

**Characterisation and Development of an Experimental Mechanical Model of  
Avascular Necrosis of the Femoral Head**

Mahsa Shahi Avadi

Submitted in accordance with the requirements for the degree of

Doctor of Philosophy

The University of Leeds

School of Mechanical Engineering

September 2016



The candidate confirms that the work submitted is his/her own and that appropriate credit has been given where reference has been made to the work of others.

This copy has been supplied on the understanding that it is copyright material and that no quotation from the thesis may be published without proper acknowledgement.

The right of Mahsa Shahi Avadi to be identified as Author of this work has been asserted by her in accordance with the Copyright, Designs and Patents Act 1988.

© 2016 The University of Leeds and Mahsa Shahi Avadi



## Acknowledgements

I would like to acknowledge and thank my supervisor Dr Sophie Williams for the support and guidance throughout the PhD. She has provided me with invaluable motivation and ideas, as well as patience in the ups and downs of the project and my personal life. I would also like to thank my secondary supervisor Prof John Fisher for thoughts and advice on the project and helping me think outside the box.

Many thanks to Dr James Anderson for infinite enthusiasm and support and being a great role model, and to my managers and colleagues at DePuy Synthes for providing the support I absolutely needed during my employment to complete my thesis.

This research would not have been possible without the support and collaboration of Prof Zhongmin Jin and Dr Manyi Wang at Xi'an Jiaotong University and Dr Meng Li and Prof Yusheng Qiu at First Affiliated Hospital of Xi'an Jiaotong University in Xi'an, China. They provided the resources that were essential for carrying out a major part of this research.

Special regards and thanks to Prof Joanne Tipper and the Centre for Doctoral Training in Medical and Biological Engineering for giving me the opportunity to undertake this research and providing opportunities for additional funding to undertake my placements in Xi'an, China. I would also like to thank Engineering and Physical Sciences Research Council for providing the funding for this project. Many thanks to DePuy Synthes for providing additional industrial funding for this project.

Many colleagues across the University of Leeds have also helped me with completion of this work. I would like to thank Rachel Pallan and Divya Baji for helping me in the laboratory. Many thanks to the technicians in University of Leeds, namely Phil Wood, Irvin Homan and Keith Dyer for their patience and technical support.

I would like to thank my parents Nasrin and Fahim Shahi for their love, support and understanding as well as always encouraging me to reach further than I think I can.

Thanks to Mehdi, Puya, Yoli, Kodee and Olivia and the rest of my family for cheering me on to become Dr Mahsa!

Finally, I would like to say thank you to my husband, Jujar Panesar, for being patient with me and not letting me give up, celebrating my achievements, lifting me up in my failures, and giving me the love and support that I undeniably needed to reach where I am now.

## Abstract

Avascular necrosis (AVN) of the femoral head is a debilitating disease of the bone that may result from a variety of aetiologies, and progresses to the death of the bone and collapse of the femoral head, and ultimately to deformation of the hip joint. *In vitro* models of AVN have been previously developed in live animals; however none of these models produce the mechanical failures that are observed in AVN femoral heads.

The aim of this study was to produce a mechanical simulation model of AVN *in vitro*. To achieve this, a series of preliminary studies were carried out. First, femoral heads from AVN patients undergoing total hip arthroplasty were studied to understand the effects of the disease on the mechanical and structural properties of the bone. The findings were compared with mechanical and structural properties of bone from non-pathological control femoral heads, and the results demonstrated mean reductions in the mechanical properties of bone with AVN.

Methods of reducing mechanical properties of bone were analysed to develop a mechanical simulation model of AVN *in vitro*. For this, chemical methods were analysed which either demineralised or dissolved the collagen matrix in the bone. The effects of treatment time were analysed on mechanical properties of bone, and it was found that demineralising bone plugs in hydrochloric acid was the most effective method of reducing the mechanical properties of bone.

In order to develop a model of AVN, porcine bone sections were treated with hydrochloric acid and returned to the femoral heads to simulate lesions in AVN. The resultant change in the structural mechanical properties of the femoral heads were analysed to determine the most suitable method of simulating AVN in porcine bone, and to provide recommendations for achieving a mechanical bone model representing the structural and mechanical properties of AVN femoral heads.





## Table of Contents

<b>Acknowledgements</b> .....	<b>v</b>
<b>Abstract</b>	<b>vii</b>
<b>List of Tables</b> .....	<b>xiii</b>
<b>List of Figures</b> .....	<b>xv</b>
<b>Abbreviations</b> .....	<b>xxxiii</b>
<b>Chapter 1. Introduction</b> .....	<b>1</b>
<b>Chapter 2. Literature Review</b> .....	<b>5</b>
<b>2.1 Basic science</b> .....	<b>5</b>
2.1.1 Anatomy of the Hip Joint.....	5
2.1.2 Anatomy of the Femoral Head.....	6
2.1.3 Mechanical Testing Methods.....	11
<b>2.2 Mechanical Testing of Bone</b> .....	<b>15</b>
2.2.1 Mechanical Properties of the Whole Bone Samples .....	16
2.2.2 Micro and Nano-Mechanical Properties .....	18
2.2.3 Mechanical Testing of Subchondral Bone.....	19
2.2.4 Factors Affecting the Mechanical Properties of Bone .....	20
2.2.5 Methods of Altering the Mechanical Properties of Bone .....	29
<b>2.3 Incidence of the Avascular Necrosis of the Femoral Head</b> .....	<b>35</b>
<b>2.4 Aetiology</b> .....	<b>37</b>
2.4.1 Stages of the Disease.....	39
2.4.2 Histological Properties .....	44
2.4.1 Legg-Calvé-Perthes Disease.....	46
<b>2.5 Diagnostic Methods</b> .....	<b>47</b>
2.5.1 Imaging Techniques.....	47
2.5.2 Staging Systems .....	48
<b>2.6 Treatment</b> .....	<b>51</b>
2.6.1 Non-operative Approach .....	51
2.6.2 Operative Approach.....	52

<b>2.7</b>	<b>Mechanical Properties of Avascular Necrosis</b> .....	<b>56</b>
<b>2.8</b>	<b>Experimental Models</b> .....	<b>57</b>
2.8.1	Non-traumatic Models .....	58
2.8.2	Traumatic Models .....	58
2.8.3	Mechanical Models of Avascular Necrosis.....	60
<b>2.9</b>	<b>Summary of Findings</b> .....	<b>61</b>
<b>2.10</b>	<b>Project Aims and objectives</b> .....	<b>63</b>
2.10.1	Aims.....	63
2.10.2	Objectives.....	63

<b>Chapter 3.</b>	<b>Mechanical Characterisation of Porcine, Ovine and Bovine Femoral Head Bone</b> .....	<b>65</b>
<b>3.1</b>	<b>Introduction</b> .....	<b>65</b>
<b>3.2</b>	<b>Materials and Methods</b> .....	<b>65</b>
3.2.1	Introduction .....	65
3.2.2	Sample Selection .....	66
3.2.3	General Materials.....	67
3.2.4	Preparation of Samples .....	68
3.2.5	Bone Plug Sample Preparation.....	69
3.2.6	Femoral Head Sample Preparation .....	71
3.2.7	Storage.....	72
3.2.8	Computed Tomography (CT) Scanning .....	72
3.2.9	Mechanical Testing.....	73
3.2.10	Results Analysis.....	74
<b>3.3</b>	<b>Results</b> .....	<b>78</b>
3.3.1	CT Images.....	78
3.3.2	Mechanical tests .....	81
<b>3.4</b>	<b>Discussion</b> .....	<b>83</b>
<b>3.5</b>	<b>Summary of Findings</b> .....	<b>89</b>

<b>Chapter 4.</b>	<b>Characterisation of Mechanical Properties of Femoral Heads with Avascular Necrosis</b> .....	<b>91</b>
-------------------	---	-----------

<b>4.1</b>	<b>Introduction</b> .....	<b>91</b>
<b>4.2</b>	<b>Materials and Methods</b> .....	<b>92</b>
4.2.1	Assessment of Properties of AVN Femoral Heads.....	93
4.2.2	Assessing Control Human Femoral Heads.....	110
4.2.3	Data Analysis for Femoral Heads in Control and AVN Groups.....	114
4.2.4	Differences between Methods Used in Testing Femoral Heads in the Control and AVN Groups .....	118
<b>4.3</b>	<b>Results</b> .....	<b>119</b>
4.3.1	Donor Characteristics.....	119
4.3.2	AVN Specimen Characterisation.....	120
4.3.3	Computer Tomography Scanning .....	125
4.3.4	Mechanical Properties .....	130
<b>4.4</b>	<b>Discussion</b> .....	<b>133</b>
4.4.1	Lesions within AVN Femoral Heads.....	134
4.4.2	Subchondral Fractures in AVN Femoral Heads.....	137
4.4.3	Structural and Mechanical Properties of Bone with AVN .....	138
4.4.4	Experimental Challenges .....	141
4.4.5	Access to AVN Specimens.....	141
4.4.6	Access to Control Specimens.....	142
4.4.7	Human Tissue Variance.....	142
4.4.8	Study Limitations.....	145
<b>4.5</b>	<b>Summary of Findings</b> .....	<b>148</b>

<b>Chapter 5.</b>	<b>Degradation of Mechanical Properties of Bone in a Disease Model of Avascular Necrosis of the Femoral Head</b> .....	<b>143</b>
<b>5.1</b>	<b>Introduction</b> .....	<b>143</b>
<b>5.2</b>	<b>Materials and Methods</b> .....	<b>144</b>
5.2.1	Materials.....	145
5.2.2	Methods.....	146
<b>5.3</b>	<b>Results Analysis</b> .....	<b>148</b>
<b>5.4</b>	<b>Results</b> .....	<b>148</b>
<b>5.5</b>	<b>Discussion</b> .....	<b>151</b>
5.5.1	Loss of Collagen Matrix.....	151

5.5.2	Decalcification of Bone Tissue .....	153
5.5.3	Reducing Mechanical Properties of Bone .....	157
<b>5.6</b>	<b>Summary of Findings .....</b>	<b>159</b>

**Chapter 6. Development of a Mechanical Simulation Model of Avascular Necrosis in Porcine Femoral Heads ..... 167**

<b>6.1</b>	<b>Introduction .....</b>	<b>167</b>
<b>6.2</b>	<b>Materials and methods.....</b>	<b>169</b>
6.2.1	Sample Preparation .....	170
6.2.2	Mechanical Characterisation.....	172
<b>6.3</b>	<b>Results analysis.....</b>	<b>172</b>
<b>6.4</b>	<b>Results.....</b>	<b>173</b>
<b>6.5</b>	<b>Discussion .....</b>	<b>174</b>
<b>6.6</b>	<b>Summary of Findings .....</b>	<b>176</b>

**Chapter 7. Overall Discussions and Conclusions..... 179**

<b>7.1</b>	<b>Research Objectives .....</b>	<b>181</b>
<b>7.2</b>	<b>Experimental Challenges.....</b>	<b>182</b>
7.2.1	Access to Human Tissue.....	183
7.2.2	Experimental Limitations.....	184
<b>7.3</b>	<b>Future Work.....</b>	<b>185</b>
7.3.1	Lesions in AVN Femoral Heads .....	186
7.3.2	Changes in BMD with AVN .....	186
7.3.3	Finalising Experimental AVN Model.....	186
7.3.4	Computational Modelling of AVN.....	187
<b>7.4</b>	<b>Conclusions.....</b>	<b>187</b>

## List of Tables

Table 2-1 - Risk factors associated with AVN, adapted from Lavernia et al. (1999); Malizos et al. (2007); Séguin et al. (2008).....	39
Table 2-2 –Ficat and Arlet staging system – Adapted from Ficat, 1985 (Ficat, 1985) and Mont et al., 2006(Mont et al., 2006).....	49
Table 2-3 – ARCO diagnostic staging system for AVN (Gardeniers, 1993b).....	49
Table 2-4 - Pennsylvania staging system established by Steinberg et al., (1995). *in these stages, depending on the severity, A-low (<15% of femoral head affected), B-Moderate (15% of femoral head affected), C-high (>30% of femoral head affected) severity is used.....	50
Table 2-5 – Clinical outcome of Core decompression, electrical simulation and combined treatment at 36 months showing successful follow-up percent. Findings of Aaron and Ciombor, (1997) .....	53
Table 3-1– Details of the tissue obtained for this study .....	66
Table 3-2 - Formulation of phosphate buffered saline tablets (MP Biomedicals, OH, US)(MP Biomedicals, 2015) .....	67
Table 4-1 – Inclusion and exclusion criteria used for patient selection for collection of AVN samples. In order for patients to be eligible for this study, they were required to meet all of the inclusion criteria and none of the exclusion criteria. ....	95
Table 4-2 - Grading criteria used for visual inspection of the femoral heads .....	98
Table 4-3- Details of assumptions made for moments analysis of the lever system used to multiply applied load (assuming use of stainless steel 316), for compression tests of femoral heads.....	104
Table 4-4 - Inclusion and exclusion criteria set for control human tissue used in this study.....	111

Table 4-5 - Summary of differences in methods used for testing AVN and control specimens.....	118
Table 4-6 - Primary and secondary causes of death, and test type used for each sample in this study .....	120
Table 4-7 – Table showing frontal medial lateral photographs and representative CT slice of each AVN specimen at the greatest diameter of the femoral head demonstrating the degree of collapse and damage to the femoral head as well as the lesions viewed in the CT images. Patient information, severity grade and specimen grouping for whole head or bone plug mechanical testing are also shown. Specimens are sorted by increasing Pennsylvania grading.....	120
Table 4-8 – Allocation of control samples to bone plug or whole head test groups for mechanical testing. ....	125
Table 5-1 - Treatments and timelines used on the bone plugs.....	147
Table 6-1 – Sample groups and treatments applied to each group.....	170

## List of Figures

- Figure 2-1 - Lateral view of the hip joint with the joint opened showing the main femoral head, acetabulum and the ligaments within the joint. Image from Tank and Gest, (2008, p141)(Reproduced with limited permission from Lippincott Williams & Wilkins).....5
- Figure 2-2 – Diagram showing cross section through the femur and acetabulum to show the blood supply into the hip joint.(Hughes et al., 2002) (Reproduced with permission from Wolters Kluwer Health, Inc.).....6
- Figure 2-3 - Image showing cortical bone and cancellous bone in the cross section of the femoral head Image from Martens et al., (1983). (Reproduced with permission form Elsevier) .....7
- Figure 2-4 – Scanning Electron Microscopy (SEM) image of (a) cortical/trabecular bone interface. The more dense area on bottom right of the image is cortical bone, and less dense region on top left of the image is trabecular bone. (b) the microporous structure in the trabecular bone, (c) the macro-pore wall, (d) Cortical bone. Image from Zhang et al. (2007). (Reproduced with permission from Elsevier) .....8
- Figure 2-5 - Diagram of a sector of the shaft of a long bone, presenting the types of bones and channels found in bone. Image from Keaveny et al. (2009), (Reproduced with permission from Elsevier) .....9
- Figure 2-6 - SEM image of a rat tibia showing the cancellous bone. The trabecular structure is visible, with the trabecular arrangements. (A) Plate-plate structure, (B) Rod-plate structure, (C) Rod-rod structure. Images from Abe et al. (1999), (Reproduced with permission from Elsevier). ..... 10
- Figure 2-7 - Vascular anatomy of the femoral head and neck. Image from Wiesel and Delahay, (2010). (Reproduced with limited permission from Springer) ..... 11
- Figure 2-8 - Typical setup of a compressive test, where an upper and lower platen are used to load the sample. In some setups, the lower platen is stationary and

the upper platen moves to subject the sample to load (L). In some cases an in-built extensometer measures the distance moved by the platens. A strain gauge may also be used to measure the change in height in the gauge area. .12

Figure 2-9 - A typical stress-strain curve showing the failure point as well as yield strength and 0.5% yield strength. The red line represents the elastic region, from which the elastic modulus (Young’s modulus) can be calculated. ....13

Figure 2-10 - An example of the progressive loading method used by Nyman et al, where the cortical bone specimens were subjected to cycles of “loading-dwell-unloading-dwell-reloading”. (i – loading instant;  $U_{im}$  – Irreversible energy dissipation;  $U_{ih}$  – hysteresis energy;  $U_{ier}$  – released elastic strain energy;  $E_0$  – initial modulus;  $E_i$  – instantaneous modulus;  $\sigma_{imax}$  – maximum stress  $\sigma_i$  – instantaneous stress;  $\epsilon_i$  – instantaneous strain;  $\epsilon_{ip}$  –plastic strain) Figure from Nyman et al., (2009) (Reproduced with permission from Elsevier). ....14

Figure 2-11 - S-N curve for the fatigue loading of human bone from a 27 year old (circles) and a 56 year old (squares) to demonstrate the typical method of calculating the fatigue properties of mineralised tissue. In this study, the data was normalised (closed circles and squares) to account for modulus variations between samples within each groups and the solid lines are the regression fits to the solid symbols. (Dashed lines show data from other studies; (a) human cortical bone fatigue data from Carter and Caler (1983); (b) Bovine cortical bone fatigue data adjusted for temperature (Carter and Hayes, 1976a); (c) Data from (b) adjusted for stiffness; (d) Fatigue data of human cortical samples as rotating cantilevers (Swanson et al., 1971) and (e) four-point bending fatigue data from human cortical bone (Choi and Goldstein, 1992) . Image from (Zioupos et al., 1996), (Image reproduced with permission from Elsevier). ....15

Figure 2-12 - Bending testing of bone. Left - Four point bending testing as performed by Martens et al., (1986). Right – Three point bending test as performed by Strømsøe et al., (1995). (Images reproduced with permission from Elsevier.)17



Figure 2-13 – Axial testing of femur at 11° adduction, as demonstrated by Cristofolini et al. (1996). (Image reproduced with permission from Elsevier.)..... 17

Figure 2-14 – influence of strain rate on the ultimate strength of compact and trabecular bone tested without marrow *in situ* by Carter and Hayes, (1976). The ultimate strength is proportional to strain rate applied. (Image reproduced with permission from The American Association for the Advancement of Science.) ..... 21

Figure 2-15 - Compressive strength of vertebral cancellous bone samples as a function of apparent density as found by Galante et al., (1970). (Image reproduced with permission from Springer.)..... 22

Figure 2-16 - Left - Graph showing the increase in porosity of cortical bone with increasing age. This results in reduction of ultimate stress (middle) and toughness (Right) of the cortical bone. (Seeman, 2008). (Image reproduced with permission from Springer.)..... 23

Figure 2-17 - The heterogeneous trabecular structure of the tibia (Boutroy et al., 2005). (Image reproduced with permission from Endocrine Society. )..... 25

Figure 2-18 - Arrangement of cancellous bone in the proximal femur can be divided into three directions (Martens et al., 1983). (Image reproduced with permission from Elsevier.) ..... 26

Figure 2-19 - Left – effects of age on porosity of cortical bone, Right - Effects of ageing on ultimate stress of the cortical bone, demonstrating the inverse relationship between porosity and ultimate stress. Figures from McCalden et al. (McCalden et al., 1993). (Image reproduced with permission from Wolter Kluwer.)..... 27

Figure 2-20 – Stiffness loss in each canine specimen group (%) versus frequency of microcracks seen in the tissue (%) in each group following application of four-point cyclic loading. (Burr et al., 1998). (Image reproduced with permission from Elsevier.) ..... 32

Figure 2-21 – Results by Wynnyckyj et al., studying the mechanical properties of male and female emu tibiae following treatment by potassium hydroxide. A significant decrease in elastic modulus and failure stress, with a significant

increase in failure strain was seen following a 14 day treatment in potassium hydroxide. A significant increase in toughness was also seen (Wynnyckyj et al., 2009). (Image reproduced with permission from Elsevier. ) .....	34
Figure 2-22 - The series of events that occur from the onset of AVN and the eventual development of osteoarthritis.....	40
Figure 2-23 – Angiogram of an avascular necrotic femoral head showing the vascular zones – AVZ – avascular zone where no arteries or arterioles are visible. RVZ- where abrupt ramification of arteries can be seen; and NVZ where smooth and unaffected arteries are seen. Image from Ohzono et al., (1992). Image reproduced with permission from Wolters Kluwer Health, Inc.....	41
Figure 2-24 - Non-diagnostic radiograph of AVN at the very early stage, Image from Steinberg et al., (1995) .....	42
Figure 2-25 - MRI of stage 0 avascular necrotic femoral heads, where a slight decrease in signal intensity is seen in both femoral heads, but still within normal limits. Image from Steinberg et al. (1995).....	42
Figure 2-26 - Left - MRI of a patient that shows decreased signal intensity in the femoral head, a sign of AVN. Right – Bone scan of a patient in early stages of AVN, which shows increased density uptake, a sign of AVN. Images adapted from Marvin E Steinberg et al., (1995) and Incavo & Pappas, (2004). .....	43
Figure 2-27 – Left – Area of increased lucency seen in radiograph, a sign of sclerosis development in the tissue. Middle – The subchondral collapse is seen by the formation of a crescent sign (shown by arrows) in the radiograph. Right – Flattening of the femoral head (shown by arrows) following high physiological loads in the joint. Images adapted from Steinberg et al., (1995). (Images reproduced with permission from The British Editorial Society of Bone and Joint Surgery) .....	44
Figure 2-28 – Microscopic pictures of histological specimens stained with haematoxylin and eosin, 100x. Left – viable osteocytes (white arrows) in osteoarthritic bone. Right- empty osteocyte lacunae (white arrows) and appositional new bone formation (black arrows) in AVN patient (Steffen et al., 2010) (Image	

reproduced with permission from British Editorial Society of Bone and Joint Surgery.) .....	45
Figure 2-29 - Histological specimen of a biopsy specimen removed from an AVN patient (Haematoxylin and eosin staining (H&E), 100x). Empty lacunae (arrows) are seen in bone trabeculae (asterisk), which is surrounded by new bone formation (two asterisks). Granulation tissue is observed in marrow tissue (Sakamoto et al., 2013). (Image reproduced with permission from Springer.)	45
Figure 2-30 – Left: Gross photograph and Right: associated specimen radiograph of necrotic femoral heads. (a) The region between the viable and necrotic region is lateral to the fovea, and (b) the fracture is in the subchondral region. (c) The interface between healthy and necrotic is deep within the femoral head, and (d) the collapse is deep within the femoral head. Image adapted from (Motomura et al., 2011).....	46
Figure 2-31 – Stages of Perthes disease from onset to healing. A and B – avascular necrosis of the bone where the epiphysis appears dense and sclerotic, with a fracture line; C and D – fragmentation of the dense epiphysis shown by presence of fissures along the epiphysis. The epiphysis may appear broken into several pieces as shown in D; E and F – revascularisation shown by formation of new bone on the periphery of the necrotic lesion; G – healing of the femoral head where mature lamellar bone replaces the dead bone. Image from Joseph, (2011), reproduced with permission from Wolters Kluwer Health, Inc.....	47
Figure 2-31 – (a) Radiograph of a right femur showing subchondral area hyperlucency as pointed with arrows in the proximal femoral head. (b) Specimen radiograph of a sectioned femoral head segment showing the subchondral fracture as seen with a crescent sign. Images from (Pappas, 2000) .....	48
Figure 2-32 - Illustration of radiographic appearance of AVN femoral heads by the Pennsylvania staging system. See Table 2-4 for description of the stages. Figure by Lavernia et al., (1999). (Image reproduced with permission from Wolters Kluwer Health, Inc.).....	51

Figure 2-33 - Cathode wire electrode coiled around graft in core decompression track with implantable current generator. Image from Aaron and Ciombor, (1997). (Image reproduced with permission from Elsevier.) .....54

Figure 2-34 –Sectioning planes and orientations of sample cubes excised and tested by Brown et al. in the apparatus shown on the right. Image from Brown et al., (1981). (Image reproduced with permission from Wolters Kluwer Health, Inc.) .....56

Figure 2-35 –Histologic sections obtained from surgery of emus that developed end-stage AVN as well as signs of crescent sign and loss of trabecular bone. (H&E, 1X) (Conzemius et al., 2002) . (Image reproduced with permission from John Wiley and Son.).....59

Figure 2-36 – Project objectives and chapter outline.....65

Figure 3-1 - Flow chart showing the experimental method for assessing mechanical properties of animal femoral heads. ....66

Figure 3-2 – (a) A porcine leg as received from the abattoir. (b) Tissue stripped from the leg. (c) Ligamentum teres being cut to separate the femoral head from the acetabulum. (d) Stripped porcine femur.....69

Figure 3-3 - The osteochondral plugs were taken from the maximum load location shown on the image on the left (Taylor et al. 2011).Image reproduced with permission from SAGE Publications. ....70

Figure 3-4 – Photographs showing the removal of bone plugs from the femoral head (in this case, porcine). The bone plugs were removed from the femoral head, and the bony end was flattened using a metal file. The cartilage was then removed using a scalpel to produce a cylindrical sample for testing. ....70

Figure 3-5 - Preparation of femoral head samples; red dotted line shows the line at which a cut will be made in the femur, and the black lines show the alignment to be used with respect to the distal end of the femur. Image adapted from 3DCADBrowser.com .....71

Figure 3-6 – XtremeCT scanner by Scanco used for obtaining CT images from the bone samples (“XtremeCT scanner,”) .....72

Figure 3-7 - Diagram showing the scanning direction in the CT scanner for the (a) osteochondral plugs and (b) whole femoral heads; the red lines represent the approximate angle of scan planes and the scanning direction is seen with the arrows. The image is not to scale. .... 73

Figure 3-8 - A - The Instron 3366 testing machine used to test bone samples in compression. B - A porcine bone plug set up and ready for compression testing. .... 74

Figure 3-9 - Diagram showing a CT image slice of a porcine bone plug, where a square area is selected in the image and then converted into a binary image..... 75

Figure 3-10 - Diagram showing a trabecular structure illustrating the trabecular thickness and spacing. The darker areas demonstrate thinner whereas lighter areas demonstrate thicker trabecular thickness. The trabecular spacing is the mean distance between trabeculae as demonstrated with the white arrows. .... 75

Figure 3-11 - A screenshot of the figure produced by the MATLAB programme and the cross-hairs requesting the manual selection of two points on the elastic region. .... 76

Figure 3-12 - An example of a graph obtained by the MATLAB programme; this graph shows the stress versus strain values for an ovine sample, where the red line shows the stress strain curve, the pink box shows the yield stress and green circle shows the 0.5% offset yield stress. The dashed line shows the line of best fit through the elastic region, from which the elastic modulus is calculated, and the Dash-dotted line shows the line parallel to the elastic line of best fit, offset by 0.5%. .... 77

Figure 3-13 - Bar chart displaying mean porosity for ovine, bovine and porcine bone samples. The error bars are standard errors of mean (n=5); there were no significant differences between any of the groups..... 78

Figure 3-14 - (a) Mean trabecular thickness and (b) mean trabecular spacing for ovine, bovine and porcine specimens with error bars indicating standard errors of mean; the red asterisks indicates significant difference between each data group and other groups ( $p < 0.05$ ). .... 79

- Figure 3-15 – Examples of CT images from the bone plugs for A-bovine, B-porcine and C-ovine femoral head tissue. It can be observed that porcine tissue has more densely packed trabeculae than bovine and ovine bone. .... 79
- Figure 3-16 – Example images of A-porcine and B-ovine femoral head CT scans. The porcine femoral head is significantly larger than the ovine femoral head with a more densely packed trabecular structure than ovine tissue, in particular near the femoral head surface. A visible growth plate is seen in the centre of the porcine femoral head, however this is only seen in the femoral neck of the ovine sample. .... 80
- Figure 3-17 – Mean bone mineral density (BMD) for bovine, ovine and porcine specimens with error bars indicating standard errors of mean; the red asterisk indicates significant difference between data group ( $p < 0.05$ ). Bovine specimens had significantly different BMD when compared with other groups. .... 80
- Figure 3-18 – Mean elastic modulus for ovine, bovine and porcine bone samples. Error bars are standard errors of mean. No significant differences were found between the data ( $P < 0.05$ )..... 81
- Figure 3-19 – Mean yield stress for ovine, bovine and porcine samples. The error bars are standard errors of mean and the red asterisk represents a significant difference with other groups ( $P < 0.05$ ). Bovine specimens had significantly different yield stress when compared with other groups. .... 82
- Figure 3-20 – Mean offset yield stress for the three animal tissue samples. The error bars are standard errors of mean and the red asterisk represents a significant difference with other groups ( $P < 0.05$ ). Bovine specimens had significantly different offset yield stress when compared with other groups. 82
- Figure 3-21 – Mean work to yield for the three animal tissue samples. The error bars are standard errors of mean and the red asterisk represents a significant difference with other groups ( $P < 0.05$ ). Bovine specimens had significantly different work to yield when compared with other groups. .... 83
- Figure 3-22 - Trabecular thickness and trabecular spacing as well as bone volume ratio (bone volume/total volume) comparison between human, ovine, bovine and

porcine greater tubercle tissue in the subcortical region; Graph adapted from results of Holzer et al. (2012).....	84
Figure 3-23 - The relationship between bone mineral density and elastic modulus for bone plug samples from the three species is shown in this figure. A regression line is fitted to each data set and all the samples combined, and R <sup>2</sup> values are shown next to each line.....	86
Figure 3-24 – The relationship between bone mineral density and yield stress for the bone plug samples from the three species, as well as the overall relationship for all samples. A regression line is fitted to each data set and all the samples combined, and R <sup>2</sup> values are shown next to each line. ....	87
Figure 3-25 – The relationship between bone mineral density and work taken to yield for bone plug samples from the three species is shown in this figure. A regression line is fitted to each data set and all the samples combined, and R <sup>2</sup> values are shown next to each line.....	87
Figure 4-1 – Summary of work leading to development of a mechanical model of AVN, with current chapter highlighted in yellow.....	91
Figure 4-2 – Summary of objectives of this study to characterise bone with AVN. ....	92
Figure 4-3 – Flow diagram demonstrating the experimental path for samples, and the outputs from each test for both AVN and control sets of samples. ....	93
Figure 4-4 - Flow diagram showing a summary of the collection, storage, test and disposal process the AVN specimens underwent in this study. ....	94
Figure 4-5 – Human femoral head (Sample 02) with AVN removed at the surgery (approximately 35mm diameter). Cavity created in the inferior position of the head during removal of the femoral head in surgery is marked by dashed circle.....	96
Figure 4-6 - A whole femoral head sample (Sample 11, medial lateral view, diameter approximately 52mm) fixed distally in PMMA cement. ....	99
Figure 4-7 – Schematic of a femoral head. The locations where bone plugs were removed from the femoral head with respect to anterior and posterior directions and ligamentum teres. All bone plugs were taken as 9mm cylindrical specimens, and for demonstration purposes, they are shown as	

elliptical shapes due to perspective and depending on location of sample. (Schematic not to scale). .....	100
Figure 4-8 – Images showing a femoral head specimen removed at surgery following removal of bone plugs. The locations from which the bone plugs were removed are demonstrated (a) laterally and (b) medially. Letters A-I correspond to Figure 4-7. Locations for bone plugs G and H are not shown in these images and are shown on Figure 4-7. ....	101
Figure 4-9 – Left: Schematic of a bone corer with serrated cutter teeth (lower portion) and internal diameter of 9mm used for removal of bone plugs. The smooth end (upper portion) was used to fix to an electrical drill. Right: The bone corer attached to a drill for removal of bone plugs. ....	101
Figure 4-10 – Diagram demonstrating the relation of object to the source and detector in the CT scanner. The X-ray source applies X-rays towards the detector, and the object that is placed between the source and detector rotates, producing cross-sectional images of the object. ....	102
Figure 4-11 – The PEEK fixture designed and developed in house to hold human tissue specimens in the CT scanner at iAMT. ....	103
Figure 4-12 - An example scout view image from the CT scanner, of the femoral head used to select the “area of interest” for scanning, as demonstrated using blue dashed lines. ....	103
Figure 4-13 - Moment diagrams for the mechanical testing lever system that was designed for experiments. (i) A simple sketch of the system, showing the location of the femoral head and supports A and B. (ii) Reaction loads $R(a)$ and $R(b)$ in the supports. (iii) Deflection ( $D$ ) and moment ( $M$ ) in the system, (iv) Location for maximum deflection – $y(max)$ . ....	105
Figure 4-14 – Diagram showing the assembly model of the loading fixture used to magnify the load applied by mechanical testing machine onto the sample, with annotations showing the individual parts of the fixture. The drawings can be found in Appendix E. ....	107
Figure 4-15 - The loading fixture that was used in mechanical testing of the samples, while it was in use on the mechanical testing machine. The crosshead of	



the machine applied load onto part 7 on the fixture. The spring was placed on the rod protruding from the base and removed prior to testing when the loading part was placed on the specimen, as shown in this image. The base was attached to the machine using the 16mm diameter hole in the centre of the base. The annotations correspond with Figure 4-14. .... 108

Figure 4-16 Mean load applied to the load cell versus the load applied by the Instron testing machine in increments onto the mechanical testing fixture shown in Figure 4-14. The error bars represent standard deviation (n=3). ..... 109

Figure 4-17 - Simplified diagram of the dimensions used for calculation of the relationship between the displacement applied by the mechanical testing machine (a) and displacement applied to the specimen (b). Angle  $x$  is the angle of the loading bar (part 2 in Figure 4-14) from horizontal. The points a and b were 180mm and 60mm from the support respectively. 109

Figure 4-18 – (a) Pelvis to mid femur stripped area as received from the tissue bank. (b) Specimen divided into left, centre and right sections. (c) and (d)– Example of a femur stripped from the rest of the right pelvis in anterior-posterior and medial-lateral views respectively..... 112

Figure 4-19 - Location of load bearing (LB) and non-load bearing (NLB) bone plug taken from femoral heads in the control group. .... 113

Figure 4-20 - Summary of image processing to analyse the area of lesions in each CT image slice of avascular necrotic femoral heads. .... 114

Figure 4-21 – Series of images showing processing of a CT image slice of a femoral head with AVN to assess the area per slice and volume of the lesions within the femoral head. (a) – Standard transverse section CT image of a femoral head as analysed. (b) A binary mask is placed on a copy of the image to provide a black and white image, where a manual threshold is selected to represent bone. (c) A closing algorithm is placed on image from (b) to dilate the trabecular bone and the normal enclosures. (d) A binary mask is placed on a different copy of the image by manually selecting the threshold to represent all viable bone and remaining tissue..... 116

Figure 4-22 – Example of a control CT image of a femoral head where the closing algorithm is applied. (a) normal CT image, (b) closed binary CT image.. 116

Figure 4-23 – Patient demographics for the specimens in this study. Means and ranges for BMI and ages of the patients at time of surgery, as well as time between first presentation to a clinician and onset of pain, and surgery are shown..... 119

Figure 4-24 – Bar chart demonstrating the frequency distribution of specimens tested as whole head or bone plug samples in mechanical testing based on initial grade according to Table 4-2..... 125

Figure 4-25 –CT slices demonstrating the variation in damage due to AVN in the femoral heads. Lesions (L) are seen in all samples; however their numbers and volumes are different in all specimens. Subchondral fractures (SF) are also seen in some samples. (a) CT slice from sample A6, demonstrating a large lesion of one side of the femoral head, as well as thin trabecular bone on the opposite side. Subchondral fracture is seen near the lesion. (b) CT slice from sample A10, demonstrating multiple lesions, as well as multiple subchondral fractures demonstrated by dense cloudy trabeculae. The surface of the femoral head is also deformed, possibly due to collapse of subchondral bone and a part of the articular surface is fractured from the rest of femoral head. (c) CT slice from sample A11, demonstrating multiple lesions of smaller size, as well as subchondral fracture, however the cortical bone is mostly intact despite presence of articular surface fractures. The hole (H) produced by surgical removal of the femoral head from patient is also seen in this slice. (d) CT slice from sample A15, showing a non-spherical femoral head due to collapse, with subchondral fracture. Smaller lesions as well as thinned trabeculae, and fractured articular surface are also seen. .... 126

Figure 4-26 – CT slices from control human femoral head samples demonstrating lesions and areas with thinned trabeculae (a) sample C2, (b) sample C3, (c) Sample C6 (L=lesion)..... 127

Figure 4-27 - Mean ratio of lesions to whole femoral head volume for each Pennsylvania stage assigned to the specimens and the control samples. The error bars represent standard error of mean, and specimen numbers are shown above each column. Kruskal-Wallis test demonstrated no significant differences between the means of groups ( $p < 0.05$ ). ..... 127

Figure 4-28 - Figure showing the distribution of samples when sorted by lesion sizes in each femoral head. Most of the samples in this study had lesions that filled 50-70% of the femoral heads..... 128

Figure 4-29 – Lesion size as percentage of femoral head versus the amount of time between onset of pain and THR surgery ( $R^2 = 0.05$ ), Age ( $R^2 = 0.16$ ) and BMI of patients ( $R^2 = 0.02$ )..... 129

Figure 4-30 – Bone mineral density plots for control bone plugs from load bearing and non-load bearing regions. Error bars demonstrate standard errors of mean. Significant differences were not found between the means of groups (Student’s t-test)( $n=3$ ). ..... 130

Figure 4-31 Elastic modulus and yield stress for the AVN heads assigned to each Pennsylvania grade and for the control head specimens. The error bars indicate standard error of mean and specimen numbers are demonstrated above each bar. Kruskal-Wallis test determined that there were no significant differences between the means of each group ( $p > 0.05$ )..... 131

Figure 4-32 - Relationships between the elastic modulus and yield stress of AVN whole head specimens and their associated bone to whole head ratio.  $R^2$  values are presented for each graph, and since the coefficient of determination is so small, the bone to whole femoral head ratio cannot determine the elastic modulus or yield stress of these samples accurately. .... 131

Figure 4-33 – Mean elastic modulus (Left) and yield stress (Right) for load bearing (LB) and non-load bearing (NLB) bone plugs from both AVN and control groups. No significant differences were found between the AVN and control groups for both parameters in load bearing and non-load bearing regions, however there were significant differences (asterisks) between

the load bearing and non-load bearing samples from both groups (Kruskal-Wallis H test and Dunn’s multiple comparison test,  $p < 0.05$ ) .... 133

- Figure 4-34 – Mean ratios of lesions to femoral head for AVN and control groups. The error bars demonstrate standard error from mean and sample numbers are above each bar. The group means were significantly different from each other (Mann-Whitney test,  $p < 0.0001$ ). ..... 134
- Figure 4-35 - The use of Kerboul angle to measure the lesion size from anterior-posterior (left) and medial-lateral (right) radiographs by adding together the angles, and therefore categorising them into small, medium and large lesions (Kerboul et al., 1974). ..... 137
- Figure 4-36 –Anterior-posterior slices from randomly selected CT images of AVN femoral heads, demonstrating the subchondral fractures (arrows) in the samples. .... 138
- Figure 4-37 - Differences in means of elastic modulus (E) and yield stress ( $\sigma$ ) between AVN and control specimens as percentages, as reported in this study and by Brown et al. (1981). ..... 139
- Figure 4-38 - Regions used by Brown et al. (1981) to group test samples into necrotic (group 1), sclerotic (group 2) and control (group 3). Image reproduced with permission from Wolters Kluwer Health, Inc. .... 140
- Figure 4-39 – High resolution pQCT images tibias of (a&c) Chinese-American and (b&d) white women, demonstrating the thicker cortical shell and more plate-like trabeculae in Chinese-American women when compared with Caucasian tibia (Cong and Walker, 2014). Image reproduced with permission from Nature Publishing. .... 145
- Figure 4-40 – (a) A binary image of a CT slice from an AVN specimen. (b) The binary image after application of the “closing” algorithm. .... 146
- Figure 4-41 – Images on the left show CT slices from samples A4, A6, and A13 respectively, and the images on the right show a binary “closed” version of the same slices. The lesions within the femoral head are shown as black, and regions of femoral head where “normally dispersed” trabeculae

exist are shown in white, allowing for measurement of the volume of the lesions rather than the volume of trabeculae..... 147

Figure 5-1 - Summary flowchart for experimental process of analysing the effects of chemical treatments on mechanical properties and bone mineral density of porcine femoral head bone samples (chemical treatment duration is in days). ..... 145

Figure 5-2 - Change in BMD of porcine bone plugs before and after treatment. Asterisks demonstrate significant differences between treatment groups, or before and after treatment (Two-way ANOVA with Bonferroni's multiple comparisons test,  $p < 0.05$ ). Error bars display standard error of mean. .... 149

Figure 5-3 - Logarithmic plot of elastic modulus of samples treated in EDTA, HCl and KOH as well as a control group. All samples had significantly different values to control samples (One-way ANOVA and Tukey's multiple comparisons test,  $p < 0.05$ ). Asterisks demonstrate significant differences between treatment groups. The asterisk above control samples indicates significant differences with all the treatment groups. Error bars display standard error of mean. .... 150

Figure 5-4 - Logarithmic plot of yield stress of samples treated in EDTA, HCl and KOH as well as a control group. All samples had significantly different values to control samples (One-way ANOVA and Tukey's multiple comparisons test,  $p < 0.05$ ). Asterisks demonstrate significant differences between treatment groups. The asterisk above control samples indicates significant differences with all the treatment groups. Error bars display standard error of mean..... 151

Figure 5-5 - A sample treated in KOH for 7 days. The sample had lost its solid structure, swelled and was destroyed in handling. .... 152

Figure 5-6 - Findings of Wynnyckyj et al. (2011), demonstrating the percent digested collagen following treatment in KOH for male and female emu tibiae. The \* and \*\* indicate that 7- and 14-day treated samples respectively had significantly greater percent digested collagen when compared to control samples. (Reproduced with permission from Elsevier)..... 153

Figure 5-7 -Relationship between elastic modulus and bone mineral density for bone plugs treated with HCl and EDTA. Solid line is a regression line and the dotted lines are areas of 95% confidence regions.  $R^2 = 0.32$  ..... 154

Figure 5-8 – Mean area of decalcified regions for bone plug samples treated with EDTA and HCl, as a percentage of the total bone plug, with a representative example CT slice from each treatment group shown above. The error bars show standard error of mean..... 155

Figure 5-9 – Relationship between the logarithmic yield stresses of bone plugs versus bone plug decalcified region percentage. A line of best fit could not be plotted for this data. .... 156

Figure 5-10 - Relationship between elastic moduli of bone plugs versus bone plug decalcified region percentage. The line is a second order polynomial non-linear regression line with 95% confidence limits shown.  $R^2 = 0.65$ . .... 157

Figure 5-11 – Figure demonstrating the percentage change in yield stress and elastic modulus of samples when compared with control samples..... 158

Figure 6-1 – Summary of studies in this thesis. Current chapter is highlighted in yellow and the studies providing direct input into the current chapter are highlighted in blue. .... 167

Figure 6-2 - A porcine bone plug that is placed back into the femoral head following treatment in HCl. The cavities (arrows) were filled with bone cement..... 171

Figure 6-3 – Flow chart demonstrating the sample preparation and treatment paths for the model and control groups..... 172

Figure 6-4 –Elastic modulus and yield stresses for femoral heads from treated groups and untreated and unmodified control groups. The error bars demonstrate standard deviation. Red brackets demonstrate significant differences between groups (ANOVA, Tukey’s multiple comparisons test,  $p < 0.05$ ). The red dashed lines demonstrate the desired mechanical properties for an AVN model, based on 14.8% decrease in elastic modulus and 4.2% decrease in yield stresses of unmodified control groups..... 174

Figure 7-1 – Number of publications per year in PubMed with “Avascular necrosis” or “osteonecrosis” in title or abstract, and related to hip or femoral head. A polynomial

trend-line is fitted, demonstrating a positive trend in publications related to avascular necrosis. (PubMed, 2016).....179

Figure 7-2 – Flowchart showing a summary of studies in this thesis, and the studies feeding into the development of an AVN model. ....181





## Abbreviations

ALDH	Aldehyde dehydrogenase
ANOVA	Analysis of Variance
ARCO	Association of Research Circulation Osseous
AVN	Avascular necrosis
BMD	Bone mineral density
CT	Computed tomography
DEXA/DXA	Dual energy X-ray absorptiometry
EDTA	Ethylenediaminetetra-acetic acid
GPRD	General Practice Research Database
HAART	Highly active antiretroviral therapy
HCl	Hydrochloric acid
HIV	Human immunodeficiency virus
KCl	Potassium chloride
KOH	Potassium hydroxide
LCPD	Legg-Calvé-Perthes disease
MRI	Magnetic resonance imaging
NaCl	Sodium chloride
NJR	National Joint Registry
PBS	Phosphate buffered saline
QCT	Quantitative computer tomography
S-N	Stress-life
THIN	The Health Improvement Network
SEM	Scanning Electron Microscopy



## Chapter 1. Introduction

Avascular necrosis (AVN) is the term given to an orthopaedic degenerative disease whereby osteocytes die as a result of interruption of blood supply to the bone (Cooper et al., 2010). It may be referred to with other terms, such as osteonecrosis, ischaemic necrosis and osseous ischemia (Jones, 2001). It commonly occurs in the femoral head of the hip, but can occur in other skeletal sites such as the knee, shoulder, and ankle (Assouline-Dayan et al., 2002). In the femoral head, it commonly results in the collapse of the femoral head following a series of pathological events. Following this point, the articular surface becomes arthritic and the patients commonly undergo total hip replacement surgery (Tofferi and Diamond, 2012).

The majority of the sufferers of AVN are younger people. The average age of patients in the Chinese population who have undergone total hip replacement due to avascular necrosis has been reported as 50 years old (Lai et al., 2008). AVN is also the most common diagnosis for patients undergoing total hip replacement in Asia (Chiu et al., 1997, 2001; Wong et al., 2005). In Europe and US, it is also the second most common reason for hip arthroplasty, after osteoarthritis (Mont and Hungerford, 1995; Cooper et al., 2010; Garellick et al., 2010; Ellams et al., 2011).

Avascular necrosis may have a variety of causes associated with it, but the endpoint of the disease always results in necrosis of the bone and collapse of the femoral head. Some of the most common causes of avascular necrosis include trauma, steroid or alcohol abuse as well as some diseases such as sickle cell disease (Lavernia et al., 1999; Gautier et al., 2000; Malizos et al., 2007).

The first stage in development of AVN is the death of the bone cells in the femoral head following blockage of blood vessels. This results in formation of a lesion of necrotic bone in the femoral head. This alters the architecture of the bone as the bone tries to self-repair. At this stage, a dense band of sclerotic bone, interrupted by focal resorption, forms around the periphery of the lesion at this stage, trying to resorb the

lesion. The necrotic and sclerotic bone is weaker than healthy bone, has a lower modulus and may collapse under the high loads applied in the hip. The articular cartilage would collapse also, leading to arthritis and destruction of the joint, at which point the patient requires total hip replacement surgery (Brown et al., 1981; Orban and Cristescu, 2009).

In the early stages, AVN can be asymptomatic, and is usually diagnosed at later stages when the patient feels pain following collapse of the articular surface, or a crescent sign representing the collapse of the head becomes visible in radiographic images. Currently, AVN is most frequently diagnosed in earlier stages only if the patient has developed symptomatic AVN in one hip and imaging is carried out on the asymptomatic hip. This has become the standard of care as there is a high chance of developing AVN in the contralateral hip (Hungerford, 2002).

Two factors affect the rate of the collapse of the femoral head: size and position of the lesion as well as the material properties of the dead and remodelling bone. Even though many studies have researched the biological pathway and consequences of AVN in the femoral head, the mechanical pathway and properties of bone with AVN are not understood. If these factors are to be studied, a laboratory mechanical model of the disease must be developed. The developed model will be advantageous both in a clinical and industrial aspect. The clinical advantages are that it will help choose the most effective treatment for patients suffering with AVN following diagnosis. It may also help to improve identification of mechanical risk-factors that could help to choose the most effective treatment for a patient. From an industrial point of view, it will allow optimisation and development of suitable orthopaedic implants aimed at treating AVN effectively.

This thesis aimed to study the mechanical and structural properties of femoral heads affected by AVN and compare them to the properties of control human femoral heads unaffected by AVN to improve the understanding of the mechanical consequences of the disease on the bone. The findings of the study were used to develop an *in vitro* simulation model of the disease using an animal femoral head. From

an industrial perspective, such a model is beneficial as allows optimisation and validation of new orthopaedic implants aimed at treating the disease.



## Chapter 2. Literature Review

### 2.1 Basic science

#### 2.1.1 Anatomy of the Hip Joint

The hip (Figure 2-1) is a ball-and-socket joint consisting of the femoral head and acetabulum as well as many muscles and ligaments which work together to make it a well-balanced and stable joint with a wide range of motion. It is a synovial joint: it has a joint cavity, in which joint surfaces are covered with articular cartilage; it is surrounded by a ligamentous capsule and it has a synovial membrane which produces synovial fluid (Byrne et al., 2010). It consists of two bony structures, the femoral head which is the proximal part of the femur, and the acetabulum which is part of the pelvis.

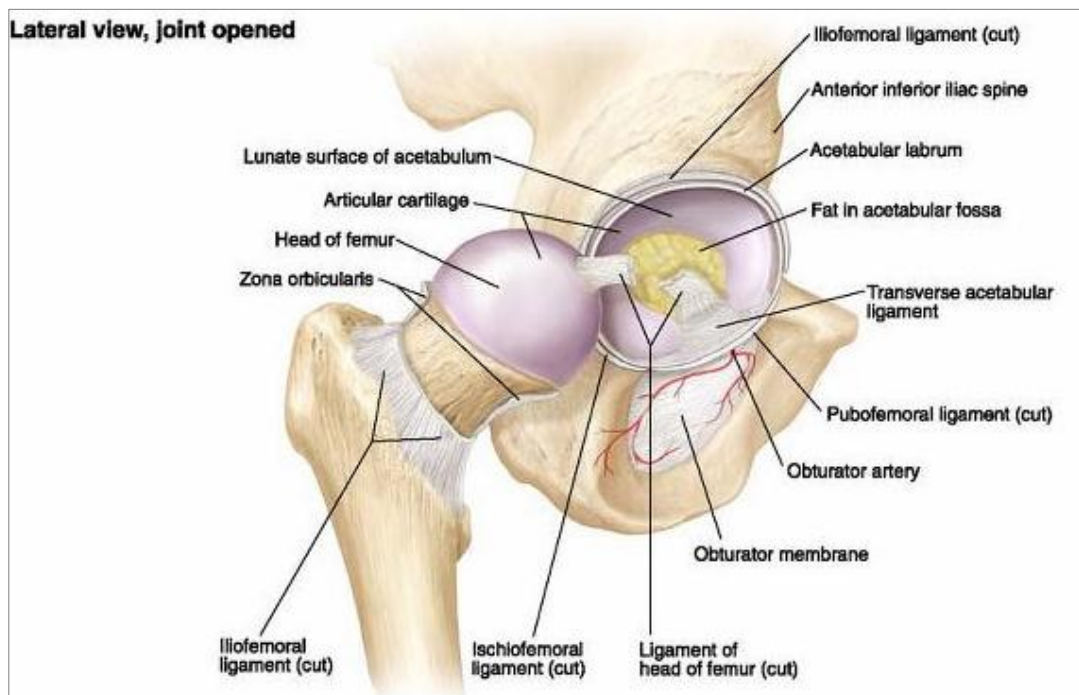


Figure 2-1 - Lateral view of the hip joint with the joint opened showing the main femoral head, acetabulum and the ligaments within the joint. Image from Tank and Gest, (2008, p141)(Reproduced with limited permission from Lippincott Williams & Wilkins)

The acetabulum receives its blood supply from three main arteries: the obturator, the superior gluteal and inferior gluteal. The femoral head and neck are mainly supplied by the medial and lateral circumflex femoral arteries. A

small proportion of the blood supply is provided through the foveal artery which enters the femoral head through fossa of the ligamentum teres (Figure 2-2)(Hughes et al., 2002).

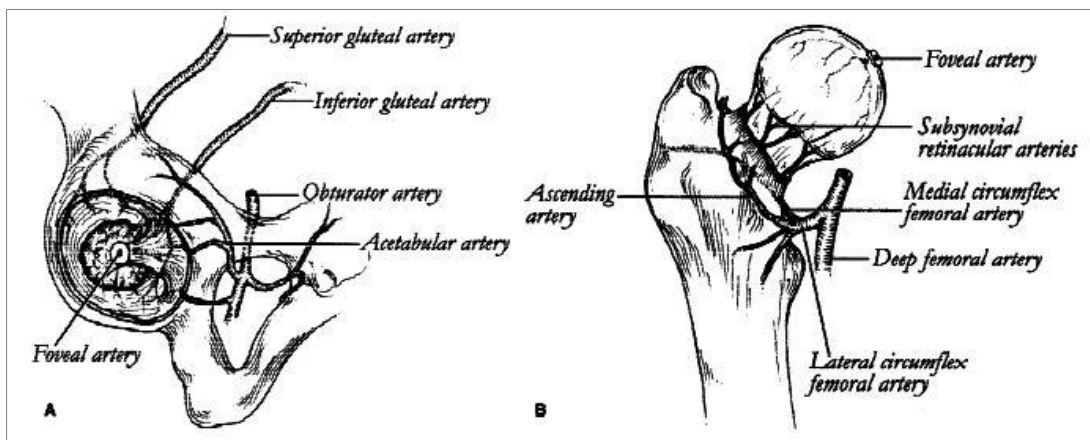


Figure 2-2 - Diagram showing cross section through the femur and acetabulum to show the blood supply into the hip joint.(Hughes et al., 2002) (Reproduced with permission from Wolters Kluwer Health, Inc.)

### 2.1.2 Anatomy of the Femoral Head

In order to understand a disease of the femoral head, its anatomy must be understood. In the macro-scale, the femur is composed of a hollow shaft (diaphysis) which transitions through an increasingly dense metaphysis into the dense epiphysis. The diaphysis is predominantly composed of cancellous bone. This structure is optimised for transferring axial compressive loads. The metaphysis and epiphysis are a mixture of trabecular and cortical bone: a reflection of the need for these regions to withstand loads in multiple orientations (Figure 2-3)(Clarke, 2008).



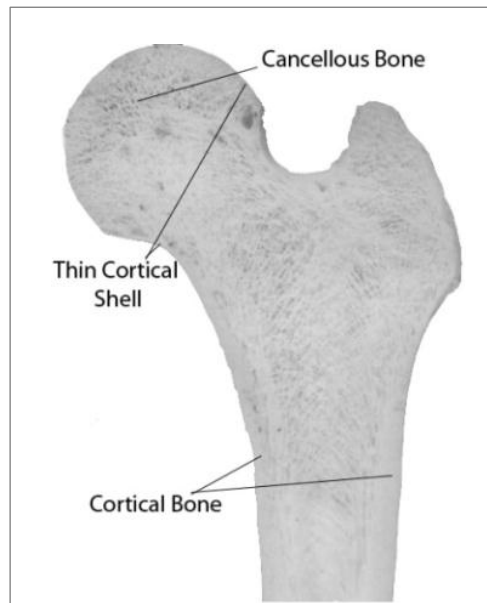


Figure 2-3 - Image showing cortical bone and cancellous bone in the cross section of the femoral head Image from Martens et al., (1983). (Reproduced with permission from Elsevier)

Cortical bone is rigid and forms the bone on the outer shells of the femur. It is composed of “regular, cylindrically shaped lamellae” (Rho et al., 1998; Clarke, 2008). Trabecular bone is made up of a very porous, honeycomb-like structure of trabeculae, the diameter of the trabecular struts typically ranges from 100-300 $\mu\text{m}$  with spaces of 300-1500 $\mu\text{m}$  between them (Figure 2-4) (Athanasίου et al., 2000; Clarke, 2008). This difference in density alongside the dissimilarity in microstructures of these two bones leads to different mechanical properties (Rho et al., 1998).

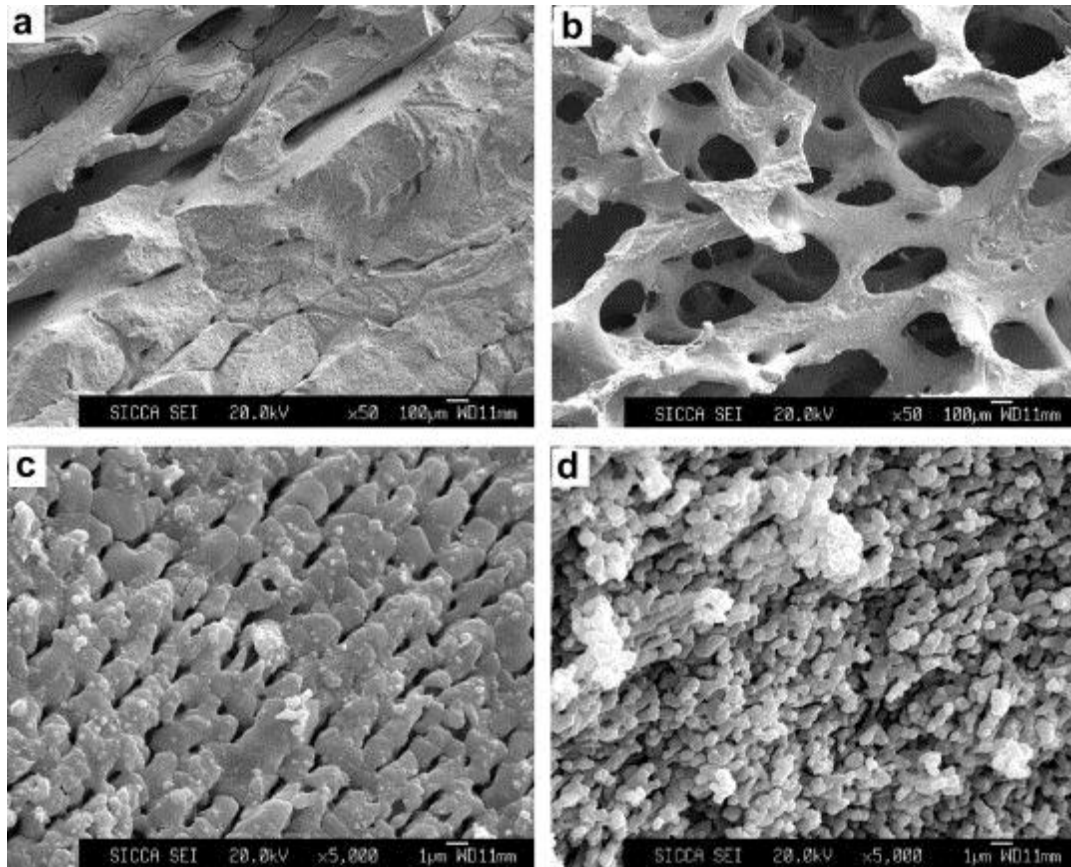


Figure 2-4 – Scanning Electron Microscopy (SEM) image of (a) cortical/trabecular bone interface. The more dense area on bottom right of the image is cortical bone, and less dense region on top left of the image is trabecular bone. (b) the microporous structure in the trabecular bone, (c) the macro-pore wall, (d) Cortical bone. Image from Zhang et al. (2007). (Reproduced with permission from Elsevier)

Bone is a highly hierarchical structure that is able to self-regenerate and self-remodel throughout the lifetime of the human (Wang et al., 2010). In the micro scale, the primary organic component of the bone consists of crystals, collagens and non-collagenous organic proteins. The bone matrix is *collagen type I*, which self-assembles into parallel fibrils (Rho et al., 1998). The plate shaped *Dahllite (or hydroxyapatite) crystals*, are the only mineral type present in mature bone (Weiner and Wagner, 1998) and they occur within the discrete spaces in the collagen fibrils in a specific crystalline orientation (Rho et al., 1998).

In adult human bone, the collagen fibres formed by the assembly of many collagen fibrils are interwoven to form *lamellae* of 3-7µm thickness (Marotti, 1993; Rho et al., 1998). These lamellae stack together to form lamellar bone, which arrange in different formats to form cortical or cancellous bones (Keaveny et al., 2009).

In cortical bone, around 3-15 lamellae are arranged in concentric cylinders around a *Haversian canal*, which is a vascular channel of about 50µm in diameter, containing blood vessel capillaries, nerves and bone cells (Figure 2-5). This then forms the *Haversian system* or *osteon*, which is a cylinder of roughly 200-250µm diameter and 1-3mm length, running parallel to the long axis of the bone. In addition to Haversian canals, *Volkman's canals* run perpendicular to the long axis of the bone, and provide a radial path for blood flow within the bone (Rho et al., 1998; Keaveny et al., 2009).

Osteocytes (bone cells) are surrounded by *lacunae*, which are thin layers of extracellular fluid arranged along the interfaces between lamellae. The osteocytes are connected to each other using processes that extend from them, called *canaliculi* (Keaveny et al., 2009).

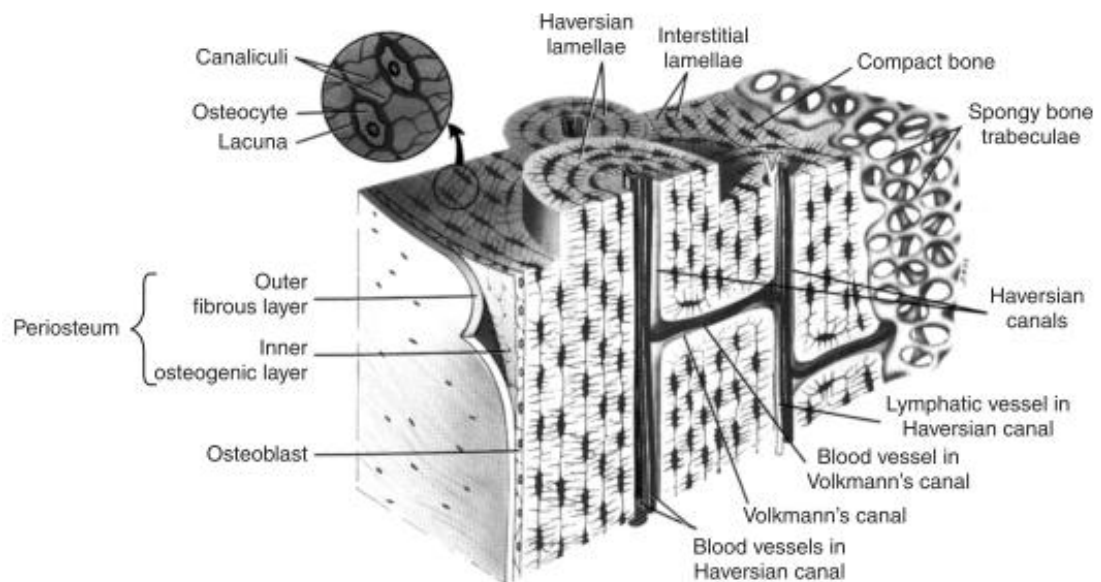


Figure 2-5 - Diagram of a sector of the shaft of a long bone, presenting the types of bones and channels found in bone. Image from Keaveny et al. (2009), (Reproduced with permission from Elsevier)

Cancellous bone comprises of a porous network of interconnected trabecular tissue of collagen fibres, filled with bone marrow. The trabeculae are irregular lattices of small rods and plates, in the following basic cellular structures: rod-rod, rod-plate, or plate-plate, varying within species, with the age of the species and the location of the bone in the body (Figure 2-6) (Rho et al., 1998; Abe et al., 1999; Keaveny et al., 2009). Within each trabeculae, three cell types are found: Osteocytes that maintain the bone matrix, osteoclasts that

degrade regions of existing structure, and osteoblasts that actively build new sections of bone (Seal and Otero, 2001).

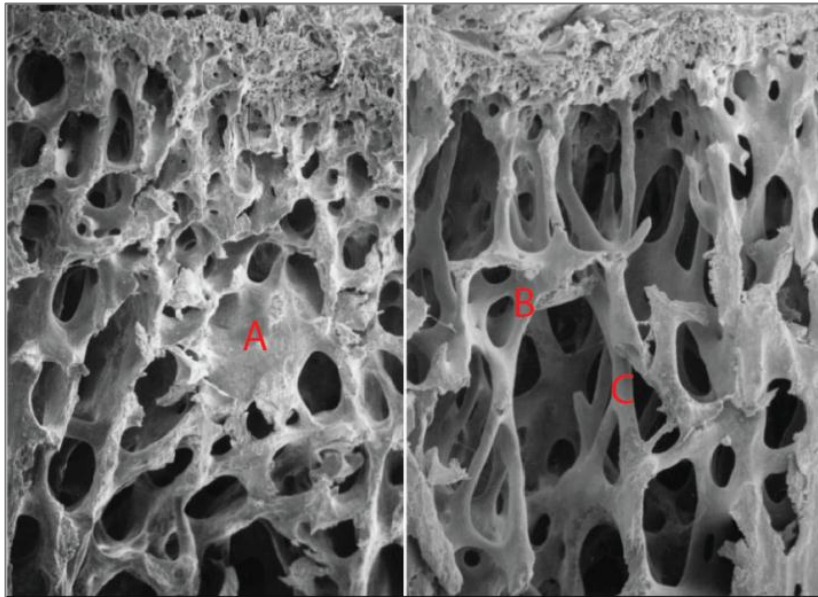


Figure 2-6 - SEM image of a rat tibia showing the cancellous bone. The trabecular structure is visible, with the trabecular arrangements. (A) Plate-plate structure, (B) Rod-plate structure, (C) Rod-rod structure. Images from Abe et al. (1999), (Reproduced with permission from Elsevier).

#### 2.1.2.1 Vascular Anatomy of the Femoral Head

The epiphyseal (or ascending) artery, a terminal branch of the medial circumflex artery, supplies most of the blood to the upper half of the femoral head. The lower area of the femoral head is vascularised by the lateral circumflex artery and its terminal branches. It is these arteries that are prone to interruption of flow due to increased intracapsular pressure from infection or trauma. The foveal artery adjacent to the ligamentum teres also supplies 10-20% of in the blood supply to the bone (Figure 2-7) (Gautier et al., 2000; Bachiller et al., 2002; Evans and Zawadsky, 2010).

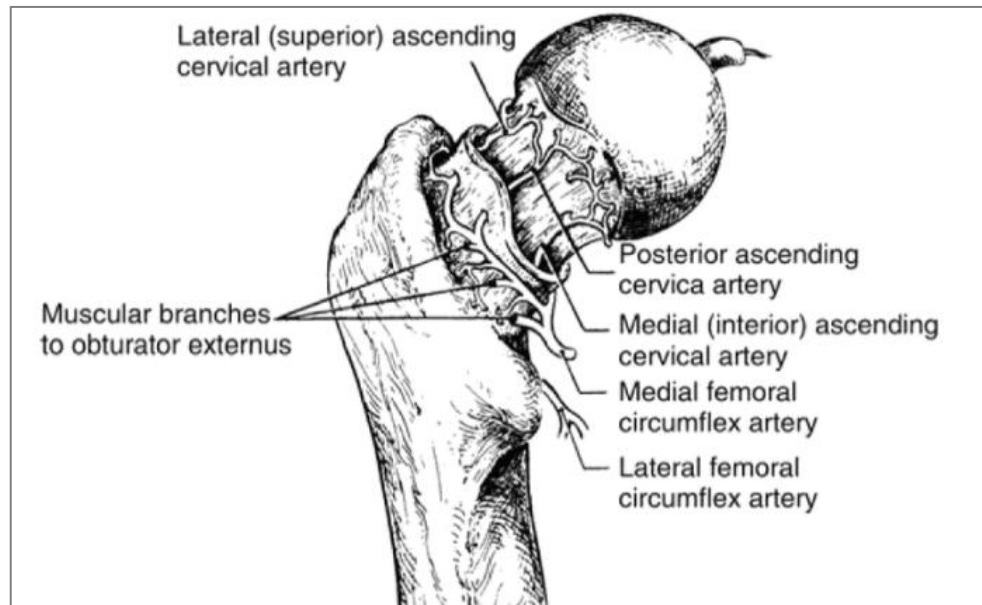


Figure 2-7 - Vascular anatomy of the femoral head and neck. Image from Wiesel and Delahay, (2010). (Reproduced with limited permission from Springer)

### 2.1.3 Mechanical Testing Methods

In order to develop a mechanical model of AVN, the mechanical properties of bone first need to be understood. Various techniques can be used to establish the mechanical properties of bone from human or animal tissue. In order to choose the most suitable testing technique, a review of the testing methods was made, a brief summary of which is reported here.

#### 2.1.3.1 Compressive Testing

Compressive tests (Figure 2-8) are the most common testing method for bone as it represents the physiological loads applied to the majority of the skeletal system. Compressive tests are carried out using uniaxial mechanical testing machines, under an axial load, or displacement/strain control. (Keaveny et al., 1994, 1997; Winwood et al., 2006; Wang et al., 2010)

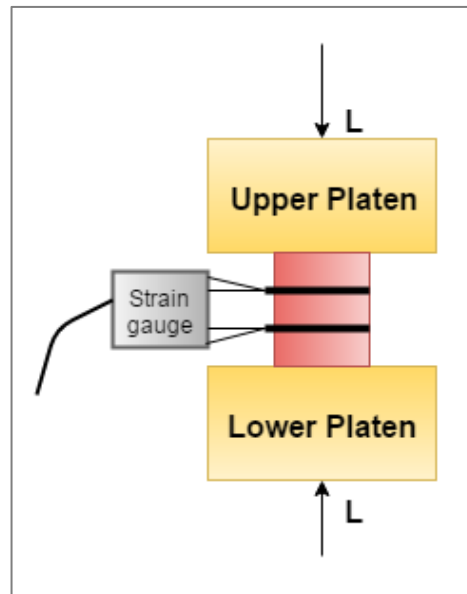


Figure 2-8 - Typical setup of a compressive test, where an upper and lower platen are used to load the sample. In some setups, the lower platen is stationary and the upper platen moves to subject the sample to load ( $L$ ). In some cases an in-built extensometer measures the distance moved by the platens. A strain gauge may also be used to measure the change in height in the gauge area.

The value of the load ( $L$ ) and change in length ( $\delta h$ ) are then used to calculate the tensile and compressive stresses ( $\sigma$ ) and strains ( $\epsilon$ ) of the bone using Equation 2-1, Equation 2-2.

$$\sigma = \frac{L}{A} \quad \text{Equation 2-1}$$

$$\epsilon = \frac{\delta h}{h_0} \quad \text{Equation 2-2}$$

A – Gauge area    P - Load Applied     $\delta h$  – Change in length     $h_0$  – Gauge length

The stress and strain values can be used to plot a graph (Figure 2-9) of the mechanical properties of the bone, and the slope of the initial linear elastic region (Equation 2-3) of the stress-strain curve can be used to calculate elastic modulus ( $E$ ). From the graph, other properties such as elastic yield strength ( $\sigma_y$ ), ultimate strength ( $\sigma_{us}$ ), offset yield strength and strain at failure ( $\epsilon_f$ ) can be obtained (Evans, 1973).

$$E = \frac{\Delta\sigma}{\Delta\epsilon}$$

Equation 2-3

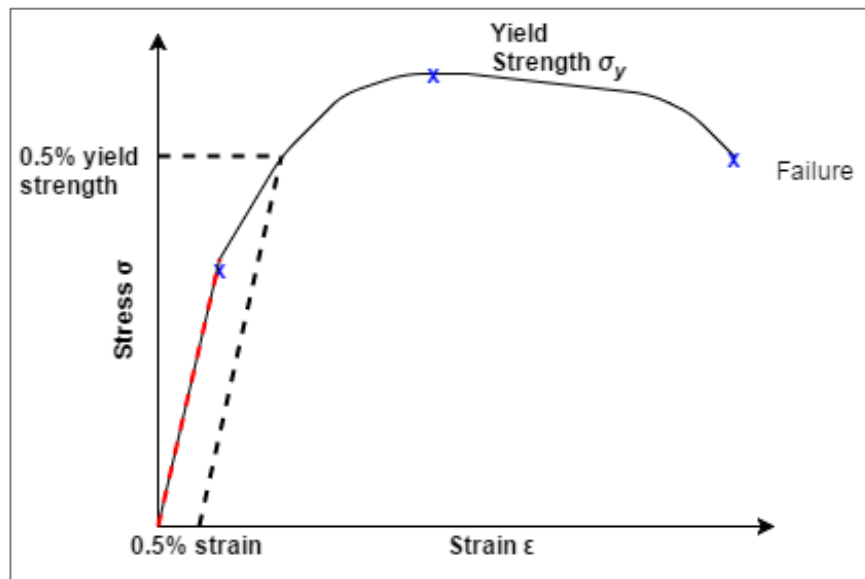


Figure 2-9 - A typical stress-strain curve showing the failure point as well as yield strength and 0.5% yield strength. The red line represents the elastic region, from which the elastic modulus (Young's modulus) can be calculated.

### 2.1.3.2 Progressive Loading

Two methods of mechanical testing on bone that have been used increasingly in the past decade are progressive loading and cyclic loading of the bone, and these are explained in this section.

During progressive loading, a series of cycles of “load-dwell-unload-dwell-reload” with incremental strains are used. This allows for measurement of elastic, plastic and viscous responses of bone and estimates several forms of energy dissipation related to permanent deformation of the bone due to hysteresis and accumulation of damage at the microscopic level (Wang and Nyman, 2007; Nyman et al., 2009).

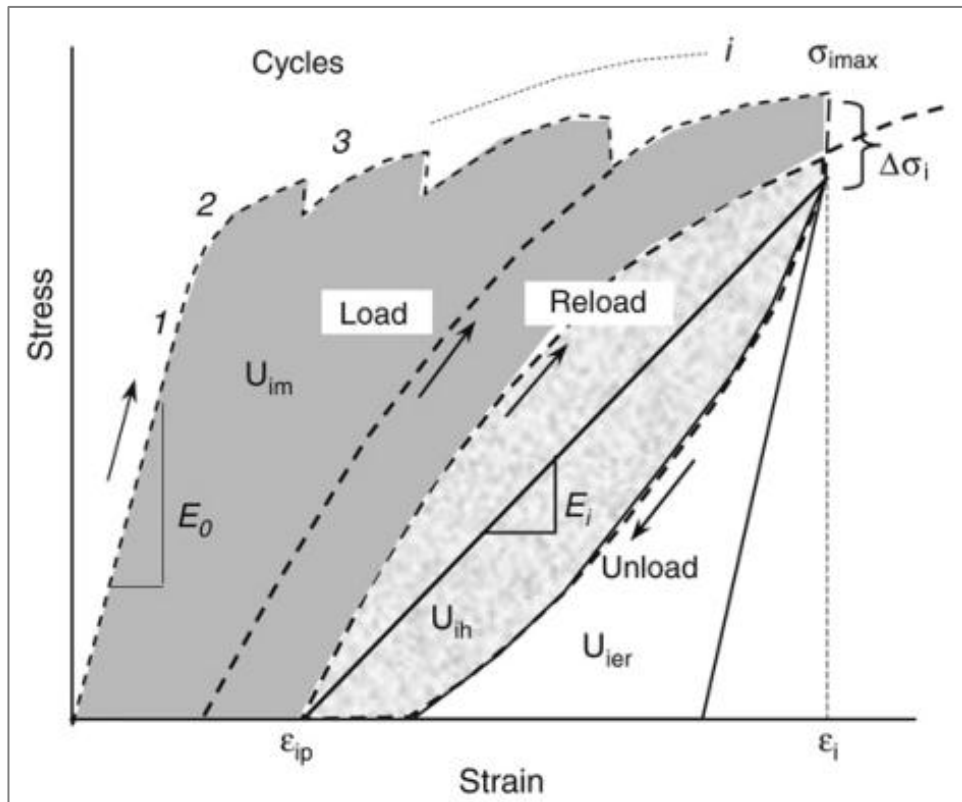


Figure 2-10 - An example of the progressive loading method used by Nyman et al, where the cortical bone specimens were subjected to cycles of “loading-dwell-unloading-dwell-reloading”. (i – loading instant;  $U_{im}$  – Irreversible energy dissipation;  $U_{ih}$  – hysteresis energy;  $U_{ier}$  – released elastic strain energy;  $E_0$  – initial modulus;  $E_i$  – instantaneous modulus;  $\sigma_{imax}$  – maximum stress  $\sigma_i$  – instantaneous stress;  $\epsilon_i$  – instantaneous strain;  $\epsilon_{ip}$  – plastic strain) Figure from Nyman et al., (2009) (Reproduced with permission from Elsevier).

### 2.1.3.3 Fatigue Testing

Fatigue testing usually involves cyclic loading of samples with one or a combination of the tensile, compressive, bending and torsional forces. Fatigue testing is usually performed under controlled conditions and, depending on the requirements of the study, can be performed on the whole bone or small sections of bone. Fatigue testing represents the anatomical conditions in the body better than all other tests, especially on the lower limbs since most loads are applied in cycles (e.g. loads in the joint during hours of walking) (Evans, 1973; Keaveny et al., 2009; Wang et al., 2010).

The results of fatigue test are usually presented on a stress-life (S-N) diagram (Figure 2-11), which shows the applied stress amplitude as a function of fatigue life.



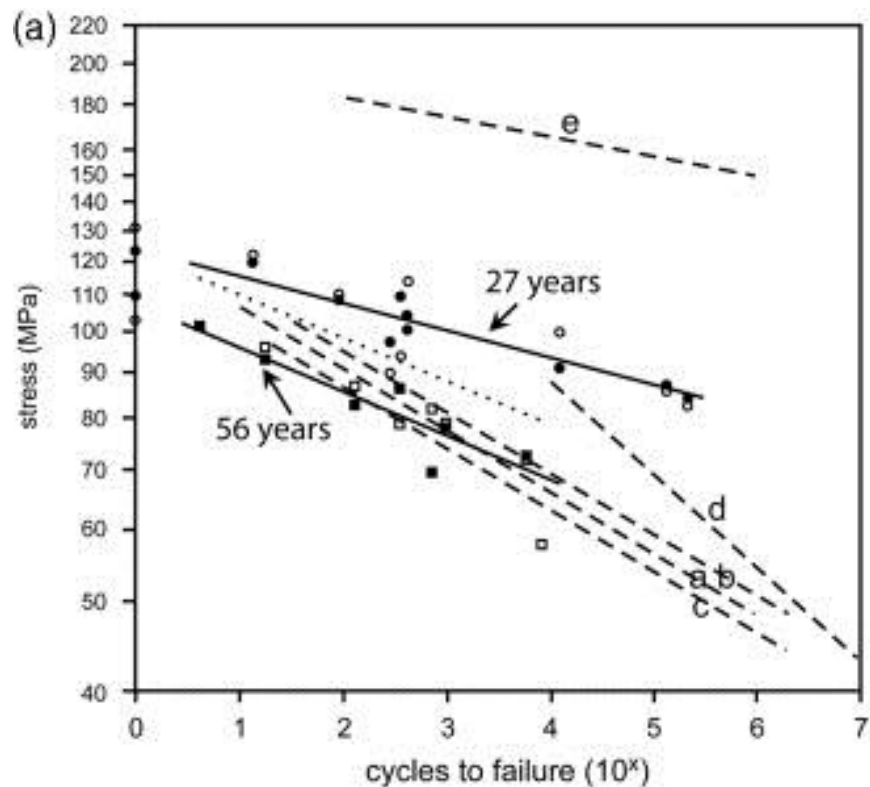


Figure 2-11 - S-N curve for the fatigue loading of human bone from a 27 year old (circles) and a 56 year old (squares) to demonstrate the typical method of calculating the fatigue properties of mineralised tissue. In this study, the data was normalised (closed circles and squares) to account for modulus variations between samples within each groups and the solid lines are the regression fits to the solid symbols. (Dashed lines show data from other studies; (a) human cortical bone fatigue data from Carter and Caler (1983); (b) Bovine cortical bone fatigue data adjusted for temperature (Carter and Hayes, 1976a); (c) Data from (b) adjusted for stiffness; (d) Fatigue data of human cortical samples as rotating cantilevers (Swanson et al., 1971) and (e) four-point bending fatigue data from human cortical bone (Choi and Goldstein, 1992) . Image from (Zioupos et al., 1996), (Image reproduced with permission from Elsevier).

## 2.2 Mechanical Testing of Bone

Mechanical testing of bone has advanced significantly since the 1970s (Currey, 1970, 2009), however there is no golden standard in mechanical testing of bone as it is a complex and anisotropic material for which the mechanical properties change in different conditions, such as age, region of bone, and other factors that will be discussed further in this report. This section contains a summary of the data available and a discussion on the variation in properties presented in the literature. The discussion is divided into two sections based on scale, whilst focusing on properties of the femoral region.

### 2.2.1 Mechanical Properties of the Whole Bone Samples

Studies on the mechanical properties of the whole bone have been performed on various locations of the skeletal system, such as the vertebrae and femur. These tests are usually performed by application of the loads that the bone would experience *in vivo*, such as torsion and bending tests combined with tensile and compressive loading.

Although clinically relevant, only a few studies have been published where the authors have tested for the mechanical properties of the whole bone. These studies usually subject samples to three-point or four-point bending. Three-point bending tests were performed by Strømsøe et al. (1995) on human femurs to analyse the relationship between bone mineral content and strength of the femur (Figure 2-12- Right). Alongside the bending test, they used quantitative computed tomography (QCT) and dual energy X-ray absorptiometry (DEXA) to measure the geometries and bone mineral properties. They found that there was a high correlation between bone mineral properties and bone mechanical strength. Although these studies provide a basic understanding of the impact of varying bone properties on the risk of bone fracture *in vitro*, they do not provide enough information about the mechanical properties of the femur *in vivo* due to the complexity of the bone structure. Another problem is that three-point loading test creates high shear stresses near the midsection of the bone, limiting the clinical relevance of this loading regime. Four-point loading tests produce pure bending between the two upper loading points (Figure 2-12 - Left). Although this reduces the transverse shear stress to zero, it still differs significantly from the typical anatomical loading of bone (Turner and Burr, 1993).

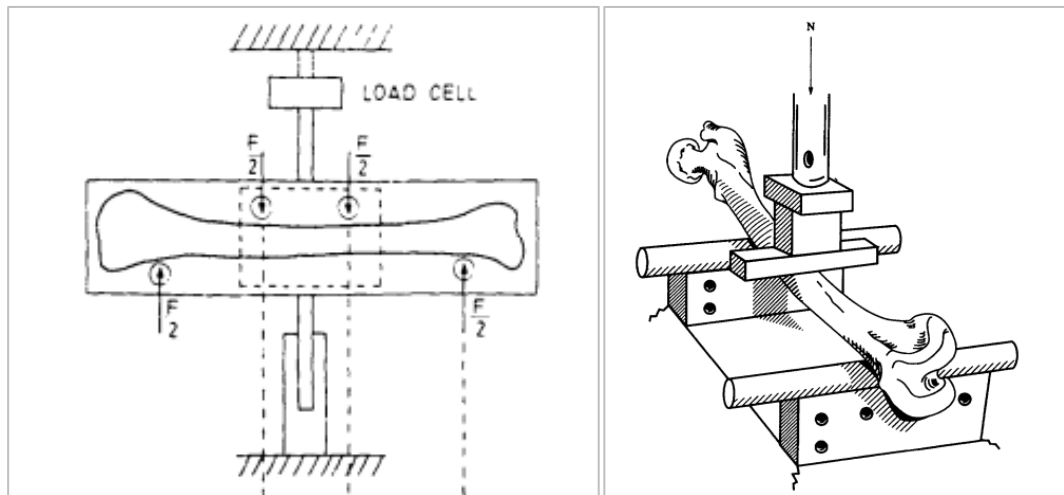


Figure 2-12 - Bending testing of bone. Left - Four point bending testing as performed by Martens et al., (1986). Right - Three point bending test as performed by Strømsøe et al., (1995). (Images reproduced with permission from Elsevier.)

Cristofolini et al. (1996) carried out a series of compression tests on human femurs and synthetic composite models of the femur in order to experimentally validate their computational model's mechanical properties with respect to human cadaveric bone. They tested for deflection and stress distribution under axial load at 11° adduction (Figure 2-13) with loads of up to 0.8kN, repeating the test 10 times for each sample. This test provided more anatomically representative torsional and bending properties of bone.

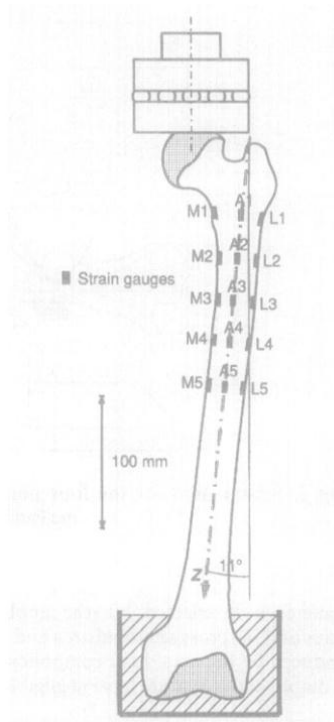


Figure 2-13 - Axial testing of femur at 11° adduction, as demonstrated by Cristofolini et al. (1996). (Image reproduced with permission from Elsevier.)

Some studies have looked at measuring the mechanical properties of bone at the femoral head and neck region, rather than the whole femur. A study by Dalén et al. (1976) measured the mechanical properties of the bone from the femoral head as well as bone mineral density at the femoral neck to understand the relationship of bone mineral content and fracture risk in that region. They measured the mechanical properties by mounting the femoral shaft in a mould, exposing the neck and femoral head and applying load to the femoral head perpendicular to the axis of the femur and recorded the force/displacement values from this test. They found a positive correlation between the bone mineral density and the ultimate compressive stress of the bone, concluding that bone mineral density can be used as a diagnostic tool to measure the risk of fracture in the femoral neck. This study demonstrated a method of testing large bone sections using a simple and reproducible compressive test.

Although mechanical testing of whole bones is more clinically relevant than micro and nano-mechanical testing, there are various factors that need to be controlled to ensure the testing is representative of the true mechanical properties of the bone and that the data is comparable to other groups. First, the output from mechanical testing of the whole bone is dependent on inputs dimensional parameters of the bone tested, such as overall size as well internal dimensions; e.g. the ratio of cortical to cancellous bone. Secondly, it is dependent on the mechanical testing parameters such as loading direction. The load applied may apply variable stresses into the bone depending on the surface area that the load is applied (An and Draughn, 2000).

### **2.2.2 Micro and Nano-Mechanical Properties**

Advances in technology allow for mechanical testing to be performed in the micro-scale on structures such as single osteons and single trabeculae (Rho et al., 1999a, 1999b, 2001; Fan et al., 2002; Kwok-Sui, 2008). In addition several studies report methods for nano-indentation testing of bone. Nano-indentation is a technique whereby a sharp indenter tip places a load on the specimen and the loads and surface deformations are continuously recorded to produce a curve of force versus displacement (Kwok-Sui, 2008; Wang et al., 2010). This can be advantageous since it provides understanding of the mechanical

properties of diseased bones at precisely discrete locations in the bone (Zysset et al., 1999; Rho et al., 2000; Morgan and Keaveny, 2001; Hengsberger et al., 2002; Kwok-Sui, 2008).

Micro-scale testing of bone using different methods (e.g. tensile, bending and torsion) have been attempted, and the one method performed more than others is the micro-tensile testing, which was originally published by Ascenzi and Bonucci (1967). Micro-tensile testing assesses the pre-yield-to-post-yield and failure behaviours of bone, and allows calculation of Young's modulus, yield strain and strength, and ultimate tensile strength of single structures of the bone (Ascenzi and Bonucci, 1967; Kwok-Sui, 2008; Currey, 2009). This type of test can be performed on osteonal and interstitial bone, as well as the rod-like single trabeculae.

### **2.2.3 Mechanical Testing of Subchondral Bone**

The properties of subchondral bone are reported to change during the progression of AVN in femoral head (Bullough and DiCarlo, 1990; Imhof et al., 2000). Very few studies have attempted to study the mechanical properties of the subchondral bone and these are reported in this section.

Li and Aspden (1997) studied the material properties of the subchondral bone plates obtained from patients with osteoarthritis or osteoporosis. They removed cylindrical cores of 9mm diameter from healthy, osteoporotic and osteoarthritic femoral heads and extracted 1mm thick discs of subchondral bone from the cylinders, to which they applied indentation loads to the specimens to measure the hardness of the bone. They showed that subchondral bone plate stiffness reduces significantly with diseases such as osteoporosis and osteoarthritis.

Day et al. (2001) studied the material properties of the subchondral bone by removing cores of the tibia and compressing them. They calculated the modulus of the tissue by using a combination of finite element modelling and mechanical testing that allowed for the effect of trabecular architecture to be derived from the results. They reported 60% reduction in bone tissue modulus

in the medial condyle of samples with damaged cartilage in early osteoarthritis when compared to non-pathological tissue.

## 2.2.4 Factors Affecting the Mechanical Properties of Bone

### 2.2.4.1 Testing Method

The method of mechanical testing of the bone can have a significant effect on the results obtained. Bone can be tested in tension, compression, torsion, and bending in order to obtain results of strength and elastic or shear modulus. A review by An and Draughn (2000) showed that tensile strength of cortical bone is about 2/3 of its compression strength. This means that the testing method can make a significant difference to the results obtained, hence it needs to be chosen carefully in order to analyse the most anatomically correct situation.

Bending mechanical properties of whole bone are dependent on geometry of the whole bone and the bone mineral content (Martens et al., 1986; Strømsøe et al., 1995). The bending mechanical properties of cortical bone are also affected by the bone mineral content, however they are also governed by the osteonal directions (Sedlin and Hirsch, 1966; An and Draughn, 2000). The strength and elastic modulus of the cortical bone by bending may be affected by other factors, such as equations used in calculations, dimensions and geometric shapes of the specimens, porosity, and collagen fibre orientation (Sedlin and Hirsch, 1966; Keller et al., 1990; Martin and Boardman, 1993).

### 2.2.4.2 Strain Rate

The rate at which bone is mechanically loaded is a factor that influences the calculated mechanical properties of bone. Wallace et al., (2013) measured the mechanical properties of normal and demineralised ovine femurs using 3-point bending at high ( $17.14 \text{ s}^{-1}$ ) and low ( $8.56 \times 10^{-3} \text{ s}^{-1}$ ) strain rates. They reported a mean 36% increase in peak stress and a 46% decrease in toughness of bone when comparing samples tested with high strain rate to low strain rate.

An earlier study by Carter and Hayes (1976) demonstrated the influence of strain rate on the ultimate strength of compact and trabecular bone without bone marrow (Figure 2-14). They suggested that in their data, the compressive strength of bone tissue was approximately proportional to the strain rate raised to the 0.06 power.

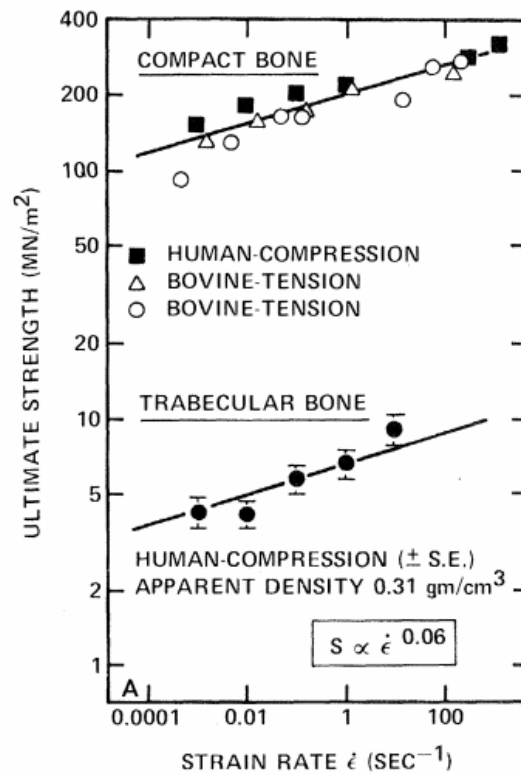


Figure 2-14 – influence of strain rate on the ultimate strength of compact and trabecular bone tested without marrow *in situ* by Carter and Hayes, (1976). The ultimate strength is proportional to strain rate applied. (Image reproduced with permission from The American Association for the Advancement of Science.)

### 2.2.4.3 Density

The strength and stiffness of cortical and cancellous bones positively correlate with the bone mineral density and bone mineral content. Many authors have tested this theory on various bone specimen types. Currey studied the effects of porosity and mineral content of bone in various mechanical tests (Currey, 1969a, 1969b, 1970, 1988a), including bending and tensile elastic modulus of cortical bone from vertebral specimens. He found that these two factors accounted for 84% of the variation in stiffness (Currey, 1988a).

Various attempts have been made to define the relationship between density and mechanical properties (Carter and Hayes, 1977; Martens et al.,

1983; Keaveny et al., 1997). The relationship between compressive strength and apparent density of vertebral cancellous bone as measured by Galante et al., (1970) can be seen in Figure 2-15.

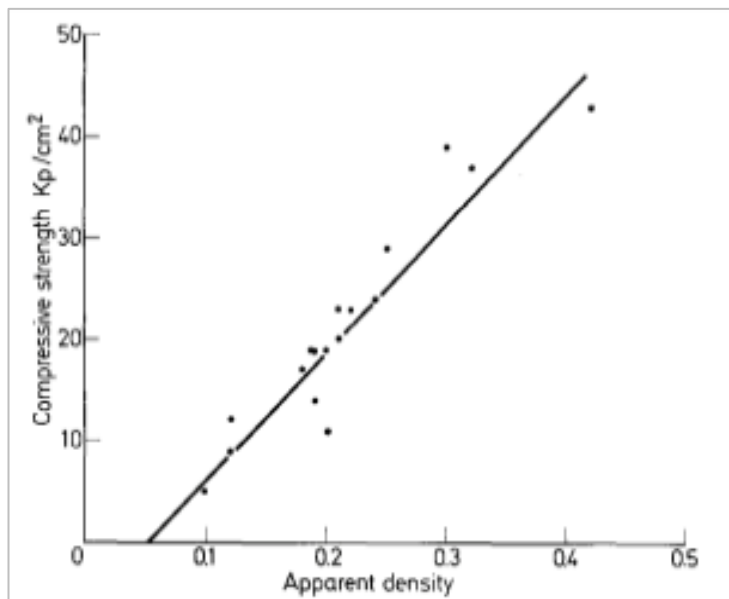


Figure 2-15 - Compressive strength of vertebral cancellous bone samples as a function of apparent density as found by Galante et al., (1970). (Image reproduced with permission from Springer.)

More recently, advances in technology and measurement techniques have allowed several studies to investigate the effects of bone mineral content and density on mechanical properties of bone on a much smaller scale (Rho et al., 1995; Vanleene et al., 2008; Wagner et al., 2011; McCormack et al., 2012). Cory et al., (2010) used micro-CT scanning to obtain the bone mineral densities of cortical and trabecular bone specimens of rat bones. They compared these findings to mechanical properties obtained by nano-indentation and uniaxial compression to failure. They found that 71-78% of the mechanical properties of cortical and cancellous bone of rats were based on equivalent mineral density over a range of common skeletal pathologies that were simulated on the rats, in vitro.

#### 2.2.4.4 Microstructure

Porosity is an important factor in determining the mechanical properties of the bone. Porosity is defined as the ratio of void volume to total volume of the bone (Lazenby, 1986), and increases with increasing age (Brockstedt et al.,



1993; Seeman, 2008)(Figure 2-16). It is obvious that the elastic modulus of the cortical bone is directly correlated with the porosity, and several authors have defined this relationship (McElhaney et al., 1970; Currey, 1988b; Schaffler and Burr, 1988). These studies found that the elastic modulus correlates with volume fraction of bone by a power law rather than by a linear relationship.

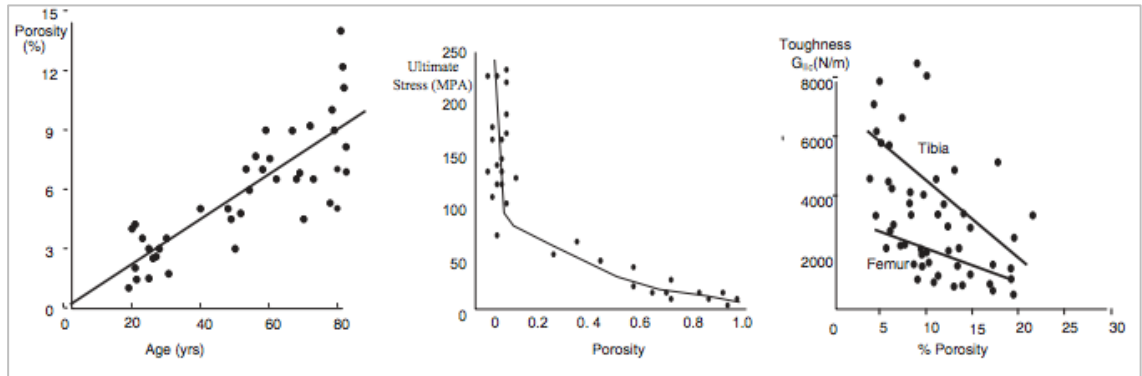


Figure 2-16 - Left - Graph showing the increase in porosity of cortical bone with increasing age. This results in reduction of ultimate stress (middle) and toughness (Right) of the cortical bone. (Seeman, 2008). (Image reproduced with permission from Springer.)

In cancellous bone, several parameters are used to define the bone structure and architecture in relation to mechanical properties (Parfitt et al., 1987). Goldstein et al. (1993) measured the trabecular plate thickness, trabecular plate separation and trabecular plate number using  $\mu$ CT imaging. They also analysed bone volume fraction, anisotropy and connectivity in isolated specimens of cancellous bone. They found that 80% of the variance in their mechanical properties could be explained by density and orientation changes in the trabecular structure.

In a finite element study that explored the relationship between the connectivity density and elastic modulus of cancellous bone, Kinney and Ladd (1998) showed that there was no functional relationship between these two factors, as connectivity is independent of the contact area, hence not affecting the load transfer on an area. However, they found that after a full cycle of atrophy, the specimens did not recover connectivity or the full elastic modulus for the equivalent trabecular bone volume, hence suggesting a relationship between the loss of connectivity and elastic modulus. These results indicate that the recovery of the mechanical function following testing depends on preservation or restoration of trabecular connectivity in cancellous bone.

#### 2.2.4.5 Anisotropy

Bone is a structurally and mechanically anisotropic material, which means it shows different mechanical properties depending on the direction in which it is loaded. This is because the collagen fibres are oriented longitudinally to the long axis of the bone. Martin and Ishida (1989) studied the effects of collagen fibre orientation along with density, porosity and mineralisation on tensile strength of bovine cortical bone samples. They found that collagen fibre orientation was a significant factor in determining the strength of cortical bone. For example, the femur is stronger under vertical compressive load, however if the same load is applied in the transverse direction it can cause fractures (Viguet-Carrin et al., 2006).

Studying the skeleton and physiological loading has led to an understanding that bone is strongest in the direction of physiological loading (Heřt et al., 1994). Martin et al., (1998) reported that in the regions which support tensile loads, the collagen fibres are oriented longitudinally, and transversely in regions supporting compressive loading. This means that in testing bone, the direction in which it is loaded must be taken in to account as it may change the results significantly.

#### 2.2.4.6 Heterogeneity

Bone is highly heterogeneous as it has many interfaces between its structures. This property of bone may have both positive and negative effects on its biomechanical properties. According to Yao et al. increased heterogeneity can “promote energy dissipation while simultaneously introducing stress concentration and strain localisation” (Yao et al., 2011). It can stop cracks from propagating due to the many “flaws” in the structure (Currey, 2005).

Cortical bone is mechanically heterogeneous, since in the middle third of the femoral shaft, the bone has higher ultimate strength and elastic modulus than the upper or lower thirds of the shaft. In addition, the lateral quadrant of the shaft has a higher ultimate tensile strength than the anterior quadrant (Evans and Lebow, 1951).

Cancellous bone is similarly heterogeneous (Figure 2-17). The cancellous bone in the lower limbs is stronger and stiffer than those of upper limbs (Goldstein, 1987). It is also heterogeneous at a given site in the body. For example, in long bones, more trabecular bone material is located at the subchondral bone plate, and becomes less concentrated towards the diaphysis. This means that the mechanical strength decreases from the subchondral bone plate toward the medullary canal (An and Draughn, 2000; Boutroy et al., 2005).

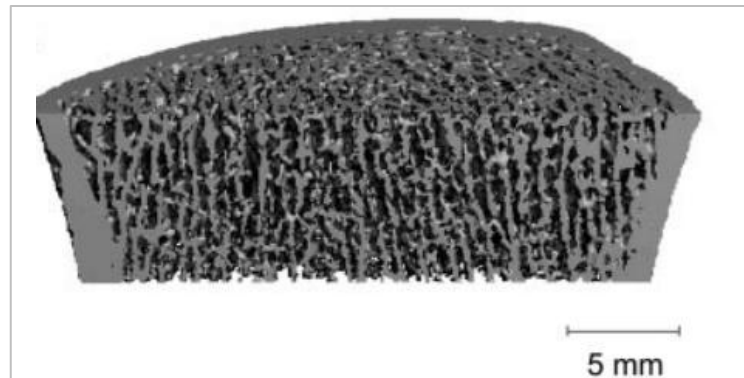


Figure 2-17 - The heterogeneous trabecular structure of the tibia (Boutroy et al., 2005). (Image reproduced with permission from Endocrine Society. )

This theory was studied by several authors (Brown and Ferguson, 1980; Augat et al., 1998). Brown and Ferguson (1980) found that in the regions where trabeculation was high, the stiffness was elevated.

In a study by Martens et al. (1983) it was found that the trabecular bone in the intertrochanteric region was stronger and stiffer than the trabecular bone at the femoral neck in horizontal loading, however it was significantly weaker in vertical loading. They believed that this was due to the unequal and anisotropic behaviour of trabeculae in various regions, based on their anatomic load-bearing behaviour as well as the arrangement of lamella (see Figure 2-18).

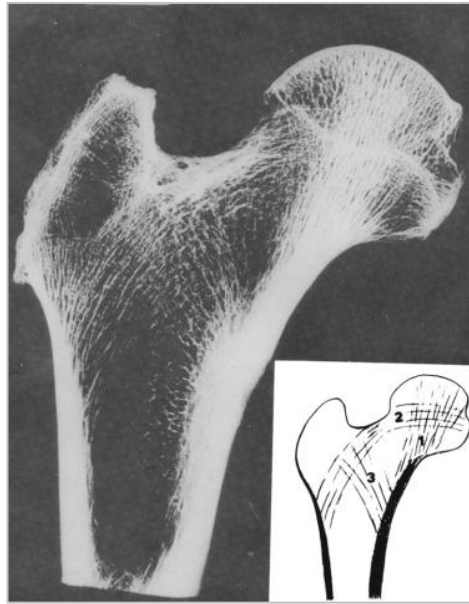


Figure 2-18 - Arrangement of cancellous bone in the proximal femur can be divided into three directions (Martens et al., 1983). (Image reproduced with permission from Elsevier.)

#### 2.2.4.7 Demographic and Environmental Factors

When testing the mechanical properties of bone, factors about the individual must be taken into account. For example, age, gender and lifestyle of the donor can significantly change the mechanical properties of the bone. *In vitro* factors that can change the mechanical properties of bone exist, and these can be embalming of tissue, as well as storage methods. Other factors also need to be considered when testing the bone, and these include the temperature and humidity of the laboratory during testing, as well as keeping the bone sample moist to prevent changes in the mechanical properties of bone. These factors are discussed in this section.

##### Age

Increasing age can increase the porosity of the bone, as well as increasing the risk of osteoporosis. This significantly reduces the quality of the bone (Burstein et al., 1976; Martin et al., 1998; Seeman, 2008), and needs to be taken into account when testing bone for mechanical properties.

A study by McCalden et al. (1993) which studied the changes in tensile strength of cortical bone with age, with regards to porosity, mineralisation and microstructure showed that the ultimate stress of the specimens decreased

significantly with increasing age, making the older population more prone to bone fracture (Figure 2-19). They also showed that the tensile modulus of the cortical bone did not change significantly with age. This result disagrees with the results of Currey (1988b), who demonstrated that Young's modulus has a roughly cubic relationship with porosity. Currey performed his tests on various animals, whereas McCalden et al.'s tests were performed on cadaveric human specimens of various ages. This suggests that the McCalden results were more based on effects of ageing rather than the inter-species differences found in the results of Currey.

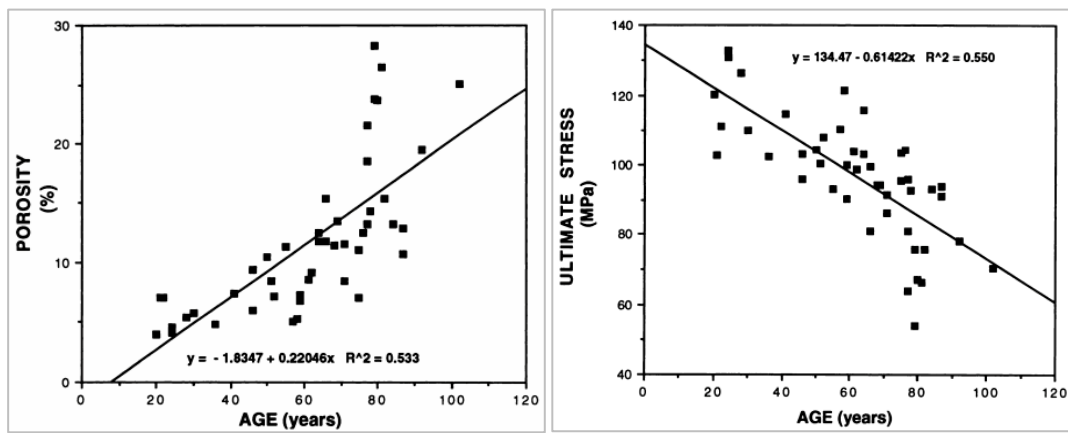


Figure 2-19 - Left – effects of age on porosity of cortical bone, Right - Effects of ageing on ultimate stress of the cortical bone, demonstrating the inverse relationship between porosity and ultimate stress. Figures from McCalden et al. (McCalden et al., 1993). (Image reproduced with permission from Wolter Kluwer.)

## Gender

Although it is known that gender does not have a direct effect on mechanical properties of bone, it may however affect the properties due to changes in mass, lifestyle and hormone changes (Lindahl and Lindgren, 1967). After menopause, female bones show accelerated resorption rates causing the porosity to increase, hence reducing the quality of bone (Boutroy et al., 2005).

## Species

This review has mainly focused on human bone, however use of animal tissue is common in testing of mechanical properties of bone. The properties of bone between species can change significantly. For example, porcine femur is weaker in tension and compression than human bone (Fung, 1993; An, 2000).

This means that care must be taken when transferring and comparing test results between species.

### Embalming or Fixation

Formalin fixation of biological tissue conserves the tissue as it has antimicrobial effects, therefore allowing for long duration tests. When a tissue is formalin-embalmed to preserve the tissue, the collagens are cross-linked, which can alter the mechanical properties of the bone. The change is dependent on the formalin concentration used and the duration of the preservation of the sample (Ohman et al., 2008).

### Storage Method

Sometimes the method by which a bone sample is stored may alter its mechanical properties. Linde and Sorensen (1993) studied the effects of freezing and thawing as well as storage by freezing and in ethanol on compressive properties of cancellous bone. They found that freezing and thawing up to five times did not alter the stiffness of the bone, however the viscoelastic properties showed small, but significant changes after 100 days of storage by both freezing and in ethanol. This change was observed by changes in hysteresis energy of the bone.

A study by Pelker et al. (1984) assessed the short term effects of freezing and freeze drying on torsion strength of long bones and compressive strength of vertebral bodies of rats. They found that freezing of bone samples to  $-20^{\circ}\text{C}$ ,  $-70^{\circ}\text{C}$ , and  $-196^{\circ}\text{C}$  for 2 weeks did not have significant effects on the strength of those bones, however freeze drying samples did result in a significant reduction in torsional strength of the long bones. Panjabi et al., (1985), conducted a series of mechanical tests on cadaveric spinal specimens that were tested in three groups: A- fresh on first day and 13 subsequent days, B- fresh on first day, frozen for 21 days, then tested for 13 consecutive days, and C- frozen for 5-7 months, then tested for 14 consecutive days. They did not find any significant differences between the mechanical properties of the three tests groups, implying that freezing and storage for up to 7 months do not significantly alter the mechanical properties of the bone.

It can be seen from the literature that freezing is the best method of storage of bone samples, as it does not significantly alter their mechanical properties.

### 2.2.5 Methods of Altering the Mechanical Properties of Bone

A search in the literature was performed to look at the methods that can be used to alter the mechanical properties of bone in order to replicate the mechanical properties found in avascular necrotic femoral heads. Many studies have been performed to understand the effects of various *in vitro* techniques on the mechanical properties of bone, with the main purpose of these studies being prevention of any alteration in mechanical properties of bone tested *in vitro*. However, since one of the objectives of the current study is to alter the mechanical properties of bone in order to create a mechanical model of AVN, the literature was reviewed using a reverse approach.

#### 2.2.5.1 Embalming

It is known that various preservation methods can alter the mechanical properties of bone, and many studies have researched the effects these techniques have on the mechanical properties of bone tested *in vitro*.

A study by McElhaney et al. (1964) on effects of embalming on bovine bone found that a significant reduction of 12% was seen in ultimate compressive strength of the bone following embalming. They also reported only very slight reduction in ultimate tensile strength, maximum strain and modulus of elasticity, as well as no significant change in hardness. Ohman et al., (2008) tested the short and long term effects of embalming on mechanical properties of human cortical bone. They found that after 8 weeks in embalming solution, the specimens had significantly lower Young's modulus (24%) and higher yield strains (20%) and ultimate strains (53%) than the control groups. No significant differences were reported in yield stress, ultimate stress and hardness. Their results agreed with results of McElhaney et al. (1964), with a difference in the compressive strength results obtained. This difference may be explained by the difference in the species tested (bovine versus human), as well as the different specimen geometries. Both studies however confirm that the

mechanical properties of the bone may change significantly following embalming.

A study by Currey et al. (1995) studied the effects of formaldehyde fixation on mechanical properties of bone. They found that the results in bending and tension loading were almost unaffected by fixation of specimens in formaldehyde, however the impact strength was decreased significantly after fixation of the specimens.

#### 2.2.5.2 Heat

Heating bone tissue can degrade the tissue extensively and alter the mechanical properties of bone. Studies have been performed where effects of boiling and autoclaving on mechanical properties of bone have been studied. A study by Borchers et al. (1995) found that both boiling and autoclaving can reduce the compressive strength of trabecular bone by 26% and 58% respectively. They also found that compressive modulus of trabecular bone whilst unaffected by boiling can be reduced by 58% following autoclaving at 127°C for 10 minutes.

Another study by Dekhtyar et al. (1995) measured the ultrasound velocity (USV) of bone, which has been known to be affected mainly by elasticity modulus (E) and bulk density ( $\rho$ ) of the material ( $USV = \left(\frac{E}{\rho}\right)^{0.5}$ ). They found that after +55°C heating of bone, there is a significant reduction in USV, meaning the young's modulus of the bone is decreasing.

A study by Wang et al. (1999) studied the effects of collagen denaturation by heating on mechanical properties of human cadaveric femurs. They heated cartilage to temperatures lower, at and beyond the denaturing temperature of collagen, and found that heating the bone specimens to +160°C denatures cartilage significantly and also changes the ultimate strength and work to fracture of the bone. They reported no significant changes in the elastic modulus of bone even when heated up to 180°C. They concluded that the toughness and strength of bone relates significantly to the integrity of collagen structure, and the stiffness of the bone is affected by the mineral phase of the bone rather than the collagen content.



The findings above have been confirmed by further studies: Viceconti et al. (1996) reported 70% decrease in compression strength of bone grafts following autoclaving at 132°C for 1 hour; Köhler et al. (1986) reported upto 20% decrease in strength and 24% decrease in stiffness after autoclaving at 121°C for 20 minutes.

#### 2.2.5.3 Storage Methods

As mentioned previously on page 28, the method by which bone is stored may alter its mechanical properties. Research has shown that cycles of freezing and thawing as well as freezing for long periods of time does not have any significant effects on the mechanical properties of bone, however freeze-drying the tissue can significantly reduce the bone strength.

#### 2.2.5.4 Sterilisation by Gamma Irradiation

Gamma irradiation is a process used to sterilise bone tissue in vitro or before implantation into a subject. The effects of this process on mechanical properties of bone have been studied, and it has been found that high doses of gamma irradiation can alter the mechanical properties of bone significantly. Knaepler et al., (1991) tested effects of heating and irradiation on mechanical integrity of trabecular bone specimens. They found that gamma irradiation ( $\text{Co}^{60}$ ) with a dose of 10kGy did not affect the compressive modulus, yield point, energy absorption and maximum stress of these specimens; however a dose of 25kGy reduced those properties by 61% to 69%. Various other studies have found similar results to the Knaepler study (Fideler et al., 1995; Salehpour et al., 1995; Currey et al., 1997; Hamer et al., 1999; Russell et al., 2013).

A study by Fink et al. (1998) studied the risk of developing AVN in patients undergoing total body irradiation during therapy, and they found that there appeared to be a higher risk in those patients receiving a total dose greater than 12Gy.

It is known that gamma irradiation causes direct molecular chain scission as well as promoting cross-linking between molecular chains in collagenous materials. The mobility of the molecules present in the material affects the

cross-linking process, and the radiation dose controls the chain scission. Tissues are usually irradiated while suspended in water, or frozen in presence of water. This reduces the mechanical influence of gamma radiation on the tissue, hence to obtain higher changes in mechanical properties of bone, the tissues must be irradiated without the presence of liquids or after freeze-drying (Smith and Kearney, 1996).

### 2.2.5.5 Micro-damage Accumulation

The effects of increased micro-crack accumulation with age have been studied, and it is known that increased micro-cracks impair the mechanical properties of bone by reducing the elastic modulus. Burr et al. (1998) studied these effects by simulating micro-cracks *in vitro*. They tested canine femurs in four-point cyclic bending under load control until they had lost between 5-43% of their original stiffness. They detected the presence of micro-damage by staining the loaded sections of the bone with basic fuchsin. They found that significant micro-damage occurred after the bone had lost 15% of its elastic modulus (Figure 2-20), and a quadratic ratio defined the crack density and stiffness loss relationship.

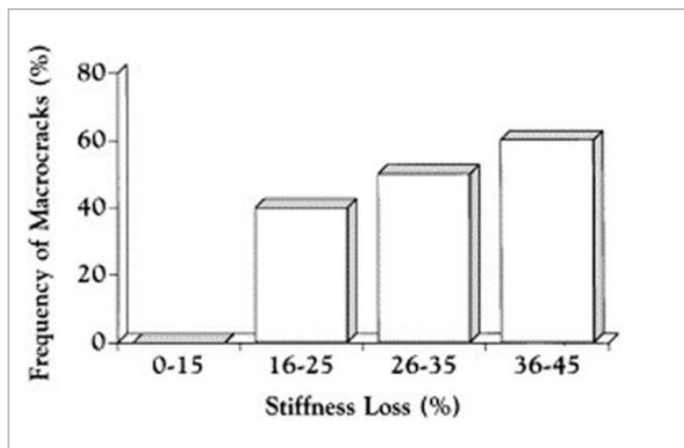


Figure 2-20 – Stiffness loss in each canine specimen group (%) versus frequency of microcracks seen in the tissue (%) in each group following application of four-point cyclic loading. (Burr et al., 1998). (Image reproduced with permission from Elsevier.)

### 2.2.5.6 Drying and Rehydrating

Currey, (1988a) believed that bone that has been allowed to dry had different mechanical properties to fresh bone, and he tested this by drying

bovine cortical bone specimens to constant weight, and then testing them in their re-wetted state. He found that this process had no significant effect on bending Young's modulus of bone; however the bending strength was reduced by 5%.

#### **2.2.5.7 Altering Mineral Content**

The importance of mineral content of bone on its mechanical behaviour has been studied in depth and understood. Mineral content of the bone is directly correlated with the work to failure and Young's modulus (Currey, 1969a, 1969b, 1988b; Dalén et al., 1976). In order to study the effects of mineral content of bone on its mechanical properties, various methods have been used and these are discussed here.

##### **Exposure to Potassium Hydroxide**

Potassium hydroxide treatment can digest the collagen fibres within bone, and this method was used in a study by Wynnyckyj et al., (2009) to understand the changes in mechanical properties of bone following collagen degradation. They found that treatment of bone for 14 days in potassium hydroxide reduced the modulus and strength of the bone while increasing ductility and toughness. They predicted that this is due to the partial de-bonding between the mineral and organic matrix, or in situ collagen degradation. The results are presented in Figure 2-21.

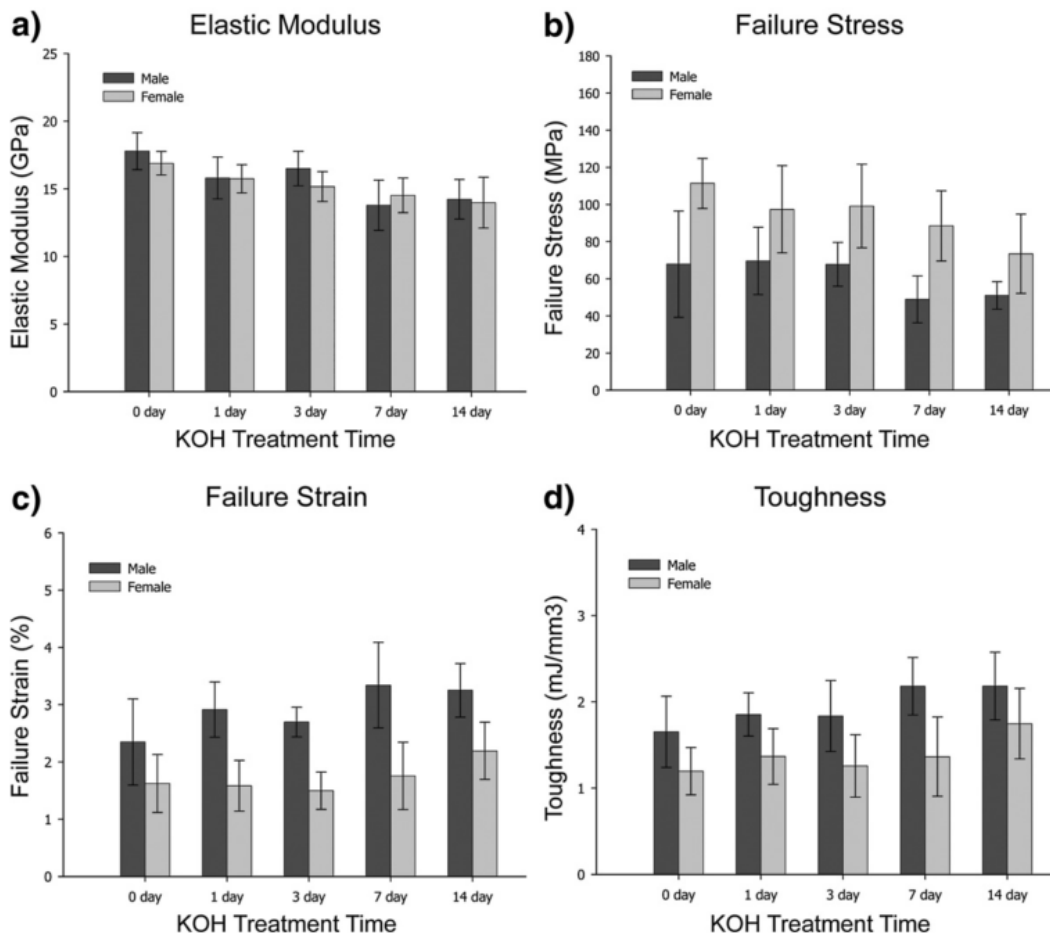


Figure 2-21 – Results by Wynnyckyj et al., studying the mechanical properties of male and female emu tibiae following treatment by potassium hydroxide. A significant decrease in elastic modulus and failure stress, with a significant increase in failure strain was seen following a 14 day treatment in potassium hydroxide. A significant increase in toughness was also seen (Wynnyckyj et al., 2009). (Image reproduced with permission from Elsevier.)

### Fluoride Exposure

Exposing the bone to fluoride can alter the mineral structure by converting hydroxyapatite to fluorapatite, leading to an increase of bone mass without increasing the whole bone failure load (Grynpas, 1993; Lafage et al., 1995; Sogaard et al., 1995; Turner et al., 1997). It is known that soaking bovine cortical bone in sodium fluoride solution for 72 hours can reduce the compressive strength of bone by 40% (Abjornson et al., 1998). Another study (Silva and Ulrich, 2000) found that soaking mouse femora in sodium fluoride solution for 12 hours can reduce the whole bone ultimate load (torque and bending moment) by 45%, reduce rigidity by 70% and increase the deformation to failure (rotation and displacement) by 80%.

Kotha et al., (1998) treated bovine cortical bone specimens in detergent to increase diffusion rates of ions across the sample, and then soaked the bone specimens in calcium fluoride and sodium chloride. They found that while sodium chloride did not affect the mechanical properties of bone tissue in tension, uniform fluoride treatment across the samples reduced the mechanical strength of bone. According to Kotha et al., this behaviour was due to the conversion of small amounts of bone mineral to calcium fluoride, reducing the structurally effective bone mineral content, hence affecting the interface bonding between the mineral and organic matrix of the bone.

### **Exposure to Hydrogen Peroxide**

Li et al., (2011) tested the effects of exposure to 30% hydrogen peroxide for various time periods (up to 72h) on cancellous bone granules from bovine femoral condyles and calculated the mechanical properties by applying compression in a materials testing machine. They found that the mineral content of the bones increased while the strength of the granules decreased substantially after 48 hours of exposure to hydrogen peroxide.

#### **2.2.5.8 Drilling**

Drilling the bone can have structural consequences on the properties of bone. Edgerton et al., (1990) carried out a finite element analysis where circular defects from 10 to 60% of bone diameter were created in paired sheep femora and bones were loaded to failure. They found that small defects (10%) have no significant torsional effect on mechanical properties of bone; however 20% defects caused 34% decrease in strength. These findings were confirmed in a similar study by Hipp et al. (1990).

## **2.3 Incidence of the Avascular Necrosis of the Femoral Head**

Avascular necrosis (AVN) of the femoral head is a destructive disease of the joint that affects mainly younger people when compared to other hip joint diseases such as osteoarthritis or osteoporosis. It is the most common

diagnosis for patients undergoing total hip replacement in Asia (Chiu et al., 1997, 2001; Wong et al., 2005).

A study by Chiu et al. (1997) reported that the 33 Chinese patients who had total hip arthroplasty in their centre were all under 40 years of age and 40% of them were diagnosed with AVN. Another study by Lai et al. (2008) that reviewed the incidence of hip arthroplasty in Taiwanese patients reported that out of the 38,323 patients who received total hip replacement between 1996-2004, 47% were diagnosed with AVN. The mean age of the patients diagnosed with AVN was 50 years, with 73% of the AVN patients under the age of 60 years. They also reported that 79% of the AVN patients were male.

The incidence rates in European countries are rather different to those observed in Asia. The National Joint Registry (NJR Annual report, (Ellams et al., 2011)) for England and Wales reported that only 2% of the patients undergoing total joint replacement were due to AVN. However, this data does not report the percentage of secondary osteoarthritis patients who developed the disease following AVN and collapse of the femoral head. In 2014, NJR for England, Wales and Northern Ireland reported that in patients under 30 years of age undergoing total hip replacement, 22% were diagnosed with AVN (Beaumont et al., 2013). A study performed by Cooper et al. (Cooper et al., 2010) reviewed the databases of General Practice Research Database (GPRD) and The Health Improvement Network (THIN) of the United Kingdom for cases of AVN reported between 1989 and 2003. They found that under the age of 60 years, men were more prone to AVN, however this finding reversed after the age of 60.

The Swedish Hip Arthroplasty Registry (Garellick et al., 2010) reported similar findings to those observed in England and Wales. They reported that between 1995 and 2010, 2.8% of the total hip replacement procedures were carried out due to AVN (6,476 cases). They also reported that the average age of patients with AVN undergoing the procedure was 67.5 years. They also reported that 32% of the cases of secondary osteoarthritis patients undergoing the procedure developed it following AVN.

As reported in the Australian Joint Registry of 2014 (Graves et al., 2014), 3.4% of total hip replacement procedures (total 280,552 cases) and 1.7% of total resurfacing hip replacements (total 15,770 cases) were performed following diagnosis of AVN. Similar to the English and Welsh registry, this report did not identify the number of secondary osteoarthritis cases following AVN.

In the United States, the actual number of the patients with AVN is not reported; however, it is estimated that there are between 10,000 and 20,000 new cases of AVN annually in the United States, with 5-12% of total hip replacement procedures following diagnosis of AVN (Orban and Cristescu, 2009).

## 2.4 Aetiology

Many causes and risk factors may lead to the development of avascular necrosis. Some of the known causes are listed in Table 2-1. According to Lieberman et al., (2004), AVN is a multifactorial disease and may develop as a result of a combination of the factors listed. It must be noted that although the conditions listed have been known as factors contributing to AVN, the direct links between all the conditions and AVN have not yet been studied.

According to Gautier et al. (2000), AVN of the femoral head is caused following obstruction of the intraosseous vessels. This may be following traumatic, or atraumatic factors. Trauma that leads to interruption of blood flow into the femoral head is the leading pathologic factor for AVN (Lavernia et al., 1999). Non-traumatic factors can be associated with intake of steroids or alcohol, which may affect blood flow into the femoral head. Other non-traumatic factors are sometimes a side effect of another pathological disease, such as sickle cell anaemia or HIV infection (Hhawker et al., 1982; Matos et al., 2007).

Dislocation of the hip is a traumatic event that may lead to AVN of the femoral head. A study by Hougaard & Thomsen (1986) examined the risk of AVN in 100 posterior hip dislocations in their study. They found that dislocations that were not reduced within 6 hours of injury had a 53% risk of producing AVN of the femoral head.

Another traumatic event that may lead to AVN is the fracture of the femoral neck. The fracture may result in interruption of the lateral and medial cervical arteries by displacement of the head, disruption to the ligament teres artery by rotation or valgus, and an obstruction effect due to increased intra-capsular pressure (Smith, 1959; Holmberg and Dalen, 1987; Swiontkowski et al., 1993; Bachiller et al., 2002; Ehlinger et al., 2011). A review of the literature has shown that 6-26% of fractures of the femoral neck lead to AVN of the femoral head (Asnis and Wanek-Sgaglione, 1994; Lu-Yao et al., 1994; Loizou and Parker, 2009).

Non-traumatic factors that lead to AVN include environmental factors such as steroid or alcohol use as well as pregnancy and sickle cell anaemia. Human immunodeficiency virus (HIV) has also been associated with AVN (Calza et al., 2003; Matos et al., 2007), however the mechanism that leads to the disease is unclear (Lafforgue, 2006). A study by Mehta et al. (2013) evaluating prevalence of AVN in 6,487 HIV patients reported that in the 22 patients who developed AVN following diagnosis of HIV, the use of highly active antiretroviral therapy (HAART) was the biggest risk factor. They also reported that diagnosis of AVN in HIV patients has increased since the rise in use of HAART for treatment of HIV.

Allogenic bone marrow transplantation is a high incidence factor, where 10% of patients receiving allograft marrow in Minnesota, USA developed AVN within 1 to 62 months post-transplantation (Enright et al., 1990).

The high prevalence of AVN in East Asian countries has been associated with a genetic polymorphism (Ramchandani, 2013). Following ethanol metabolism, acetaldehyde is produced via oxidation by aldehyde dehydrogenase (ALDH). The low-activity form of ALDH, which is ALDH2\*2 is found in about half of East Asian population and not observed in Caucasian population (Thomasson et al., 1991; Shen et al., 1997). This variant allele does not exhibit any ethanol oxidising capability *in vitro*. This results in accumulation of acetaldehyde levels thus sensitivity reaction such as facial flushing, increased heart rate and avascular necrosis (Peng et al., 2002; Chao et al., 2003; Peng and Yin, 2009).



Table 2-1 - Risk factors associated with AVN, adapted from Lavernia et al. (1999); Malizos et al. (2007); Séguin et al. (2008).

Traumatic factors	
Femoral neck fracture	Hip dislocation
Extensive burns	Vessel trauma
Non-traumatic factors	
Intake of steroids	Radiation
Alcoholism	Contraceptive use
Smoking	Pregnancy
Allogenic bone marrow transplantation	
Diseases	
Sickle cell anaemia	Ehler–Danlos syndrome
Hyperparathyroidism	Raynaud’s disease
Myelodysplastic syndromes	Diabetes mellitus
Coagulopathies	Antiphospholipidemic antibodies
Erythematosus	Hemophilia
Hypercholesterolemia	Hemoglobinopathies
Intramedullary hemorrhages	Chron’s disease
Hyperlipidemia	Decompression disease
Collagen diseases	Hemodialysis
Human immunodeficiency virus infection (HIV)	Deficit of antithombine III, protein C or protein S
Gout	Deficit of plasminogen activator
Cushing disease	Resistance to activated protein C
Gaucher disease	Ulcerative colitis
Pancreatitis	Use of chemotherapeutic agents
Inflammatory bowel disease (IBD)	Familial thrombophilias

#### 2.4.1 Stages of the Disease

AVN of the femoral head occurs as a result of disruption of the blood flow into the femoral head, and results in death of the bone and bone marrow in the region. It occurs in a number of stages, which are described in this chapter.

AVN is often diagnosed in later stages, which has resulted in the limited understanding of the early events of the disease. Attempts have been made to study the early stages of the disease in animal models; however these studies include total devascularisation of the joint or large doses of glucocorticoid

steroids, which only represent extremes of the disease. These attempts are also hampered by the large potential for healing in animals when compared to humans (Lafforgue, 2006).

The events that lead to end stage of AVN are shown in Figure 2-22. There are a series of factors that can contribute to onset of AVN, and although the way by which it leads to the disease may vary, the way the disease progresses is similar in majority of the patients.

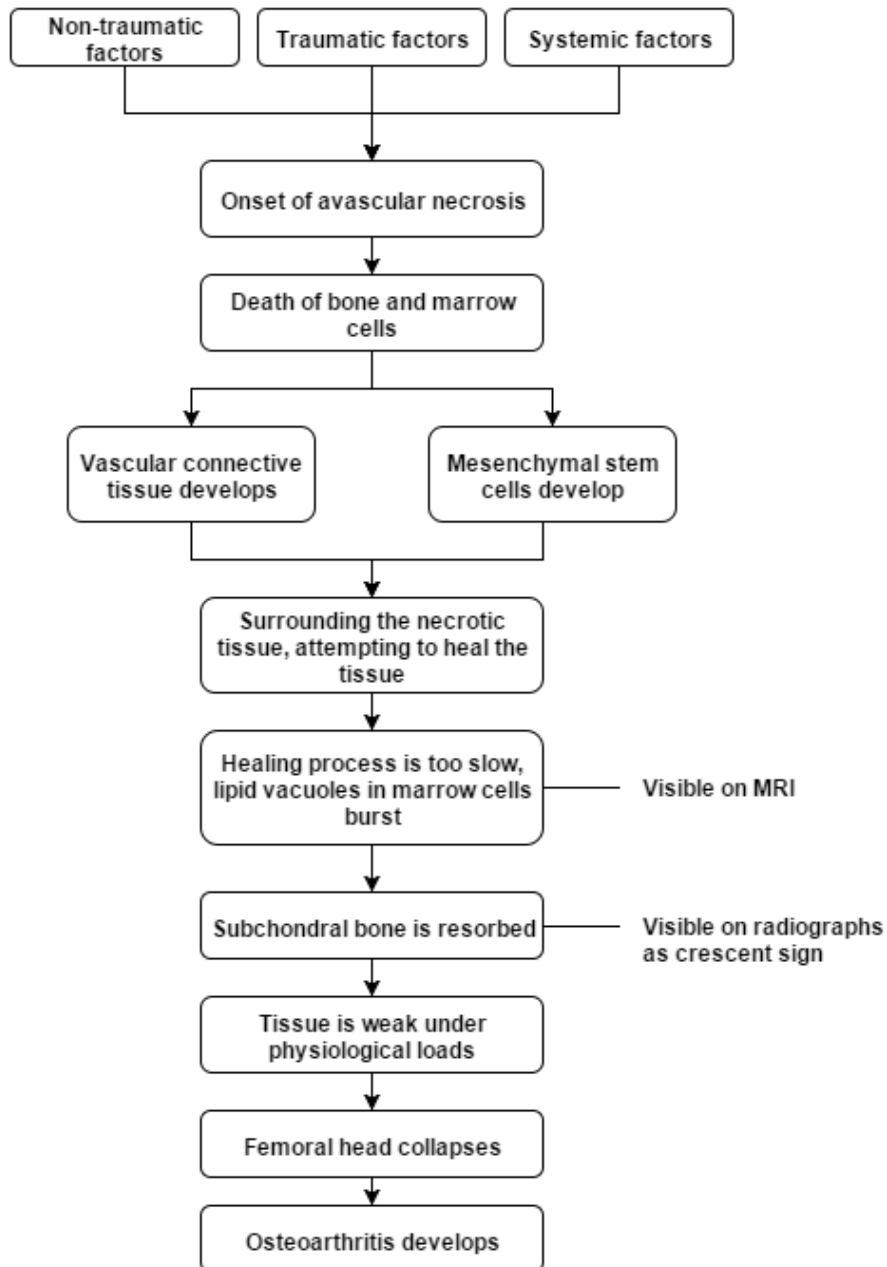


Figure 2-22 - The series of events that occur from the onset of AVN and the eventual development of osteoarthritis.

It starts with blockage of the blood vessels and arteries leading to or within the femoral head. This progresses depending on the main risk factor for the disease. Gluco-corticosteroid use may promote fat embolus formation in the bone, which directly or by triggering intravascular coagulation leads to ischemia of vessels. In sickle cell disease, sickle cell formation may lead to intraluminal vascular obliteration and necrosis of the bone.

A study by Ohzono et al. (1992) carried out micro-angiographic stratification of 38 femoral heads with AVN, and found that there are generally three vascular zones in the diseased heads: Avascular necrotic, reparative vascular and normal vascular zones (Figure 2-23). They compared these images to histological findings, and found that the extent of the necrotic area was related to the extent and number of involved arteries which were blocked.

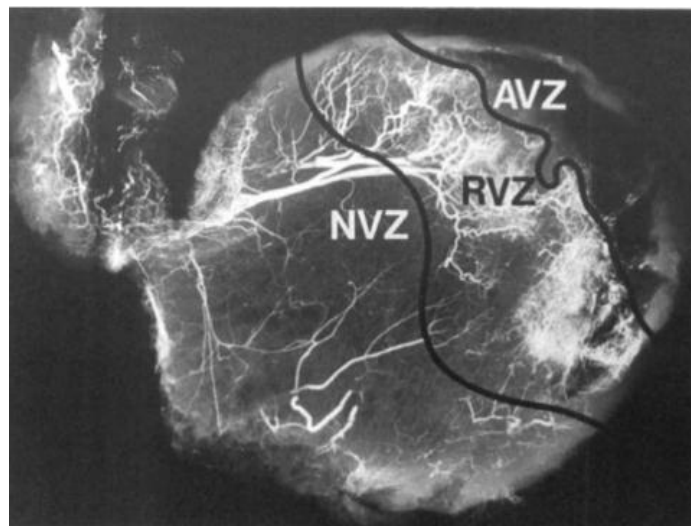


Figure 2-23 – Angiogram of an avascular necrotic femoral head showing the vascular zones – AVZ – avascular zone where no arteries or arterioles are visible. RVZ- where abrupt ramification of arteries can be seen; and NVZ where smooth and unaffected arteries are seen. Image from Ohzono et al., (1992). Image reproduced with permission from Wolters Kluwer Health, Inc..

When the onset of AVN occurs, the progress of the disease is fast and it affects all the cell types in the bone and marrow (osteocytes, hematopoietic cells, and adipocytes) (Lafforgue, 2006). AVN develops at sites such as the femoral head as the marrow is composed predominantly of adipocytes (yellow marrow). These adipocytes have small nuclei and cytoplasm, and are composed mainly of huge triglyceride-predominant lipid vacuoles. These vacuoles are hardly affected by cell death, and hence they remain unchanged for some time, making the Magnetic Resonance Imaging (MRI) signal received

from the necrotic bone seem normal initially (Figure 2-24 and Figure 2-25) (Hernigou et al., 1989; Lafforgue, 2006).



Figure 2-24 - Non-diagnostic radiograph of AVN at the very early stage, Image from Steinberg et al., (1995)

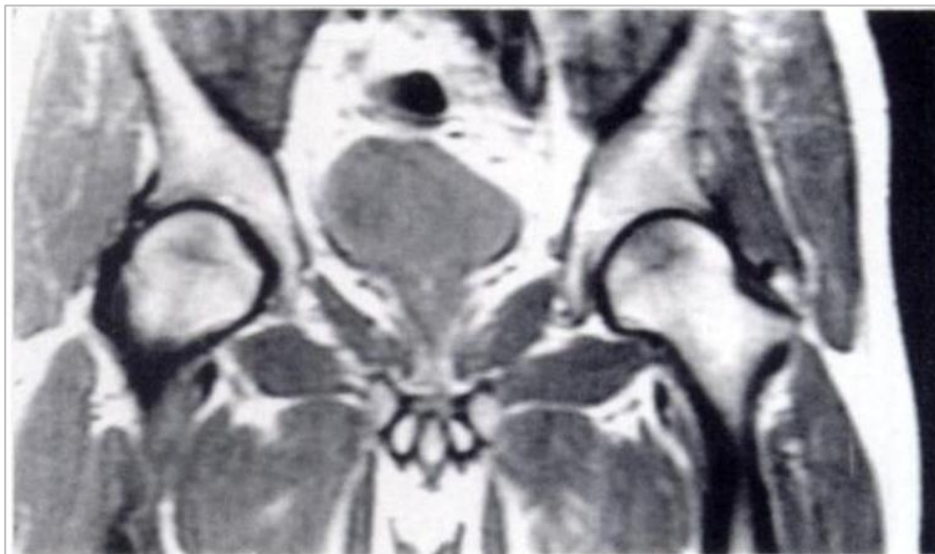


Figure 2-25 - MRI of stage 0 avascular necrotic femoral heads, where a slight decrease in signal intensity is seen in both femoral heads, but still within normal limits. Image from Steinberg et al. (1995).

Within a few days or weeks from the start of bone death, vascular connective tissue and primitive, undifferentiated mesenchymal stem cells develop and surround the necrotic bone. This active interface allows diagnosis of AVN by scintigrams, and as changes progress, by radiography. The interface also contains the lesion and promotes healing by promoting osteocytes, histiocytes and vascular elements. Osteoclasts are called in to degrade the dead

bone and osteoblasts initiate new bone. Mechanical degradation of AVN however progresses at a higher rate than the healing rate; hence the repair is counterproductive and has limited effectiveness (Assouline-Dayana et al., 2002). Following development of the sclerotic tissue, the lipid vacuoles within the adipocytes burst, and their contents undergo denaturation and calcification. Following this event, MRI shows signs of necrosis in the bone (Figure 2-26 - Left) (Hernigou et al., 1989; Bluemke and Zerhouni, 1996; Lafforgue, 2006). At this point it is also possible to see increased density in the femoral head in bone density scans as shown in Figure 2-26 - Right (Steinberg et al., 1995).

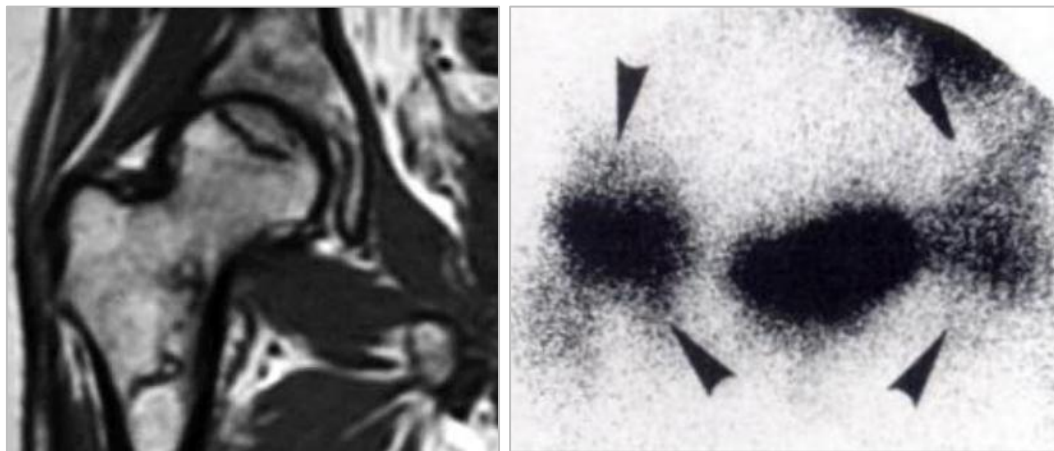


Figure 2-26 - Left - MRI of a patient that shows decreased signal intensity in the femoral head, a sign of AVN. Right - Bone scan of a patient in early stages of AVN, which shows increased density uptake, a sign of AVN. Images adapted from Marvin E Steinberg et al., (1995) and Incavo & Pappas, (2004).

The bone remodelling process is slow and ill-adapted to the local constraints in the necrotic tissue (Figure 2-27 - Left) (Glimcher and Kenzora, 1979a; Lafforgue, 2006). This results in the resorption of subchondral bone, weakening the biomechanical properties of bone. When the bone's mechanical properties are weaker than the physiological forces in the joint, stress fractures through the dead bone occur, resulting in a fracture line, represented in radiographs by a "crescent sign" (Figure 2-27 - Middle) (Glimcher and Kenzora, 1979b; Lafforgue, 2006).

Progression to collapse occurs within 1 to 5 years after the onset of symptoms (Lee et al., 1980; Meyers, 1988; Aaron et al., 1997; Iorio et al., 1998). At this point, the patient experiences severe pain and the femoral head "collapses" under the physiological forces. The end stage of the disease is

osteoarthritis following the alteration of the spherical shape of the femoral head (Figure 2-27 – Right) (Glimcher and Kenzora, 1979b; Lafforgue, 2006).



Figure 2-27 – Left – Area of increased lucency seen in radiograph, a sign of sclerosis development in the tissue. Middle – The subchondral collapse is seen by the formation of a crescent sign (shown by arrows) in the radiograph. Right – Flattening of the femoral head (shown by arrows) following high physiological loads in the joint. Images adapted from Steinberg et al., (1995). (Images reproduced with permission from The British Editorial Society of Bone and Joint Surgery)

It must be noted that a small yet definite number of patients may not progress to collapse or further radiologic stage (Meyers, 1988; Koo et al., 1995; Jergesen and Khan, 1997; Nishii et al., 2002b). Some lesions may also decrease in size over time, with pain and MRI evidence completely disappearing in some patients (Kopecky et al., 1991; Sakamoto et al., 1997; Ito et al., 2003). The risk of collapse of the femoral head is related to the size of the lesion. Many authors have proposed methods of measuring the lesion size, however many inter- and intra-observer errors can affect the measurements obtained (Holman et al., 1995; Steinberg et al., 1999; Nishii et al., 2002b).

#### 2.4.2 Histological Properties

Bone necrosis is generally recognised in histological studies by the loss of osteocytes from the lacunae in the trabecular bone (Catto, 1977; Steffen et al., 2010). Steffen et al., (2010) measured the mean percentage of empty lacunae for AVN samples versus OA and reported 85% empty osteocyte lacunae for AVN versus only 9% for OA (Figure 2-28). Other studies have also reported sites of necrotic bone replacing the bone marrow (Maeda et al., 2003) (Figure 2-29), formation of fat-filled spaces (Catto, 1977) and appositional new bone formation (Steffen et al., 2010; Sakamoto et al., 2013).

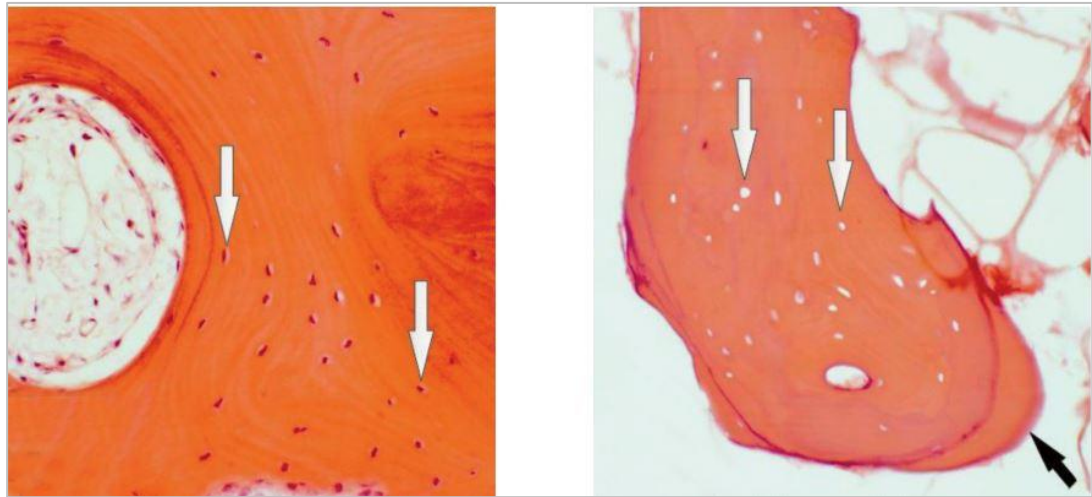


Figure 2-28 – Microscopic pictures of histological specimens stained with haematoxylin and eosin, 100x. Left – viable osteocytes (white arrows) in osteoarthritic bone. Right- empty osteocyte lacunae (white arrows) and appositional new bone formation (black arrows) in AVN patient (Steffen et al., 2010) (Image reproduced with permission from British Editorial Society of Bone and Joint Surgery.)

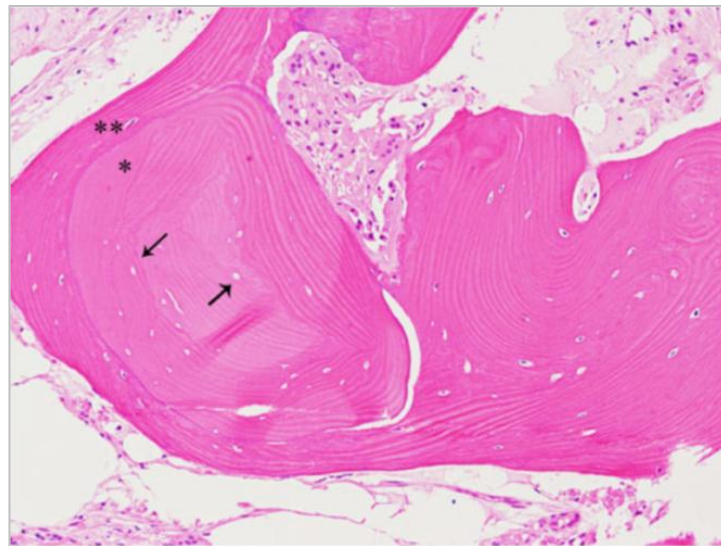


Figure 2-29 - Histological specimen of a biopsy specimen removed from an AVN patient (Haematoxylin and eosin staining (H&E), 100x). Empty lacunae (arrows) are seen in bone trabeculae (asterisk), which is surrounded by new bone formation (two asterisks). Granulation tissue is observed in marrow tissue (Sakamoto et al., 2013). (Image reproduced with permission from Springer.)

Motomura et al. (2011) assessed whether the collapsed region in femoral heads with AVN was associated with the size of the necrotic lesion. They reported that collapse in the subchondral region was largely associated with location of the medial boundary of the necrotic lesion (Figure 2-30). In cases where the necrotic region was limited to the proximal part of the femoral head before the fovea, the collapsed regions were limited to the subchondral region. In cases where the necrotic region was large and the interface between the

necrotic and viable bone was below the distal part of the fovea, the collapse was also on the distal portion of the femoral head.

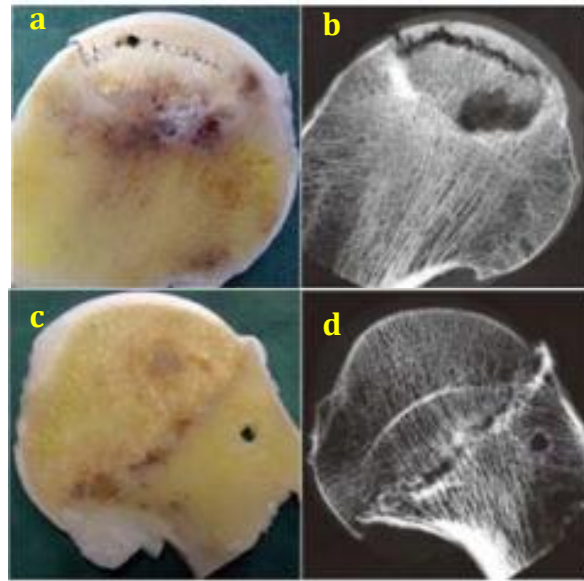


Figure 2-30 – Left: Gross photograph and Right: associated specimen radiograph of necrotic femoral heads. (a) The region between the viable and necrotic region is lateral to the fovea, and (b) the fracture is in the subchondral region. (c) The interface between healthy and necrotic is deep within the femoral head, and (d) the collapse is deep within the femoral head. Image adapted from (Motomura et al., 2011).

#### 2.4.1 Legg-Calvé-Perthes Disease

The Legg-Calvé-Perthes disease (Calvé, 1910; Legg, 1910; Perthes, 1913) also known as Perthes disease or LCPD is a form of avascular necrosis of the developing femoral head, with an average onset in children between 4 and 8 years of age, usually occurring in male to female patient ratios of 4:1 (Loder and Skopelja, 2011).

Although the precise cause of LCPD is not clear, it results as a form of vascular insult and leads to death of bone cells in the femoral head (Joseph, 2011). It was discussed in section **Error! Reference source not found.** that AVN in adults leads to collapse of the femoral head in most cases however LCPD is different to AVN in that it is mostly self-limiting as the blood supply to bone gets restored. This is by either of two mechanisms; the existing vessels are rapidly re-canalised within weeks or new vessels are formed within months to years (Figure 2-31)(Conway, 1993). If the bone is not healed, the femoral head may become enlarged (coxa magna), ovoid or deformed (coxa irregularis)



(Saito et al., 1985). In these cases, the acetabulum in younger children may remodel to fit that of the femoral head (Joseph, 2011).



Figure 2-31 – Stages of Perthes disease from onset to healing. A and B – avascular necrosis of the bone where the epiphysis appears dense and sclerotic, with a fracture line; C and D – fragmentation of the dense epiphysis shown by presence of fissures along the epiphysis. The epiphysis may appear broken into several pieces as shown in D; E and F – revascularisation shown by formation of new bone on the periphery of the necrotic lesion; G – healing of the femoral head where mature lamellar bone replaces the dead bone. Image from Joseph, (2011), reproduced with permission from Wolters Kluwer Health, Inc.

## 2.5 Diagnostic Methods

Patients with avascular necrosis commonly approach physicians with deep and throbbing pain that appears suddenly in the groin. There may also be painful and limited range of motion on examination (Ficat, 1985; Amanatullah et al., 2011). This may be associated with elevated intraosseous pressure (Ficat and Arlet, 1980; Ficat, 1985; Koo et al., 1999; Hungerford, 2002), and may also be correlated with radiographic evidence of collapse in the early follow up (Nishii et al., 2002a).

### 2.5.1 Imaging Techniques

Several imaging techniques are discussed in the literature to diagnose AVN in the early stages. The most common method is radiographic evaluation where a crescent sign is seen after collapse of the subchondral bone (Figure 2-32). The findings from the radiographic images can be used to stage the disease according to the Ficat-Arlet staging system, explained in Table 2-2.

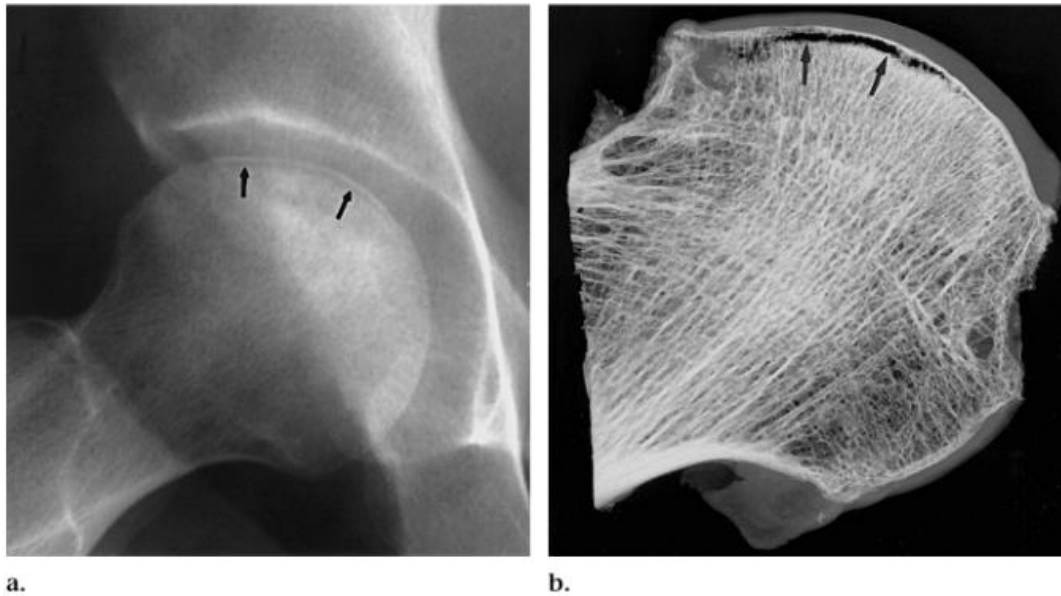


Figure 2-32 – (a) Radiograph of a right femur showing subchondral area hyperlucency as pointed with arrows in the proximal femoral head. (b) Specimen radiograph of a sectioned femoral head segment showing the subchondral fracture as seen with a crescent sign. Images from (Pappas, 2000)

In recent years, MRI has been used successfully to identify AVN in patients with minimal symptoms and insignificant radiographic changes. MRI is used due to its high sensitivity to detect the signal changes associated with osteocyte death and marrow fat cell replacement (Thickman et al., 1986; Gardeniers, 1993a; Amanatullah et al., 2011).

Some studies have looked at the accuracy of MRI in diagnosis of AVN when compared with other imaging techniques. A study by Thickman et al., (1986) reported that MRI is very sensitive in detection of early AVN, when compared with radionuclide imaging. Another study by Mitchell et al., (1986), which compared the efficacy of MRI versus CT scans and Bone scans, showed that MRI is the most sensitive imaging technique for the early diagnosis of AVN.

### 2.5.2 Staging Systems

Many authors have published various diagnostic-staging systems. One of the first staging systems published for AVN is that of Ficat and Arlet, who developed their system in 1960s (see Table 2-2) (Arlet and Ficat, 1960; Ficat and Arlet, 1980; Mont et al., 2006). This system, which started as a three stage system, and has evolved into four and then six stages, is still in use by many surgeons. Many other classification systems such as the ARCO staging system

(Gardeniers, 1993a, 1993b), which was then adapted into the Pennsylvania staging system (Steinberg et al., 1995) have evolved from the Ficat and Arlet system.

Table 2-2 –Ficat and Arlet staging system – Adapted from Ficat, 1985 (Ficat, 1985) and Mont et al., 2006(Mont et al., 2006)

<b>Stage</b>	<b>Radiographic findings</b>
<b>1</b>	None (evident on magnetic resonance images)
<b>2</b>	Diffuse sclerosis, cysts (visualised on radiographs)
<b>3</b>	Subchondral fracture (crescent sign, with or without head collapse)
<b>4</b>	Femoral head collapse, acetabular involvement, and joint destruction (osteoarthritis)

Ficat and Arlet system mainly focused on observations in radiographic findings, therefore development of staging systems that took into account more advanced imaging and diagnostic techniques was necessary. The ARCO (Association Research Circulation Osseous) system established by the ARCO committee (Gardeniers, 1993b) is a staging system that considers radiologic findings as well as Scintigraph and MRI findings, which show signs of sclerosis, osteolysis and focal porosis (stage 2) more clearly than radiography alone (Table 2-3).

Table 2-3 – ARCO diagnostic staging system for AVN (Gardeniers, 1993b).

<b>Stage</b>	<b>Findings</b>
<b>0</b>	All of X-ray, CT(Computerised Tomography), Scintigraph and MRI images are normal
<b>1</b>	X-ray, CT are normal, at least one of either Scintigraph or MRI are positive
<b>2</b>	X-ray abnormal, signs of sclerosis, osteolysis and focal porosis seen on any of: X-ray, CT, Scintigraph, MRI
<b>3</b>	X-ray and CT show crescent sign on the x-ray and/or flattening of articular surface of femoral head (collapse)
<b>4</b>	Osteoarthritis seen, joint space narrowing, acetabular changes visible, joint destruction seen, all on X-ray.

The Pennsylvania staging system is different to Ficat and Arlet and the ARCO system in the sense that in addition to radiography and MRI, it also incorporates bone scanning (Table 2-4). It also has a severity scale in each stage, taking into account the percentage of bone affected (Figure 2-33), similar to that introduced in the ARCO system (Steinberg et al., 1995; Lavernia et al., 1999).

Table 2-4 - Pennsylvania staging system established by Steinberg et al., (1995). \*in these stages, depending on the severity, A-low (<15% of femoral head affected), B-Moderate (15% of femoral head affected), C-high (>30% of femoral head affected) severity is used.

<b>Stage</b>	<b>Findings</b>
<b>0</b>	Normal or non-diagnostic radiographs, bone scan and MRI
<b>I*</b>	Normal radiograph, abnormal bone scan and/or MRI
<b>II*</b>	Abnormal radiograph showing 'cystic' and sclerotic changes in the femoral head
<b>III*</b>	Subchondral collapse, producing crescent sign
<b>IV*</b>	Flattening of the femoral head
<b>V*</b>	Joint narrowing with or without acetabular involvement
<b>VI</b>	Advanced degenerative changes

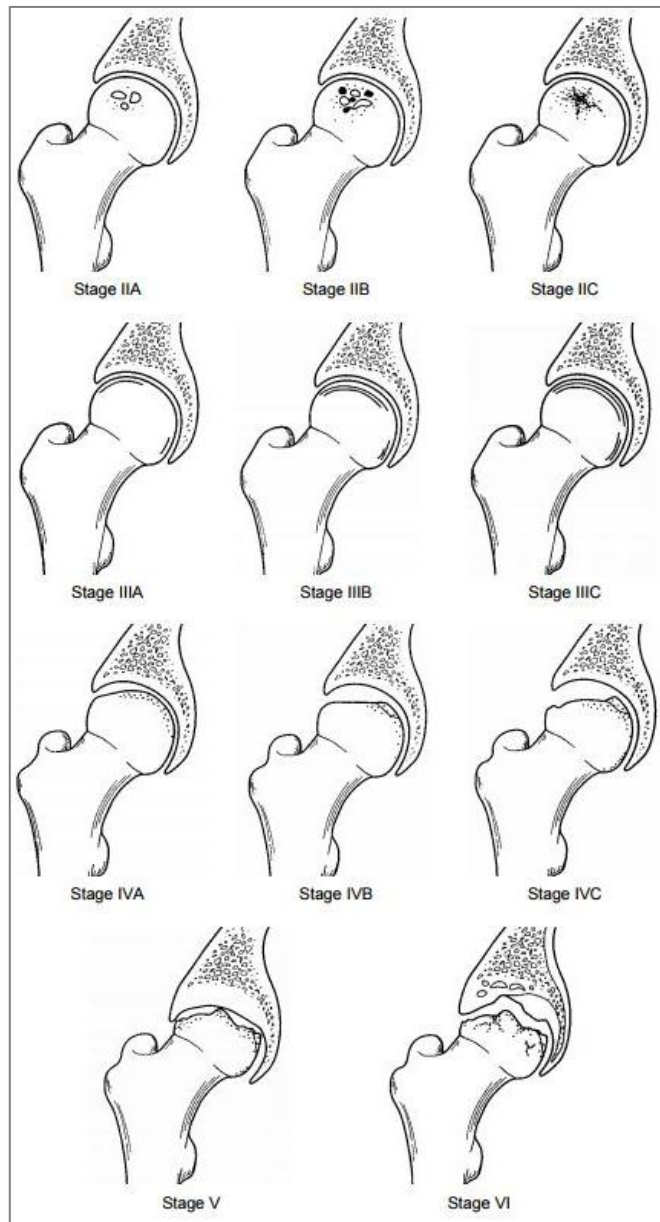


Figure 2-33 - Illustration of radiographic appearance of AVN femoral heads by the Pennsylvania staging system. See Table 2-4 for description of the stages. Figure by Lavernia et al., (1999). (Image reproduced with permission from Wolters Kluwer Health, Inc..)

## 2.6 Treatment

Both non-operative and operative approaches have been taken to treat AVN of the femoral head. The results of these treatments are discussed here.

### 2.6.1 Non-operative Approach

A few studies show the results of activity modification, reduced weight bearing (Merle D'Aubigné et al., 1965) and physiotherapy (Neumayr et al.,

2006) following diagnosis of AVN, and found that the majority of treated patients required further operative treatment (Mont et al., 1996a).

Another series of studies have reported the results of bisphosphonate treatment on patients with AVN. Bisphosphonates are a class of compounds that inhibit osteoclasts and therefore reduce the rate of bone remodelling and turn over. This prevents the resorption of bony matrix and the collapse of the femoral head (Amanatullah et al., 2011). A series of studies have shown an improvement in Ficat stages I and II AVN of the femoral head following treatment by bisphosphonates (Astrand and Aspenberg, 2002; Agarwala et al., 2005, 2009; Lai et al., 2005; Nishii et al., 2006; Ramachandran et al., 2007; Peled et al., 2009); however some adverse effects were also reported, where development of AVN of the jaw following treatment is the most common (Papapetrou, 2009).

A study by Massari et al. (2006) analysed the effects of pulsed electromagnetic field treatment on different Ficat stages of AVN. They reported that 94% of Ficat stage-I and II hips and 48% of Ficat stage III hips were preserved following this treatment. They believed that this treatment enhances bone healing by stimulation of local production of growth factors, promoting new vessel formation and reduction of bone re-absorption.

Other non-operative treatments such as extracorporeal shockwave therapy (Ludwig et al., 2001; Wang et al., 2005, 2008) and hyperbaric oxygen therapy (Reis et al., 2003) have also been studied, however, although successful, further research is needed before they can be recommended for routine clinical use.

## **2.6.2 Operative Approach**

### **2.6.2.1 Core Decompression**

One of the common operative approaches to treat AVN is core decompression, which was developed by Ficat and Arlet with the aim of relieving the elevated intraosseous pressure within the femoral head and to allow blood flow. Although clinical reports vary, the majority agree that core decompression is more suitable for AVN at Ficat stage I and II when compared

to physiotherapy (Stulberg et al., 1990; Fairbank et al., 1995; Mazières et al., 1997; Lieberman, 2004; Wei and Ge, 2011). However, the effect of core decompression in comparison to other operative treatment methods is not well established yet. Some authors have reported high complications such as fractures and infection (Camp and Colwell, 1986; Hopson and Siverhus, 1988), and others believe that it is ineffective (Kristensen et al., 1991; Koo et al., 1995).

Some studies have used core decompression along with other non-operative techniques to stimulate bone growth and improve the outcome of treatments. Aaron and Ciombor (1997) compared the results of treatments by core decompression plus electrical simulation (Figure 2-34) versus other treatments, and their results are presented in Table 2-5. Clinically, it can be seen that the success rate of core decompression plus electrical simulation is higher than core decompression alone, however lower than electrical simulation alone on patients at Ficat stage II.

Table 2-5 – Clinical outcome of Core decompression, electrical simulation and combined treatment at 36 months showing successful follow-up percent. Findings of Aaron and Ciombor, (1997)

<b>Treatment group</b>	<b>Ficat stage (follow-up success rate)</b>		
	<b>I (%)</b>	<b>II (%)</b>	<b>III (%)</b>
<b>Core Decompression</b>	100	67	40
<b>Electrical Simulation</b>	100	80	60
<b>Core Decompression plus electrical simulation</b>	-	77	69

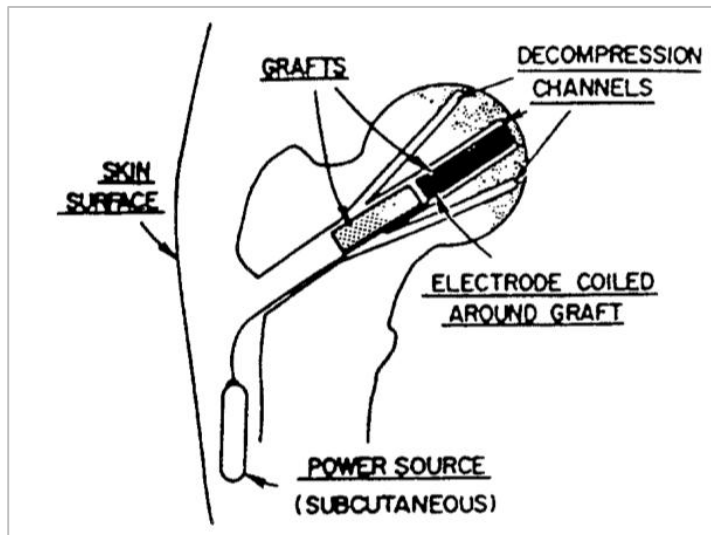


Figure 2-34 - Cathode wire electrode coiled around graft in core decompression track with implantable current generator. Image from Aaron and Ciombor, (1997). (Image reproduced with permission from Elsevier.)

Some users have tested bone grafts, either vascularised or non-vascularised, to improve the support of the femoral head and to boost repair. Vascularised bone grafting has been used as a supplement to core decompression, and is recommended for Ficat II and III (Iwata et al., 1993; Coogan and Urbaniak, 1997; Marciniak et al., 2005; Yen et al., 2006; Zhao et al., 2006).

### 2.6.2.2 Rotational Osteotomy

Rotational osteotomy is a method where the femoral head is rotated anteriorly or posteriorly around the longitudinal neck axis, thus reducing the weight bearing on the necrotic region of the femoral head and reducing the vascular pressure in the region (Sugioka, 1984). A follow up study by Sugioka and Yamamoto (2008) found that out of 43 hips that underwent rotational osteotomy, 70% did not develop osteoarthritis within 1.2-21 years (mean = 12 years). The success rate of the osteotomy was higher in hips with lower ARCO stages (100% in ARCO III-A when compared to 33% in ARCO IV stage). Another follow-up study by Mont et al., (1996b) reported a lower success rate for patients that were diagnosed with AVN following use of corticosteroids when compared to other etiologies.

A study by Matsusaki et al. (2005) reported the results of vascularised pedicle iliac bone graft combined with trans-trochanteric anterior rotational



osteotomy, where 90 degrees of anterior rotation of the femoral head is carried out. This treatment was carried out on 17 patients with the purpose of supplying vascularity and mechanical strength to the femoral head. 12 of 17 patients showed no disease progression following this treatment; however the five unsuccessful hips were reported to have insufficient iliac bone graft insertion position or poor circulation to bone graft.

### 2.6.2.3 Arthroplasty

So far, the final treatment method for AVN is arthroplasty. There are various arthroplasty techniques used to treat AVN, and there is controversy regarding their effectiveness.

With the advancing of hip resurfacing procedures, hemiresurfacing arthroplasty became a popular technique in treating AVN; however the results of these procedures have not been excellent, leading to many investigators suggesting that hemi-resurfacing arthroplasty is an “interim treatment for young patients with large necrotic lesions” (Adili and Trousdale, 2003; Jones and Hungerford, 2004). Adili and Trousdale (2003) reported survival rates of 93.5% at 1 year and 75.9% at 3 years for femoral head resurfacing.

Total hip arthroplasty has often been used as the final treatment for patients with post-collapse AVN (Brinker et al., 1994; Al-Mousawi et al., 2002; Fyda et al., 2002; Dudkiewicz et al., 2004; Lim et al., 2012). The outcomes reported from this procedure vary greatly between different studies. A review by Johansson et al., (2011) looked at the reasons for these variations and reported a series of variables that affect the revision rate reported. They found significant correlation between some diagnoses such as renal failure and/or transplant, heart transplant, idiopathic AVN and sickle cell disease, and their associated THA revision rates. They also reported that in studies where surgeries were performed before 1990, the average revision rate was 17%, which fell to average 3% for surgeries which were performed in 1990 or later. This shows that the advances in THA techniques in the last few decades have improved the outcomes for AVN patients undergoing this surgery.

## 2.7 Mechanical Properties of Avascular Necrosis

There have been very few studies looking at mechanical changes in the hip joint as a result of AVN. A paper by Brown et al. (1981) studied the mechanical characteristics of bone in femoral AVN. They machined eight post-collapse and one pre-collapse femoral heads into cubical specimens and loaded them in a uniaxial compression testing machine as shown in Figure 2-35. They divided the cubes into three groups – completely necrotic, at the fibrotic/sclerotic margin of the lesion and immediately adjacent to the lesion. They demonstrated consistent reduction in stiffness (72%) and strength (51%) in the fully necrotic cubes. The changes in strength of the sclerotic group and adjacent to lesion groups were not statistically significant from the non-pathologic controls; however both groups demonstrated substantial reduction in stiffness ( $\approx 60\%$ ). A similar reduction in strength (41%) and stiffness (59%) was also reported in the only pre-collapse sample in this study with a significant change in modulus reduction seen between pre and post collapse cases. This demonstrates that most of the deficit in mechanical properties occurs in early stages, with a slower but significant change occurring in later stages.

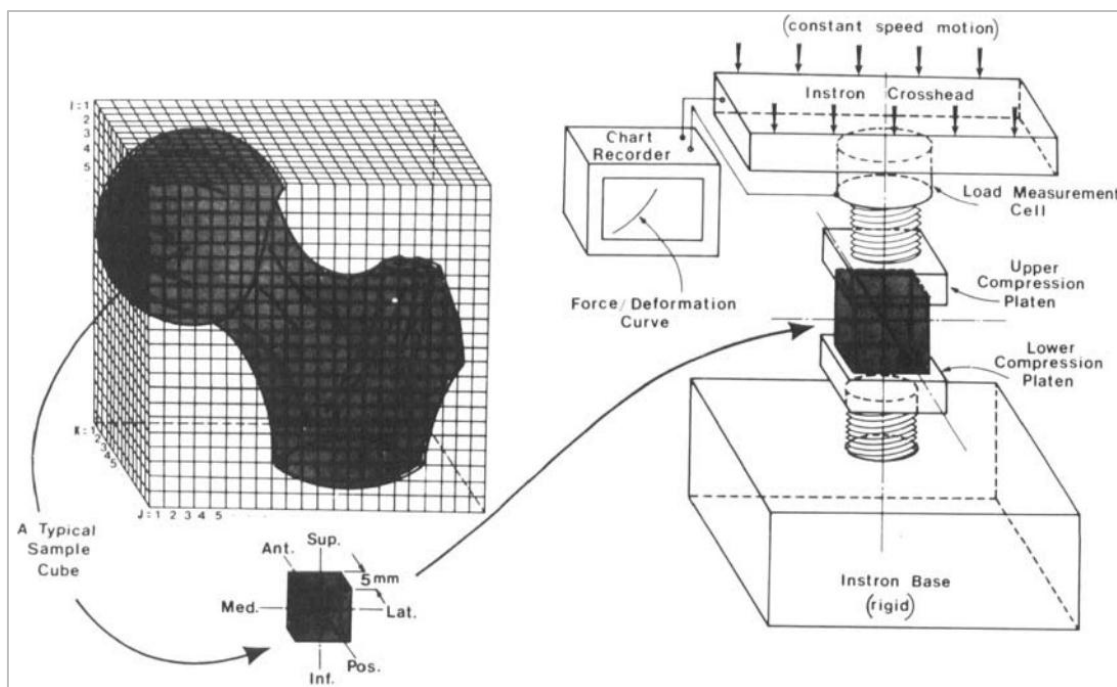


Figure 2-35 –Sectioning planes and orientations of sample cubes excised and tested by Brown et al. in the apparatus shown on the right. Image from Brown et al., (1981). (Image reproduced with permission from Wolters Kluwer Health, Inc.)

Following this study, Brown et al. went on to study the mechanical properties of AVN using finite element modelling. In a three-dimensional finite element study (Brown et al., 1992), they looked at effects of a mechanically uncompromised subchondral plate on protecting the underlying bone weakened due to AVN. They found that if the mechanical integrity of the subchondral plate was preserved, stress levels in the at-risk subjacent necrotic cancellous bone were over 70% of the stress levels in the subchondral bone. They suggested that the onset of collapse in AVN is probably dominated much more strongly by the degree of structural degradation of the cancellous bone within the main infarct body than by the degree of structural degradation within the subchondral plate.

Magnussen et al. studied the degeneration of cartilage in post collapse cases of AVN of the femoral head (Magnussen et al., 2005a, 2005b). They carried out a series of tension, compression and shear strength tests on cartilage and the underlying subchondral bone, and found that the decreasing cartilage tensile strength correlated with histologic evidence of degeneration in patients with AVN. They however found lower correlation with shear and compressive properties. They also compared their findings to results from mechanical and histological tests on osteoarthritic samples. It was reported that the cartilage degeneration in AVN patients has different mechanical and histological characteristics to cartilage degeneration seen in regular osteoarthritis. They thought that the histological difference, where more proteoglycan loss and less surface fibrillation was seen when compared to osteoarthritic group, is due to the cartilage disuse rather than irreversible degeneration of cartilage.

## **2.8 Experimental Models**

Several attempts have been made to create a valid model that represents AVN of the femoral head with the same biological and mechanical characteristics that are found in the natural progression of the disease in human femoral heads. To date, all of these models have been animal models, where AVN is induced and the animal is sacrificed following progression of disease to understand the mechanical and biological properties of the disease.

### 2.8.1 Non-traumatic Models

Since administration of high doses of corticosteroid is a major risk factor for developing AVN (Weinstein, 2012), many authors have used this factor as a way of inducing AVN in animal models of the disease. Various animals including mice (McLaughlin et al., 2002; Yang et al., 2009), rats (Wang et al., 2002; Kondo et al., 2006; Takano-Murakami et al., 2009), rabbits (Fisher et al., 1972; Motomura et al., 2004; Wang et al., 2006; Ma et al., 2008; Kang et al., 2010), chickens (Cui et al., 1997), pigs (Ikeda et al., 2003; Pufe et al., 2003; Drescher et al., 2004b) and ponies (Glade and Krook, 1982) have been used to model AVN induced by corticosteroids. Although many of these models do lead to similar biological outcomes seen in natural AVN, none of them have produced the same mechanical changes that lead to the collapse of the joint. This could be due to these models being quadrupeds rather than bipedals, as well as the multifactorial nature of AVN that occurs in humans (Jones and Allen, 2011).

Other risk factors seen in humans such as alcohol use have been used to induce AVN in animal models. A study by Manggold et al., (2002) produced alcohol induced sheep model of AVN by injecting ethanol directly into the femoral head to create a necrotic lesion, and reported the development of a necrotic lesion, however the models did not lead to mechanical collapse of the femoral head in 12 weeks after injection.

Other novel methods have been used to stimulate AVN in animal models, and these include: hormone induced AVN in rabbits (Wen et al., 2008), activation of immune system in rats (Okazaki et al., 2009), intravascular coagulation in rats (Jones, 1992), rabbits (Yamamoto et al., 1995) and pigs (Drescher et al., 2004), inducing hypersensitivity reactions in rabbits (Matsui et al., 1992; Nakata et al., 1996; Takao et al., 2009), injecting radiopaque lipidols in rabbits (Jones and Sakovich, 1966) and inducing oxidative stress via glutathione depletion and cryogenic freezing in rats (Ichiseki et al., 2006).

### 2.8.2 Traumatic Models

Traumatic models to replicate AVN have been created using various techniques in various animals. Traumatic AVN occurs when there is a

disruption to the circulation to or from the femoral head. In humans, the most common cause for traumatic AVN is the fracture of the femoral neck. Seiler et al. (1996) created a model of traumatic AVN in miniature swine by carrying out an osteotomy to simulate fracture of the head. They reported a decrease in blood flow into the joint during the monitored 8 week period, and histological evaluation showed signs of AVN development.

Some authors have described a method of inducing AVN by sectioning the ligamentum teres and tying a silk ligature around the base of the femoral neck to reduce blood flow into the femoral head (Kim et al., 2001; Menezes et al., 2007; Shapiro et al., 2009). They reported development of AVN of the femoral head in the animals as well as reduced height of the femoral head in MRI images, indicating deformation of the head (Shapiro et al., 2009).

Conzemius et al. (1999) carried out a study on femoral head bones from emus in order to stimulate AVN of the femoral head in a model that progresses to a human-like mechanical failure. Their theory was that models of the disease in quadrupeds generally failed to progress to end-stage femoral head collapse due to the anatomy in those animals. They suggested emus due to their bipedality and their high activity levels represent a more challenging biomechanical environment and therefore result in possible mechanical failure of the hip following initiation of AVN. Of the 19 emus where AVN was induced using ischemic and cryogenic insults, 18 showed histological appearance of end stage AVN, with 6 showing a crescent sign (Figure 2-36). Even though this study demonstrated a model of AVN where mechanical fracture was seen, it does not compare the properties of the collapsed bone to that seen in human femoral heads.

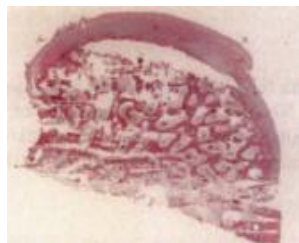


Figure 2-36 –Histologic sections obtained from surgery of emus that developed end-stage AVN as well as signs of crescent sign and loss of trabecular bone. (H&E, 1X) (Conzemius et al., 2002) . (Image reproduced with permission from John Wiley and Son.)

### 2.8.3 Mechanical Models of Avascular Necrosis

An extensive search in literature found no studies that looked at a mechanical model of AVN. All of the animal models researched either focused on a similar biological representation of the disease, or could not progress enough for the mechanical changes to be seen in the model. This presents a large gap in literature that will be very useful, if a successful treatment that addresses both biological and mechanical problems of the disease is to be designed.

## 2.9 Summary of Findings

AVN of the femoral head is a degenerative disease that affects a younger generation, and is the most common diagnosis for patients undergoing total hip replacement in Asia (Chiu et al., 1997, 2001; Wong et al., 2005). Many causes and risk factors may lead to the development of AVN; however they all lead to disruption of blood flow into the femoral head, resulting in death of the bone and bone marrow in the region. This leads to AVN following a series of events listed in Figure 2-22.

AVN is usually asymptomatic in early stages, and is diagnosed when patients approach physicians with deep and throbbing pain from the groin, with painful and limited range of motion (Ficat, 1985; Amanatullah et al., 2011). At this stage, there may be radiographic evidence of AVN presented by a region of dense sclerotic bone, or possibly collapse of the head under the joint loads (Nishii et al., 2002a). Other diagnostic tools such as magnetic resonance imaging or biopsy histology may be used to diagnose the disease.

Various treatment approaches have been taken for AVN, and these include bisphosphonate treatment, pulsed electromagnetic field treatment, shockwave therapy as well as surgical interventions such as core decompression, vascularised bone grafting and arthroplasty. Although some successes have been reported with these treatments, there have also been many failures. The most common approach currently is core decompression for early stage AVN and arthroplasty for late stages however arthroplasty can have poor outcomes, if the bone has been significantly weakened.

A very small selection of research on AVN has looked at the mechanical properties of bone in the disease. The most significant study was by Brown et al. (Brown et al., 1981), where they sectioned avascular necrotic femoral heads obtained following arthroplasty into very small cubes and characterised the mechanical properties of the bone in order to create a map of the properties. This research provided information regarding the differences between necrotic and non-necrotic regions of bone, however does not provide enough information regarding the mechanical characteristics of the overall femoral head.

Various experimental models of AVN have been introduced; however they have all involved live animals – mainly quadrupeds, which do not lead to the mechanical collapse of the bone seen in AVN in humans. A model by Conzemius et al., (1999) recreated AVN in emus, which eventually led to end-stage femoral head collapse seen in humans. This collapse was seen due to the bi-pedality and high activity level of the animal. Even though this study demonstrated a model of AVN where mechanical fracture was seen, it does not compare the properties of the collapsed bone to that seen in human femoral heads and it is not clear if this model can be used to test future interventions for the disease.

In order to understand the mechanical properties of femoral heads with AVN, various methods to test the mechanical features of bone may need to be used. The method by which bone is tested can have a significant effect on the results obtained (An and Draughn, 2000), therefore many methods were reported in this review. Although all the present methods study the mechanical properties of bone in smaller dimensions or in whole and provide a good comparison basis for research, further work is needed to understand the mechanical behaviour of bone in anatomical positions.

In order to create a valid in vitro model of AVN, a review of the literature on methods of degrading mechanical properties of bone was carried out. Most of these methods were originally studied in order to understand the different effects of drugs or preservation techniques on mechanical properties of bone to possibly eliminate these effects. These methods include preservation techniques such as freezing and drying, altering mineral content with use of chemicals such as potassium hydroxide and hydrogen peroxide, and mechanical methods such as drilling or micro-fracture. Sterilisation by Gamma irradiation also seemed to have a degrading effect on the mechanical properties of bone.



## 2.10 Project Aims and objectives

This project aims to develop a validated simulation model of AVN of the femoral head. This model will have both clinical and industrial benefits: Clinically, it may help to improve identification of mechanical risk-factors that could help to choose the most effective treatment for a patient; from an industrial perspective, such a model would allow optimisation and validation of new orthopaedic interventions aimed at treating the disease.

### 2.10.1 Aims

The aim of this project was to study the mechanical properties of femoral heads affected by AVN, and use the results to develop an *in vitro* simulation model of the disease on animal femoral head tissue. This model could then be used in testing treatments and interventions for AVN, and possibly as a diagnostic tool for the clinicians.

### 2.10.2 Objectives

The objectives of the study were as follows:

- 1) Develop techniques to characterise the mechanical properties of bone. These techniques included CT scanning and mechanical compression testing on various dimensions of bone samples from femoral head.
- 2) Compare mechanical properties of bone from porcine, ovine and bovine femoral head tissue and choose the most suitable species for further testing and the final model of the disease.
- 3) Compare mechanical properties of animal tissue with mechanical properties of healthy human bones received from a tissue bank.
- 4) Establish possible methods of changing the material properties of bone that could be used in a later stage to create the model. These included consideration to heating, freezing and degradation using chemicals.
- 5) Mechanical properties of femoral heads with AVN will be studied using the techniques established and used on the animal femoral heads. The

mechanical properties were recorded and the results were used to develop a model of the disease.

- 6) The findings from characterisation of diseased bones and animal tissue were combined with the methods established to change the material properties of bone to create an in vitro model of AVN in animal femoral heads.

A diagram showing the project objectives and the data used in onward chapters (arrows) can be viewed in Figure 2-37.

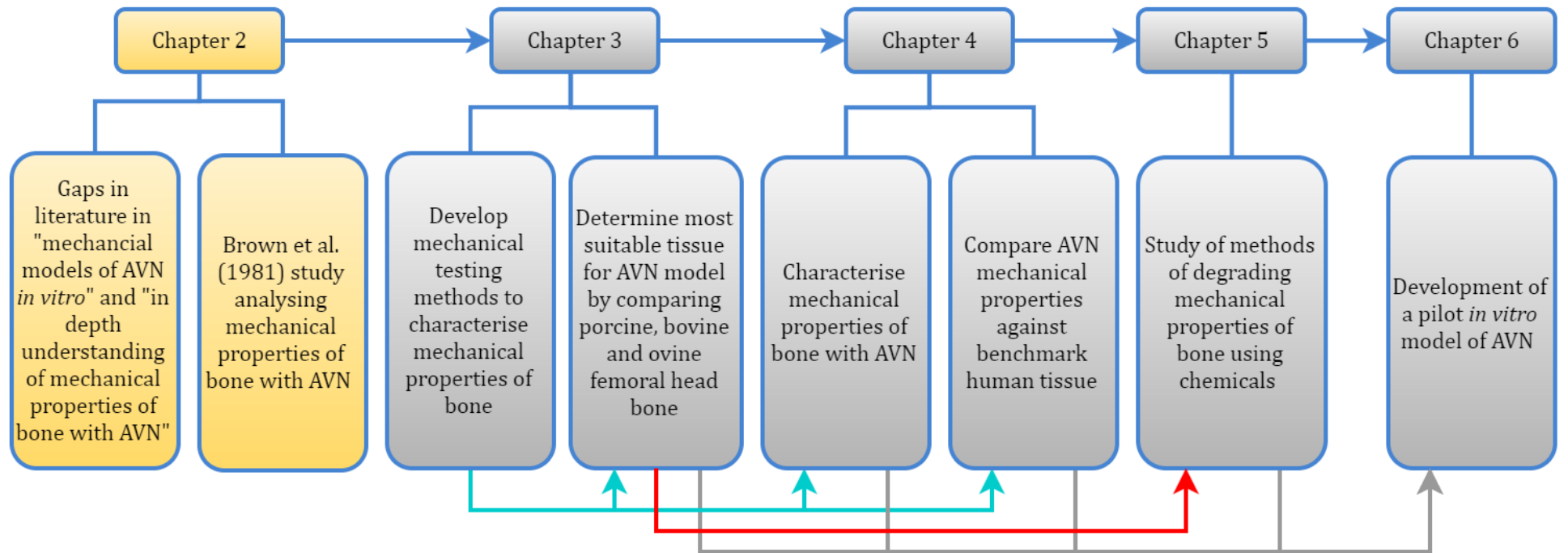


Figure 2-37 – Project objectives and chapter outline.



## Chapter 3. Mechanical Characterisation of Porcine, Ovine and Bovine Femoral Head Bone

### 3.1 Introduction

The mechanical properties of bone vary between different species (Fung, 1993; An, 2000). These mechanical properties are affected by the size of the animal and the function the bone plays in the body. The mechanical properties of bone are also dependent on the method used to calculate the properties, as factors such as strain rate, loading direction and location of bone may affect the calculated mechanical properties. Human bone has been compared to various animal species in order to find matching mechanical properties that can be used in modelling human bone *in vitro*. In order to develop a valid animal mechanical model of AVN, suitable and comparable animal bones need to be used. In order to find the most suitable species, the properties of animal bone need to be assessed and compared with human femoral head tissue.

The aim of this study was to provide the necessary data and information to develop a protocol for further bone characterisation. Secondly, the data obtained from this study would provide the information for basic mechanical properties of healthy animal femoral heads prior to degradation. This data was used as control data for mechanical properties and compared to properties of bone following degradation in Chapter 5.

### 3.2 Materials and Methods

#### 3.2.1 Introduction

The radiographic and mechanical properties of bone samples from porcine, bovine and ovine specimens were analysed using CT imaging and compression testing of bone samples. The results were analysed to compare the mechanical behaviour of the bone from the three species to human tissue and were used to

determine a suitable species for the *in vitro* model of avascular necrosis. The method can be seen in Figure 3-1.

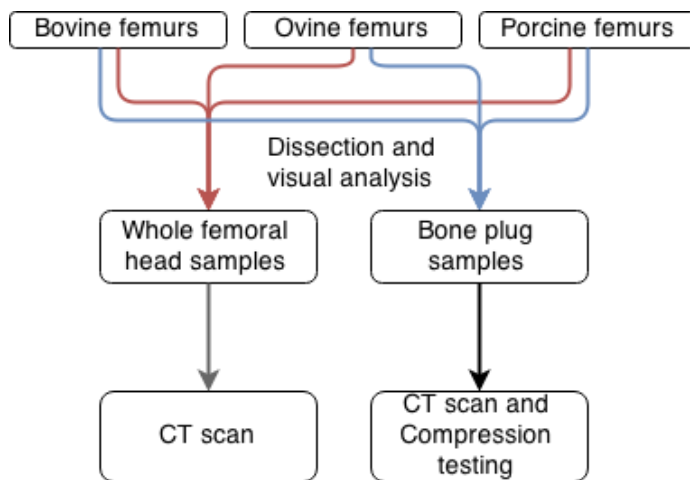


Figure 3-1 - Flow chart showing the experimental method for assessing mechanical properties of animal femoral heads.

### 3.2.2 Sample Selection

In order to characterise and select a material for the mechanical model of AVN, bone samples from three quadrupeds commonly used in scientific bone research were used. These were bovine, porcine and ovine tissue taken from immature animals. These samples were selected firstly due to ease of purchase from local abattoirs as they are commonly available in the food chain and secondly as they have some similar geometrical and mechanical properties to human femoral head tissue (Taylor et al., 2011). Details of the tissues used in this experiment are outlined in Table 3-1.

Table 3-1- Details of the tissue obtained for this study

Species	Source	Age	Condition	Quantity
Ovine	M&C Meats, Sherwood Park, Leeds, UK	1-2 years	Full leg and surrounding tissue	10
Porcine	John Penny & Sons Abattoir, Rawdon, Leeds, UK	5-6 months		10
Bovine	UK	18-24 months	Femur only	10

The samples were divided into two sets for experiments on the overall femoral head to determine the structural properties of bone, and on a small bone plug removed from the load-bearing region of the femoral head, to determine the mechanical properties of bone. CT scans and visual analysis was carried out on all samples to compare the sample geometries and morphologies. The bone plug samples were additionally tested in compression to assess mechanical properties.

### 3.2.3 General Materials

#### 3.2.3.1 Phosphate Buffered Saline

In order to maintain the tissue hydration throughout the study, a water based buffer solution was used. The phosphate buffered saline (PBS) (MP Biomedicals, OH, United States) was prepared following the manufacturer's instructions by dissolving one tablet in every 100ml of sterile water (Baxter, UK). The formulation for the PBS tablet is listed in Table 3-2.

Table 3-2 - Formulation of phosphate buffered saline tablets (MP Biomedicals, OH, US)(MP Biomedicals, 2015)

<b>Component</b>	<b>Concentration (mg/l)</b>	<b>Molecular weight (DA)</b>	<b>Molarity (mM)</b>
Potassium Chloride [KCl]	200	74.55	2.68
Potassium Phosphate Monobasic [KH <sub>2</sub> PO <sub>4</sub> ]	200	136.09	1.47
Sodium Chloride [NaCl]	8000	58.44	136.89
Sodium Phosphate Dibasic [Na <sub>2</sub> HPO <sub>4</sub> ]	1150	141.96	8.10

#### 3.2.3.2 Bone Cement

In some parts of the experiments, tissues were potted in cement following dissection. The prepared bone cement mixture comprised of two materials: rapid repair liquid and cold cure powder (both WHW plastics, Hull, UK). In order to prepare the bone cement mix, a scale was used to measure the powder

mass, and the liquid part was added onto the powder. An approximate mass ratio of 2 powder parts for 1 liquid part was used to make the bone cement, and the amount of cement produced each time depended on the amount required at each session.

#### 3.2.4 Preparation of Samples

All samples were dissected and prepared using a local operating procedure in place for animal tissue dissection (SOP06.1). Legs from different species were received in different conditions. Porcine legs were received from the abattoir as full legs from pelvis to toes with all the muscles and skin attached. Ovine legs were obtained as full legs from pelvis to ankle with the skin removed in the abattoir. Only the bovine femur with most of the muscles and soft tissues pre-removed were obtained. This resulted in different dissection methods for each species.

All samples were dissected between 18-28 hours after slaughter. The legs were stored in a fridge prior to delivery to the laboratory.

In order to access the femoral head in the porcine and ovine legs most of the surrounding tissue was removed using a scalpel (Figure 3-2). Care was taken to prevent damage to the femoral head tissue. The ligamentum teres was carefully cut using a scalpel in order to separate the femoral head from the pelvis. The femur was then separated from the rest of the leg in order to allow for further preparation in a bench vice. Bovine legs were ready for further sample preparation at receipt.





Figure 3-2 - (a) A porcine leg as received from the abattoir. (b) Tissue stripped from the leg. (c) Ligamentum teres being cut to separate the femoral head from the acetabulum. (d) Stripped porcine femur.

### 3.2.5 Bone Plug Sample Preparation

From each femoral head selected for bone plug testing, osteochondral plugs of 9mm diameter and approximately  $15 \pm 5$ mm length were removed from the maximum load-bearing region of the femoral head. This was done using a stainless steel corer and an electrical drill, halfway between the ligamentum teres/articular cartilage junction and the articular

cartilage/femoral neck junction (Figure 3-3), as it is the primary weight bearing region of the femoral head (Taylor et al., 2011). The distal end of the samples was flattened using a bone clipper and a file, and the cartilage was removed using a scalpel, leaving approximately 8-12mm of bone for testing (Figure 3-4).

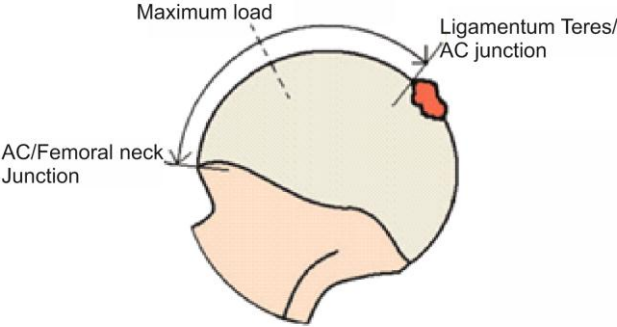


Figure 3-3 - The osteochondral plugs were taken from the maximum load location shown on the image on the left (Taylor et al. 2011).Image reproduced with permission from SAGE Publications.

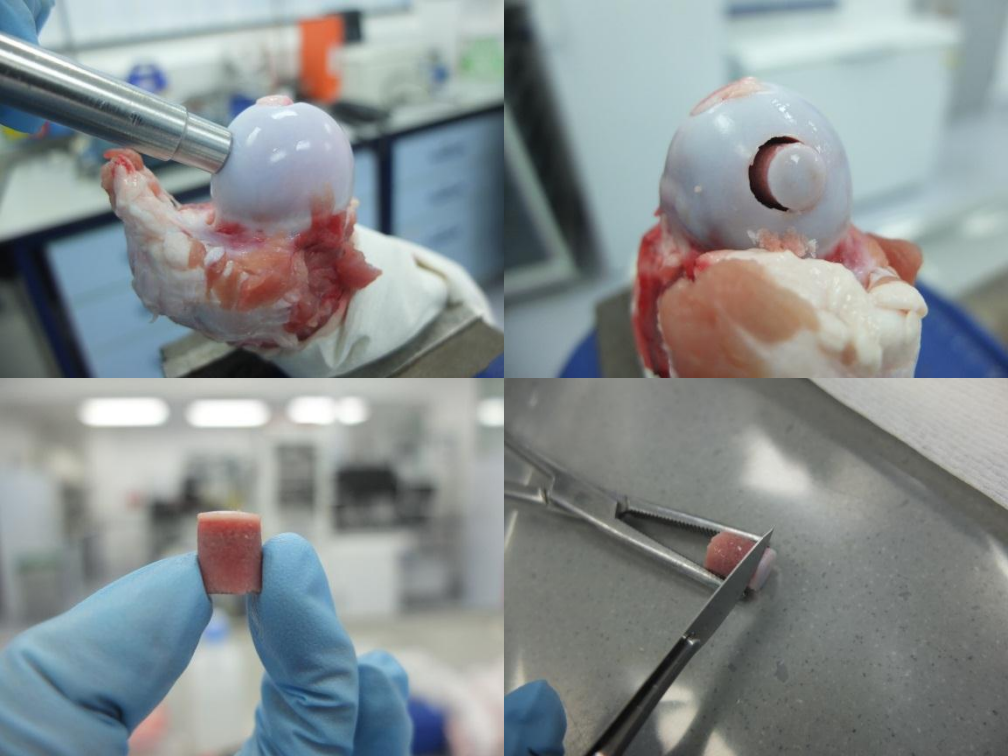


Figure 3-4 - Photographs showing the removal of bone plugs from the femoral head (in this case, porcine). The bone plugs were removed from the femoral head, and the bony end was flattened using a metal file. The cartilage was then removed using a scalpel to produce a cylindrical sample for testing.

### 3.2.6 Femoral Head Sample Preparation

In order to analyse the morphological properties of the overall femoral head, one porcine and one ovine femoral head were prepared by separating the femoral head from the femur. This was only carried out on porcine and ovine species as bovine femoral heads were larger than the CT scan fixture.

The distal end of the femur was used to align the femur. The femurs were placed on a flat table, with a flat surface laid against the distal end of the femur. A ruler was aligned at 90 degrees to the flat surface, and marks were placed on the proximal end of the femur, where cuts were to be made according to the plan shown in Figure 3-5 using the red dotted lines.



Figure 3-5 - Preparation of femoral head samples; red dotted line shows the line at which a cut will be made in the femur, and the black lines show the alignment to be used with respect to the distal end of the femur. Image adapted from 3DCADBrower.com

The prepared femoral head was then potted in bone cement. The bone cement was a mixture ratio of 1ml liquid part (methyl methacrylate based liquid, CAT ref 01CCL1, WHW Plastics, Hull, UK) to every 2g powder part (polymer blend based on methyl methacrylate and 2-ethyl hexyl acrylate, CAT ref 01TSC3, WHW Plastics, Hull, UK). Following mixing for about 10 seconds, the mixture was poured into a round metal potting fixture (diameter: 7cm, height 2cm) to a height of 3-5mm. After approximately 5 minutes of curing of the cement, the femoral head was placed flat side down inside the fixture, and more bone cement (height of 10mm) was poured to secure the sample inside

the cement. The cement inside the fixture was left to cure for approximately 30 minutes before they were stored or tested.

### 3.2.7 Storage

During sample preparation, where possible a tissue paper soaked in PBS solution was placed on the femoral head to maintain hydration of the tissue. Following preparation of samples, they were wrapped in a tissue paper soaked in the PBS solution, enclosed in plastic packaging and placed in freezer at -20°C until testing. Between tests, the samples were placed back in freezer until further testing.

### 3.2.8 Computed Tomography (CT) Scanning

The CT scanner (Figure 3-6, Scanco Medical XtremeCT, Switzerland) was used to obtain CT images of the bone samples, which provided geometrical and morphological details. It was calibrated using a calibration phantom on the day of the use. All bone plug samples and the whole femoral head samples of porcine and ovine tissue were scanned using a high-resolution peripheral quantitative CT scanner prior to mechanical loading. A testing program was created with the scanning parameters (voxel size (slice thickness) of 82µm and integration time of 300ms) and was used throughout. A new sample number was created for each specimen scanned.



Figure 3-6 – XtremeCT scanner by Scanco used for obtaining CT images from the bone samples (“XtremeCT scanner,”)

The samples were orientated in the scanner as demonstrated in Figure 3-7, where images were taken in the transverse plane of the samples. The data were saved and images were analysed using the built-in Scanco microCT systems software of the scanner as well as ImageJ image processing software (Rasband, 1997) with the BoneJ Plug-in (Doube et al., 2010).

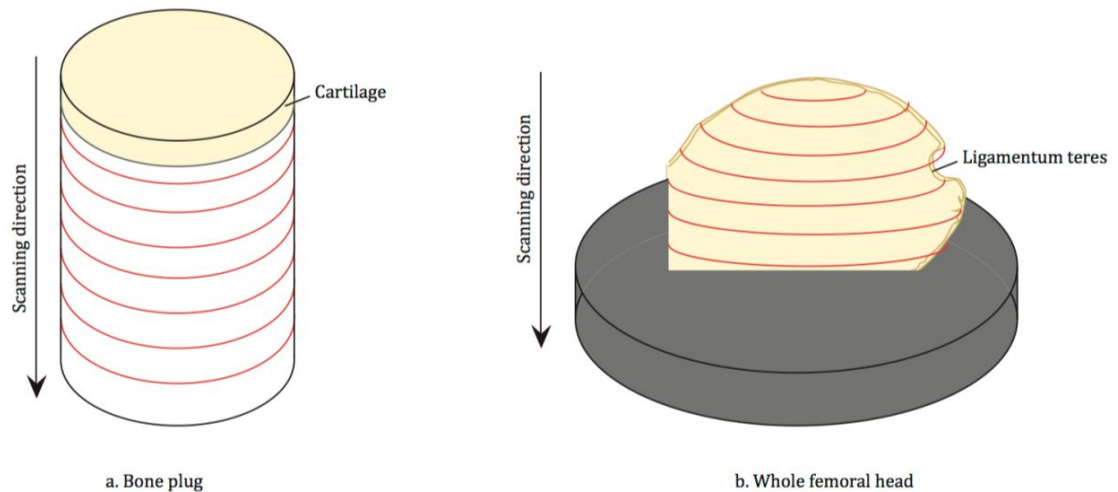


Figure 3-7 - Diagram showing the scanning direction in the CT scanner for the (a) osteochondral plugs and (b) whole femoral heads; the red lines represent the approximate angle of scan planes and the scanning direction is seen with the arrows. The image is not to scale.

### 3.2.9 Mechanical Testing

A mechanical testing machine (Figure 3-8 - A, Instron 3366, High Wycombe, UK) with a 10kN load cell was used to carry out compression tests on bone plugs. Bluehill testing software (Instron, High Wycombe, UK) was used to control the loads applied and for data acquisition. The samples were initially pre-loaded to 1N in compression (Figure 3-8 - B). An axial load was applied under displacement control onto the samples at strain rate of  $0.01 \text{ mms}^{-1}$  until failure (Carter and Hayes, 1976). Failure was defined as the point where plastic deformation was initiated and this was recognised by a significant drop in the compression load during testing. The test was stopped manually at this point. The load-displacement data was recorded at a rate of 10Hz.

The original heights of the plugs were measured using callipers. A pressure sensitive film (Fujifilm; Tokyo, Japan) was placed between the sample and the compression platen to estimate the contact area during loading. ImageJ image

processing software (Rasband, 1997) was used to calculate the contact area on digitally scanned and scaled images of the pressure sensitive films.

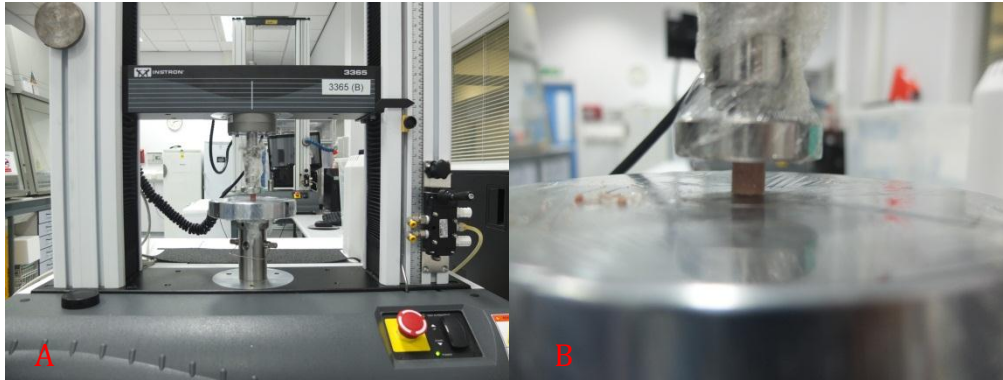


Figure 3-8 – A – The Instron 3366 testing machine used to test bone samples in compression. B – A porcine bone plug set up and ready for compression testing.

### 3.2.10 Results Analysis

The properties that needed to be observed from this test were the material properties and mechanical behaviour of each tissue. These were analysed along with comparative findings in literature.

The datasets were statistically analysed using analysis of variance (ANOVA) to determine significant difference between the groups, and Tukey-Kramer multiple comparison test was carried out to determine the groups that were significantly different from others ( $p < 0.05$ ).

#### 3.2.10.1 CT Image Analysis

The built-in Scanco microCT systems software was used to calculate the bone mineral density (BMD) of bone plugs. The entire bone plug was selected during the analysis as a circular region of interest (ROI) in each slice and the overall BMD was calculated.

The CT images were then analysed using the ImageJ Software (Schneider et al., 2012) with a BoneJ plugin (Doube et al., 2010). The images were analysed for porosity, trabecular thickness and trabecular spacing. To calculate these parameters, the stacks of images were divided into a series of stacks with 10 images per stack. This was done to improve the quality of the binary image as the properties of the bone change with increasing depth into the sample, and therefore need different thresholds to obtain binary images. A square area of

5.74mm side was selected in the centre of the circular bone plug in the first CT image in each 10-image stack. This was then converted into a stack of binary images, where white indicated bone and black indicated non-bone areas as shown in an example in Figure 3-9.

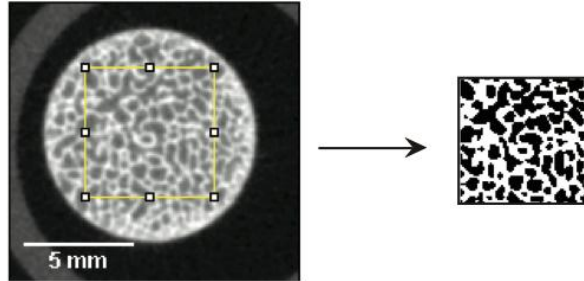


Figure 3-9 – Diagram showing a CT image slice of a porcine bone plug, where a square area is selected in the image and then converted into a binary image.

Following conversion of the image to binary, the BoneJ plug-in then calculated the ratio of area covered by bone in each 10-image stack. This value was then subtracted from 1 to calculate a ratio of porosity of bone as shown in equation 3.1.

$$Porosity = 1 - \frac{Bone\ Volume(BV)}{Total\ Volume(TV)} \quad \text{Equation 3.1}$$

Trabecular thickness was calculated as the mean thickness of the trabeculae in the scan. Trabecular spacing was calculated as the mean distance between trabeculae in the image (see Figure 3-10).

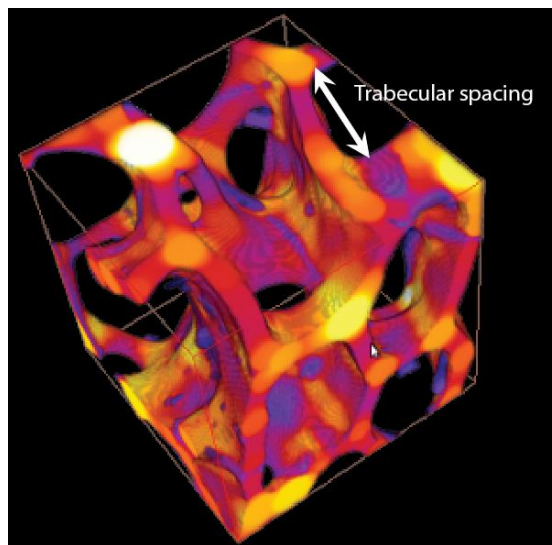


Figure 3-10 - Diagram showing a trabecular structure illustrating the trabecular thickness and spacing. The darker areas demonstrate thinner whereas lighter areas demonstrate thicker trabecular thickness. The trabecular spacing is the mean distance between trabeculae as demonstrated with the white arrows.

### 3.2.10.2 Mechanical Testing Analysis

The data from the mechanical tests were obtained in a raw file in a comma separated values (CSV) format, where load and extension at time-points were recorded. The data along with initial contact area and original length values were imported into MATLAB (2011b, MathWorks, Massachusetts, USA) where a loop programme was set up in order to calculate the values of engineering stress and engineering strain for all imported data. This was calculated using equations 3.2 and 3.3.

$$\text{Stress } (\sigma) = \frac{\text{Load (P)}}{\text{Contact Area (A)}} \quad \text{Equation 3.2}$$

$$\text{Strain } (\epsilon) = \frac{\text{Displacement } (\delta L)}{\text{Original Length } (L_0)} \quad \text{Equation 3.3}$$

In order to remove the toe region of the graphs, the programme removed any data below the 50N preload value, and shifted the displacement values, so that at 50N, the displacement was 0mm.

The stress and strain values obtained were used to plot a graph (Figure 3-12), and the first major peak in the stress (defined as the first major peak with 20 lower points on either side of the peak) was used as the yield stress. A pair of cross-hairs was used in the MATLAB programme to manually select two points on the elastic region of the graph, which is defined as the linear portion of the stress-strain curve, before deformation becomes plastic (Figure 3-11). A line of best fit was then fitted through the elastic region of the curve. The gradient of this line was calculated to provide the elastic modulus.

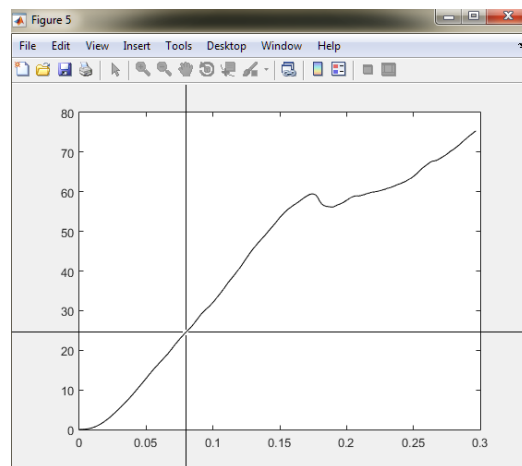


Figure 3-11 – A screenshot of the figure produced by the MATLAB programme and the cross-hairs requesting the manual selection of two points on the elastic region.



The area under the stress-strain curve between zero and the yield stress value was calculated to obtain the work to yield value. A parallel line to the elastic line, which intersected the strain axis at 0.005, was drawn to show the 0.5% offset line. The point at which this line crossed the stress-strain curve was defined as the 0.5% offset stress. The programme wrote the data obtained from these calculations to an output file, which was then used in the statistical analysis of the information. Further details of the MATLAB programme used in calculation of mechanical properties bone can be found in Appendix A.

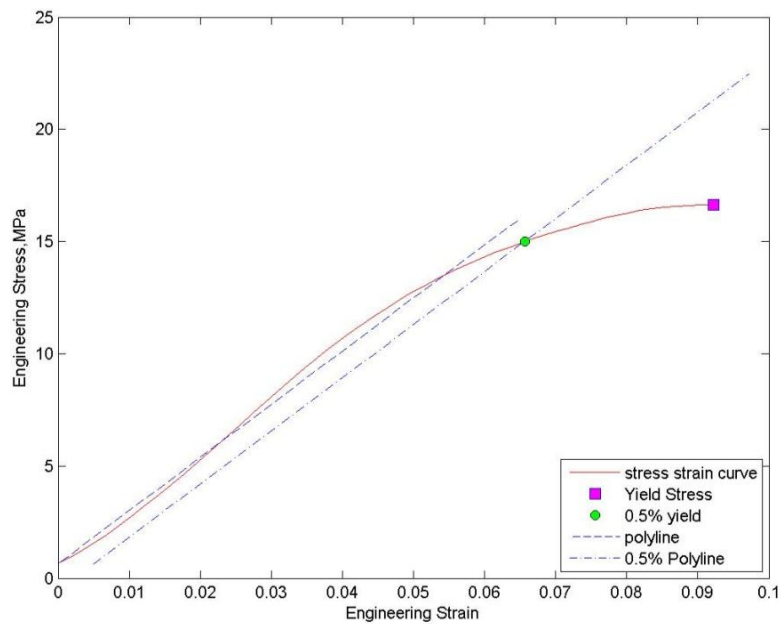


Figure 3-12 - An example of a graph obtained by the MATLAB programme; this graph shows the stress versus strain values for an ovine sample, where the red line shows the stress strain curve, the pink box shows the yield stress and green circle shows the 0.5% offset yield stress. The dashed line shows the line of best fit through the elastic region, from which the elastic modulus is calculated, and the Dash-dotted line shows the line parallel to the elastic line of best fit, offset by 0.5%.

### 3.2.10.3 Statistical Analysis

A separate MATLAB programme was used to carry out statistical analysis on the output of the data obtained. This programme imported the output data which consisted of elastic modulus, yield stress, work to yield and offset yield stress as well as CT image analysed data, BMD, porosity and trabecular thickness and spacing. Graphs of the data were then obtained to compare the values of these variables for each animal species used – ovine, bovine and porcine. The boxplots show the median line, with the upper and lower quartiles, as well as the highest and lowest data values.

An analysis of variance (ANOVA) was carried out to check for any significant differences between the datasets. An ANOVA table was produced by the programme, which was used to check for significant differences, and to calculate where these differences lie. A red star was placed above the groups which had significant differences ( $p < 0.05$ ) with the other datasets.

### 3.3 Results

The aim of this study was to assess mechanical properties of femoral head bone from three animal species and to compare the findings with human femoral head bone properties. In order to do this, CT images were obtained and analysed from the bone samples and the samples were tested in compression for mechanical properties. The results are presented in this section.

#### 3.3.1 CT Images

Charts of porosity for the three species are shown in Figure 3-13. There are no significant differences in the porosity data for the different tissue types. The range of porosity observed between samples is higher in bovine samples when compared to ovine samples.

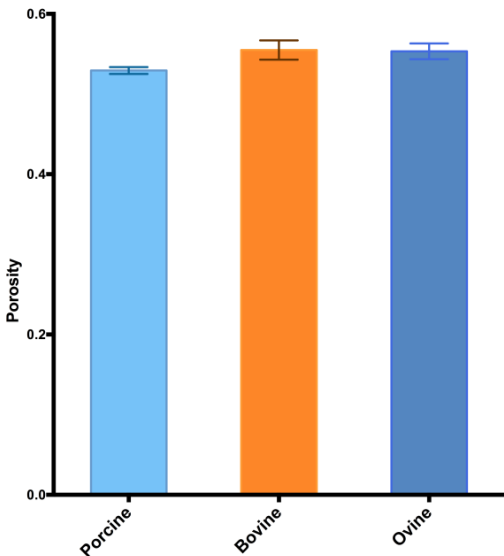


Figure 3-13 – Bar chart displaying mean porosity for ovine, bovine and porcine bone samples. The error bars are standard errors of mean ( $n=5$ ); there were no significant differences between any of the groups.

There were significant differences between trabecular thickness and spacing of all groups. Bovine samples had the highest values and porcine

samples had the lowest values for both parameters (Figure 3-14(a) and (b)). This finding was also visually seen in bone plug CT scans for the three specimens in Figure 3-15, where it can be seen that porcine samples have a very dense structure and thinner trabeculae when compared to ovine or bovine samples. This however was not reflected in the porosity data as it means that the ratio of bone to marrow is not affected by the trabecular thickness and spacing in these specimens.

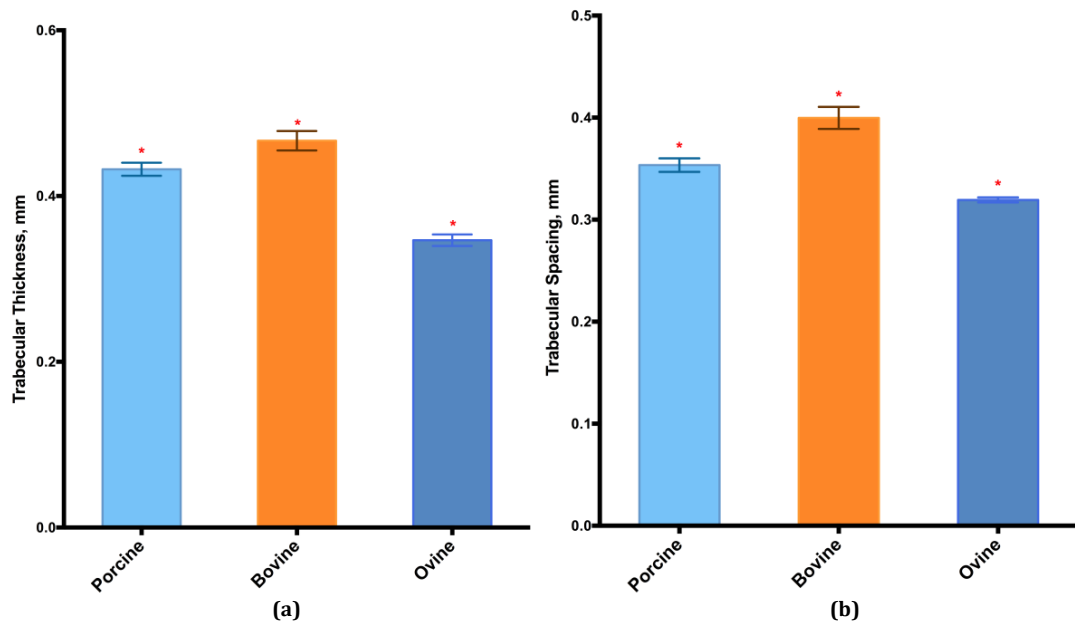


Figure 3-14 – (a) Mean trabecular thickness and (b) mean trabecular spacing for ovine, bovine and porcine specimens with error bars indicating standard errors of mean; the red asterisks indicates significant difference between each data group and other groups ( $p < 0.05$ ).

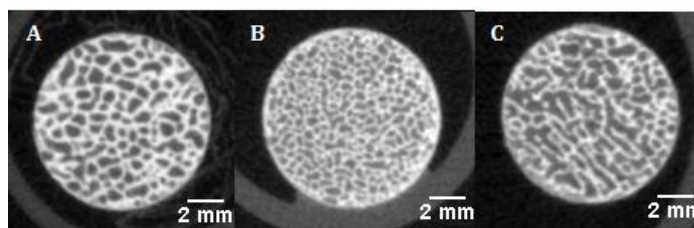


Figure 3-15 – Examples of CT images from the bone plugs for A-bovine, B-porcine and C-ovine femoral head tissue. It can be observed that porcine tissue has more densely packed trabeculae than bovine and ovine bone.

Images of the whole femoral heads for porcine and ovine tissue (Figure 3-16) show that trabecular arrangement is visually different between the two species. Another major difference between these tissue types is the growth plate in the centre of the porcine femoral head versus the growth plate in the neck of the ovine femur. The porcine femoral head is also more densely packed

near the surface of the femoral head whereas the ovine femoral head is equally structured throughout the head.

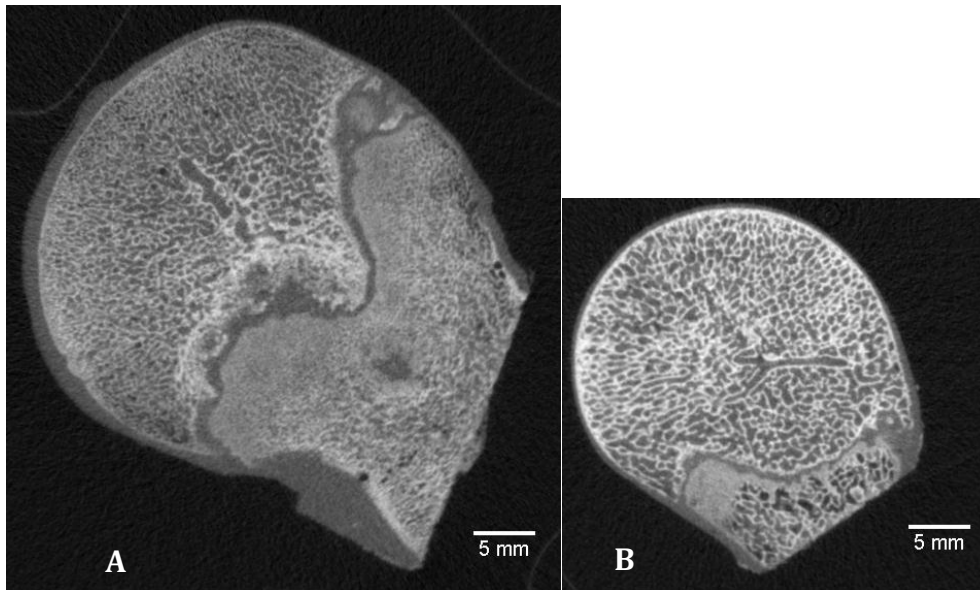


Figure 3-16 – Example images of A-porcine and B-ovine femoral head CT scans. The porcine femoral head is significantly larger than the ovine femoral head with a more densely packed trabecular structure than ovine tissue, in particular near the femoral head surface. A visible growth plate is seen in the centre of the porcine femoral head, however this is only seen in the femoral neck of the ovine sample.

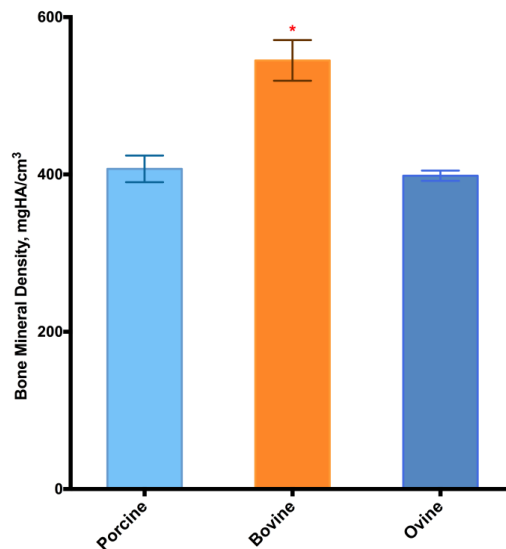


Figure 3-17 – Mean bone mineral density (BMD) for bovine, ovine and porcine specimens with error bars indicating standard errors of mean; the red asterisk indicates significant difference between data group ( $p < 0.05$ ). Bovine specimens had significantly different BMD when compared with other groups.

As well as a larger trabecular thickness and spacing, the bovine samples also demonstrated significantly larger BMD values when compared with ovine or porcine specimens (Figure 3-17).

### 3.3.2 Mechanical tests

Results of analysis of mechanical properties of bone from bovine, ovine and porcine tissues are presented in this section.

Elastic modulus was calculated for all analysed samples and the mean values along with range of values are presented in Figure 3-18. There were no significant differences between the means of the groups; however a very large range was observed for all samples, in particular for ovine samples (75-232MPa). The ovine samples also had a smaller mean elastic modulus when compared to porcine or bovine samples.

The mean yield stress (Figure 3-19) for the bovine samples was significantly higher than that of ovine or porcine samples. A large range in yield stress was seen in the ovine samples (4.7-16.7MPa) and bovine samples (18-28.6MPa). Similar findings were seen for the offset yield stress (Figure 3-20) and the work taken to yield the samples (Figure 3-21), where bovine samples showed significantly higher values than ovine or porcine tissue.

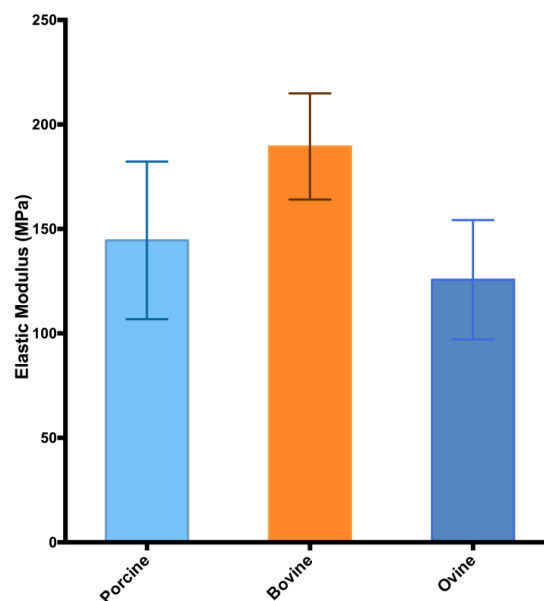


Figure 3-18 – Mean elastic modulus for ovine, bovine and porcine bone samples. Error bars are standard errors of mean. No significant differences were found between the data ( $P < 0.05$ ).

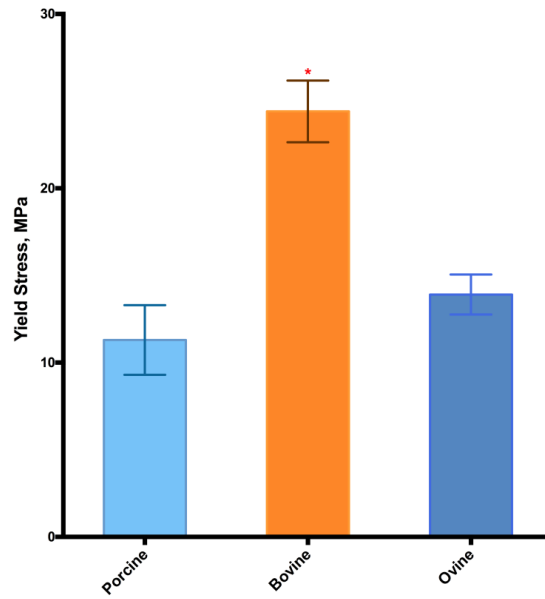


Figure 3-19 – Mean yield stress for ovine, bovine and porcine samples. The error bars are standard errors of mean and the red asterisk represents a significant difference with other groups ( $P < 0.05$ ). Bovine specimens had significantly different yield stress when compared with other groups.

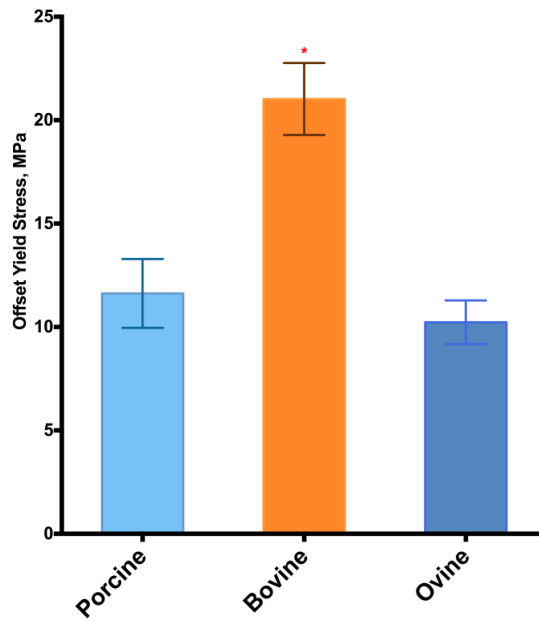


Figure 3-20 – Mean offset yield stress for the three animal tissue samples. The error bars are standard errors of mean and the red asterisk represents a significant difference with other groups ( $P < 0.05$ ). Bovine specimens had significantly different offset yield stress when compared with other groups.

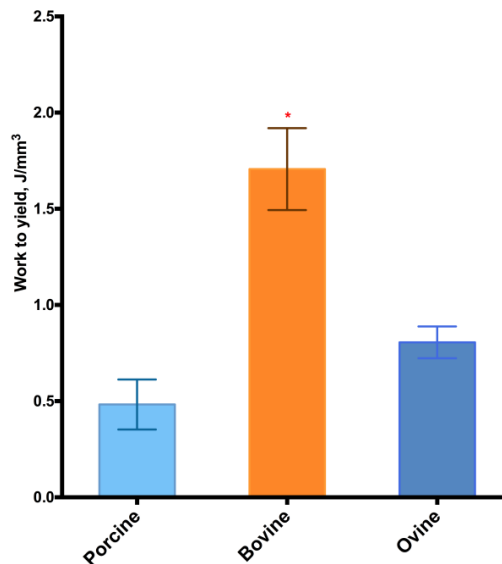


Figure 3-21 – Mean work to yield for the three animal tissue samples. The error bars are standard errors of mean and the red asterisk represents a significant difference with other groups ( $P < 0.05$ ). Bovine specimens had significantly different work to yield when compared with other groups.

Although all of the species groups had similar stiffness, it can be seen that the bovine samples were significantly stronger in compression and required more energy to yield than ovine or porcine samples.

### 3.4 Discussion

A previous study by Currey (1988) demonstrated that the mechanical properties of bone in bending and tension vary between animals of different species. In order to choose the right species for use in the final model of avascular necrosis, it is important to understand the differences between bones from various animals. In this study, bones from bovine, ovine and porcine tissue were analysed.

The findings of this study show that bovine samples were significantly stronger in compression than porcine or ovine samples. These findings correlated with the significantly higher bone mineral density, trabecular spacing and thickness found in bovine samples when compared to porcine or ovine samples. It was also noticeable that the bovine femoral heads were larger in size than ovine or porcine tissue (Taylor et al., 2011)(Figure 3-16). This is acceptable as bovine species are larger in size than porcine or ovine species.

There have not been any previous studies comparing the bone mass density or porosity of femoral head tissue between various animals. Hölzer et al. (2012) studied the differences in a series of microstructural parameters between human, ovine, bovine and porcine greater tubercle tissue and this data is presented in Figure 3-22. This study showed that human tissue had different trabecular separation and thickness when compared to the three animal species. Within the animal species, porcine tissue had the lowest trabecular spacing when compared with bovine and ovine tissue. Although the study by Hölzer agrees with this study that there are differences between trabecular structures of the three specimens, the reported variations are different to this study. This may be due to the tissue being obtained from different regions of the leg; in the case of the Hölzer study, from the greater tubercle of the humeri, a non-load-bearing region, whereas in this study they were taken from the load bearing region of the femoral head.

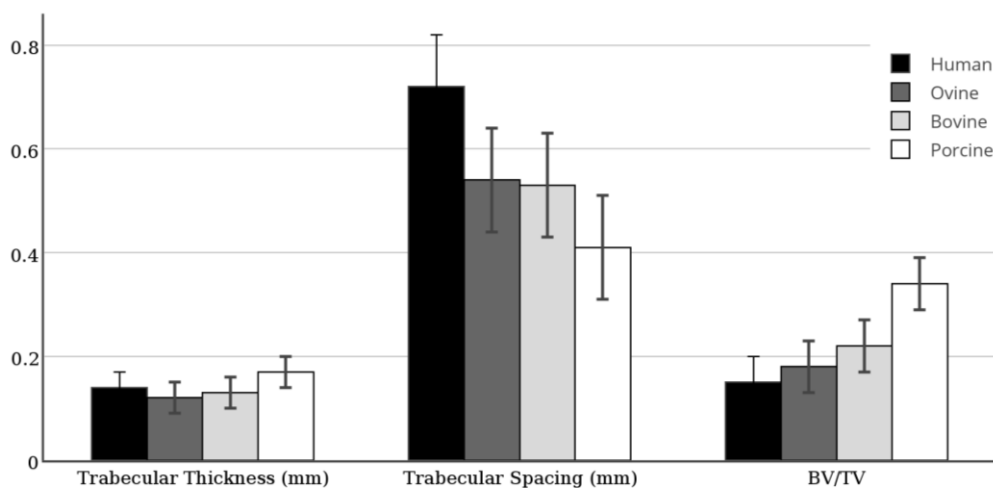


Figure 3-22 - Trabecular thickness and trabecular spacing as well as bone volume ratio (bone volume/total volume) comparison between human, ovine, bovine and porcine greater tubercle tissue in the subcortical region; Graph adapted from results of Holzer et al. (2012).

Another study by McLure (2012) showed that the bovine BMD was significantly higher than porcine and ovine BMD in the lateral femoral condyle and the tibial plateau, which agree with the findings of this study. There are no data regarding BMD interspecies changes for the femoral head. Since the porosity and BMD of the bone can affect the mechanical properties of bone (Friedman, 2006), it is important to understand these parameters in various species.



In this study, CT scan images of the samples were obtained prior to mechanical testing. This was done to calculate morphological properties such as porosity and BMD of the femoral head specimens, and make a cross-comparison between the bones from various species. The bovine specimens had higher BMD and as well as trabecular thickness and spacing than ovine and porcine samples. This correlated with the significantly higher yield stress and work taken to yield seen in bovine samples when compared to other specimens. This suggested that the bone mineral density and trabecular structure have a direct relationship with its mechanical properties.

Previously studies have shown that non-destructive imaging techniques that measure structural parameters and bone mineral density can be used to predict the strength of bone (Carter and Hayes, 1977; Li and Aspden, 1997; Kaneko et al., 2004). A study by Perilli et al., (2012) used dual energy X-ray absorptiometry (DXA) to measure bone mineral density in human spinal vertebrae, and they found that BMD was a good predictor of the ultimate load in the bone. Another study by Habu et al., (2012) compared BMD of osteoarthritic femoral heads measured by dual-energy X-ray absorptiometry (DXA) and quantitative computer tomography (QCT) with elastic modulus and found that the elastic modulus correlated with BMD measured using both techniques ( $r^2 = 0.69$  for DXA and  $r^2 = 0.73$  for QCT).

In the current study, plots of these parameters and bone mineral density were analysed. When all the samples were analysed there was no significant correlation between bone mineral density and elastic modulus ( $R^2 = 0.105$ ). The samples were then analysed individually, and again no correlation was seen between BMD and elastic modulus of ovine and bovine samples ( $R^2 = 0.086$  for ovine samples and  $R^2 = 0.00001$  for bovine samples). However, a correlation was seen for the porcine samples ( $R^2 = 0.530$ ) (Figure 3-23). When all the samples were analysed as one dataset, no correlation was seen between BMD and elastic modulus ( $R^2 = 0.105$ ).

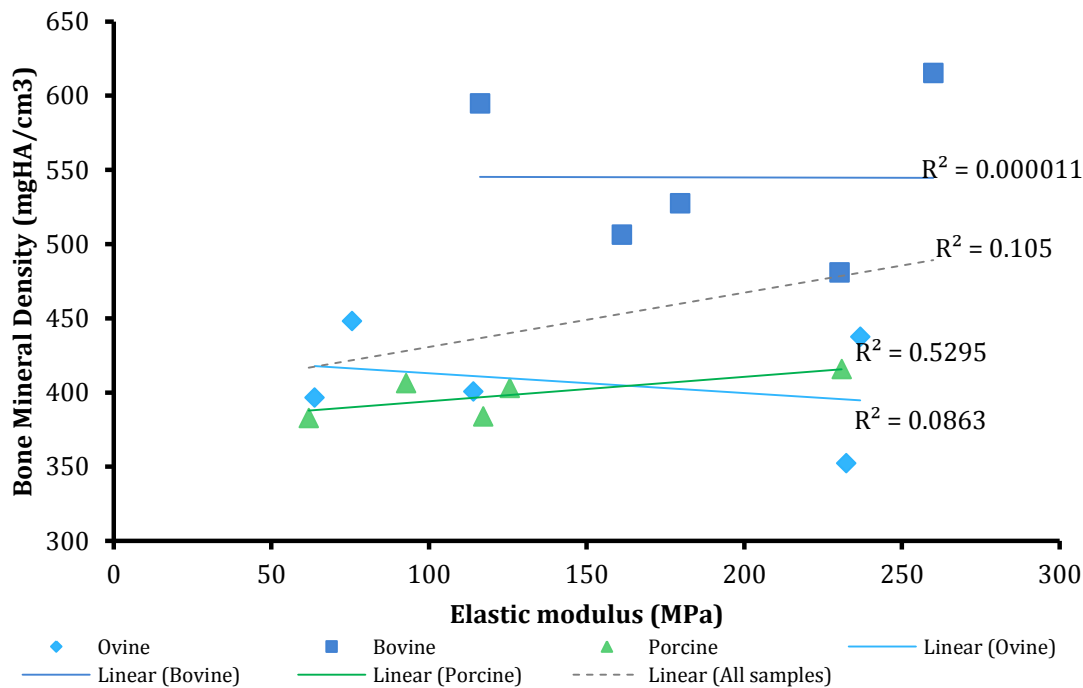


Figure 3-23 - The relationship between bone mineral density and elastic modulus for bone plug samples from the three species is shown in this figure. A regression line is fitted to each data set and all the samples combined, and R<sup>2</sup> values are shown next to each line.

A correlation was seen for BMD versus yield stress ( $r^2 = 0.5869$ ) and work to yield ( $r^2 = 0.614$ ), as shown in figures Figure 3-24 and Figure 3-25, however when these parameters were analysed for individual species groups, no correlations were seen except for the porcine BMD versus yield stress ( $R^2 = 0.449$ ). This means that although bone mineral density may be a possible tool for estimating the rough values for yield stress and work taken to yield, it is not very accurate for the bone samples tested in this study.

Previous studies in the literature have reported higher elastic moduli for human bone than those found in the animal tissues tested in this study. Martens et al., (1983) reported elastic modulus of  $900 \pm 710$  MPa and compressive strength of  $9.3 \pm 4.5$  MPa in human femoral head specimens. The strength values are comparable to those of porcine tissues analysed, however the elastic modulus is significantly higher in humans than the animal tissues in this study. A comparative study has been carried out on bone samples from the load bearing region of control human femoral heads and is reported in chapter 4.

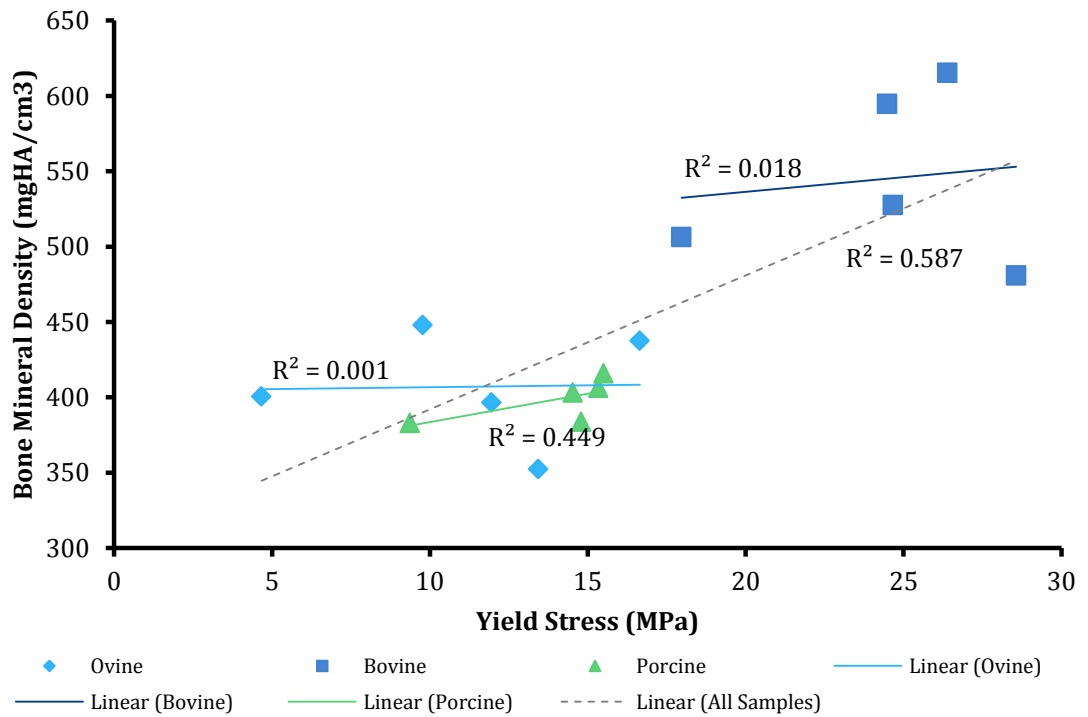


Figure 3-24 – The relationship between bone mineral density and yield stress for the bone plug samples from the three species, as well as the overall relationship for all samples. A regression line is fitted to each data set and all the samples combined, and R<sup>2</sup> values are shown next to each line.

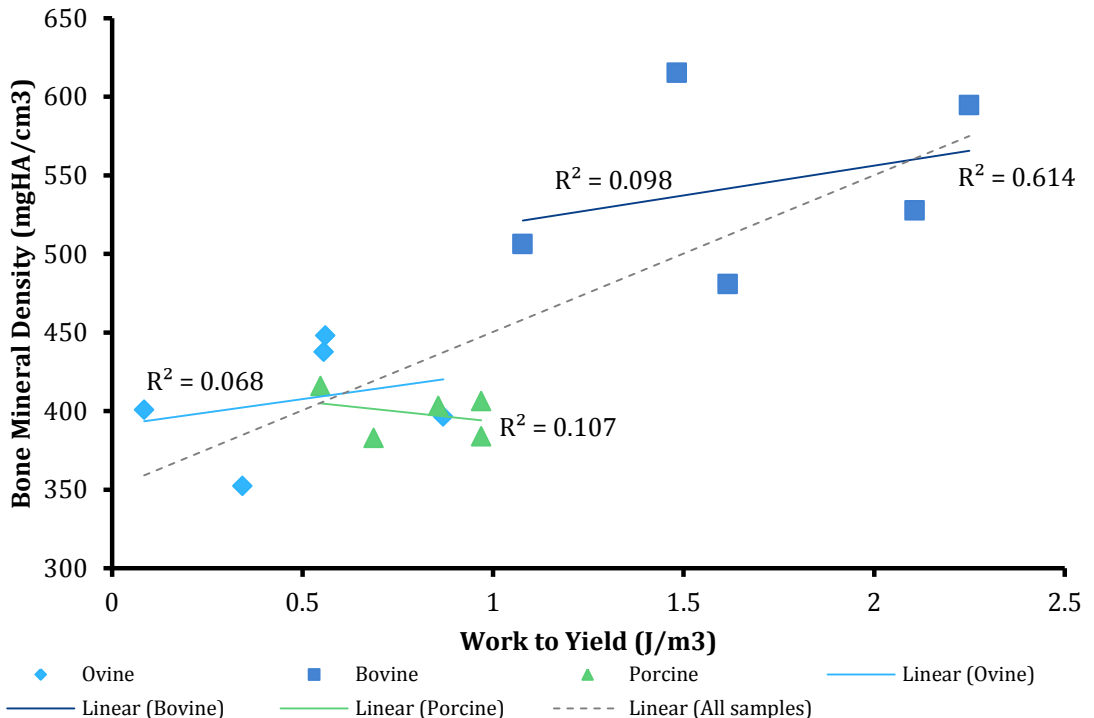


Figure 3-25 – The relationship between bone mineral density and work taken to yield for bone plug samples from the three species is shown in this figure. A regression line is fitted to each data set and all the samples combined, and R<sup>2</sup> values are shown next to each line.

For porcine tissue, the ages of the animals varied between 24-26 weeks at the time of slaughter- representing immature porcine tissue. According to Rasoulia et al., (2013), porcine bone reaches maturity at 2 years. A growth plate was visible in all porcine femoral heads tested in this study. The size and location of the growth plate was not analysed in this study and the bone plugs tested were taken from areas unaffected by the growth plate. Previous studies have characterised the growth plate and its mechanical properties (Sergier et al., 2009; Villemure and Stokes, 2009); however there have been no studies on the effect of the presence of the growth plate on the mechanical properties of the overall femoral head.

The aim of this study was to characterise femoral head bone from bovine, porcine and ovine samples and use the findings to choose a suitable species for use in a mechanical model of avascular necrosis. The factors that were considered were availability of tissue of constant age, sizes of the femoral heads in comparison with human femoral heads, morphology and mechanical properties of the femoral heads. It was reported that porcine femoral heads have a more similar diameter to those of human. Porcine tissue that is tested in this study also showed comparable compression strength to human femoral heads reported in literature (Martens et al., 1983). The availability of the animal tissue in the laboratories were also analysed, and it was found that bovine and porcine tissues were more available in a smaller age range compared to ovine tissue, which is seasonal.

### **3.5 Summary of Findings**

In order to establish the techniques for mechanical evaluation of bone, and to choose the suitable final species for the simulation model of avascular necrosis, CT images were obtained from bone plugs of porcine, ovine and bovine species and tested in compression. Following evaluation of the data, porcine tissue was found to be the most suitable tissue. The data obtained in this study will also be used as benchmark in Chapter 6 during development of a mechanical model of AVN.

## Chapter 4. Characterisation of Mechanical Properties of Femoral Heads with Avascular Necrosis

### 4.1 Introduction

AVN is a disease that initiates from biological disruptions within the hip and it progresses to a mechanical failure of the joint (Conzemius et al., 2002). In order to develop a valid mechanical model of AVN (Figure 4-1), the mechanical and structural properties of the tissue affected by this pathology need to be understood and compared with those of non-diseased femoral head tissue. This was to develop an understanding of the extent of mechanical damage caused in the femoral head tissue as a result of AVN, and to replicate this damage extent *in vitro*.

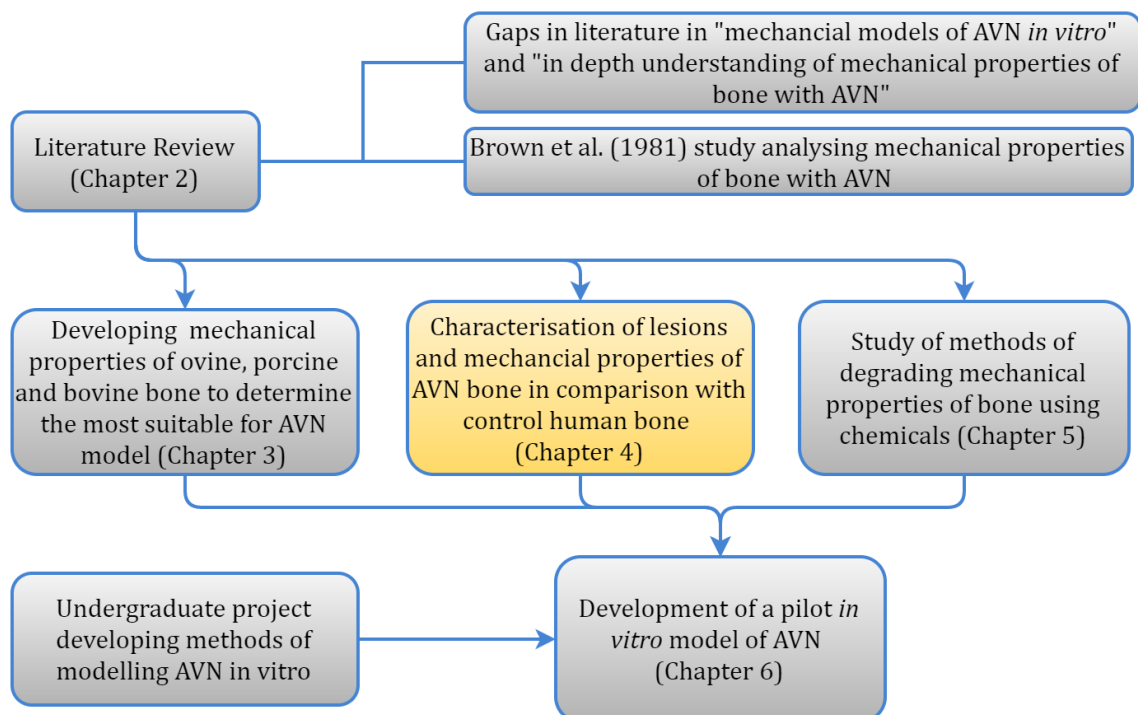


Figure 4-1 – Summary of work leading to development of a mechanical model of AVN, with current chapter highlighted in yellow.

The mechanical changes that occur following onset of AVN are not researched thoroughly. A study by Brown et al. (1981) assessed the mechanical properties of cubical bone specimens from different regions of femoral heads affected by AVN

and they found that necrotic regions had significantly lower yield strength (reduced by 52%) and elastic modulus (reduced by 72%) when compared to non-pathological bone tissue. The study was carried out on nine osteonecrotic femoral heads and the findings were compared with spatially matched data from control non-pathological femoral heads. A limitation in the study was that the mechanical properties were not compared to the radiological degradation observed with AVN. It was also assumed that the necrotic regions were limited to the proximal-medial side of the femoral head and all cubic samples were grouped into either “necrotic”, “sclerotic” or “non-pathological” based on visual observations.

Since the study by Brown et al. (1981), there have been no further reported research into characterisation of mechanical properties of femoral head bone with AVN.

This study aimed to characterise the mechanical and structural properties of bone with AVN and to compare the findings with the properties of control human tissue. To do this, a series of objectives were produced, and these are summarised in Figure 4-2.

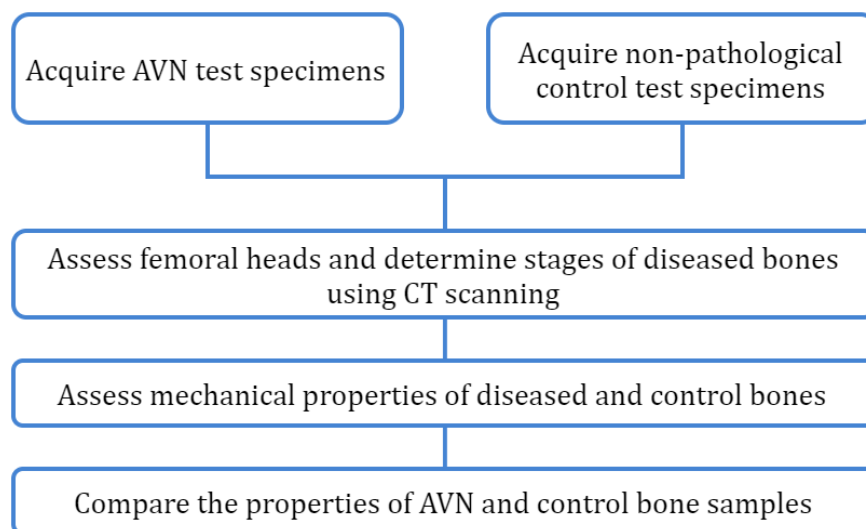


Figure 4-2 – Summary of objectives of this study to characterise bone with AVN.

## 4.2 Materials and Methods

In order to understand the mechanical and structural properties of AVN femoral head tissue, AVN human femoral head specimens as well as a set of control femoral heads were obtained. CT imaging of specimens was carried out and the specimens were tested in compression to obtain mechanical properties.

The specimens in this study were obtained from two different sources: the AVN samples were from patients undergoing THR for AVN in Xi'an, China and the control tissues were obtained from a human tissue bank. Since the AVN tissues could not be transported to United Kingdom for tests, the experimental work on these tissues was also carried out in Xi'an, China. Although the AVN samples were tested in a different location to control femoral heads using different equipment, as many parameters as possible were kept constant between the two sets of experiments, to maintain the comparability of the data groups. A summary of the methods applied to studies on AVN and control samples is shown in Figure 4-3.

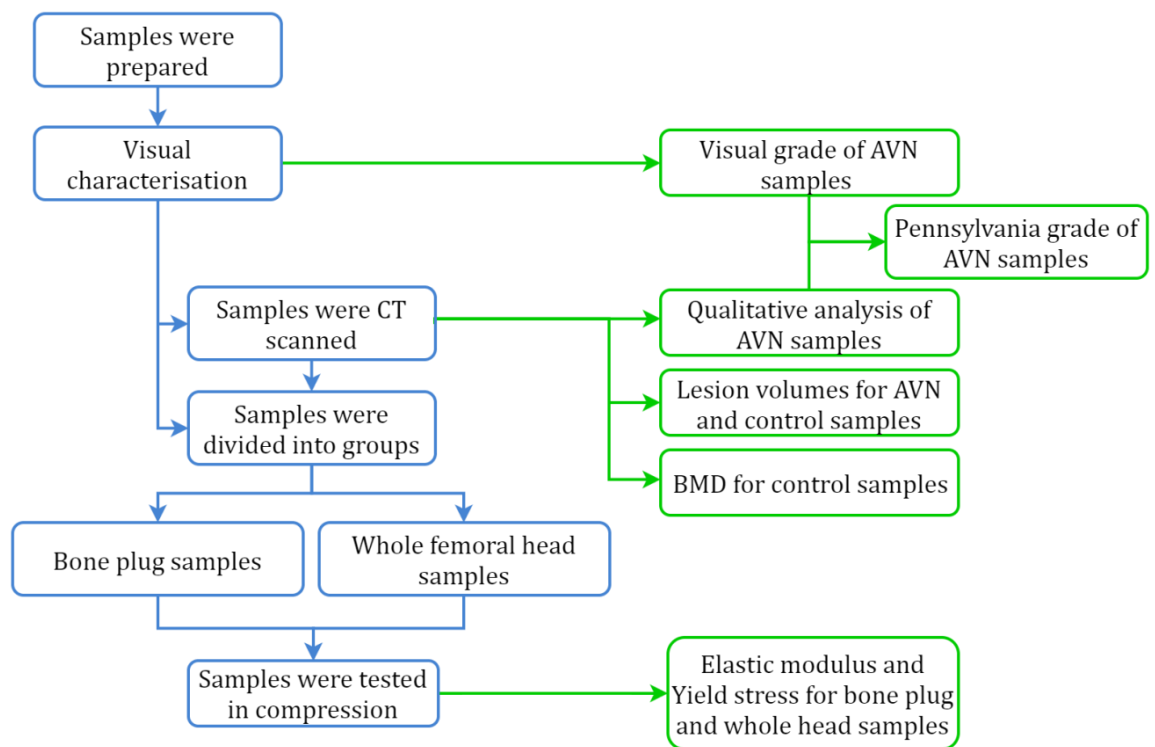


Figure 4-3 – Flow diagram demonstrating the experimental path for samples, and the outputs from each test for both AVN and control sets of samples.

## 4.2.1 Assessment of Properties of AVN Femoral Heads

### 4.2.1.1 Specimen Acquisition

In order to characterise the mechanical and structural properties of bone with AVN, whole femoral head specimens with AVN were required. These could have been collected in surgery from AVN patients undergoing total hip replacement. An attempt was made to contact orthopaedic surgeons in United Kingdom in order to receive AVN specimens, however due to the small number of AVN cases in UK (2%

of 80,642 THR cases during 2014 (NJR, 2015)) and time constraints on the PhD project, a sufficient number of specimens could not be collected. Since AVN is more prevalent in East Asia, Chinese hospitals were considered.

Professor Zhongmin Jin at Xi'an Jiaotong University was contacted, and a collaborative agreement was set up between University of Leeds, Xi'an Jiaotong University and its affiliated hospitals. The agreement included collection of femoral head specimens from patients undergoing total hip replacement for AVN by surgeons at Xi'an Affiliated Hospitals. The specimens were then transferred to Xi'an Jiaotong University, where they were stored and tested.

A summary of the collection, storage, test and disposal process the specimens underwent is shown in Figure 4-4.

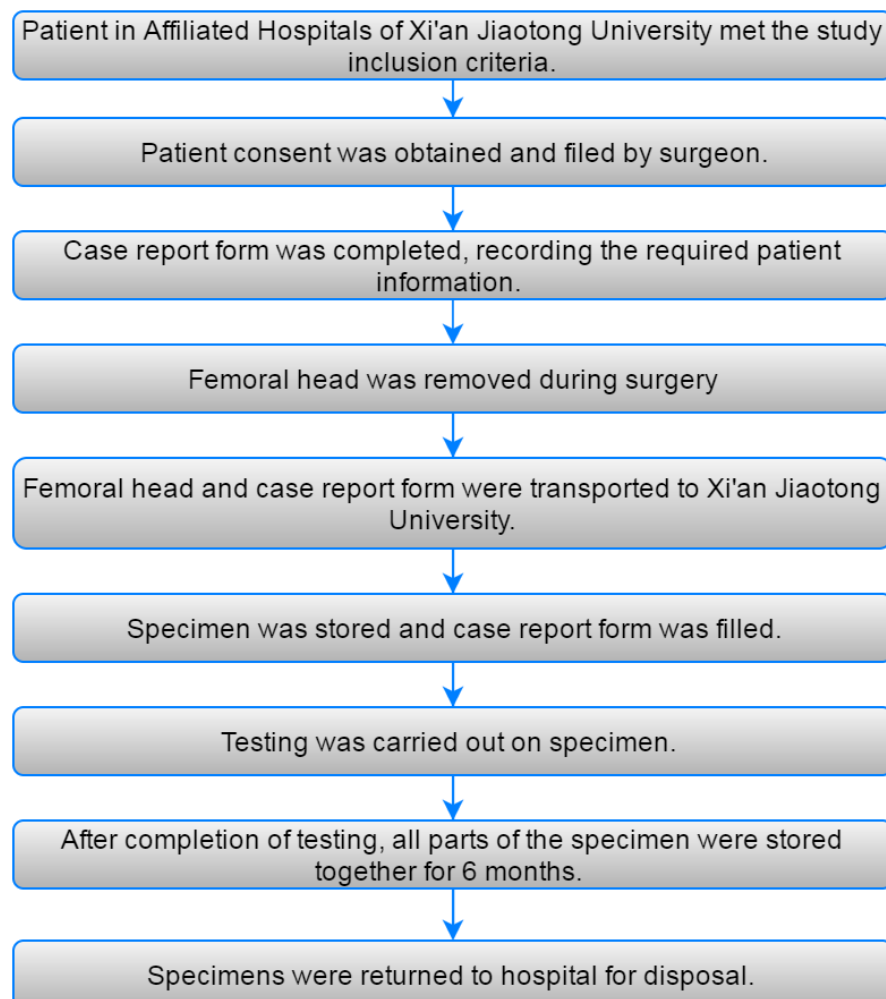


Figure 4-4 - Flow diagram showing a summary of the collection, storage, test and disposal process the AVN specimens underwent in this study.



#### 4.2.1.2 Ethics

Since the AVN specimens used in this study were obtained from human subjects, an ethics proposal was prepared and submitted to University of Leeds Ethics Committee for approval. Following approval (MEEC 13-001), the proposal was translated to Mandarin Chinese and submitted to the ethics committee for Xi'an Jiaotong University Affiliated Hospitals, and received approval (Approval no. KYLLSL-2014-002-01).

The ethics proposal (Appendix D) included a detailed protocol for patient selection, approaching patients and obtaining consent. It also included transport, storage and disposal methods as well as protocol for appropriate handling of the specimens.

#### 4.2.1.3 Specimen Collection

A set of inclusion and exclusion criteria (Table 4-1) were defined in the ethics protocol and followed for the collection of specimens. Patients who met all inclusion criteria and none of the exclusion criteria were approached by the surgeons at Xi'an Jiaotong University Affiliated Hospitals for informed consent. Specimens were collected during surgery from the patients who had consented to take part in the study.

Table 4-1 – Inclusion and exclusion criteria used for patient selection for collection of AVN samples. In order for patients to be eligible for this study, they were required to meet all of the inclusion criteria and none of the exclusion criteria.

Inclusion criteria	<ul style="list-style-type: none"><li>• Male or female subjects aged 18 years or above and skeletally mature at the point of screening for participation</li><li>• Subjects with avascular necrosis of the femoral head</li><li>• Subjects undergoing total hip replacement procedure as part of their standard treatment routine</li><li>• Subjects who were able to give voluntary, written informed consent to participate in this clinical investigation</li></ul>
--------------------	--

Exclusion criteria	<ul style="list-style-type: none"><li>• Subjects who, in the opinion of the Clinical Investigator, had an existing condition that would compromise their participation in this study.</li><li>• Subjects who had previously undergone any type of surgery for avascular necrosis in the affected hip</li><li>• Subjects who had marked atrophy or deformity in the upper femur</li><li>• Subjects who were unable to give informed consent</li><li>• Subjects with transmissible diseases</li><li>• Subjects with active local or systemic infection</li></ul>
--------------------	--

Twenty femoral head specimens were collected from patients diagnosed and undergoing total hip replacement surgery due to AVN of the femoral head. They were provided as proximal parts of femurs as removed during surgery. The femoral heads were cut at the femoral neck using a saw and a corkscrew was placed in the inferior side of the femoral head to remove it. This resulted in a cavity in the femoral head (Figure 4-5). Although this potentially affected the integrity of specimens received, it was part of the surgical procedure and could not be altered.

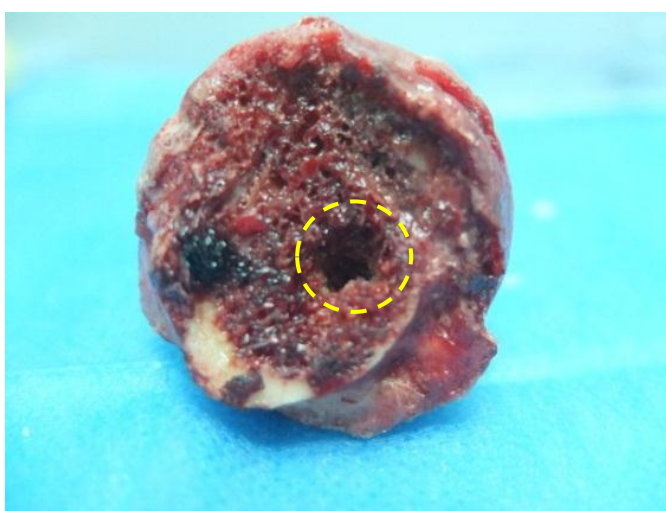


Figure 4-5 - Human femoral head (Sample 02) with AVN removed at the surgery (approximately 35mm diameter). Cavity created in the inferior position of the head during removal of the femoral head in surgery is marked by dashed circle.

The specimens were collected over a period of 13 months, between February 2014 and March 2015. The first eight specimens were analysed in October 2014 and the further 12 specimens were analysed in April 2015.

The surgeons completed a case report form for each collected specimen. This included:

- The side of the hip
- Age
- Gender of patient
- Mass and height at surgery
- Dates of surgery
- Date of first onset of pain
- The date the patient first presented to the clinician with hip pain

#### 4.2.1.4 Specimen Transport and Storage

After collection at surgery, the specimens were placed in protective packaging to transfer to Xi'an Jiaotong University. This packaging included an inner sealed bag and an outer sealed bag, which were placed inside a temperature controlled box with ice-bags to prevent degradation of the specimens. The specimens were transported to the Institute of Advanced Manufacturing Technology (iAMT) in Xi'an Jiaotong University, where the sample inside the inner sealed bag was stored in a freezer at -20°C for 1-33 weeks until testing. Specimens were thawed in a refrigerator (5°C) for up to 15 hours before testing. Samples were also stored for 1-3 days between tests under similar conditions. If there were gaps of more than three days between tests, they were placed back into the freezer for storage until further use.

#### 4.2.1.5 Risk Assessment

The experiments were carried out in the Bio-fabrication Laboratories of iAMT in Xi'an Jiaotong University, Xi'an, China. As the laboratory did not have the practices that are inherent in the culture in the University of Leeds when conducting experimental work and in order to prevent incidents as well as maximise efficiency of the experimental work due to cost and time constraints, a risk assessment was prepared (Appendix E).

To prepare the risk assessment, the hospital, laboratories and the work offices of iAMT where the work was to be carried out were visited. During this visit, any potential risks of working in a foreign laboratory were highlighted, and any needs for extra test equipment or fixtures were noted.

#### 4.2.1.6 Visual Characterisation

Specimens were characterised visually following thawing. Photographs were taken of the specimens using a digital camera (Fujifilm X10, Tokyo, Japan) and a severity grade as detailed in Table 4-2 was given to the specimens based on their appearance from photographs. This rating was used for assignment of specimens to different test methods. Specimens were also photographed and heights and diameters of the femoral heads were measured.

Table 4-2 - Grading criteria used for visual inspection of the femoral heads

<b>Grade</b>	<b>Condition</b>
<b>1</b>	No or little visible damage to femoral head
<b>2</b>	Some visible damage to articular surface
<b>3</b>	Deformed shape of femoral head
<b>4</b>	Severe damage to head

Following receipt of CT images of the samples, they were also graded using the Pennsylvania grading system (Steinberg et al., 1995). This method took into account the severity of the articular surface as well as the lesions present in the femoral head. This grading was used in further grouping of samples during data analysis.

#### 4.2.1.7 Specimen Fixation for CT Scanning and Mechanical Testing

All specimens were prepared for mechanical fixation following the method explained in section 3.2.6. Since the femoral heads were already separated from the rest of the femur as part of the surgical procedure explained in section 4.2.1.3, most of the specimens did not require further dissection. A handheld saw was used

to create a flat surface on the distal part of the femoral head and to remove excess bone where required.

To prevent movement during CT scanning as a result of rotation of specimen, all femoral specimens were fixed into a cylindrical mould designed to fit within the internal dimensions of the CT scanner fixture. They were fixed using poly methyl methacrylate (PMMA). To prepare the mould, petroleum gel (Vaseline, Surrey, UK) was applied to the inner walls and base to prevent the PMMA from adhering to the cylindrical mould. The PMMA resin (Denture base resin type II, Shangchi, Shanghai Medical Devices Co., Ltd., Shanghai, China) consisted of a powder and liquid part. To prepare the resin, a powder to liquid ratio of 2:1 was measured (e.g. 20g of powder for every 10ml of liquid) and combined to make up the required volume. Initially, a small amount of resin was poured into the mould, up to 5mm, and left to set for about 30 minutes. The inferior part of the specimen was then placed in the cylindrical mould above the first layer of resin and more PMMA resin was poured around the specimen, between 5-10mm. The resin was left to set for up to one hour, and removed from mould when set (Figure 4-6). Care was taken to ensure the specimens did not dehydrate by placing a tissue soaked in PBS over the specimen when possible. In between testing, specimens were wrapped in tissue paper soaked in PBS and packaged in plastic wrapping.

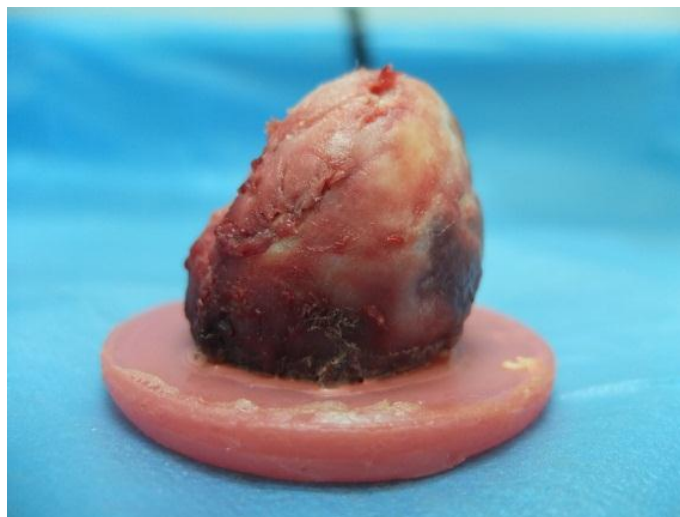


Figure 4-6 - A whole femoral head sample (Sample 11, medial lateral view, diameter approximately 52mm) fixed distally in PMMA cement.

#### 4.2.1.8 Specimen Groups

Following grading by visual inspection (explained in section 4.2.1.6), specimens from all grades were divided into whole femoral head test group and bone plug test group. The specimens were divided depending on their severity grade (Table 4-2), and also the overall condition of the femoral head –i.e. whether bone plugs could be removed from the damaged surface of the femoral head. In cases where bone plug removal was not possible, specimens were allocated to the whole head group; hence more specimens from visual grade 4 were allocated to whole head testing.

#### 4.2.1.9 Whole Femoral Head Preparation

Whole femoral head specimens did not require further preparation after the fixation as detailed in section 4.2.1.7.

#### 4.2.1.10 Bone Plug Preparation

Multiple bone plug specimens for mechanical testing were prepared from each femoral head. The bone plugs were removed from defined zones where possible as shown in Figure 4-7 and Figure 4-8. In some of the femoral heads, due to size or condition of the bone, bone plugs could not be removed from all areas, and were only removed from areas where it was possible to do so.

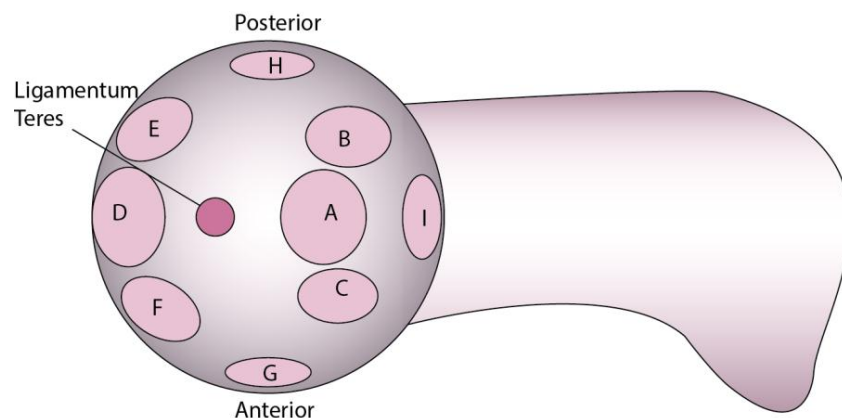


Figure 4-7 – Schematic of a femoral head. The locations where bone plugs were removed from the femoral head with respect to anterior and posterior directions and ligamentum teres. All bone plugs were taken as 9mm cylindrical specimens, and for demonstration purposes, they are shown as elliptical shapes due to perspective and depending on location of sample. (Schematic not to scale).

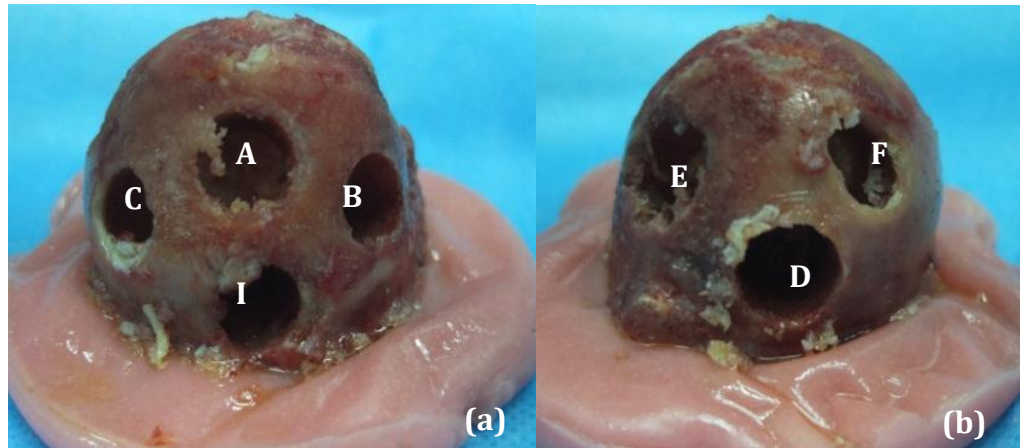


Figure 4-8 – Images showing a femoral head specimen removed at surgery following removal of bone plugs. The locations from which the bone plugs were removed are demonstrated (a) laterally and (b) medially. Letters A-I correspond to Figure 4-7. Locations for bone plugs G and H are not shown in these images and are shown on Figure 4-7.

Bone plugs were removed using a custom-made stainless steel corer with cutting teeth (Figure 4-9) and an internal diameter of 9mm. The smooth end of the cutter was attached to an electric drill, which allowed for rotation of the corer into the bone to cut the bone plug. A different bone plug corer with smooth cutting end was then placed in the cut out area and a swinging motion was applied to the bone to fracture the distal end of the bone plug. This allowed for removal of the bone plug using the corer, and a rod was used to push out the bone plug. The bone plug was then placed in a tissue soaked in PBS and placed in a vial for storage.

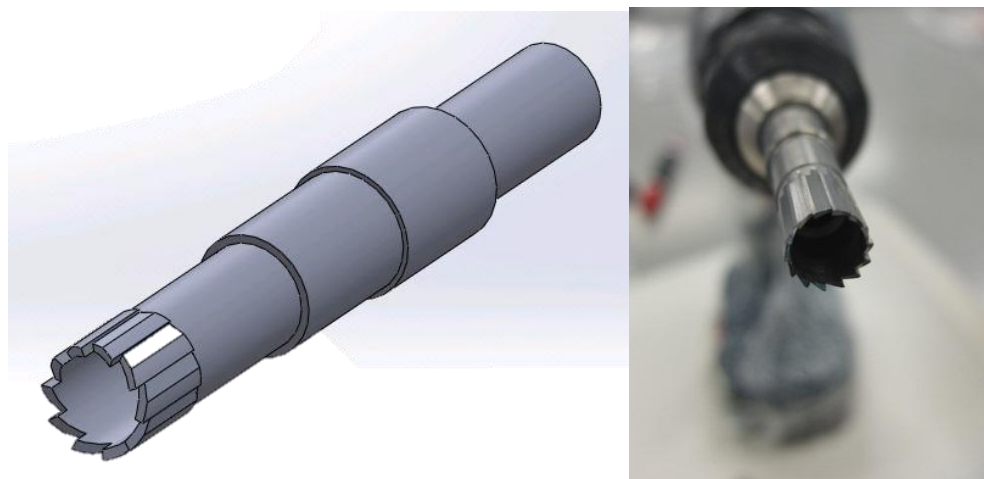


Figure 4-9 – Left: Schematic of a bone corer with serrated cutter teeth (lower portion) and internal diameter of 9mm used for removal of bone plugs. The smooth end (upper portion) was used to fix to an electrical drill. Right: The bone corer attached to a drill for removal of bone plugs.

#### 4.2.1.11 Computer Tomography Scanning

The CT scanner (Y-Cheetah Microfocus X-ray System, YXLON, Germany) that was used for scanning AVN femoral head samples consisted of a stationary source and detector with a rotating object holder as shown in Figure 4-10.

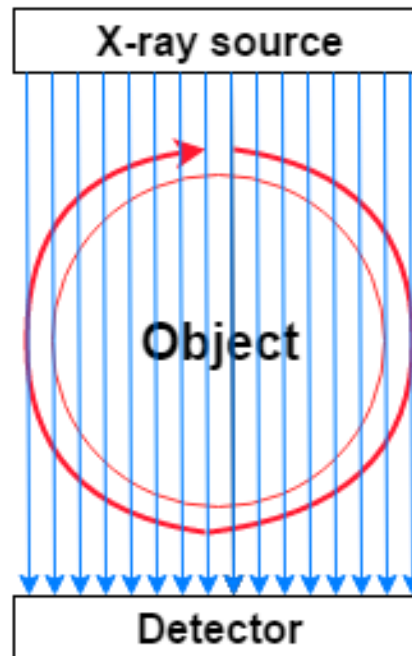


Figure 4-10 – Diagram demonstrating the relation of object to the source and detector in the CT scanner. The X-ray source applies X-rays towards the detector, and the object that is placed between the source and detector rotates, producing cross-sectional images of the object.

In order to secure the specimens on the rotating object holder, a fixture was required. The fixture (Figure 4-11) was made using Polyether ether ketone (PEEK), which is a radio-opaque material to allow for CT imaging of the specimen. It was designed to fit the dimensions of the attachment part of the rotating object holder of the CT scanner in the iAMT, and it also provided a lidded enclosure to prevent leakage of fluids from human tissue into the CT scanner and maintenance of the hydration of the specimens. The fixture had the same internal diameter as the fixation mould used in section 4.2.1.7, which meant that the PMMA fixed samples fitted into the fixture for CT scanning.



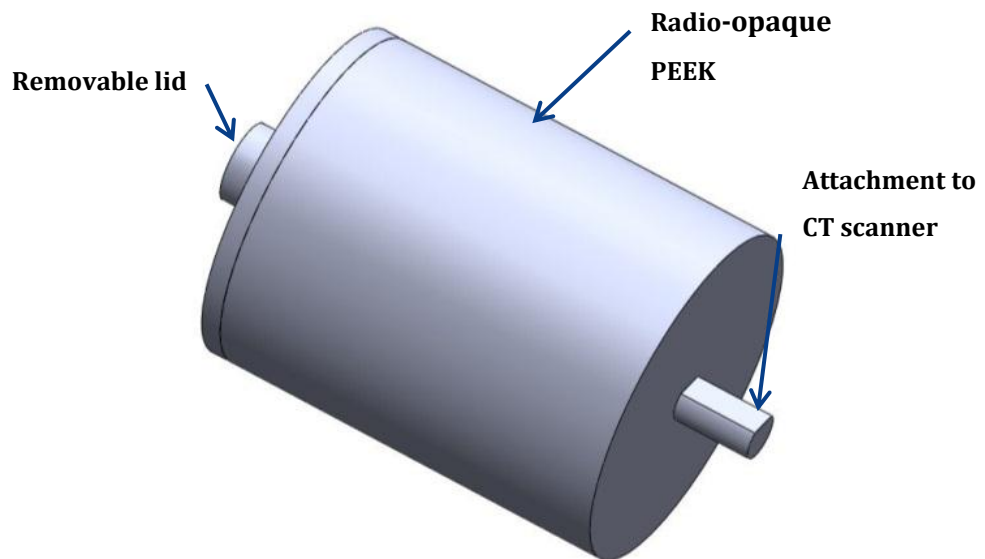


Figure 4-11 – The PEEK fixture designed and developed in house to hold human tissue specimens in the CT scanner at iAMT.

Following potting in PMMA cement, specimens were placed in the CT fixture, and the cemented part was secured onto the base of the cylinder using double sided tape. The scanning fixture holding the specimen was placed in the CT scanner. Initially, a scout view of the specimen was generated from the scanner, showing a longitudinal scan of the core, to select the femoral head in the built-in software of the scanner as “area of the interest” for scanning (Figure 4-12). The cross sectional images of the specimen were captured by the CT scanner by rotation of the specimen between the X-ray beam and detector (Figure 4-10) using a resolution of  $67.8\mu\text{m}$  per pixel. The images were exported as .RAW and .DICOM files and saved for further analysis.

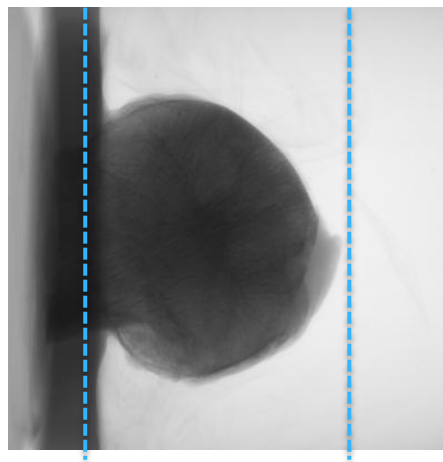


Figure 4-12 - An example scout view image from the CT scanner, of the femoral head used to select the “area of interest” for scanning, as demonstrated using blue dashed lines.

#### 4.2.1.12 Mechanical Characterisation

##### Development of Test Fixtures

The facilities available in Xi'an Jiaotong University provided a mechanical testing machine with a load cell capable of up to 5kN in compression, which was estimated as an insufficient capability. Due to limitations in the facilities available in the university in Xi'an and the possibility of loads higher than 5kN being required, alternative methods were sought for mechanical testing of human femoral heads with AVN. A fixture incorporating a lever system was designed to increase the load applied by the machine.

In order to design the fixture, moments analysis (Figure 4-13) was carried out to calculate the maximum deflection in the lever based on the assumed beam length and material properties (McKenzie, 2013).

A ratio of 2:1 was used for  $a:L$ , where  $a$  is the distance between femoral head and loading point and  $L$  is distance between femoral head and lever end point,  $A$ .  $P$  is the load applied by the testing machine and  $B$  is the load applied onto the specimen.  $R$  is the reaction load at the point specified. The calculations assumed use of Stainless Steel 316 as the material for the beam (AK-Steel, 2007).

Table 4-3- Details of assumptions made for moments analysis of the lever system used to multiply applied load (assuming use of stainless steel 316), for compression tests of femoral heads.

<b>Young's modulus, E</b>	200GPa
<b>Breadth, b</b>	40mm
<b>Depth, d</b>	40mm
<b>Length, L</b>	40mm
<b>a</b>	80mm
<b>Load applied by machine, P</b>	5kN

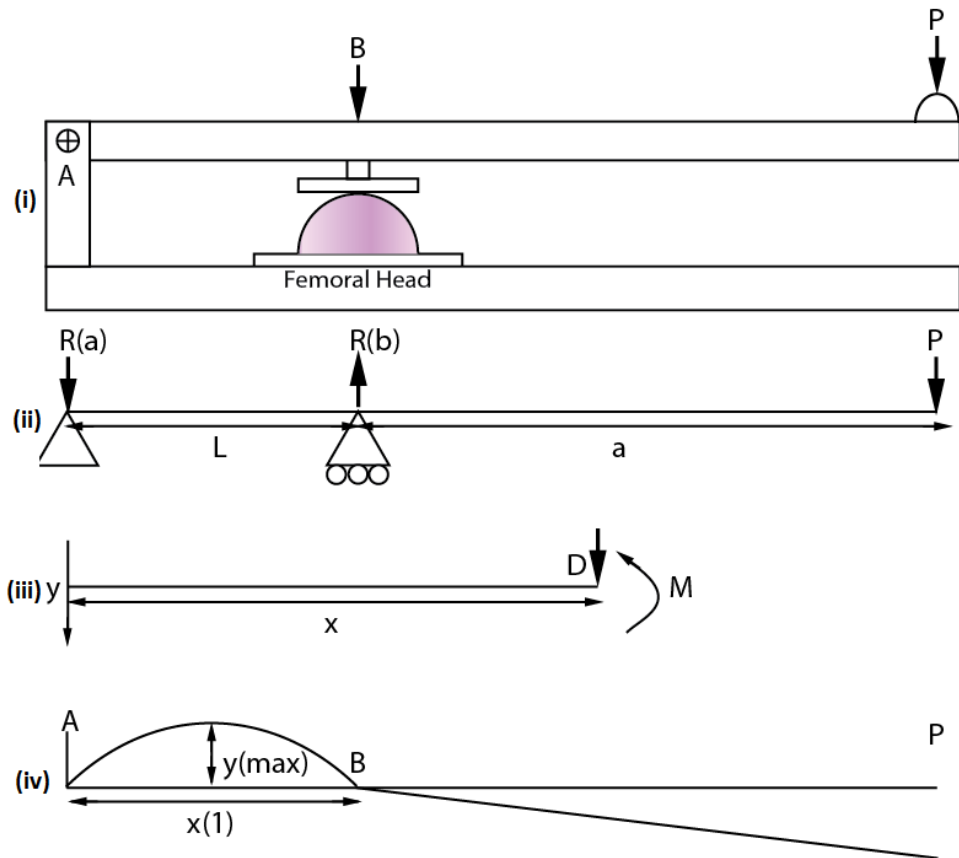


Figure 4-13 - Moment diagrams for the mechanical testing lever system that was designed for experiments. (i) A simple sketch of the system, showing the location of the femoral head and supports A and B. (ii) Reaction loads R(a) and R(b) in the supports. (iii) Deflection (D) and moment (M) in the system, (iv) Location for maximum deflection - y(max).

The second moment of area (I) for the beam was calculated using Equation 4-1. The reaction forces  $R_A$  and  $R_B$  at points A and B (Figure 4-13) are given using Equation 4-2 and Equation 4-3. The bending moment is given in Equation 4-4. Integrating this twice, first in Equation 4-5 and then in Equation 4-6, and substituting the values at Equation 4-7, and with further rearranging of equations (Equations 4.8 to 4.13),  $y_{max}$ , the maximum deflection at point P can be found using Equation 4-14. The maximum deflection ( $y_{max}$ ) in this system was found to be  $7.22 \times 10^{-4}mm$  with application of 5kN load at point P, which is considered negligible in comparison to the strains applied in this study. This lever system also allowed for the load to be magnified on application to the specimen, by increasing the applied load (P) to the load at application point ( $R_B$ ).

$$I = \frac{bd^3}{12} = \frac{40 \times 40^3}{12} = 213333mm^2 \quad \text{Equation 4-1}$$

$$R_A = P \frac{a}{L} = 2P = 10kN \quad \text{Equation 4-2}$$

$$R_B = P \left(1 + \frac{a}{L}\right) = 3P = 15kN \quad \text{Equation 4-3}$$

$$M = -\frac{Pax}{L} = -2Px = EI \frac{d^2y}{dx^2} \quad \text{Equation 4-4}$$

$$EI \frac{dy}{dx} = -\frac{1}{2}P \frac{a}{L}x^2 + c_1 \quad \text{Equation 4-5}$$

$$EIy = -\frac{1}{6}P \frac{a}{L}x^3 + c_1x + c_2 \quad \text{Equation 4-6}$$

$$\text{At } x = 0, y = 0 \rightarrow c_2 = 0 \quad \text{Equation 4-7}$$

$$\text{At } x = L, y = 0 \rightarrow EI(0) = -\frac{1}{6}P \frac{a}{L}L^3 + c_1L \Rightarrow c_1 = +\frac{1}{6}PaL \quad \text{Equation 4-8}$$

$$EI \frac{dy}{dx} = -\frac{1}{2}P \frac{a}{L}x^2 + \frac{1}{6}PaL \Rightarrow \frac{dy}{dx} = \frac{PaL}{6EI} \left[1 - 3\left(\frac{x}{L}\right)^2\right] \quad \text{Equation 4-9}$$

$$EIy = -\frac{1}{6}P \frac{a}{L}x^3 + \frac{1}{6}PaLx \Rightarrow y = \frac{PaL^2}{6EI} \left[\frac{x}{L} - \left(\frac{x}{L}\right)^3\right] \quad \text{Equation 4-10}$$

$$\frac{dy}{dx} = 0 \Rightarrow 0 = \frac{PaL}{6EI} \left[1 - 3\left(\frac{x_1}{L}\right)^2\right] \quad \text{Equation 4-11}$$

$$x_1 = \frac{L}{\sqrt{3}} = 0.577L \quad \text{Equation 4-12}$$

$$\frac{x_1}{L} = 0.577 \quad \text{Equation 4-13}$$

$$y_{max} = \frac{PaL^2}{6EI} [(0.577 - (0.577)^3)] \quad \text{Equation 4-14}$$

$$y_{max} = 0.0642 \frac{PaL^2}{EI} \quad \text{Equation 4-15}$$

$$y_{max} = \frac{0.0642 \times 5 \times 60 \times 40^2}{200 \times 213333} = 7.22 \times 10^{-4} \text{mm} \quad \text{Equation 4-16}$$

### Terms in equations 4-1 to 4-16

I	Moment of inertia	R <sub>B</sub>	Reaction force at point B
b	Breadth	M	Bending moment
d	Depth	x	Point on beam
R <sub>A</sub>	Reaction force at point A	y	Point on beam
P	Applied force	c	Equation constants
a	Distance between R <sub>B</sub> and P	E	Young's modulus
L	Distance between R <sub>A</sub> and R <sub>B</sub>	y <sub>max</sub>	Maximum deflection

The design of the fixture was started following confirmation through calculations in equations 4-1 to 4-16 that the maximum deflection in the beam of the fixture was negligible and that the load applied by machine at P would be magnified by about 3 times at application onto specimen. The fixture (Figure 4-14) was designed using Solidworks 2014 (Dassault Systèmes SOLIDWORKS Corp., Waltham, Massachusetts, USA) as an assembly of seven parts made of stainless steel grade 316. The support (part 4 in Figure 4-14) was secured onto the base (part 3 in Figure 4-14) using three M16 bolts. The base of the fixture was secured to the mechanical testing machine using the 16mm hole in the centre of the base and an M16 bolt (Figure 4-15). A threaded nut (Part 6 in Figure 4-14) was placed around the threaded loading part (part 1 in Figure 4-14), and was used to adjust the height of the loading part when placing specimens. In the final part assembly, in order to hold the top part (part 2 in Figure 4-14) above the sample during set up, a rod was glued to the base and a removable spring was placed around the rod. The rod and the spring that were removed during testing can be seen in the final fixture in Figure 4-15.

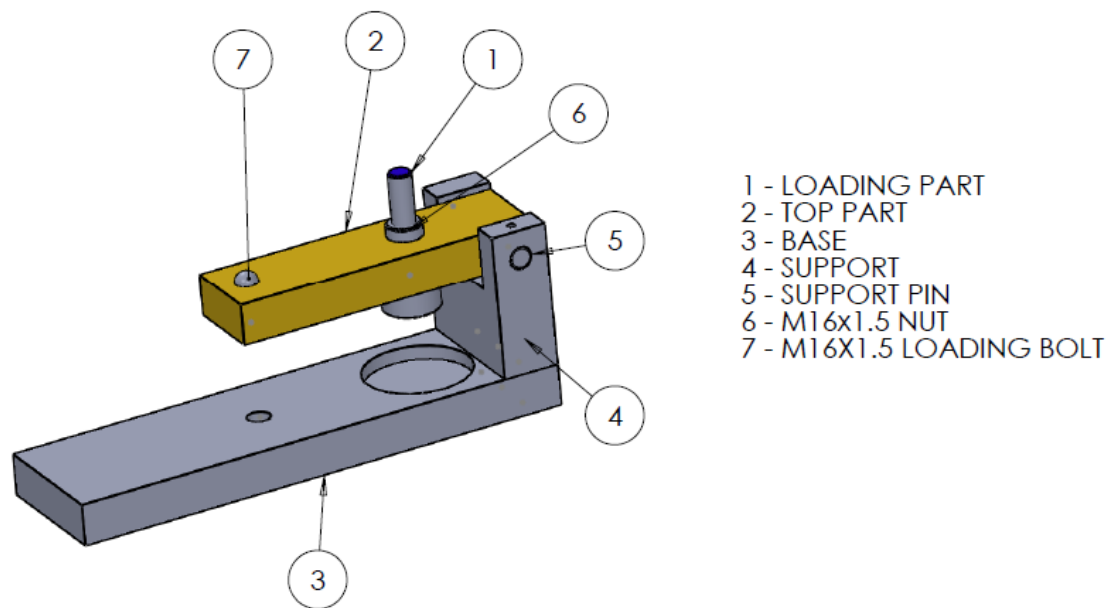


Figure 4-14 – Diagram showing the assembly model of the loading fixture used to magnify the load applied by mechanical testing machine onto the sample, with annotations showing the individual parts of the fixture. The drawings can be found in Appendix E.

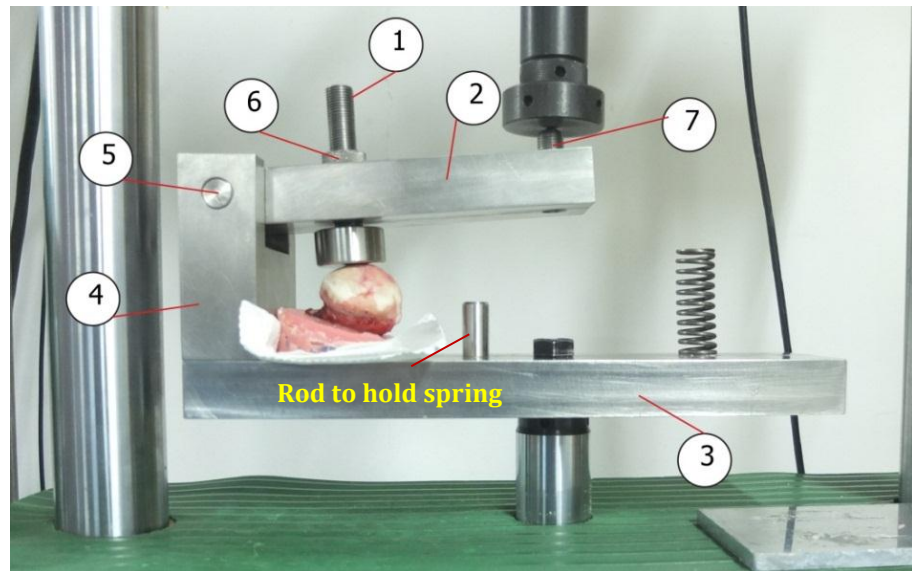


Figure 4-15 - The loading fixture that was used in mechanical testing of the samples, while it was in use on the mechanical testing machine. The crosshead of the machine applied load onto part 7 on the fixture. The spring was placed on the rod protruding from the base and removed prior to testing when the loading part was placed on the specimen, as shown in this image. The base was attached to the machine using the 16mm diameter hole in the centre of the base. The annotations correspond with Figure 4-14.

In order to ensure that the fixture multiplied the load as designed and met its functional outcome, it was verified. To do this, the fixture was placed in a mechanical testing machine (Instron 3369) and an independent 50kN load cell (KAM-B, Angewandte System Technik GmbH, Dresden, Germany) was placed under the loading part. Incremental loads of 100N were then applied to the fixture, and the output load was measured and recorded. This was repeated three times, and mean and standard deviation were calculated. The results from this are presented in Figure 4-16 and were used to calculate the equation for converting load applied by machine to load applied to the specimen (Equation 4-17).

$$y = 2.4398 x + 0.039657 \quad \text{Equation 4-17}$$

where y is the load applied to the specimen (kN) and x is the load applied by machine (kN)

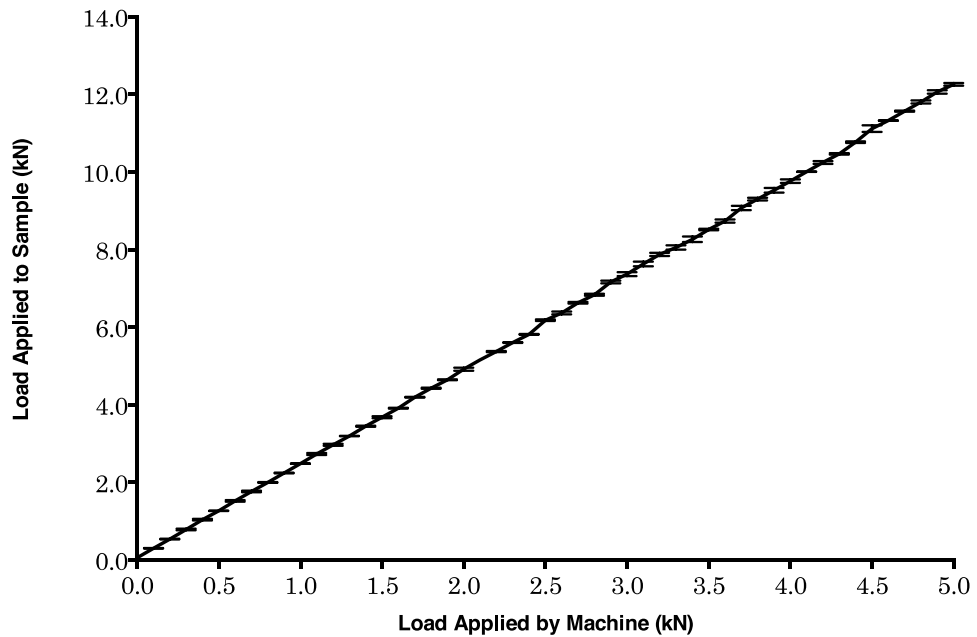


Figure 4-16 Mean load applied to the load cell versus the load applied by the Instron testing machine in increments onto the mechanical testing fixture shown in Figure 4-14. The error bars represent standard deviation (n=3).

In order to calculate the displacement applied to the specimen, the compression displacement applied by the mechanical testing machine required conversion to compression displacement applied to the specimen. To do this, simple trigonometry was used to calculate the displacements with respect to the angle at the lever point at the length of the loading bar. The relationship was defined as shown in Figure 4-17.

$$\tan x = \frac{a}{120} = \frac{b}{60} \Rightarrow a = 2b \quad \text{Equation 4-18}$$

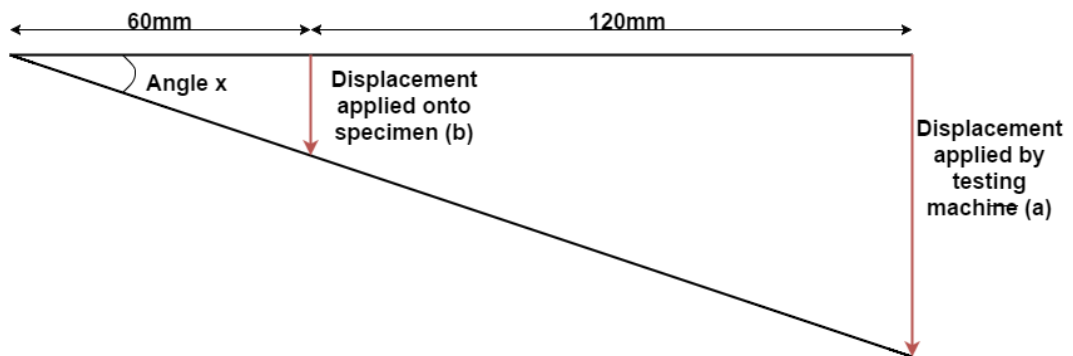


Figure 4-17 - Simplified diagram of the dimensions used for calculation of the relationship between the displacement applied by the mechanical testing machine (a) and displacement applied to the specimen (b). Angle x is the angle of the loading bar (part 2 in Figure 4-14) from horizontal. The points a and b were 180mm and 60mm from the support respectively.

#### 4.2.1.13 Mechanical Testing Method

The load cell (CELTRON PSD-500kg-SJTT, Vishay Precision Group, Malvern, PA, USA) attached to the crosshead on the mechanical testing machine (LETRY Dynamic Stiffness Testing Machine, Xi'an Material Testing Technology Co., Xi'an, Shaanxi, China) was calibrated using the built-in software before use and before attachment of any fixtures. The custom-made mechanical testing fixture (Figure 4-15) was placed in the mechanical testing machine, and the specimens were placed under the loading part of the fixture (Part 1 in Figure 4-14). The whole femoral heads were placed directly onto the fixture (Figure 4-15). The bone plugs were raised by 10mm by placing an aluminium plate under the loading part (Part 2 on Figure 4-15) and placing the specimens on top. This improved the ease of adjusting the height of loading part when testing as bone plugs were shorter and did not affect the results of the test.

The crosshead on the testing machine was lowered onto the fixture using the built-in software at a rate of 1mm per minute. The resultant load was measured using the load cell attached to the crosshead and recorded electronically at a frequency of 10 s<sup>-1</sup>.

#### 4.2.2 Assessing Control Human Femoral Heads

The control femoral heads used in this study were obtained from a different source to the AVN femoral heads. The experimental work to assess properties of control heads was carried out in the University of Leeds, and therefore using a different set of equipment. As many parameters as possible were maintained constant in assessing AVN and control femoral heads.

##### 4.2.2.1 Ethics

Samples in this study were obtained from Platinum Training, Phoenix, AZ, United States (2015) following approval of ethics application from University of Leeds Ethics Committee (Approval number: MEEC 13-002). Platinum Training is a company that provide an ethical donor network for healthcare research and training purposes. They provided tissues that met the inclusion and exclusion criteria set in Table 4-4



Table 4-4 - Inclusion and exclusion criteria set for control human tissue used in this study.

Inclusion Criteria	<ul style="list-style-type: none"> <li>• Donors who meet Platinum Training’s requirements regarding tissue donation and have signed a consent form</li> <li>• Male or female donors aged 18-65 years</li> <li>• Donors with no history of osteoarthritis in the hip, or suffered a broken hip, or had hip surgery</li> </ul>
Exclusion Criteria	<ul style="list-style-type: none"> <li>• Donors that have osteoarthritis in the hip, or suffered a broken hip, or had hip surgery</li> <li>• Donors with serological results indicating a transmissible disease</li> </ul>

Six pelvises with attached proximal femurs were used in this study. The tissue obtained was divided to provide samples for a series of studies within the department and these are detailed in the ethics protocol found in Appendix B. The handling, storage and disposal of tissue were carried out following the ethics protocol. All was performed in a strictly confidential and respectable manner to the donor, where samples were traced with a unique identification code associated with that tissue.

#### 4.2.2.2 Visual characterisation

All samples were visually inspected for visual abnormalities prior to further testing.

#### 4.2.2.3 Sample Preparation

Six femoral heads from the right side of pelvises were used in this study. The preparation of the samples was done carefully to not damage the articular surface. The pelvis that was received (Figure 4-18 (a)) was separated into three parts: Right, Left and Centre sections (Figure 4-18 (b)). The centre and left parts were stored for a different study. The femoral capsule (Figure 4-18 (c&d)) and the ligaments around the joint were carefully removed from the right section using a scalpel. The acetabulum and the right side of the pelvis were stored for a different study.

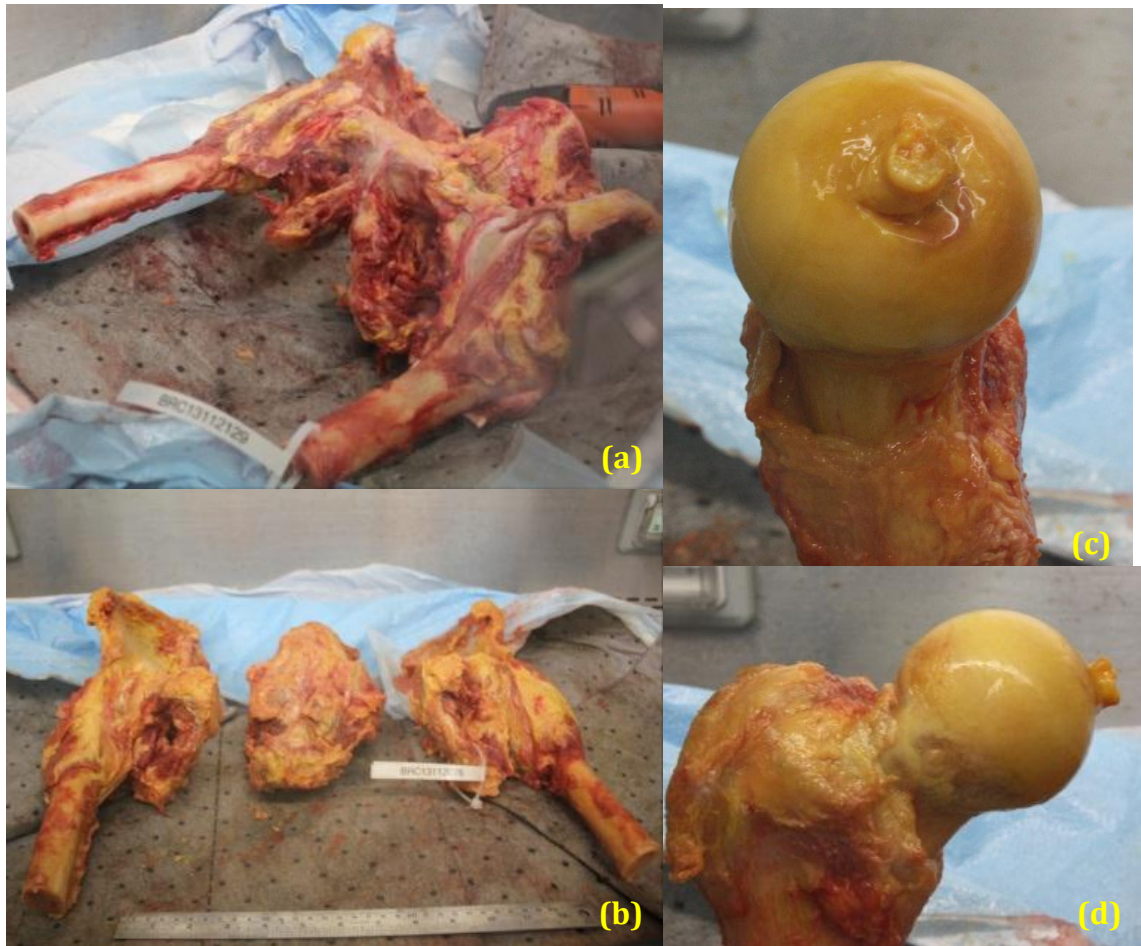


Figure 4-18 – (a) Pelvis to mid femur stripped area as received from the tissue bank. (b) Specimen divided into left, centre and right sections. (c) and (d)– Example of a femur stripped from the rest of the right pelvis in anterior-posterior and medial-lateral views respectively.

#### 4.2.2.4 Computer Tomography Scanning

All femoral head samples were CT scanned as whole proximal femurs before they were prepared for mechanical testing. They were scanned with pixel sizes of  $82\mu\text{m}$  in presence of a hydroxyl-apatite calibration phantom in the XtremeCT machine (Scanco Medical, Brüttisellen, Switzerland), using the protocol and parameters that were used in section 3.2.8. The data were recorded as DICOM files which were further analysed. After CT scanning, further preparation of the samples was carried out to produce bone plugs and whole femoral head specimens.

#### 4.2.2.5 Whole head samples

Three femoral heads were randomly selected for whole head testing. To prepare for testing, an electric saw was used to remove the femur shaft from the

femoral head. The femoral heads were prepared and potted in bone cement as described in section 3.2.6.

#### 4.2.2.6 Bone plug samples

Three femoral heads were randomly selected for bone plug testing. Bone plugs of 9mm diameter were removed from the load bearing and non-load bearing regions of the femoral head as shown in Figure 4-19. The method of removal of bone plug has been described in section 3.2.5.

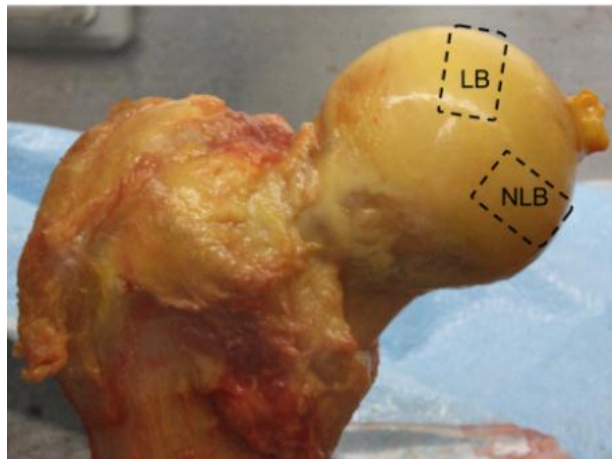


Figure 4-19 - Location of load bearing (LB) and non-load bearing (NLB) bone plug taken from femoral heads in the control group.

#### 4.2.2.7 Mechanical Characterisation

All whole head and bone plug samples were tested in compression. This was carried out following potting of whole head samples in bone cement to assist in fixation in the machine. The tests on bone plug samples were carried out by placing the bone plugs upright in the testing machine, and applying compression in the vertical direction.

The tests were carried out using an Instron 3300 dual column universal testing system (Instron, MA, US) following the protocol explained in section 3.2.9. The compression rate used was  $0.01\text{mm s}^{-1}$ .

### 4.2.3 Data Analysis for Femoral Heads in Control and AVN Groups

#### 4.2.3.1 CT Image Analysis

CT images of AVN and control were analysed to characterise the specimens morphologically. A bone density calibration phantom was not present at the time of CT imaging of AVN samples, therefore the bone mineral density could not be measured; however dimensional measurements were carried out as well as general visual characterisations of the images. This included calculation of the grey areas in the images where lesions and decalcified tissue were present, and presenting that as a ratio of the whole specimen.

#### Lesion Volumes

Slices of CT images taken in the transverse plane relative to the femoral head were analysed. A MATLAB program was created to analyse the volumes of femoral head and lesions. To do this, a loop script was created to analyse the slices in bulk in order to reduce the processing time per image. A flow diagram showing the steps of image processing for each slice is shown in Figure 4-20.

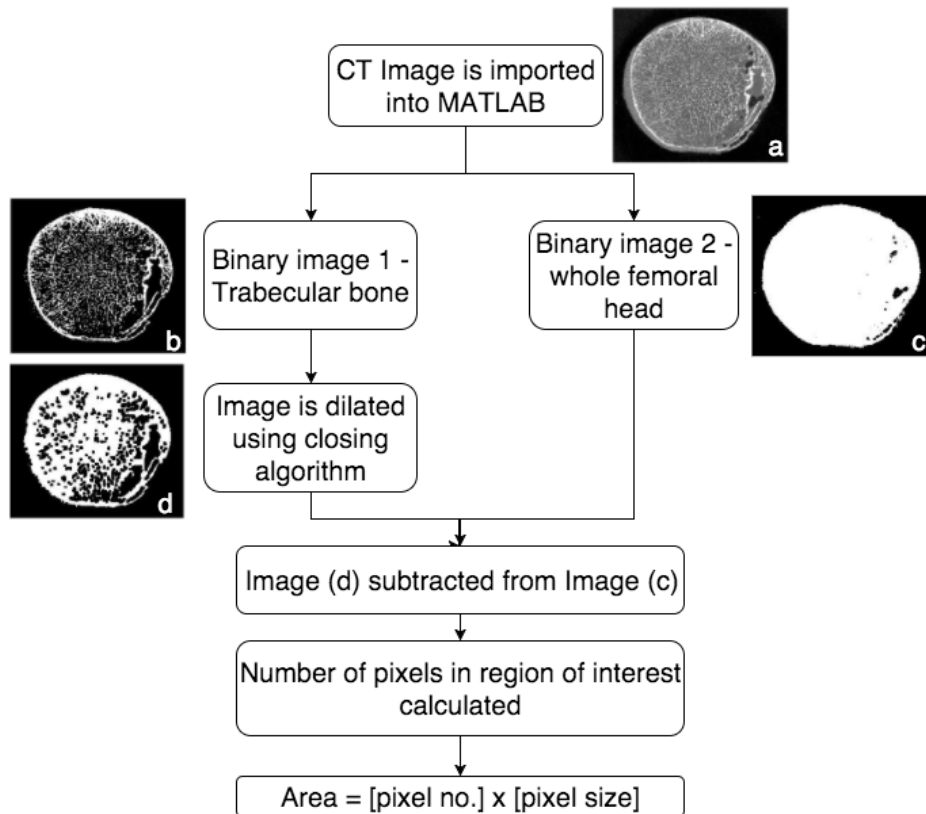


Figure 4-20 - Summary of image processing to analyse the area of lesions in each CT image slice of avascular necrotic femoral heads.

For each slice (Figure 4-21 (a)), a binary image was produced, where trabecular bone was selected using the pre-selected thresholds for each sample (Figure 4-21 (b)). The binary image of the trabecular bone was then dilated using a closing algorithm, in which the neighbouring pixels of the white pixels were also converted to white (Figure 4-21 (c)). This was done to define the areas where normal trabecular bone was present and to eliminate the spacing in the bone, present due to normal bone structure. A separate binary image with a threshold that selected the whole femoral head including the soft tissue and marrow regions within the image was then produced and the femoral head was selected as a region of interest (Figure 4-21 (d)). The area of white pixels for each slice was then calculated for the closed image and whole femoral head image within the region of interest in mm<sup>2</sup> and their mean over the slices of interest were calculated. The total volume of the “normal bone” and the volume of the overall femoral head were then calculated by using

Equation 4-19. Further details of the algorithms used can be found in the MATLAB programmes in Appendix C.

$$Volume_{normal\ bone\ or\ femoral\ head} = Mean\ Area_{normal\ bone\ or\ femoral\ head} \times n_{slices} \times Pixel\ Size$$

Equation 4-19

Following calculation of the bone volume and the femoral head volume, their ratio was calculated to represent the amount of spacing in the bone defined as lesions present in the femoral head. This allowed for volumetric estimation of bone degradation within the femoral head with the disease.

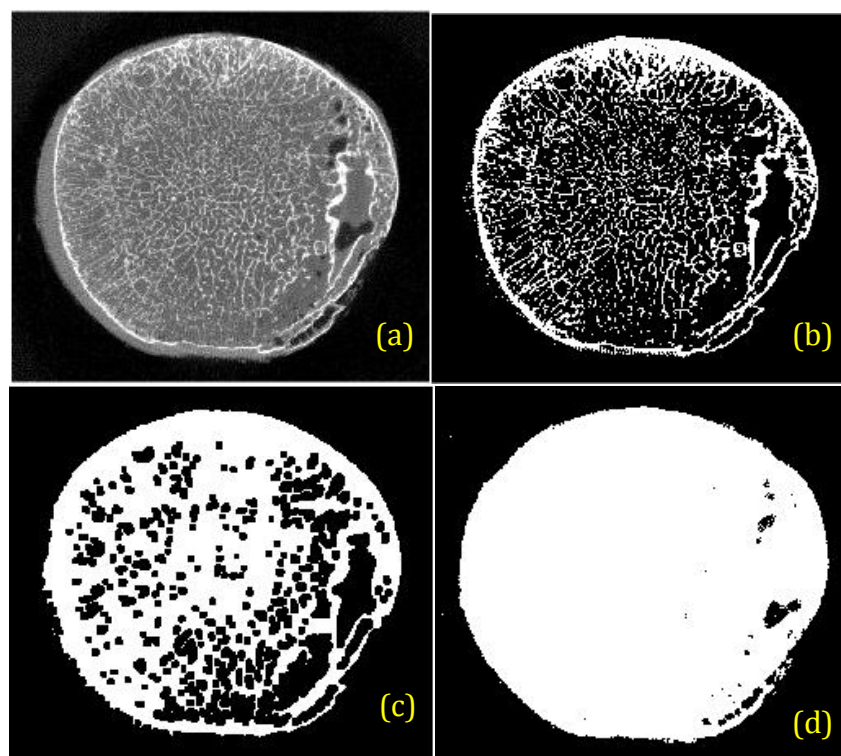


Figure 4-21 – Series of images showing processing of a CT image slice of a femoral head with AVN to assess the area per slice and volume of the lesions within the femoral head. (a) – Standard transverse section CT image of a femoral head as analysed. (b) A binary mask is placed on a copy of the image to provide a black and white image, where a manual threshold is selected to represent bone. (c) A closing algorithm is placed on image from (b) to dilate the trabecular bone and the normal enclosures. (d) A binary mask is placed on a different copy of the image by manually selecting the threshold to represent all viable bone and remaining tissue.

To check the validity of this method on a range of femoral heads, it was also used on CT images of control specimens. The same closing algorithm was applied to CT images of control femoral heads, and as shown in an example in Figure 4-22, it successfully filled in the areas that represented normal looking trabeculae, and produced gaps within areas with less visible trabeculae.

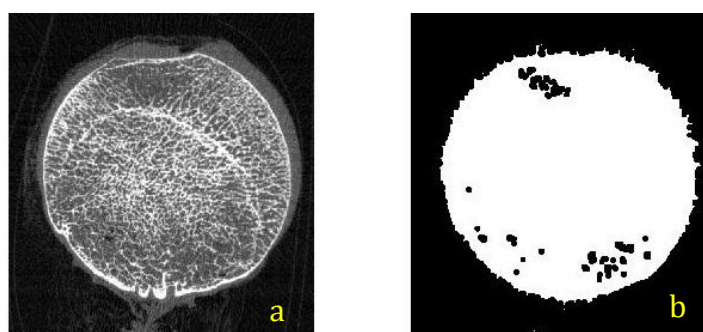


Figure 4-22 – Example of a control CT image of a femoral head where the closing algorithm is applied. (a) normal CT image, (b) closed binary CT image.

In order to calculate the sizes of lesions as a percentage of the femoral head volume, Equation 4-20 was used. Ratio of bone to femoral head is the volume

selected by Matlab code and is demonstrated in Figure 4-21 (d). The lesion size is the remaining non-viable bone areas in the femoral head.

$$\text{Lesion Size (\%)} = (1 - \text{Ratio of bone to femoral head}) \times 100\% \quad \text{Equation 4-20}$$

### **Bone Mineral Density of Control Specimens**

The built-in Scanco XtremeCT systems software was used to calculate the bone mineral density (BMD) of bone plugs from femoral heads in the control group. The entire bone plug was selected during the analysis as a cylindrical volume of interest and the overall BMD was calculated using a built-in algorithm.

#### **4.2.3.2 Mechanical Properties Data Analysis**

Mechanical testing data was used to calculate the mechanical properties of the specimens. In the case of AVN samples, Equation 4-17 was used to calculate the true load applied to the specimen from the original data. The displacement applied by the machine was used with Equation 4-18 to calculate the true displacement. These values were then used to calculate the stress and strain applied to the specimen using equations defined previously in section 3.1.1.4. For control specimens, the load and extension values were obtained from the uniaxial testing machine in comma separated value (.csv) files, and these were saved for further analysis.

A MATLAB programme was developed and used to analyse the data and calculate stress, strain, yield stress and elastic modulus of the samples using the load and extension values along with area of load application and gauge height of the samples. Further details of the MATLAB programme used to calculate these properties can be found in section Appendix C.

Graphs of stress versus strain were plotted for each specimen, and the Young's modulus and Yield Strength were calculated for the specimens using the MATLAB programme described in section 3.1.1.4.

The results of mechanical properties of the specimens were grouped into structural properties of whole femoral head and mechanical properties of bone plug groups. The bone plug specimens were then divided into load-bearing or non-load bearing groups.

### 4.2.3.3 Statistical Analysis

In most data analysis carried out in this study, sample sizes were not equal between groups, and therefore to analyse data statistically and to compare groups, Mann-Whitney U tests were performed when comparing two groups and Kruskal-Wallis H tests were performed when more than two groups were compared (Pena-Rodriguez, 2013). When Kruskal-Wallis H test returned with p-value of lower than 0.05, Dunn's multiple comparisons test was used to compare groups with each other.

Where sample sizes between compared groups were equal, student's unpaired t-test was carried out to test similarity between the two groups.

### 4.2.4 Differences between Methods Used in Testing Femoral Heads in the Control and AVN Groups

Although the experimental work carried out on the AVN and control samples were in two different institutes with different sets of equipment, as many factors as possible were kept constant between the studies. The differences between the methods are summarised in Table 4-5.

Table 4-5 - Summary of differences in methods used for testing AVN and control specimens

	<b>AVN Specimens</b>	<b>Control Specimens</b>
<b>Experiment location</b>	Xi'an Jiaotong University, Xi'an, Shaanxi, China	University of Leeds, Leeds, West Yorkshire, United Kingdom
<b>Sample origin</b>	Chinese Patients undergoing total hip replacement for AVN	Human tissue bank in USA
<b>Sample group</b>	Randomly based on visual grade	Randomly
<b>CT scanner</b>	Y-Cheetah Microfocus X-ray system	Scanco XtremeCT
<b>CT resolution</b>	67.8µm	84µm
<b>Mechanical</b>	LETRY Dynamic Stiffness Testing	Instron 3300 Dual Column



testing machine	Machine	Universal Testing System
Compression rate	0.01mm/s	0.01mm/s
Sample storage time (weeks) (Mean ± standard deviation)	91±17	18±15

### 4.3 Results

#### 4.3.1 Donor Characteristics

##### 4.3.1.1 AVN Femoral Heads

The metadata of patients were recorded by the surgeon in case report forms before surgery and summary data are presented in Appendix G. In total, 20 hips (11 left hips and 9 right hips) were removed from 18 patients, where 50% of specimens were from female patients. The age at surgery and BMI were  $59 \pm 15$  years and  $22.5 \pm 9.6$  respectively (Mean ± standard deviation). The date of the hip replacement surgery and hence specimen retrieval was  $169 \pm 146$  months (Mean ± standard deviation) after patients presented to a clinician with hip pain (Figure 4-24).

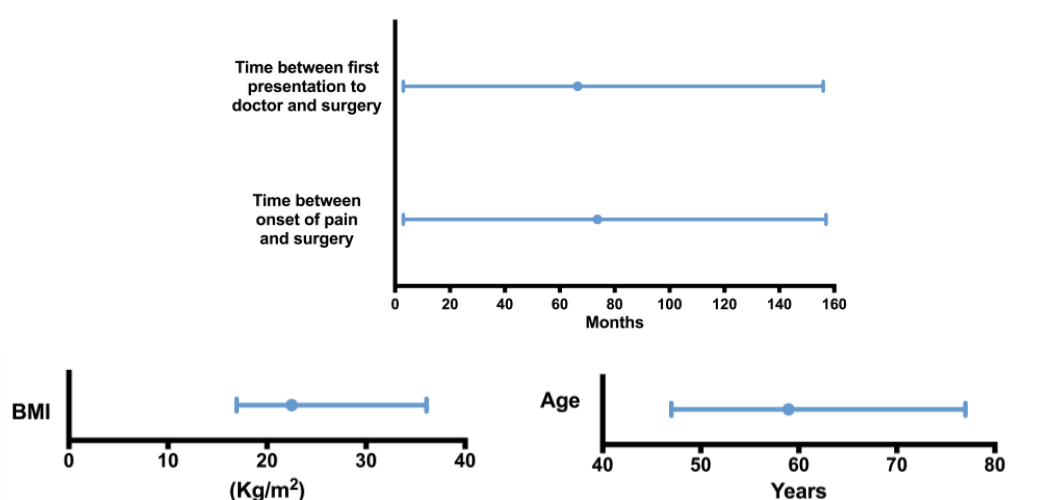


Figure 4-23 – Patient demographics for the specimens in this study. Means and ranges for BMI and ages of the patients at time of surgery, as well as time between first presentation to a clinician and onset of pain, and surgery are shown.

### 4.3.1.2 Control Femoral Heads

The control specimens in this study were obtained from three male and three female donors. All samples were from white caucasian donors. The donors at the time of death had mean age of 63.67 years (SD=6.26) and mean BMI of 27.8 kg/m<sup>2</sup> (SD=6.9). They were all deceased from non-bone related diseases. The primary and secondary causes of death for each donor as well as the sample type used for testing are listed in Table 4-6.

Table 4-6 - Primary and secondary causes of death, and test type used for each sample in this study


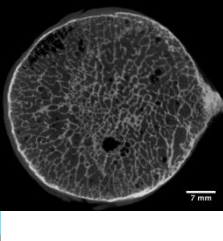
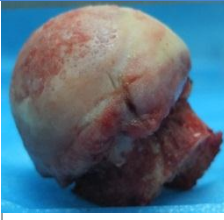
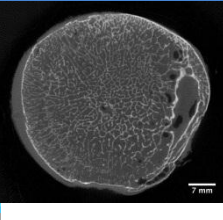
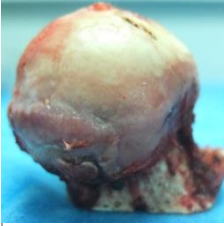
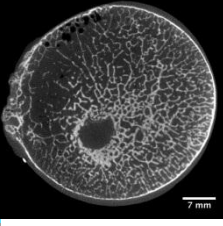
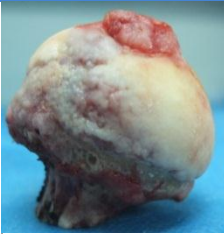
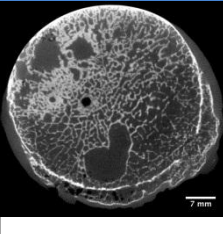

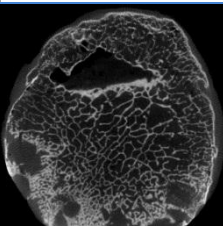
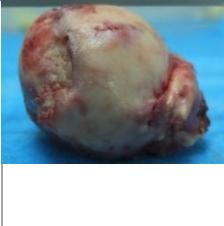
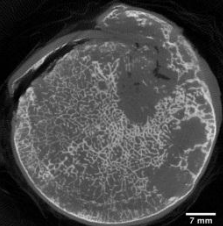
Donor no.	Primary Cause of Death	Secondary Cause of Death
C1	Pancreatic cancer	Respiratory Failure
C2	Myocardial infarction	Respiratory Failure
C3	Prescription drug overdose	Respiratory Failure
C4	Metastatic breast cancer	Respiratory Failure
C5	Alcoholic cirrhosis of the liver	Respiratory Failure
C6	Malignant tongue cancer	Respiratory Failure

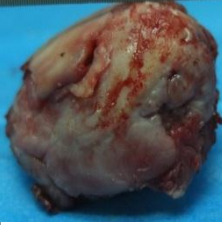
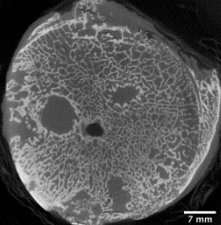

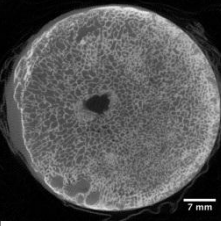

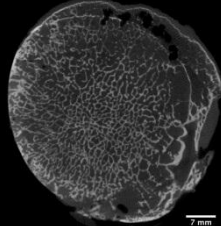
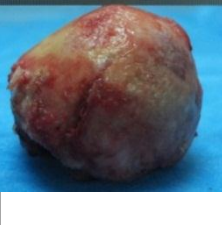


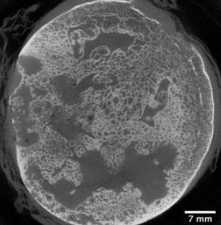

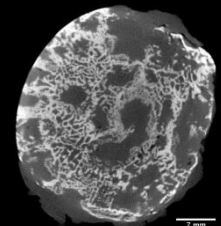
### 4.3.2 AVN Specimen Characterisation

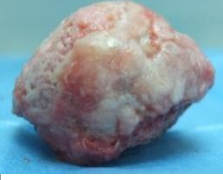
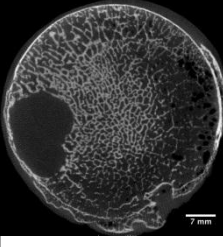
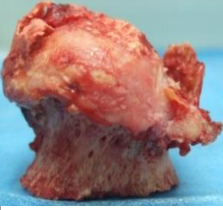
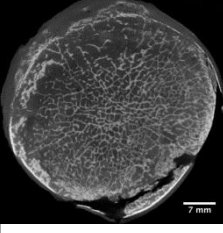
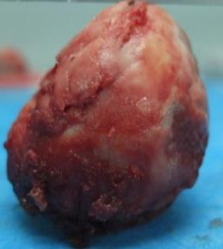
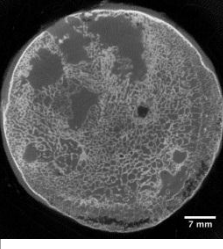

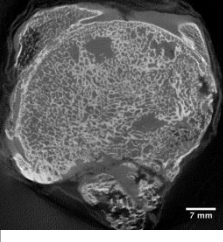
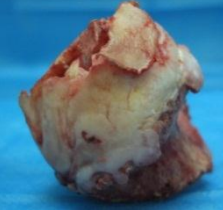
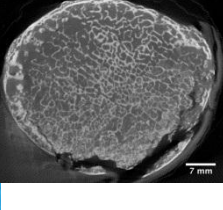
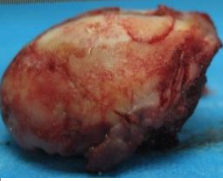
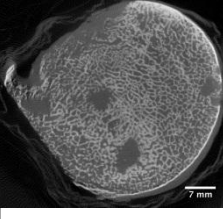
The AVN specimens were visually characterised before any destructive testing was carried out. They were characterised using the parameters shown in Table 4-2, and following receipt of CT scans, they were also characterised using Pennsylvania grading (explained in Table 2-4). They were divided into groups for whole femoral head testing and bone plug testing based on their visual grade. Details of specimens sorted by increasing Pennsylvania grade are shown in Table 4-7.


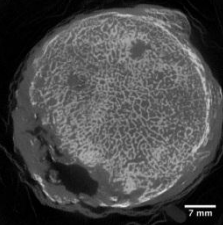
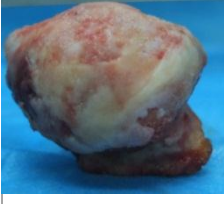
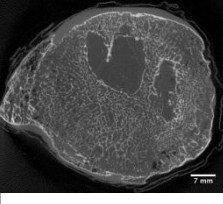
Table 4-7 – Table showing frontal medial lateral photographs and representative CT slice of each AVN specimen at the greatest diameter of the femoral head demonstrating the degree of collapse and damage to the femoral head as well as the lesions viewed in the CT images. Patient information, severity grade and specimen grouping for whole head or bone plug mechanical testing are also shown. Specimens are sorted by increasing Pennsylvania grading.

Specimen no.	Pennsylvania grade Grading by Table 4-2	Frontal M-L Photograph of sample	Specimen CT slice	Age (years)	Gender	BMI (kg/m <sup>2</sup> )	Side of hip	Months between onset of pain and surgery	Mechanical testing group
--------------	--	-------------------------------------	-------------------	-------------	--------	--------------------------	-------------	---	-----------------------------

Specimen no.	Pennsylvania grade	Grading by Table 4-2	Frontal M-L Photograph of sample	Specimen CT slice	Age (years)	Gender	BMI (kg/m <sup>2</sup> )	Side of hip	Months between onset of pain and surgery	Mechanical testing group
A2	3	1			65	F	16.9	L	97	Bone plug
A19	3	2			56	F	18.4	R	156	Bone plug
A3	4	1			60	F	21.0	R	121	Whole head
A4	4	2			77	F	23.3	L	40	Whole head
A5	4	2			63	F	26.8	L	13	Bone plug
A10	4	3			63	M	18.7	L	28	Whole head

Specimen no.	Pennsylvania grade	Grading by Table 4-2	Frontal M-L Photograph of sample	Specimen CT slice	Age (years)	Gender	BMI (kg/m <sup>2</sup> )	Side of hip	Months between onset of pain and surgery	Mechanical testing group
A12	4	4			59	M	18.2	R	27	Whole head
A17	4	3			51	M	20.8	L	111	Bone plug
A8	5	2			65	F	24.6	L	3	Bone plug
A9	5	2			56	F	22.4	L	111	Whole head
A13	5	3			47	M	36.1	R	150	Whole head
A1	6	4			51	F	22.7	R	157	Whole head

Specimen no.	Pennsylvania grade	Grading by Table 4-2	Frontal M-L Photograph of sample	Specimen CT slice	Age (years)	Gender	BMI (kg/m <sup>2</sup> )	Side of hip	Months between onset of pain and surgery	Mechanical testing group
A6	6	3			60	F	19.3	R	51	Bone plug
A7	6	4			62	M	21.3	L	11	Bone plug
A11	6	4			47	M	36.1	L	150	Bone plug
A14	6	4			52	M	21.6	R	49	Whole head
A15	6	4			62	M	22.7	R	14	Whole head
A16	6	3			65	M	21.7	R	19	Bone plug

Specimen no.	Pennsylvania grade	Grading by Table 4-2	Frontal M-L Photograph of sample	Specimen CT slice	Age (years)	Gender	BMI (kg/m <sup>2</sup> )	Side of hip	Months between onset of pain and surgery	Mechanical testing group
A18	6	4			62	M	18.6	L	13	Whole head
A20	6	3			56	F	18.4	L	156	Whole head

All AVN specimens had visual signs of deformation due to disease, demonstrated by lack of spherical shape, worn articular surface, exposed trabecular bone and in most of the cases, the specimens had collapsed and the spherical surface of the femoral head had deformed completely. In some specimens – e.g. specimens A7 and A15, the articular surface of the femoral head was severely damaged (Table 4-7).

The specimens in this study were graded visually according to Table 4-2. This method was used initially rather than the established grading methods such as ARCO or Pennsylvania since X-rays or CT scans were not available at the beginning of the study to establish the scale of collapse in the femoral head. Once CT images were obtained, the samples were also graded using the Pennsylvania staging system (Mont et al., 2006).

The AVN specimens were divided into two groups for whole head and bone plug mechanical testing (Figure 4-24). More samples were allocated to whole head testing in grade 4, as most of the samples in this grade, such as specimens 14, 15 and 16, were extremely damaged and surfaces were not available for bone plug removal.

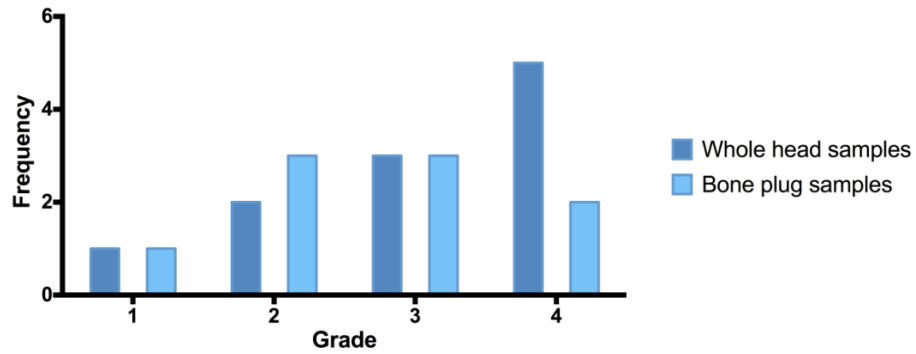


Figure 4-24 – Bar chart demonstrating the frequency distribution of specimens tested as whole head or bone plug samples in mechanical testing based on initial grade according to Table 4-2.

#### 4.3.2.1 Control Human Femoral Heads

The control samples were visually characterised for any visible abnormalities. None were noticed in these samples. Particular attention was paid to samples from donors C3 and C5, where prescription drug overdose and alcoholic cirrhosis of the liver were the primary causes of death, as there was a chance that this may have affected the blood supply to the femoral head and caused bone damage, however no visual differences were seen in these samples.

Samples were randomly selected for whole head or bone plug testing and these are also listed in Table 4-8.

Table 4-8 – Allocation of control samples to bone plug or whole head test groups for mechanical testing.

Compression test group	Donor no.
Bone plug	C1, C4, C6
Whole head	C2, C3, C5

#### 4.3.3 Computer Tomography Scanning

CT images for AVN femoral head specimens were obtained in .RAW format. These were converted to .DICOM images using MATLAB and saved for further analysis. The CT images from control femoral heads were exported in DICOM format.

##### 4.3.3.1 Lesions

The images were analysed following the methods described in section 4.2.3.1. Volumes of lesions and femoral heads were calculated from these images, and

these values were used to determine the ratio of lesion to healthy bone within femoral heads. Some samples also demonstrated fracture of subchondral bone as well as missing or partial cortical bone around the femoral heads. Lesions were seen in all of the femoral head. The size of each of the lesions were different: while some AVN samples had many small lesions, several also presented with large lesions (Figure 4-25).

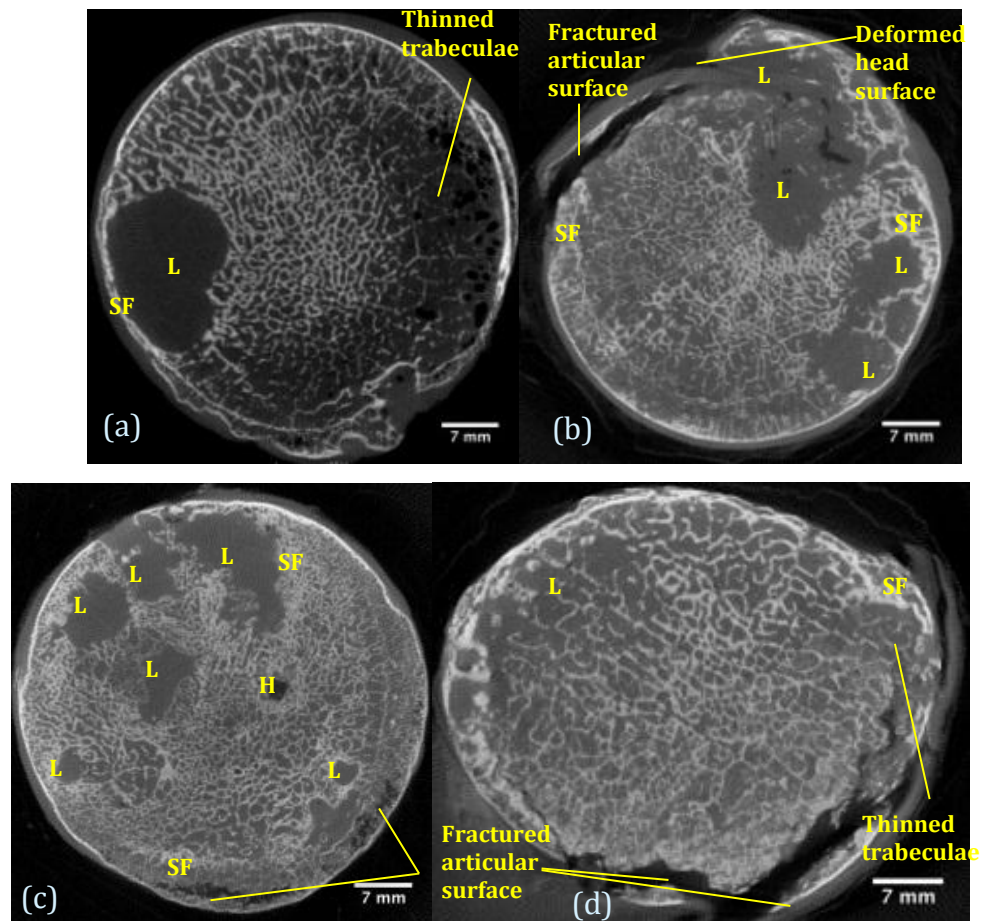


Figure 4-25 –CT slices demonstrating the variation in damage due to AVN in the femoral heads. Lesions (L) are seen in all samples; however their numbers and volumes are different in all specimens. Subchondral fractures (SF) are also seen in some samples. (a) CT slice from sample A6, demonstrating a large lesion of one side of the femoral head, as well as thin trabecular bone on the opposite side. Subchondral fracture is seen near the lesion. (b) CT slice from sample A10, demonstrating multiple lesions, as well as multiple subchondral fractures demonstrated by dense cloudy trabeculae. The surface of the femoral head is also deformed, possibly due to collapse of subchondral bone and a part of the articular surface is fractured from the rest of femoral head. (c) CT slice from sample A11, demonstrating multiple lesions of smaller size, as well as subchondral fracture, however the cortical bone is mostly intact despite presence of articular surface fractures. The hole (H) produced by surgical removal of the femoral head from patient is also seen in this slice. (d) CT slice from sample A15, showing a non-spherical femoral head due to collapse, with subchondral fracture. Smaller lesions as well as thinned trabeculae, and fractured articular surface are also seen.



The control femoral heads were also analysed for lesion volume, and although the samples were from donors without evident bone diseases, small lesion-like areas were seen in some samples (Figure 4-26).

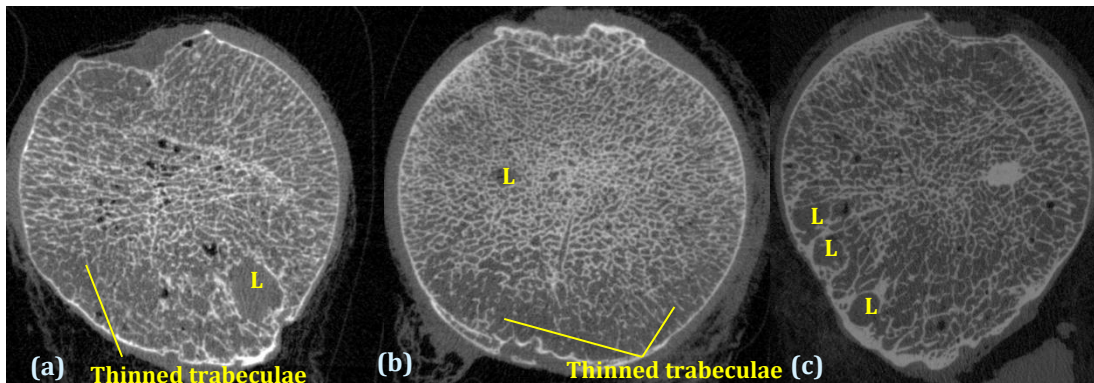


Figure 4-26 – CT slices from control human femoral head samples demonstrating lesions and areas with thinned trabeculae (a) sample C2, (b) sample C3, (c) Sample C6 (L=lesion)

The ratios of “lesion” volume to femoral head volume were statistically analysed to determine patterns within the data. The calculated ratios were combined as characterised using the Pennsylvania system. The mean ratios for each grade along with control data were then plotted in Figure 4-27. No significant differences were found in the means of the groups when compared within grades or with control data.

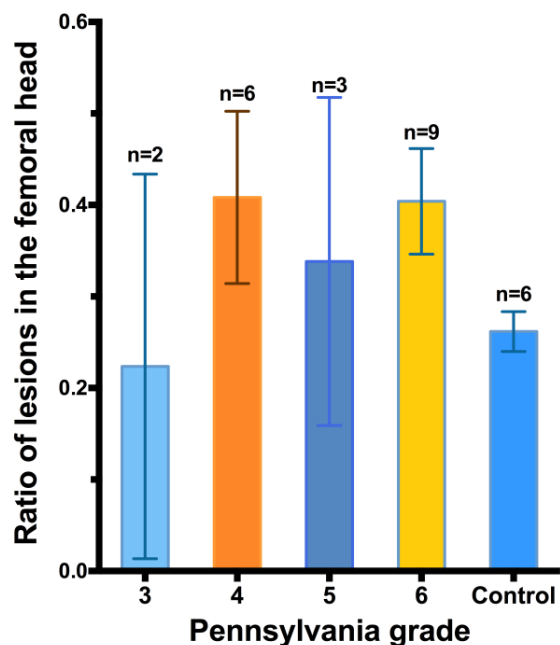


Figure 4-27 - Mean ratio of lesions to whole femoral head volume for each Pennsylvania stage assigned to the specimens and the control samples. The error bars represent standard error of mean, and specimen numbers are shown above each column. Kruskal-Wallis test demonstrated no significant differences between the means of groups ( $p < 0.05$ ).

The lesion volumes for the AVN samples were grouped according to lesion size (Figure 4-28). Most of the samples in this study had lesions between 50-70% of the femoral head volume. Two samples had lesions that were less than 10 percent of the total femoral head volume.

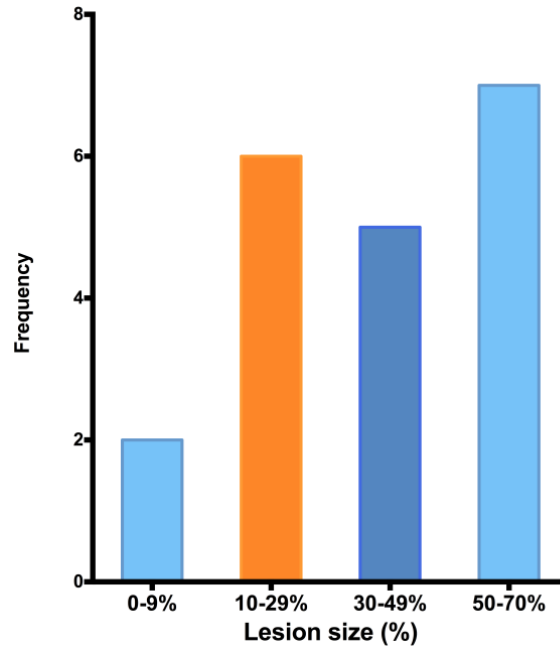


Figure 4-28 - Figure showing the distribution of samples when sorted by lesion sizes in each femoral head. Most of the samples in this study had lesions that filled 50-70% of the femoral heads.

The lesion volumes of the AVN samples were also compared with other demographic factors from the patients in order to establish any correlations. No correlations were seen between lesion size when compared with time between onset of pain and surgery, age or BMI of the patients (Figure 4-29).

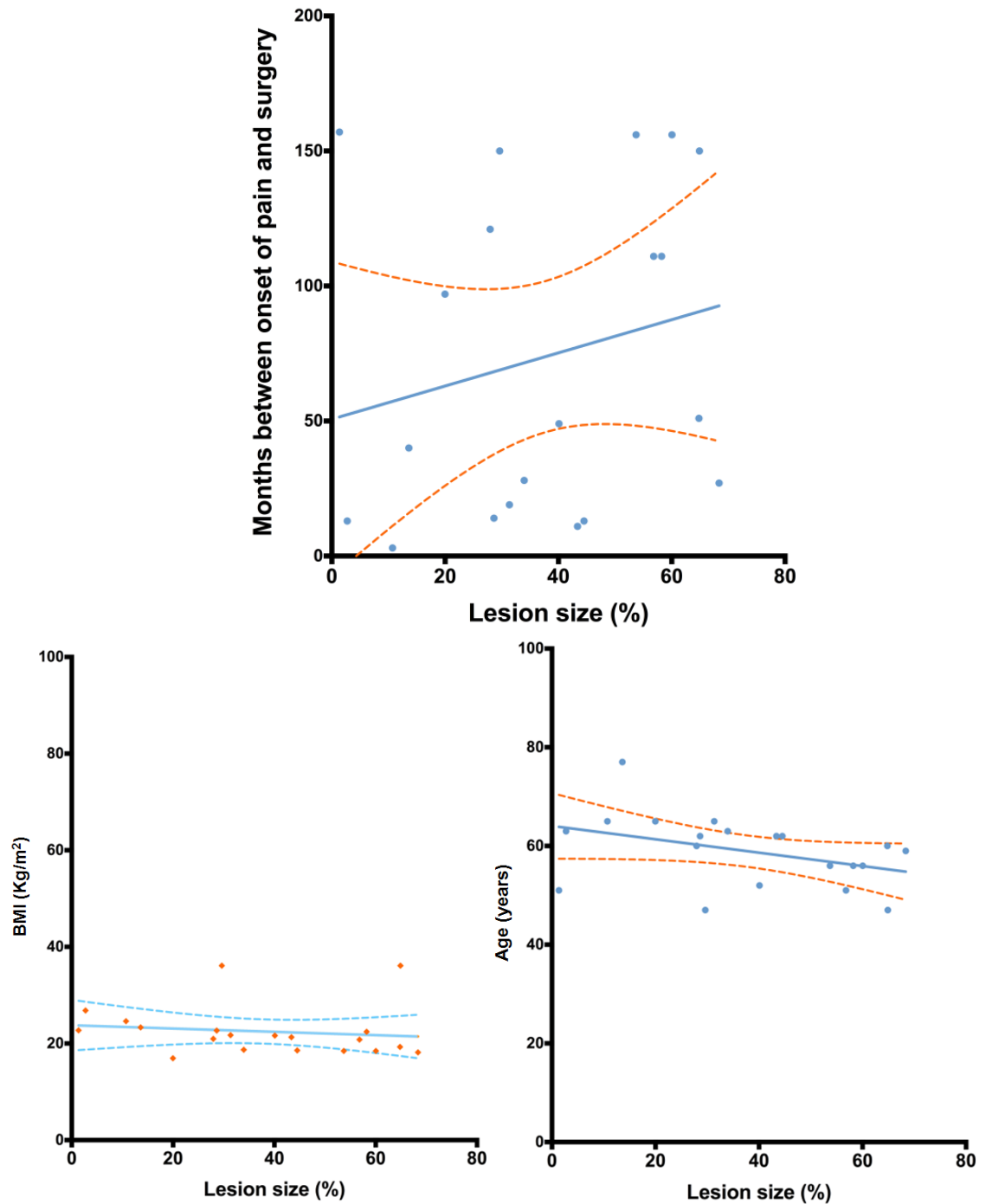


Figure 4-29 – Lesion size as percentage of femoral head versus the amount of time between onset of pain and THR surgery ( $R^2 = 0.05$ ), Age ( $R^2 = 0.16$ ) and BMI of patients ( $R^2 = 0.02$ ).

#### 4.3.3.2 Bone Mineral Density

The bone mineral densities (BMD) were measured for bone plugs from control human samples. The mean BMDs were 807.1 mgHA/cm<sup>3</sup> (Standard error of mean (SEM)= 46.15) and 642.5 mgHA/cm<sup>3</sup> (SEM = 97.18) for load bearing and non-load bearing groups respectively. There were no significant differences between the means of the groups.

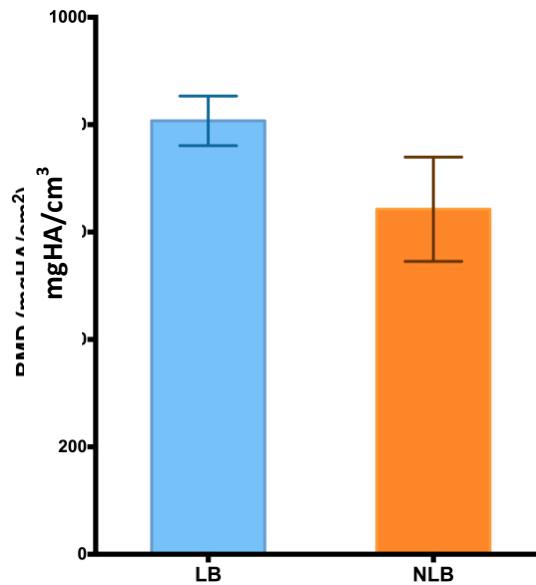


Figure 4-30 – Bone mineral density plots for control bone plugs from load bearing and non-load bearing regions. Error bars demonstrate standard errors of mean. Significant differences were not found between the means of groups (Student’s t-test)(n=3).

#### 4.3.4 Mechanical Properties

The mechanical characteristics of the specimens were analysed in two sets – structural properties of whole head specimens and mechanical properties of bone plug specimens.

##### 4.3.4.1 Structural Properties of Whole Head Specimens

A total of 11 AVN specimens and 3 control specimens were tested in this group. The elastic modulus and yield stress were calculated for all specimens.

In order to determine the relationship between these structural properties and the other observed factors in this study, further comparisons were made. Firstly, the relationship between the structural properties and the Pennsylvania grade applied was calculated. The mean elastic modulus and yield stress values for each identified grade are shown in Figure 4-31. A Kruskal-Wallis test was carried out to compare the means between the groups. No significant differences were found between the elastic modulus and yield stresses of different grades of AVN and control femoral heads.

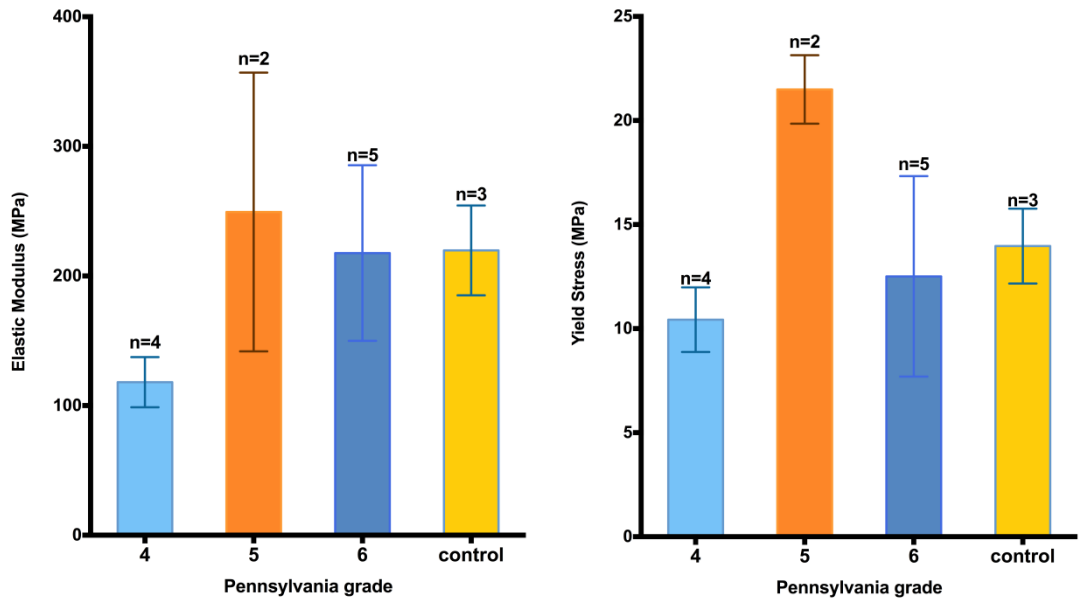


Figure 4-31 Elastic modulus and yield stress for the AVN heads assigned to each Pennsylvania grade and for the control head specimens. The error bars indicate standard error of mean and specimen numbers are demonstrated above each bar. Kruskal-Wallis test determined that there were no significant differences between the means of each group ( $p > 0.05$ ).

Further analysis was carried out to compare the structural properties to the ratio of bone to whole femoral head volume (section 4.2.3.1). The graphs in Figure 4-32 show the relationship between these properties. The calculated  $R^2$  values for the graphs were very small indicating that the bone to femoral head ratio does not determine the structural properties of the bone in this group.

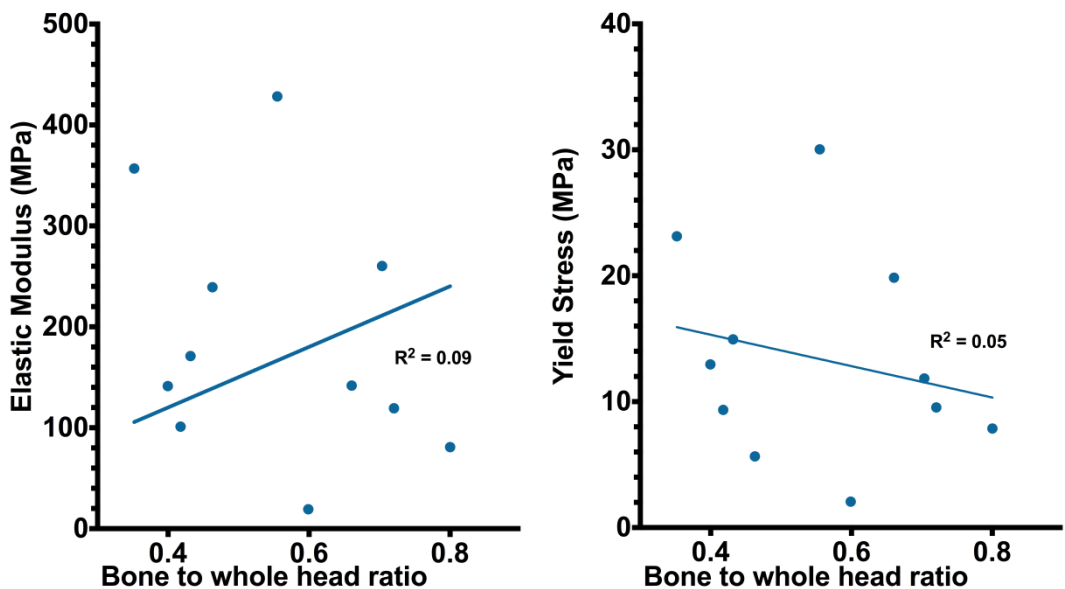


Figure 4-32 - Relationships between the elastic modulus and yield stress of AVN whole head specimens and their associated bone to whole head ratio.  $R^2$  values are presented for each graph, and since the coefficient of determination is so small, the bone to whole femoral head ratio cannot determine the elastic modulus or yield stress of these samples accurately.

#### 4.3.4.2 Mechanical Properties of Bone Plug Specimens

In order to determine the mechanical properties of bone plug specimens, the specimens were divided into specimens from load bearing and non-load bearing regions for AVN and control specimens. This was done by grouping all specimens removed from the femoral head regions A, B, C and I into load bearing group (LB) and specimens D, E and F into non-load bearing group (NLB) (Figure 4-7 for region descriptions).

The LB AVN specimens (n=28) had mean elastic modulus of 116.6 MPa (SEM=11.69) and yield stress of 6.19 MPa (SEM=0.73). The NLB AVN specimens (n=6) had mean elastic modulus of 54.88 MPa (SEM=12.35) and yield stress of 2.34 MPa (SEM=0.59). The mean elastic modulus for control samples was 146.12 MPa (SEM=23.78) for the load bearing bone plugs (n=3) and 35.96 MPa (SEM=10.51) for the non-load bearing bone plugs (n=3). Mean yield stress of control samples was 8.07 MPa (SEM=1.49) for samples from load bearing region and 1.91 MPa (SEM=0.24) for samples from non-load bearing region.

The mean elastic modulus and yield stress for LB and NLB groups of bone plugs for both control and AVN samples were significantly different from each other (Figure 4-33), which demonstrated that the load bearing region of these femoral heads have higher mechanical strength and elasticity than the non-load bearing regions. There were no significant differences between the properties of samples, when samples from the same regions were compared with each other.

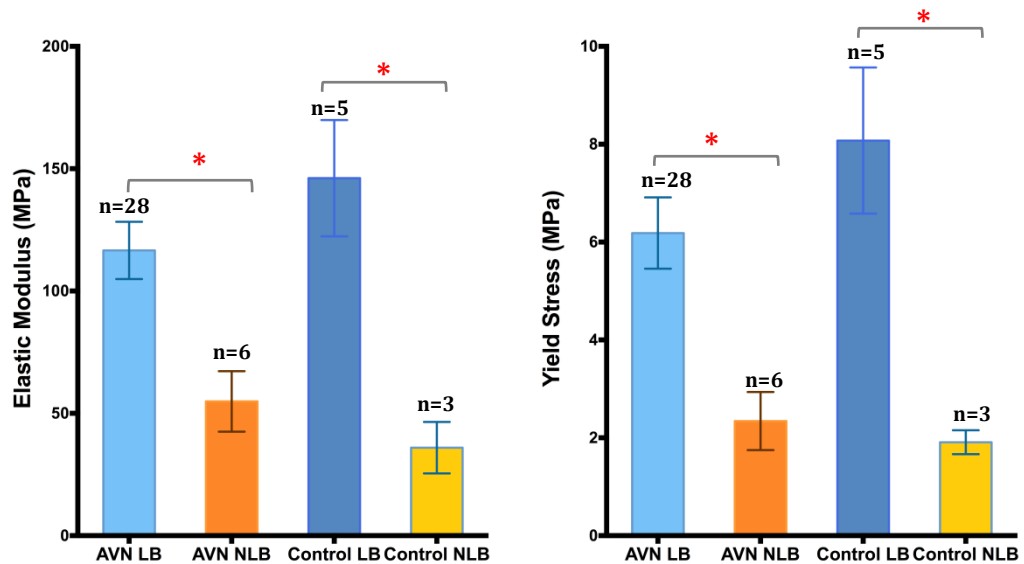


Figure 4-33 – Mean elastic modulus (Left) and yield stress (Right) for load bearing (LB) and non-load bearing (NLB) bone plugs from both AVN and control groups. No significant differences were found between the AVN and control groups for both parameters in load bearing and non-load bearing regions, however there were significant differences (asterisks) between the load bearing and non-load bearing samples from both groups (Kruskal-Wallis H test and Dunn’s multiple comparison test,  $p < 0.05$ )

#### 4.4 Discussion

This study had the following two aims:-

1. To characterise femoral head bone from patients with AVN
2. To compare the properties of bone with AVN to control human bone to characterise the degree of change from non-pathologic to diseased bone.

In order to meet these aims, femoral head specimens were obtained from AVN patients undergoing THA, and the characteristics of these were compared with those of control femoral heads obtained from a human tissue bank. The findings of this study are divided into the following sections:-

1. Lesions and subchondral fractures in AVN femoral heads
2. Mechanical difference between AVN and control femoral heads
3. Challenges
  - a. Experimental challenges
  - b. Challenges with access to human tissue
  - c. Human tissue variance
  - d. Other limitations of the study

#### 4.4.1 Lesions within AVN Femoral Heads

Detailed ex-vivo CT imaging of human AVN tissue has not been carried out in any published studies. Clinical imaging techniques have been used to characterise bone with AVN, however these have mostly considered the diagnostic characterisations of necrotic bone, such as presence of a crescent or changes in the opacity of the image when compared with non-pathologic femoral head images. These changes are discussed in section 2.4.1. Characterisation of the samples visually and using the CT scans in this study provided information about the types, frequency and volumes of lesions within femoral heads with AVN.

Pennsylvania stages were used to divide the groups to analyse the mean ratio of lesions to whole femoral head volume and no significant differences were found between the different stages and control specimens. The mean ratio of lesions within the femoral head for control and AVN specimens were compared (Figure 4-34), the AVN femoral heads had significantly higher ratio lesions within the femoral head tissue when compared to control samples.

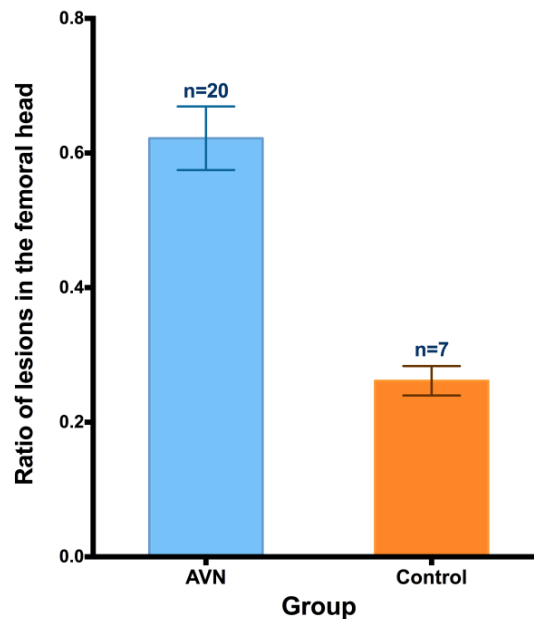


Figure 4-34 – Mean ratios of lesions to femoral head for AVN and control groups. The error bars demonstrate standard error from mean and sample numbers are above each bar. The group means were significantly different from each other (Mann-Whitney test,  $p < 0.0001$ ).

All the heads in this study were in Pennsylvania stages 3-6, and the lesion volume does not differentiate the femoral heads using the Pennsylvania score. It may be possible that the ARCO system may be a better choice to differentiate the



stages with the lesion size as it also includes an orientation characterisation as well as volume.

The presence of lesions in the femoral head is a diagnostic marker for AVN. Steinberg et al. (1999) studied lesions in femoral heads of patients undergoing core decompression and bone grafting for AVN, using MRI in Pennsylvania Stage I and radiographs in Stage II to determine if the lesion size affected the outcome of treatment. They then divided the groups based on their lesion sizes, and reported that more patients with lesion sizes larger than 30% required total hip replacement when compared to patients with small lesion sizes, suggesting that lesion size can predict the outcome of core decompression in early stages.

Kubota et al., (2014) studied 48 hips in vivo with pre and post collapse cases of AVN using X-rays, MRI and DEXA and reported that the BMD measured with DEXA of the lateral sides of the femoral heads, i.e. non-load bearing regions were significantly greater in collapse groups when compared to non-collapse groups. They reported no significant differences in the BMDs of the load bearing regions, trochanter and the femoral neck. This study however did not consider the possibility of increased BMD as a result of denser bone produced by the collapse in the femoral head. It also did not compare their findings to the BMD of non-pathological samples. The study by Kubota et al. does not agree with the findings of the current study, where smaller volumetric ratios of calcified bone to whole femoral head are present in AVN specimens when compared to control samples. This evidently affects the BMD of the samples, due to lower volume of calcified tissue, however due to limitations in the experimental equipment the BMD of these samples could not be measured.

Another study by Beckmann et al. (2009) compared  $\mu$ CT parameters from 1cm<sup>3</sup> samples from AVN and osteoarthritis (OA) femoral heads, and demonstrated that there were no significant differences between the bone volume, connectivity density and trabecular parameters of the two groups. The limitation of the study by Beckmann et al. was that the AVN samples were compared to bone from OA rather than non-pathological femoral heads, and they did not evaluate whether the OA was secondary to AVN. The findings discussed in this chapter are compared to bone from donors that did not demonstrate pathologies rather than bones removed from OA patients undergoing hip arthroplasty. Also, the results of

Beckmann et al. are supported by studies which induced AVN in animals, however as discussed in section 2.7, and by Jones and Allen, (2011), animal models of AVN currently do not replicate the mechanical failure seen in human cases of AVN and cannot be used as an acceptable comparison to clinical AVN.

In this study it was demonstrated that most of the specimens had lesion sizes greater than 50% and were in stage 6 in the Pennsylvania grade of the disease. The results of this study therefore cannot be compared directly with the results by Steinberg et al., (1999), where all of the patients were within stages I and II of the disease and showed lesion sizes under 30% of the volume of the femoral. The findings of the current study however provide details of the types of lesions seen within femoral heads requiring total hip replacement and therefore in later stages of the disease. Another major difference between the current study and that by Steinberg et al. is in the way the lesion sizes were calculated. Steinberg et al. calculated the size of the lesion from single slices of MRIs in stage I and in A-P radiographs in stage II, rather than the 3D CT imaging and the repeatable automated segmentation technique that was used in this study. The lesions in A-P radiographs do not represent the true size of the lesions as it limits them to the load bearing region of the femoral head, however as the current study has shown, lesions can vary in location, size and frequency in the femoral head.

In a separate study, Steinberg et al., (2006) measured volumetric lesion sizes in AVN patients by combining anterior-posterior and medial-lateral radiographs. This method used the Combined Necrotic Angle of Kerboul et al., (1974), where the angles of the necrotic regions in AP and ML views are added (Figure 4-35). They reported that the combined necrotic or “Kerboul” angle regularly overestimated the size of lesions due to the irregular shapes and locations of lesions. The Kerboul method assumes that the majority of the lesion is in the subchondral region and that measurement of the angle of the lesion from the centre of the femoral head provides an estimate of the lesion size. However, as Steinberg et al., (2006) discussed and is demonstrated in this study (Figure 4-25), necrotic lesions are not limited to the subchondral region of the femoral head, and several lesions may be present which may be difficult to detect in radiographs. Steinberg et al., (2006) also proposed a volumetric quantitative method to calculate the necrotic lesion volumes by measuring the number of pixels in the necrotic region of the image and

dividing by the pixels in the entire head, producing a percentage. This is carried out in both AP and ML radiographs, and combined to determine the percent volume of the head that is necrotic. Whether this volumetric percentage is a true clinical representation of the necrotic lesion size cannot be determined without comparing the method to the technique of determining the lesion size used in this study

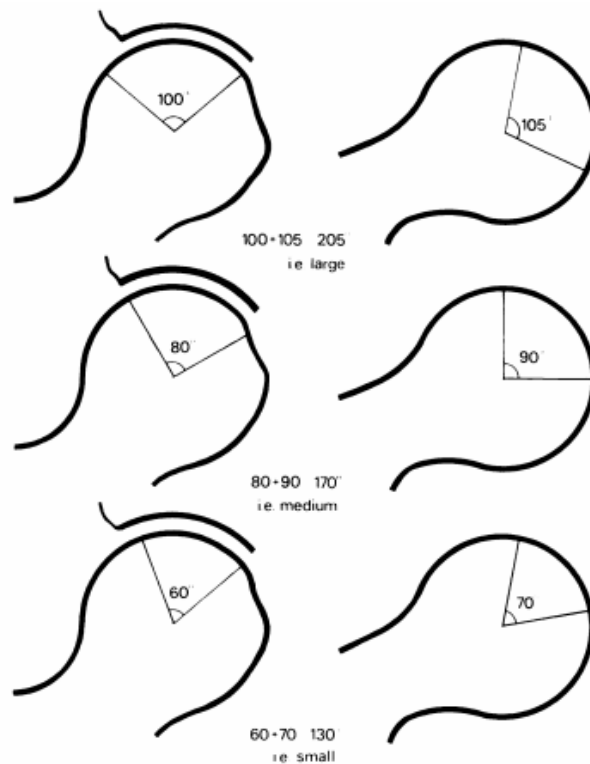


Figure 4-35 - The use of Kerboul angle to measure the lesion size from anterior-posterior (left) and medial-lateral (right) radiographs by adding together the angles, and therefore categorising them into small, medium and large lesions (Kerboul et al., 1974).

#### 4.4.2 Subchondral Fractures in AVN Femoral Heads

Subchondral fractures in bone with AVN are common and indicate biomechanical compromise in the femoral head (Mont and Hungerford, 1995; Stevens et al., 2003). They are indicative of later stage AVN, and result in very dense bone, sometimes separated from the articular surface by a space. This eventually results in collapse and deformation of the femoral head. They may be present anywhere in the femoral head as a result of AVN, however they mostly result in collapse and deformity of the femoral head in the load bearing regions (Bullough and DiCarlo, 1990).

In this study, subchondral bone fracture was defined as areas in the femoral head, near the articular surface with dense bone (Stevens et al., 2003). Subchondral bone fractures were identified in all of the CT scans of AVN femoral heads. This is typical of AVN in the later stages as the crescent sign is generally visible in plain radiographs, one of the main diagnostic and staging tools for AVN patients.

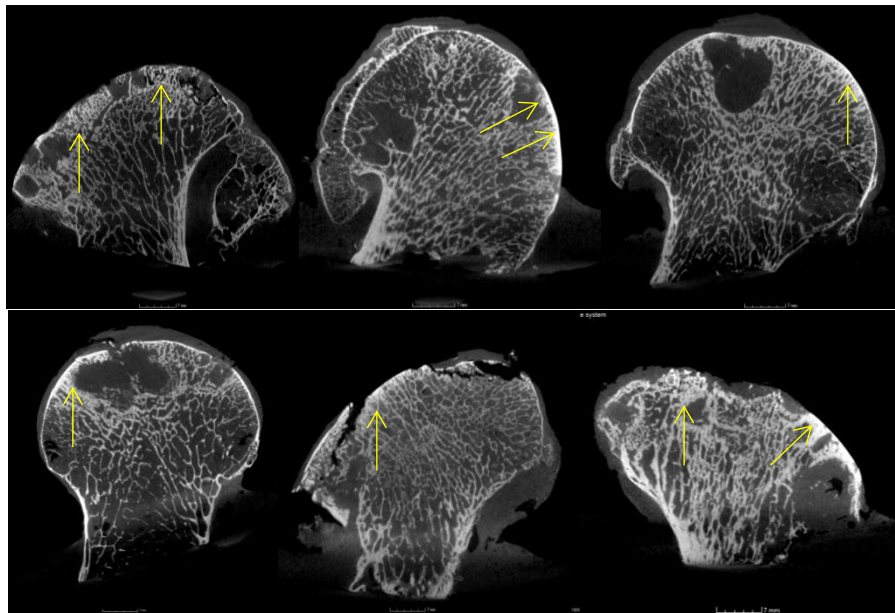


Figure 4-36 –Anterior-posterior slices from randomly selected CT images of AVN femoral heads, demonstrating the subchondral fractures (arrows) in the samples.

There have been recent reports suggesting that presence of subchondral fractures without any evidence of predisposing AVN may be a different condition to the more commonly diagnosed AVN (Polesello et al., 2009; Yamamoto, 2012). It is a condition commonly seen in elderly women with osteoporosis, rather than the AVN seen in younger patients. It is suggested that it needs to be suspected when the crescent sign is seen without any lesions in the femoral head, suggesting that the bone is alive and viable.

#### 4.4.3 Structural and Mechanical Properties of Bone with AVN

In order to develop a valid mechanical model of AVN, mechanical parameters of bone with AVN such as elastic modulus and yield stress need to be understood and replicated in the model. To generate an in vitro simulation in animal tissue, the degree of change from healthy tissue to diseased tissue need to be understood.

The structural and mechanical properties of bone with AVN were compared to the findings for control human femoral head samples. This was done for whole femoral heads and bone plugs. No significant differences were observed between the structural properties of whole heads and mechanical properties of bone plugs of AVN and control groups.

Following comparison of elastic modulus ( $E$ ) and yield stress ( $\sigma$ ) of bone plugs of AVN and control groups, the degree of change in mean mechanical properties was calculated as ratios of the control means (Figure 4-37). The data from this calculation will be used in Chapter 6 to produce a mechanical model of AVN. Although a reduction in structural properties of whole head samples and load bearing regions of samples were seen in AVN samples when compared with control samples, there was an increase in the elasticity and strength of the bone plugs in non-load bearing regions. This, along with the reduction in the elasticity and strength of the bone plug has resulted in a combined small reduction in structural properties of whole head specimens.

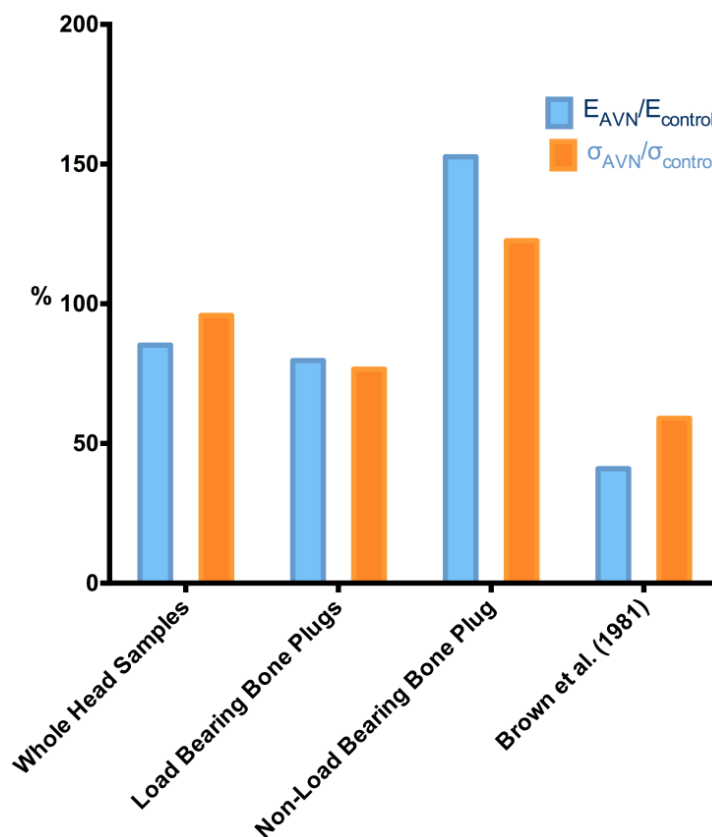


Figure 4-37 - Differences in means of elastic modulus ( $E$ ) and yield stress ( $\sigma$ ) between AVN and control specimens as percentages, as reported in this study and by Brown et al. (1981).

The findings of this study were also compared to those reported by Brown et al. (1981). In this study, necrotic bone samples demonstrated smaller changes with respect to control samples than that reported by Brown et al., and this is due to many differences in experimental methods between the two studies. Brown et al. (1981) compared the elastic modulus and yield strength of cubic samples removed from necrotic, sclerotic and live (control) regions of necrotic femoral heads (Figure 4-38) as well spatially matched control samples from non-pathological femoral head specimens. They demonstrated that the yield strength of the samples from the three different regions did not vary, whereas significant changes were seen between the elastic moduli of necrotic and sclerotic samples when compared with control group. Hence the results of this study disagree with the findings of Brown et al. It may be argued that in the latter stages of the disease, the lesions can be present in various sizes and quantities throughout the femoral head and are not limited to the load bearing region of the femoral, and to assume the necrotic region as a singular large area within the femoral head is incorrect. More details of the method used to distinguish between the different regions of the femoral head were not provided in the study by Brown et al.

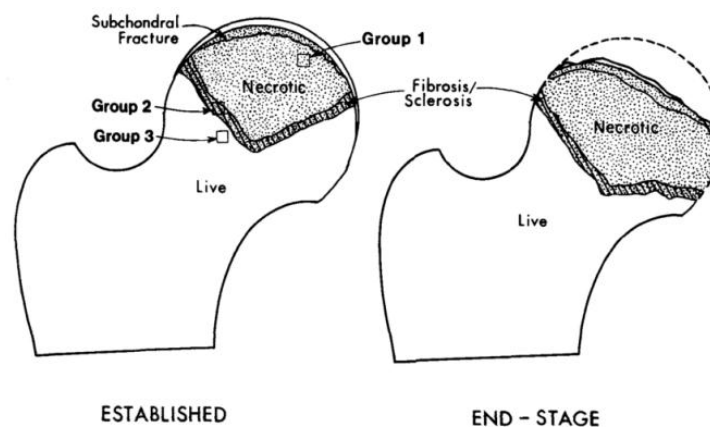


Figure 4-38 - Regions used by Brown et al. (1981) to group test samples into necrotic (group 1), sclerotic (group 2) and control (group 3). Image reproduced with permission from Wolters Kluwer Health, Inc.

Another factor that was not considered in the study by Brown et al. was that there are differences in mechanical properties of bone from load bearing and non-load bearing regions of the same femoral head. Areas with load bearing burden in the femoral head have higher bone volume, trabecular thickness and anisotropy than non-load bearing areas (Chiba et al., 2013). This results in higher strength in

the load bearing region when compared to the inferior non-load bearing region of the femoral head (Munemoto et al., 2016).

#### 4.4.4 Experimental Challenges

#### 4.4.5 Access to AVN Specimens

The AVN specimens in this study were from patients undergoing total hip arthroplasty following diagnosis of AVN. As discussed in Chapter 2, THA is normally the final treatment option for most patients affected with AVN, and due to its invasive nature, it is only undertaken in severe cases of AVN. The samples obtained in this study were categorised into stages 3-6 on the Pennsylvania system, which are also considered “late-stage”. As discussed in Chapter 2, the pathology of AVN is complicated; however it results in the final collapse of the femoral head seen in most patients. The results of this study can therefore only be representative of late stage AVN rather than all AVN cases.

Obtaining femoral heads for mechanical studies from early stage AVN is very limited for three reasons:

- In early stages, AVN is either undiagnosed, or when diagnosed, it is treated with less invasive hip preserving methods such as core decompression and bone grafting.
- It is a disease that affects younger demographics, and therefore obtaining AVN samples from tissue banks is highly unlikely.
- It is a very common disease in Asian demographics, and access to samples from Asia Pacific countries for a study in UK carries a set of challenges and limitations, as observed in this study.

The experimental work of this study was carried out on samples removed in THA surgery, and in Xi'an Jiaotong University in Xi'an, China. The main motivation for this was that AVN of the femoral head is more common in countries in Asia Pacific such as China than it is in the western continents. It is the most common diagnosis for patients undergoing total hip replacement procedures in Asia Pacific (Chiu et al., 1997, 2001; Lai et al., 2008) compared to the 2% reported in England and Wales (Ellams et al., 2011).

#### 4.4.6 Access to Control Specimens

The control samples in this study were collected as part of a larger research project, details of which can be found in the ethics protocol in Appendix B. This meant that six pelvises were shared between different studies. From the six pelvises obtained from the tissue bank, all right-side femoral heads were contributed to this study.

#### 4.4.7 Human Tissue Variance

The AVN Specimens were collected from patients who met the inclusion/exclusion criteria as explained in section 4.2.1.3. In order to collect a suitable number of specimens and to characterise bone in AVN in this study, the stage of disease was not set as a limiting factor. This meant that the AVN specimens collected in this study were from patients in later stages of the disease and therefore severely deformed. This has also meant that bone from earlier stages of AVN could not be characterised in this study.

The AVN specimens were collected from patients from a wide range of demographics as explained in section 4.3.1. The femoral heads were from equal numbers of male and female patients, with 11 left and nine right hips. Two pairs of specimens were collected from the left and right hips of the same patients. In this study the mean age of patients was 59 years. This is higher than the value seen in a paper by Lai et al. (2008), who looked at the incidence of AVN in Taiwanese patients for nine years. There was a large range in the time taken for the patients to undergo surgery from the time they had first onset of pain (3-157 months) or first presentation to a clinician for hip pain (3-156 months). This is likely a cultural issue, since Chinese people are more likely to withhold from having surgery for severe hip pain than patients in other countries. This was discussed in a paper by Tan et al. (2009), who looked at women from Indian, Malay and Chinese backgrounds and their perception of labour pain. They found that Chinese patients reported the lowest pain scores and were taking the least amount of morphine during the study, suggesting that they were more modest in their pain perception. They also found that paying patients were less likely to report high pain scores than non-paying patients. The average cost of a straightforward total hip replacement procedure in China is £4250 which is beyond the reach of many



people in the country (Huang et al., 2012), where average annual income was £6280 in 2015 (Trading Economics, 2015). This may also be a contributing factor for the long time between pain onset and surgery in this study.

The samples in this study were retrieved over a period of 13 months and were stored in a freezer for 1-33 weeks until testing. Due to the long distance between the home university and the institute where this study was carried out, the tests were carried out over two periods of 2 weeks each. A concern was that the long term freezing may have impacted the structural and mechanical properties of bone, however studies by van Haaren et al. (2008) and Kaye et al. (2012) have demonstrated that long term freezing does not reduce the mechanical properties of bone more significantly than the natural variation seen in the samples.

All control samples in this study were from deceased donors. Table 4-6 shows the primary and secondary causes of death for each donor. Three donors died from cancer unrelated to bone, one from a myocardial infarction, which is a form of heart attack, one from a drug overdose, and the final from alcoholic cirrhosis of the liver. Although, the cancer or heart attack probably did not affect the properties of bone in these donors, there is a possibility that the drug overdose or alcoholic cirrhosis of the liver may have had an effect on the properties of bone.

Obtaining legal and ethical human tissue for research, is normally difficult and limited, and can be obtained either following removal of tissue as a routine part of a surgical procedure such as hip replacement or from tissue banks where donated tissue from deceased donors are collected. When tissues are obtained from surgical procedures, they are normally severely damaged by disease (such as bone with AVN obtained from hip replacement procedure) and cannot be used as representatives of healthy tissue. When tissues are obtained from tissue banks, they are from donors who have had either physical or systemic causes of death, and more likely from an older age group. Although some of these factors can be controlled with use of an inclusion and exclusion criteria, if the factors are not diagnosed at time of death or reported in the donor report form, the screening may be ineffective. This means that there is a likelihood of presence of pathologies in tissues from donors who may have had factors contributing to loss of tissue integrity in areas of interest. In cases where donors have deceased from causes such as alcoholism or drug overdose as found in this study, it is not known

whether this has had an impact on the morphology of the bone tissue received. Alcohol abuse is a major factor contributing to AVN (Jones and Hungerford, 2004) as well as osteoporosis (Laitinen and Välimäki, 1991). Intravenous drug overdose is a factor that may lead to damage of the blood vessels in the femoral head, therefore leading to AVN of bone (Kerachian et al., 2006). Although AVN is rare in Caucasian population, the risk of AVN with alcoholism or drug overdose needed to be considered in this study.

The method used for mechanical testing of samples was kept constant between AVN and control specimens. In both studies, the 9mm bone plugs were removed from locations defined in section 4.2.1.10. The loading rate of the samples was constant between both tests. A factor that may have led to different mechanical properties of AVN and control bone in this study, and could not be kept constant was the morphological differences in the sample groups. Although the ethnic backgrounds of the AVN patients in this study are not known, it can be assumed that most likely AVN samples are from Chinese patients, whereas the control samples were from white Caucasian donors in USA. This may have contributed to differences in their mechanical properties. A study by Cong and Walker (2014) argued that lower areal BMD (BMD measured using DXA rather than volumetric BMD measured using CT imaging) seen in Chinese groups when compared to Caucasian groups may have been compensated by thicker cortices and more plate-like trabeculae rather than rod-like in their bone as well as greater buckling and compressive strength in their hips due to shorter femoral neck length. Similar findings are also reported by Liu et al. (2011).

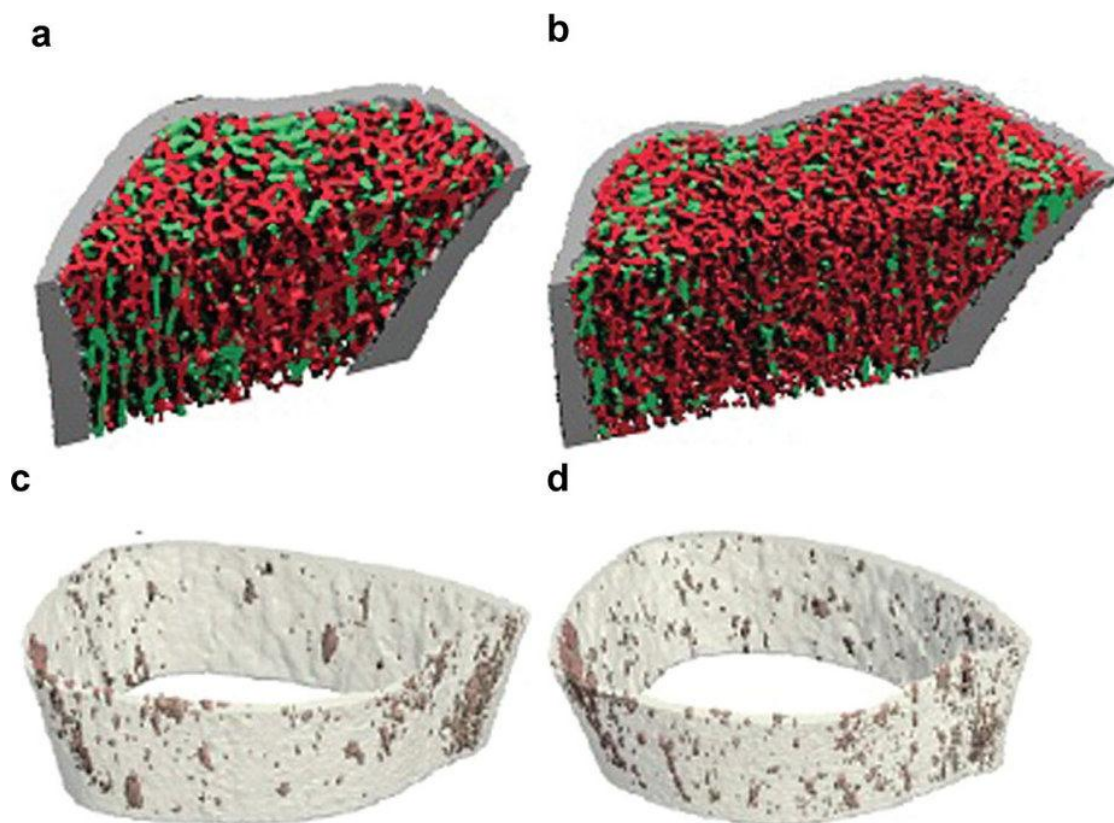


Figure 4-39 – High resolution pQCT images tibias of (a&c) Chinese-American and (b&d) white women, demonstrating the thicker cortical shell and more plate-like trabeculae in Chinese-American women when compared with Caucasian tibia (Cong and Walker, 2014). Image reproduced with permission from Nature Publishing.

#### 4.4.8 Study Limitations

Due to limited availability of technical equipment locally, compromises were made to the study and these are explained in this section.

Analysing CT images qualitatively is a challenging activity and quantitative analysis of the images is normally conducted in research. The most commonly used analysis technique for bone images is measurement of bone mineral density of specimens and comparing the findings between diseased and healthy tissue (Huber et al., 2008; Wu et al., 2009). This is possible with CT scanners where a calibration phantom designed for measurements of bone mineral density is used either in calibration of the scanner or is present in the image. The CT scanner available for this experiment in Xi'an Jiaotong University did not have the calibration phantom needed to measure the bone mineral density. Alternative quantitative and qualitative methods were considered. Initially, the plan was to qualitatively determine the locations of the subchondral fractures in the bone and quantify them using a visual grading technique. Following the CT scan of the first

set of specimens, this method was refined to the method used in section 4.2.3.1., which calculated the amount of calcified bone present in each femoral head, and used this to estimate the ratios of lesions to the overall volume of the femoral head. This method (using MATLAB) identified the volume of the femoral head, and the volume of “normal bone” within, and calculated a ratio – compensating for gaps within the trabecular bone that would normally exist within a healthy femoral head. This was done by using a “closing” algorithm, where the white areas of the image were dilated to close the regions that were denser and represented healthy bone. The difference between an AVN binary image and the “closed” image can be seen in Figure 4-40. The ratio of bone to overall femoral head was calculated for all specimens and compared in section 4.3.3. The method was also used to assess the “lesions” in control human femoral heads (Figure 4-41).

This method was preferred as opposed to the more conventional method of measuring trabecular volume within the femoral head; this method represented the volume of lesions observed in AVN rather than the volume of calcified bone. It can be seen in the CT slices from AVN specimens that although some very dense regions exist, some large lesions were also present within the femoral heads.

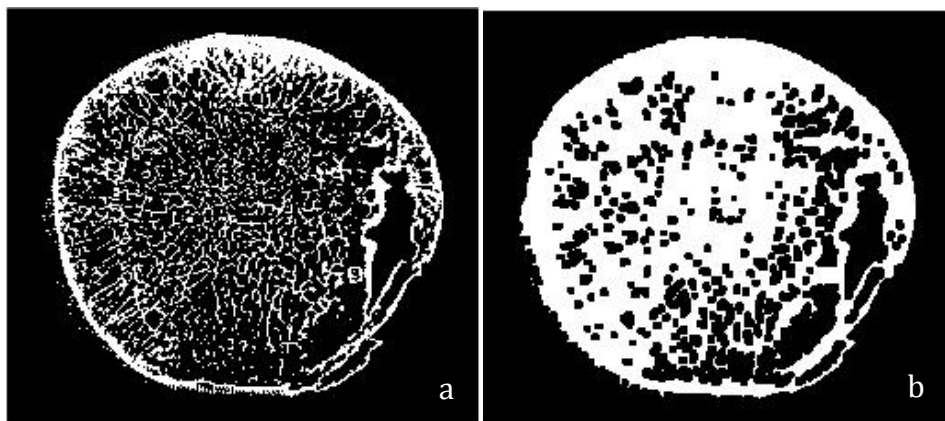


Figure 4-40 – (a) A binary image of a CT slice from an AVN specimen. (b) The binary image after application of the “closing” algorithm.

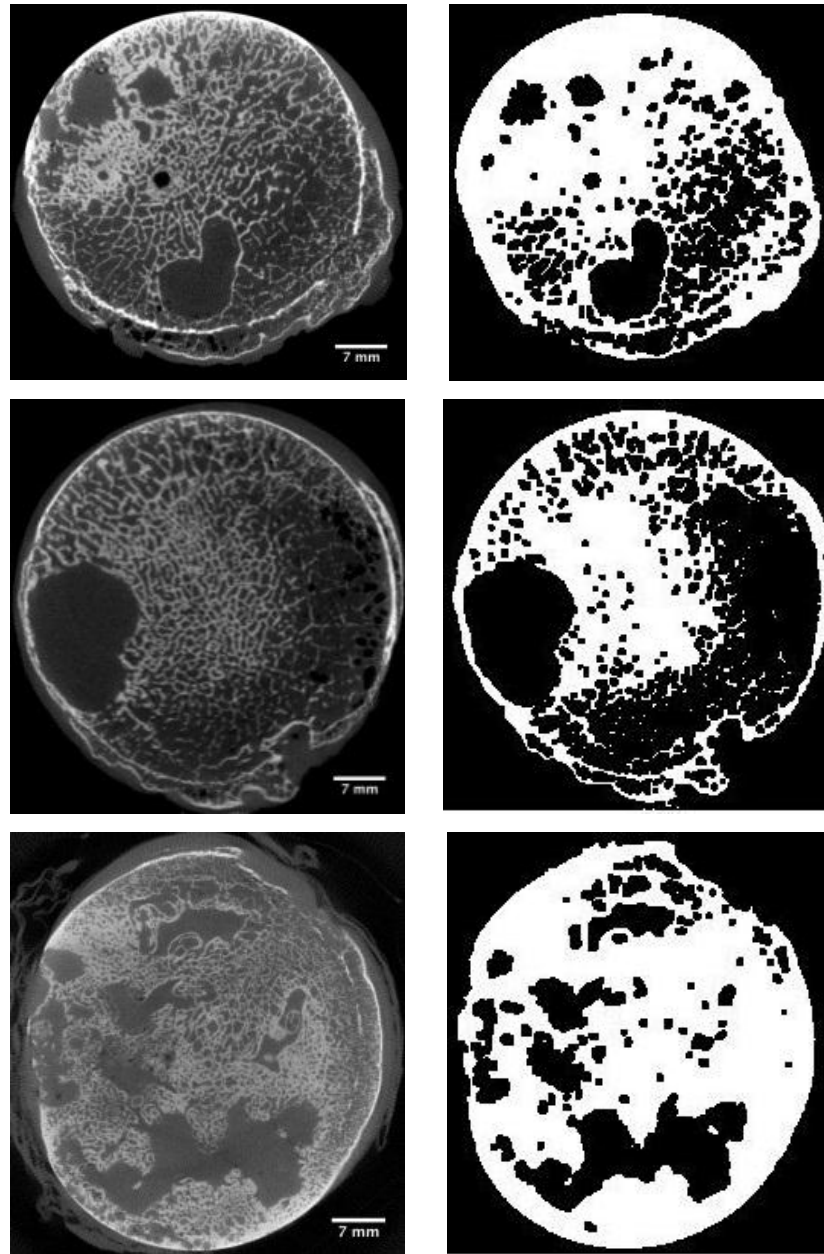


Figure 4-41 – Images on the left show CT slices from samples A4, A6, and A13 respectively, and the images on the right show a binary “closed” version of the same slices. The lesions within the femoral head are shown as black, and regions of femoral head where “normally dispersed” trabeculae exist are shown in white, allowing for measurement of the volume of the lesions rather than the volume of trabeculae.

Availability of mechanical testing machine with capability of loading specimens to up to 10kN was a challenge in this study. The highest capability available for this study in Xi’an Jiaotong University was 5kN. This was a unique issue, and due to the short term of the placement and financial limitations, acquirement of a new mechanical testing machine for the laboratory in China was deemed infeasible. To overcome this issue, alternative methods of increasing the load to the desired load were researched. A fulcrum system was thought to be the

ideal option and after further calculations and development of a fixture, this was incorporated into the study as shown in section 4.2.1.12. Although the beam theory and the fulcrum system used in this study are not new discoveries, the use of this technique to increase the load capability of mechanical testing machine has not been published previously, and can be considered in similar situations where loading capabilities are a limit in a study.

#### **4.5 Summary of Findings**

In order to understand the implications of AVN on structural and mechanical properties of bone, CT scans and compression tests of samples were carried out. It was demonstrated that the lesion volumes in AVN heads can be up to 70% of the volume of the femoral head. This was significantly higher than “lesions” or open spaces seen in control femoral heads. The lesions were also spread throughout the femoral heads and were not limited to a particular region. Subchondral fractures were also present around the lesions.

The AVN femoral heads samples demonstrated 14.8% decrease in elastic modulus and 4.2% decrease in yield stress when compared with control femoral heads. This was as a result of increased mechanical properties in non-load bearing regions of the femoral head and decreased mechanical properties in load-bearing regions.

## Chapter 5. Degradation of Mechanical Properties of Bone in a Disease Model of Avascular Necrosis of the Femoral Head

### 5.1 Introduction

Several attempts have been made to create a valid model that represents AVN of the femoral head with the same biological and mechanical characteristics that are found in the natural progression of the disease in human femoral heads. To date, all of these models have been animal models, where AVN is induced in live animals (Manggold et al., 2002; Jones and Allen, 2011). Although the initiation of AVN has been successfully induced in these animals, none of the models have presented comparable mechanical properties to those seen in human AVN (Conzemius et al., 2002). There is therefore a need to develop a mechanical model of AVN, which shows comparable mechanical and failure properties to those seen in human AVN in order to allow for optimisation of treatment modes aimed at AVN.

In order to develop a valid mechanical model of AVN, bone mechanical properties need to be altered to represent similar changes seen in AVN. To do this, various methods of reducing the mechanical strength of bone were considered and tested in vitro. Previously, the following chemicals have been indicated to possibly affect the mechanical properties of bone; potassium hydroxide (KOH), ethylene diamine tetra-acetic acid (EDTA), and hydrochloric acid (HCl).

KOH has been previously used to degrade collagen molecules in bone and was thought to have a weakening effect on bone (Wynnycky et al., 2011). EDTA is a decalcifying agent used in histology of bone, and is therefore thought to reduce the strength of bone (Wallace et al., 2013). HCl is another acid that is used in decalcification of bone as it reduces the mineral density of bone and hence the mechanical strength (Bancroft and Gamble, 2001).

The aim of this study was to investigate a chemical method to degrade mechanical properties of bone in order to replicate the reduction in mechanical strength seen in avascular necrosis of the femoral head. The three chemicals previously used in literature, KOH, EDTA and HCl were considered. The chemicals have different mechanisms and rates by which they reduce the mechanical strength of bone. These were considered in the development of test protocol, and the length of treatment by chemicals was decided based on findings from the literature.

The study of mechanical properties of bone with AVN and control human tissue (Chapter 4) showed that bone with AVN has an elastic modulus that is reduced by 14.8% and a yield strength that is reduced by 4.2% when compared with control bone. In order to replicate this difference in mechanical properties of bone in animal tissue, the different chemicals and treatment durations were tested in this chapter.

## **5.2 Materials and Methods**

A flow chart illustrating the experimental process is shown in Figure 5-1.

The effects of chemical treatment in EDTA, HCl and KOH on mechanical properties of bone were investigated. Porcine femoral head bone plugs were treated for specified durations in the chemicals mentioned and changes in their bone mineral density and mechanical properties were recorded.



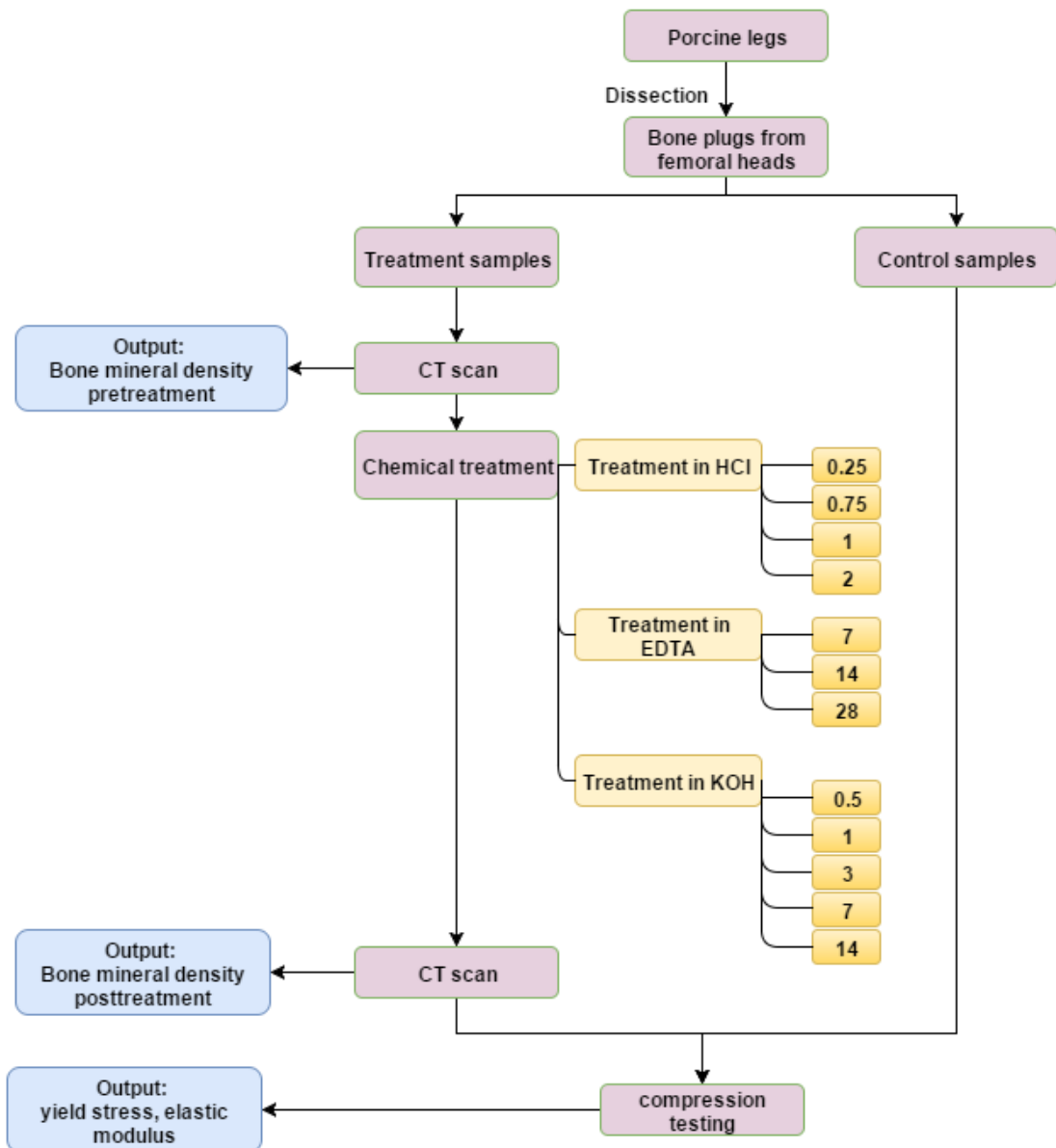


Figure 5-1 - Summary flowchart for experimental process of analysing the effects of chemical treatments on mechanical properties and bone mineral density of porcine femoral head bone samples (chemical treatment duration is in days).

## 5.2.1 Materials

### 5.1.1.1 Bone Samples

Right side porcine femurs were obtained from an abattoir (John Penny & Sons, Leeds, UK) at 5-6 months of age at time of slaughter. The tissues were obtained and dissected within 24 hours of slaughter. Bone plugs of 9mm diameter were removed from the load-bearing region of the femoral head using a corer and drill. Further details of the sample preparation method are described in section 3.2.4. Following dissection and preparation of samples,

they were either used for experiments on the day of preparation, or placed in a freezer (-20°C) for a maximum of 60 days. Three samples were allocated to each treatment and duration combination. Three samples were tested without any treatment to provide control measurements.

#### **5.1.1.2 EDTA**

A solution of EDTA (12.5% (w/v)) concentration was prepared by dissolving 125g EDTA powder (Fisher Scientific, Loughborough, UK; Cat no: 11843-0010) with 875ml of distilled water. Following stirring for 1 hour, 15g of sodium hydroxide pellets (Fisher Scientific, Cat. no: BPE359-500) were added to the solution, and it was stirred again. The pH of the solution was adjusted to 7.0 by adding drops of hydrochloric acid (6M) or potassium hydroxide (6M) solutions.

#### **5.1.1.3 HCl**

A solution of 1M HCl was prepared by diluting 12M HCl. To do this, 83ml of 12M HCl was added to 1 litre of distilled water to make up 1M HCl.

#### **5.1.1.4 KOH**

To prepare a 1M KOH solution, 56g (1 mole) of KOH pellets were added to 1L water, and stirred using a magnet stirrer for 1 hour.

#### **5.1.1.5 Chemical Storage**

The chemicals were stored in a dark cupboard at room temperature, and were used within 1 month of the preparation date.

### **5.2.2 Methods**

#### **5.1.1.6 Computed Tomography of Samples and BMD Assessment**

The treatment samples were scanned using a CT scanner (XtremeCT, Scanco Medical, Switzerland) before initiation of treatment and within two

hours of end of treatment. The CT scanner was calibrated using a phantom on the day of scanning.

The scans were carried out at a resolution of 82µm per pixel and integration time of 300ms. The scanned images were saved as DICOM files and BMD of the samples before and after treatment was calculated using the built-in software of the machine and recorded. The BMD values were calculated by selecting the overall bone plug image throughout all scanned slices.

### 5.1.1.7 Treatment of Bone Samples

The samples (n=3 for each group) were treated using the solutions in Table 5-1, for the timescales stated. HCl is a stronger acid than EDTA, and therefore samples were treated for shorter durations in HCl than EDTA. Strength of KOH was based on the reports in literature on its effects on collagen degeneration (Wynnyckyj et al., 2011); the samples were treated for 1-14 days in KOH.

Table 5-1 - Treatments and timelines used on the bone plugs

Solution	Timeline (days)				
	14	7	3	1	0.5
Potassium Hydroxide 1M (KOH)	14	7	3	1	0.5
ethylenediaminetetra-acetic acid 12.5% (w/v) (EDTA)	28	14	7	-	-
hydrochloric acid 1M (HCl)	2	1	0.75	0.25	-

During the treatment, samples were soaked in the stated solution at room temperature and with agitation at 160rpm. A solution change was carried out every 1-3 days for samples that were undergoing treatment duration of over 2 days. Following treatment, the samples were lightly rinsed with water.

### 5.1.1.8 Mechanical Tests

Following stated treatment times, samples were CT scanned again. The samples treated in potassium hydroxide for 14 days had dissolved into the liquid and were therefore excluded from further CT scanning or mechanical testing. Moreover, samples treated in potassium hydroxide for 7 days had lost

their solid structure due to exposure to the treatment, and were therefore excluded from the mechanical testing.

The heights of the bone plugs were measured using callipers. The samples were then tested using an Instron 3365, 5kN load cell (High Wycombe, UK) using a compression rate of 0.01mm/s recorded at 10Hz. Samples were tested to failure, where failure was defined as yield, or until samples reached a displacement change of over 70%.

### 5.3 Results Analysis

The BMD outputs from the CT scanned images before and after treatment were recorded by the built-in software of the scanner (Scanco Medical XtremeCT, Switzerland). The BMD was calculated for the whole bone plug. The data obtained was statistically analysed to compare findings before and after treatment. ANOVA was carried out to test for statistically significant difference between groups, followed by Tukey's means comparison test to locate the treatment groups that were significantly different.

Compression data were collected using Bluehill 2, the built-in software of Instron. The raw data were collected in comma separated (.csv) files. These files were imported into a programme on MATLAB as used in previous chapters. Yield stress and elastic modulus were calculated from the graphs. The findings were compared using ANOVA for statistically significant difference between treatment groups and the control group ( $p < 0.05$ ). Tukey's means comparison test was used to select the groups that were significantly different.

### 5.4 Results

The results obtained for bone mineral density before and after treatment are shown in Figure 5-2. Statistically significant reductions in BMD were seen in all groups that were treated with EDTA and HCl ( $p < 0.05$ ). Longer treatment times resulted in further reduction in BMD. Samples treated in EDTA at 28, 14 and 7 days had significant differences in BMD to 3 day EDTA samples. An average reduction of 97% in BMD was seen when samples were treated for 28

days in EDTA. This change was on average 19% in samples treated for only 3 days in EDTA.

Samples that were treated in HCl demonstrated significant differences in BMD before and after treatment at all-time points. Samples treated in HCl for 48 hours had significantly different BMD values to those treated only for 6 hours. An average reduction of 96% in BMD was seen in samples that were treated for 48 hours, whereas this average reduction was 61% in samples treated for 6 hours in HCl.

Only samples treated in potassium hydroxide for 7 days demonstrated statistically significant reduction of 30% in BMD. The rest of the potassium hydroxide treated samples did not show significant differences before and after treatment.

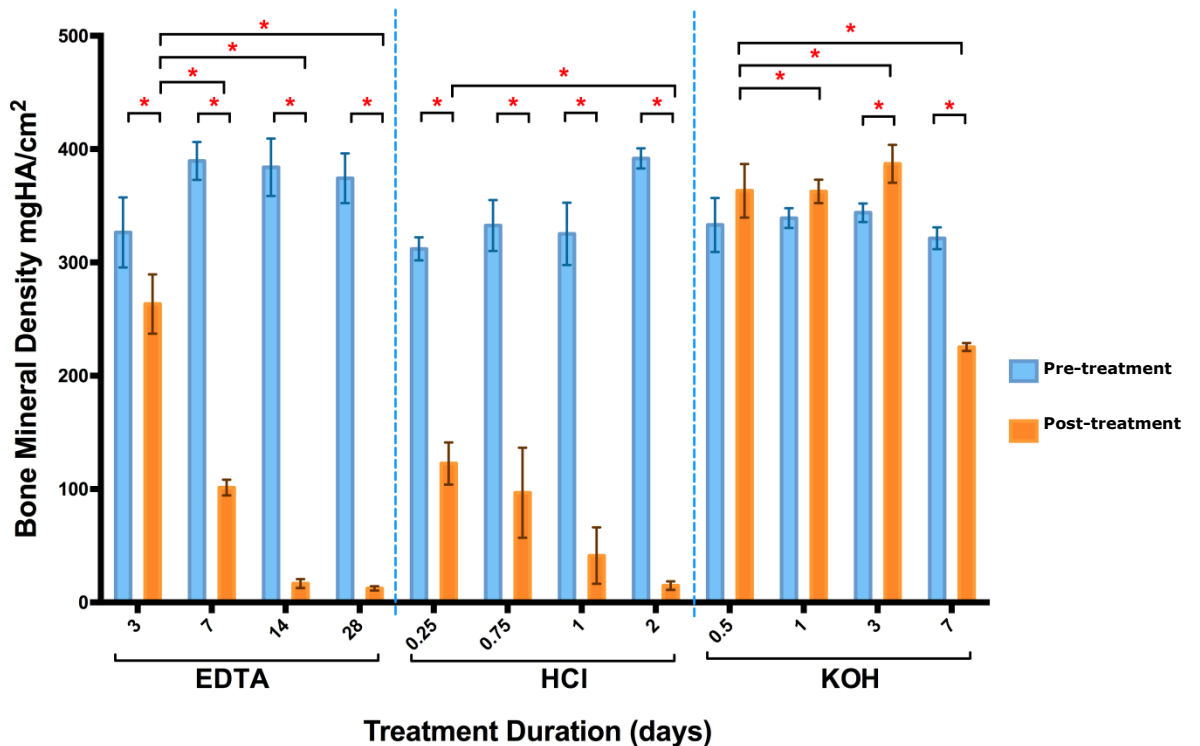


Figure 5-2 - Change in BMD of porcine bone plugs before and after treatment. Asterisks demonstrate significant differences between treatment groups, or before and after treatment (Two-way ANOVA with Bonferroni's multiple comparisons test,  $p < 0.05$ ). Error bars display standard error of mean.

A statistically significant reduction was seen in elastic modulus and yield stress of samples that were treated in all of the treatment groups, when compared to control samples. For EDTA treated samples, a significant reduction in elastic modulus was seen between samples that were treated for 14 and 28

days, when compared to 3 days. No significant differences in elastic modulus were seen between samples that were treated with hydrochloric acid or potassium hydroxide.

The yield stress of samples treated in EDTA for the various durations were significantly different when compared with 3 day treatment group, reducing further with increasing treatment duration. 7+ days of treatment in EDTA and the HCl treatments reduced the yield stress to nearly 0MPa. For KOH samples, the samples treated for 1 and 3 days had significantly lower yield stress when compared to 0.5 day treatment samples.

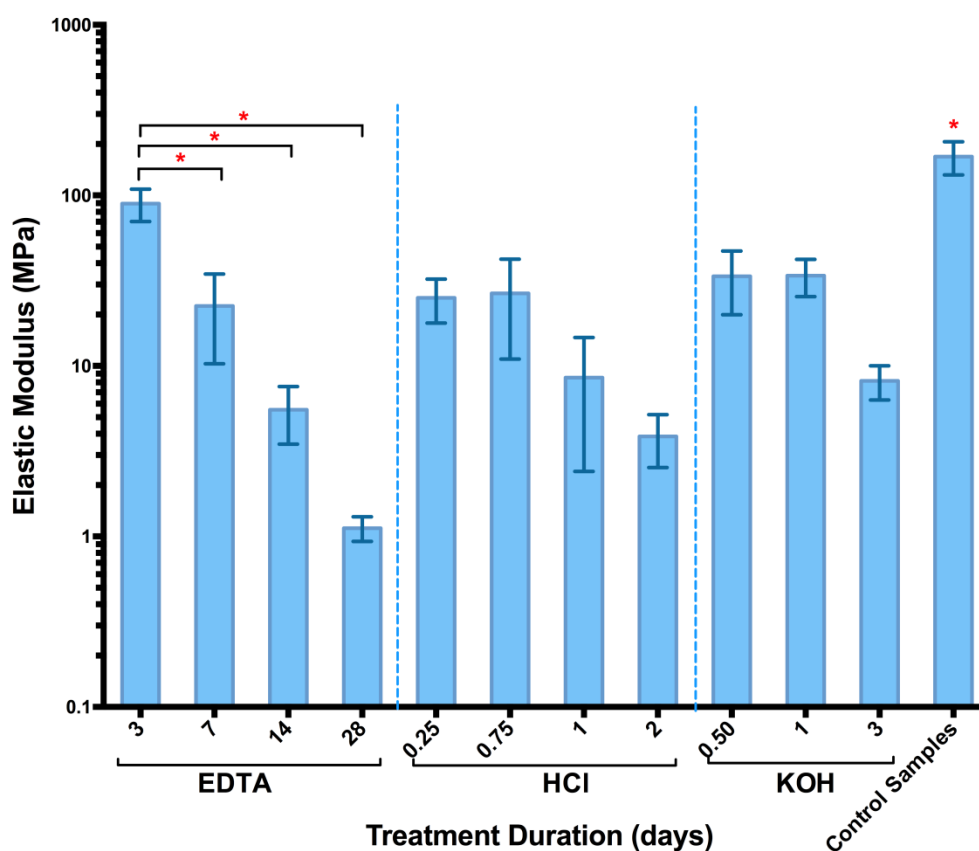


Figure 5-3 – Logarithmic plot of elastic modulus of samples treated in EDTA, HCl and KOH as well as a control group. All samples had significantly different values to control samples (One-way ANOVA and Tukey’s multiple comparisons test,  $p < 0.05$ ). Asterisks demonstrate significant differences between treatment groups. The asterisk above control samples indicates significant differences with all the treatment groups. Error bars display standard error of mean.

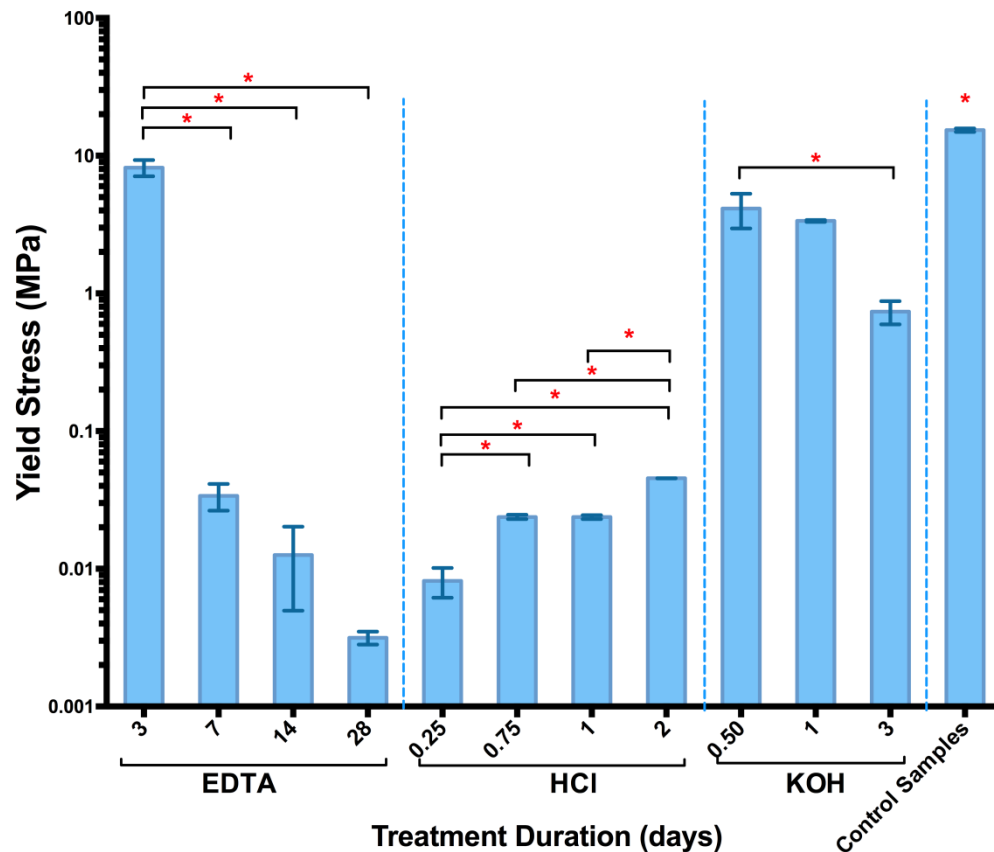


Figure 5-4 – Logarithmic plot of yield stress of samples treated in EDTA, HCl and KOH as well as a control group. All samples had significantly different values to control samples (One-way ANOVA and Tukey’s multiple comparisons test,  $p < 0.05$ ). Asterisks demonstrate significant differences between treatment groups. The asterisk above control samples indicates significant differences with all the treatment groups. Error bars display standard error of mean.

## 5.5 Discussion

This study was designed to determine the most suitable method of degrading the mechanical properties of bone in order to replicate the degeneration observed in AVN of the femoral head. In order to do this, bone plugs were treated using three degenerating chemicals: ethylene diamine tetraacetic acid (EDTA), hydrochloric acid (HCl) and potassium hydroxide (KOH).

### 5.5.1 Loss of Collagen Matrix

KOH is an agent that is used in removal of bone matrix by degrading the collagen network in the bone (Wynnyckyj et al., 2011). As collagen is very important in providing structural integrity to bone (Wang et al., 2001), it was assumed that collagen degeneration by KOH treatment would provide the loss of strength required to represent mechanical properties of avascular necrosis

of bone. Samples treated using KOH for 7 and 14 days had lost most of their solid structure (Figure 5-5), so much that mechanical testing could not be performed on these samples and they were excluded. A CT image was obtained for samples treated in KOH for 7 days, and the BMD had reduced significantly when compared to BMD of samples pre-treatment. Since KOH does not have a decalcifying effect on bone, this reduction of BMD in the 7-day treatment sample may be explained by swelling of the sample, which increased the volume of the sample, hence the BMD reduction in a selected area of the image that was used for calculations.



Figure 5-5 - A sample treated in KOH for 7 days. The sample had lost its solid structure, swelled and was destroyed in handling.

Following mechanical testing of samples treated in KOH for 0.5, 1 and 3 days, significant reductions in yield stress and elastic modulus were seen when compared with control samples. A study by Wynnyckyj et al. (2011) analysed the effects of KOH treatment on emu bone collagen content using  $\alpha$ -chymotrypsin digestion assay, and found that samples treated in KOH for 7 and 14 days had significantly higher percent of denatured collagen when compared to control samples (Figure 5-6). This matches with the findings of the current study, where treating samples in KOH for 7 and 14 days reduced the solidity of samples. Wynnyckyj et al. (2011) explained that the weakness in mechanical integrity of bone is due to the penetration of KOH into the bone, swelling the collagen, hence resulting in a disorganised structure. This is also consistent with the findings of the current study, where swelling was seen in samples treated with KOH.



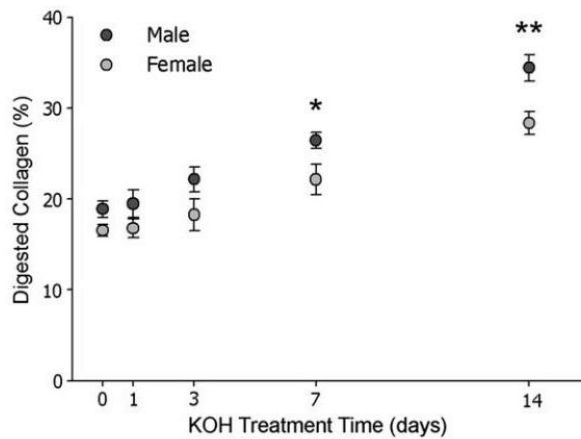


Figure 5-6 - Findings of Wynnykyj et al. (2011), demonstrating the percent digested collagen following treatment in KOH for male and female emu tibiae. The \* and \*\* indicate that 7- and 14-day treated samples respectively had significantly greater percent digested collagen when compared to control samples. (Reproduced with permission from Elsevier)

### 5.5.2 Decalcification of Bone Tissue

HCl and EDTA are decalcifying agents used commonly in biological experiments, where histological analysis of bone is required (Prasad and Donoghue, 2013; Castania et al., 2015). This is due to ability of HCl and EDTA to remove calcium from the mineralised tissue and therefore allow for precision slicing of samples, to be viewed under the microscope. In this study, this effect was observed in CT images of samples following treatment by EDTA and HCl. A reduction of the overall bone mineral density was seen in these samples, as demonstrated in Figure 5-2.

The relationship between bone mineral density and elastic modulus of samples treated in EDTA and HCl is shown in a regression analysis in Figure 5-7. It can be seen that with increasing BMD, the elastic modulus also increases. Although most samples lay within the 95% confidence limit of this regression line, four samples were slight outliers, and one sample was on the border of the 95% confidence limit. A linear relationship for BMD versus elastic modulus for samples with BMD lower than 100mgHA/cm<sup>3</sup> is shown, however the results show this data cannot be used to predict the elastic modulus of the bone using BMD for samples with BMD higher than 100mgHA/cm<sup>3</sup>.

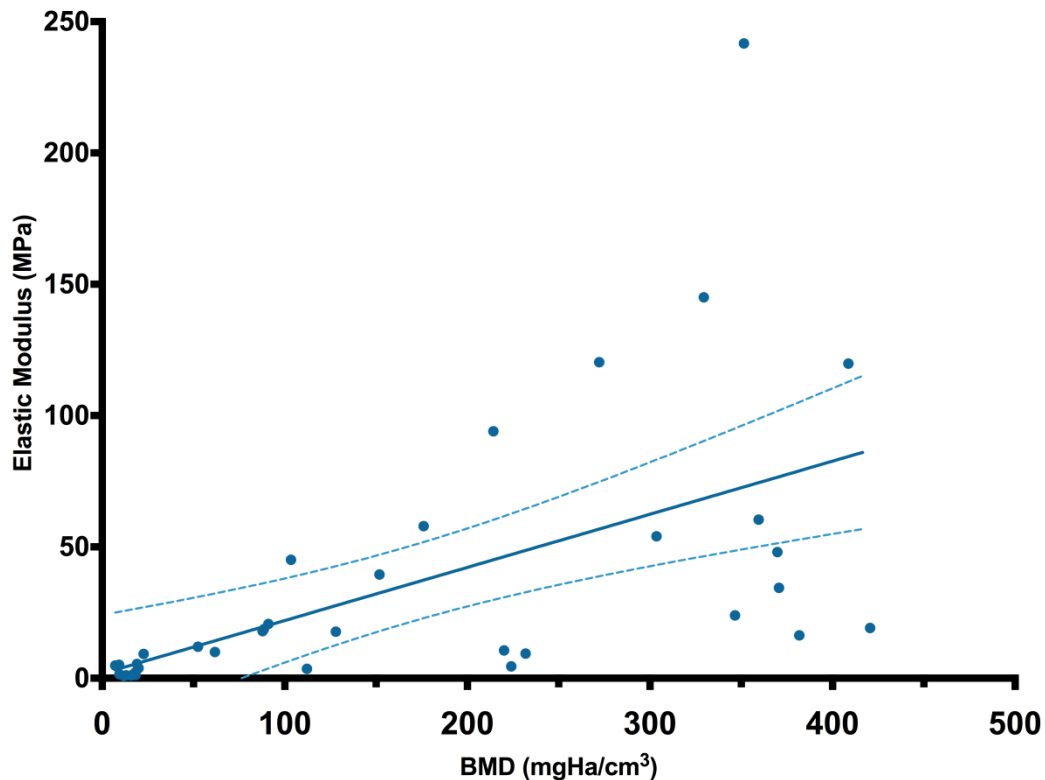


Figure 5-7 -Relationship between elastic modulus and bone mineral density for bone plugs treated with HCl and EDTA. Solid line is a regression line and the dotted lines are areas of 95% confidence regions.  $R^2 = 0.32$

The relationship between BMD and mechanical properties of bone has been studied previously. Wachter et al. (2002) showed a correlation between qCT derived BMD and compressive yield stress ( $r = 0.64$ ) and elastic modulus ( $r = 0.69$ ) of cortical bone extracted from human femoral lateral diaphysis. Another study by Duchemin et al., (2008) demonstrated similar findings for human femoral mid-diaphysis cortical bone samples, and their CT BMD and compressive yield stress ( $r^2 = 0.72$ ) and elastic modulus ( $r^2 = 0.43$ ). Similarly, Haba et al. (2012) reported a linear relationship between the structural modulus of human femoral head trabecular samples and DXA BMD of samples measured *in vivo* ( $r^2 = 0.79$ ) and *in vitro* ( $r^2 = 0.82$ ).

The CT images showed that the reduction in bone mineral density did not occur uniformly over the bone plugs and the area decalcified in the images increased with increasing treatment duration in EDTA or HCl, as shown in Figure 5-8. It is observed that the samples had a central calcified region, and an outer decalcified region following penetration of the decalcifying agent into the

bone trabeculae. After 28 days of treatment with EDTA and 2 days with HCl, samples were respectively 100% and 95% decalcified.

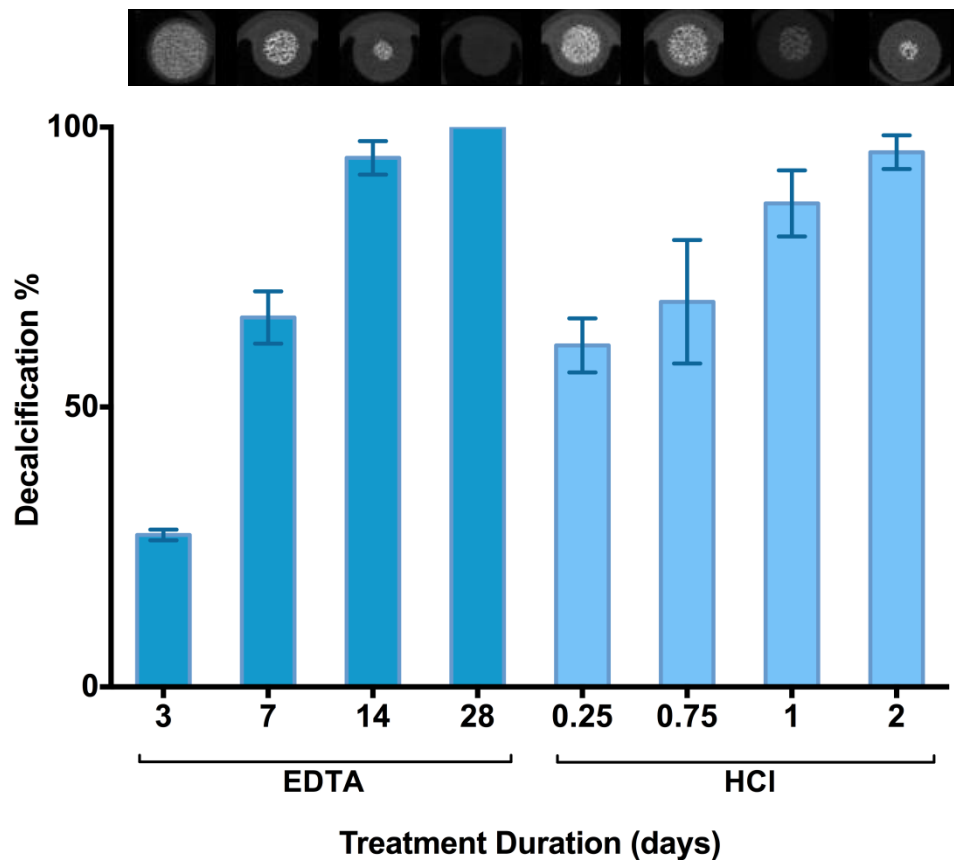


Figure 5-8 – Mean area of decalcified regions for bone plug samples treated with EDTA and HCl, as a percentage of the total bone plug, with a representative example CT slice from each treatment group shown above. The error bars show standard error of mean.

These results are consistent with the findings of Ching-yi Lee et al. (2011),. They used EDTA to decalcify porcine lumbar vertebrae in order to develop an experimental model of osteoporosis, and they reported that in samples treated with EDTA for 6 weeks, 80% of volume of vertebrae was osteoporotic, suggesting that the outer regions of the bone were more decalcified than the inner regions.

The relationship between the mechanical properties of bone and the decalcified region for these samples is presented in Figure 5-9 and Figure 5-10. It can be seen that as the percent decalcified increases, both the yield stress and elastic modulus are decreased. It was seen that the yield stress of samples were 5-10MPa for samples that were below 40% decalcification, however the yield stress was reduced to ~0MPa with further decalcification. Therefore it can be

argued that the region within the bone plug that remains calcified does contribute to the yield strength of the bone plug.

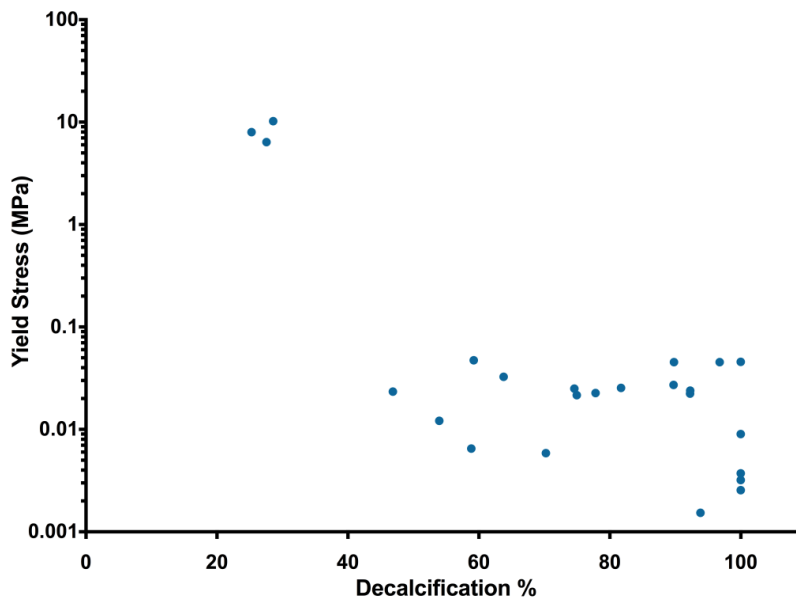


Figure 5-9 – Relationship between the logarithmic yield stresses of bone plugs versus bone plug decalcified region percentage. A line of best fit could not be plotted for this data.

A non-linear regression line was drawn for elastic modulus versus percent decalcified to demonstrate the relationship between the two findings (Figure 5-10). It showed that a negative relationship can be assumed for elastic modulus and the percent decalcified, where increasing percent decalcified leads to decreased elastic modulus. Four out of 24 samples in this study were anomalies which lay beyond the 20% error region, indicating that further work is required to narrow down an accurate relationship between these two factors.

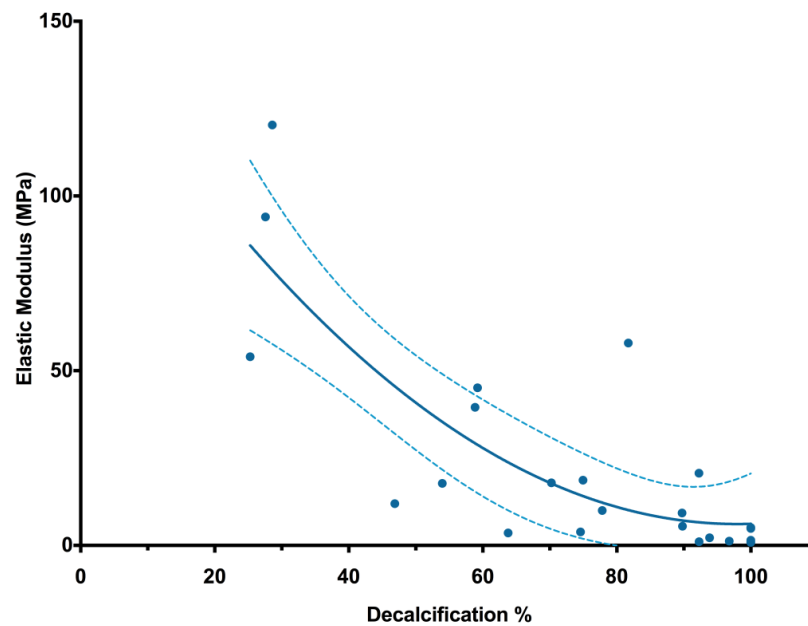


Figure 5-10 - Relationship between elastic moduli of bone plugs versus bone plug decalcified region percentage. The line is a second order polynomial non-linear regression line with 95% confidence limits shown.  $R^2 = 0.65$ .

### 5.5.3 Reducing Mechanical Properties of Bone

The aim of this study was to determine the effects of degrading chemicals on the mechanical properties of porcine bone. This was so that the effects could be translated into a method to develop disease models of AVN in Chapter 6. It was shown that treating bone plugs with the chemicals in this study can reduce the mechanical properties of the bone by affecting its overall integrity.

The findings in this study showed that treatment of bone with EDTA and HCl which are decalcifying chemicals, can affect its mechanical properties by altering the mineral content of the bone, resulting in lower volumetric BMD values and weaker mechanical properties following treatment.

The overall BMD measured in the bone samples treated with HCl and EDTA may be a useful tool in estimating the yield strength and elastic modulus of bone in a non-invasive manner. The percentage of area decalcified over total volume of the bone sample was also assessed for correlation with mechanical properties, and it can be useful in estimating the mechanical properties.

Collagen dissolving chemicals such as KOH affect the bone collagen matrix, and therefore weakening its structure. The yield stress and elastic modulus of

bone decreased with increasing treatment time in all three solutions used in this study.

Significant reductions in yield stress and elastic modulus of treated samples were seen when compared with the mechanical properties of control samples. Yield stress was reduced by 46.51% after 3 days in EDTA and up to 99.98% after 28 days in EDTA. Similarly, reductions of 47.02% were seen in elastic modulus of samples after 3 days in EDTA and up to 99.34% after 28 days treatment in EDTA. A comparison was made between the elastic modulus and yield stress of AVN samples with control samples, and it was reported that reductions of 20.2% in mean yield stress and 23.4% in mean elastic modulus were seen when compared with control samples. This means that in this study, the degree of degradation of bone mechanical properties were beyond that percentage change seen in AVN bone plug samples.

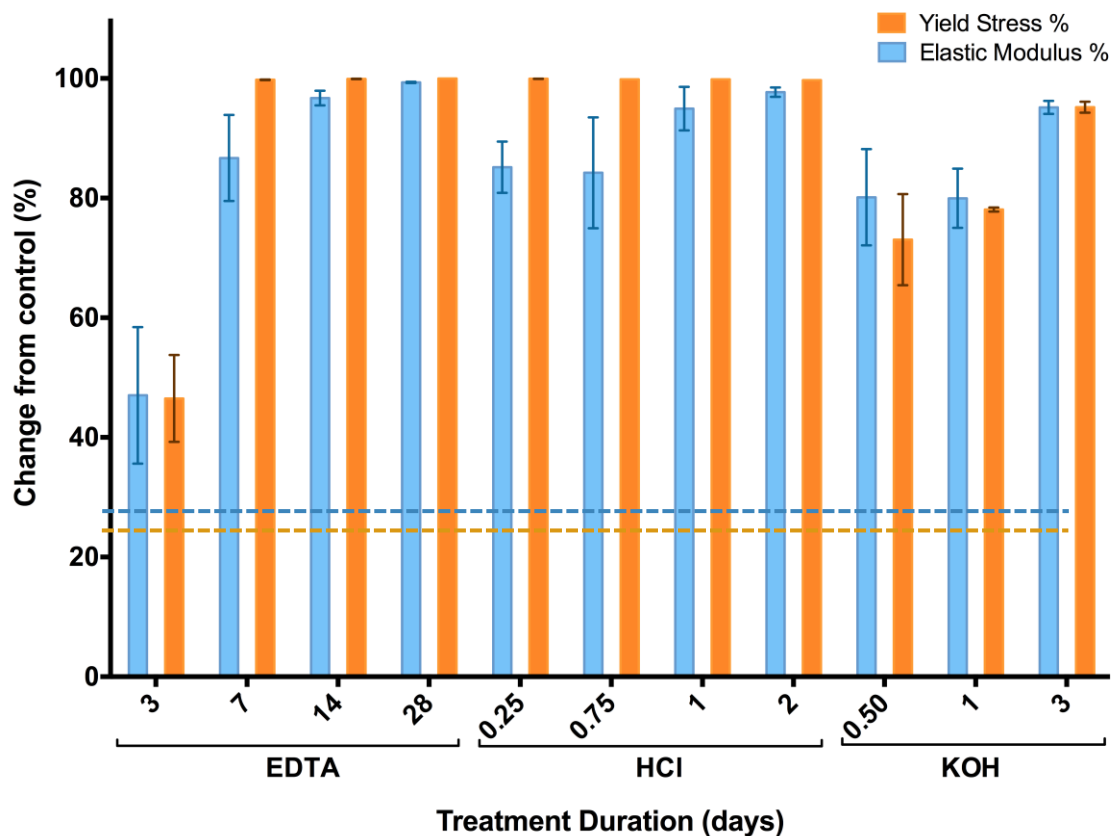


Figure 5-11 – Figure demonstrating the percentage change in yield stress and elastic modulus of samples when compared with control samples.

It was shown in the study of mechanical properties of bone plugs with AVN in Chapter 4 that the elastic modulus and yield strength of samples were

different depending on the location taken from the femoral head. The samples from the load bearing regions of the AVN femoral heads had significantly higher yield stress and elastic modulus than those from the load bearing regions. The current study demonstrated successful reduction of mechanical properties of individual bone plugs, however the effect of this change on the overall whole head structure is not known and is analysed in Chapter 6.

## 5.6 Summary of Findings

The aim of this study was to understand the effect of degradation techniques on mechanical properties of bone and find a suitable treatment method that can be used to replicate the mechanical degradation of bone seen in avascular necrosis of the femoral head. Following treatment of samples in KOH, EDTA and HCl for various durations it can be seen that HCl was most effective in reducing mechanical properties of bone in shorter time and may be more suitable in in vitro model development of avascular necrosis on whole femoral heads. EDTA showed similar results to HCl following longer treatment periods.

KOH samples showed a different behaviour to that seen in EDTA and HCl samples. Where the demineralised samples kept their structural integrity and demonstrated reduction in strength due to lower BMD, KOH samples did not have reductions in BMD as seen in demineralised samples. They also swelled up during treatment and at longer treatment times dissolved in the KOH solution.

The findings in this study show that the mechanical reduction as shown by Brown et al. and reported in experimental study in Chapter 4 can be achieved using all three methods. The applications of these methods in developing an in vitro simulation model of AVN are explored in Chapter 6.





## Chapter 6. Development of a Mechanical Simulation Model of Avascular Necrosis in Porcine Femoral Heads

### 6.1 Introduction

The aim of this PhD thesis was to understand the mechanical properties of avascular necrosis and use the findings to simulate avascular necrosis in a laboratory setting. The outputs from this model may be used in two ways – firstly it can be a model to simulate the disease that could be used for testing mechanical treatment modes for AVN. Secondly, it could be used to improve diagnostic tools used for AVN by demonstrating a comparative set of data for femoral head images with AVN and their associated mechanical properties.

Four studies contributed to the development of this study, and these are presented in Figure 6-1.

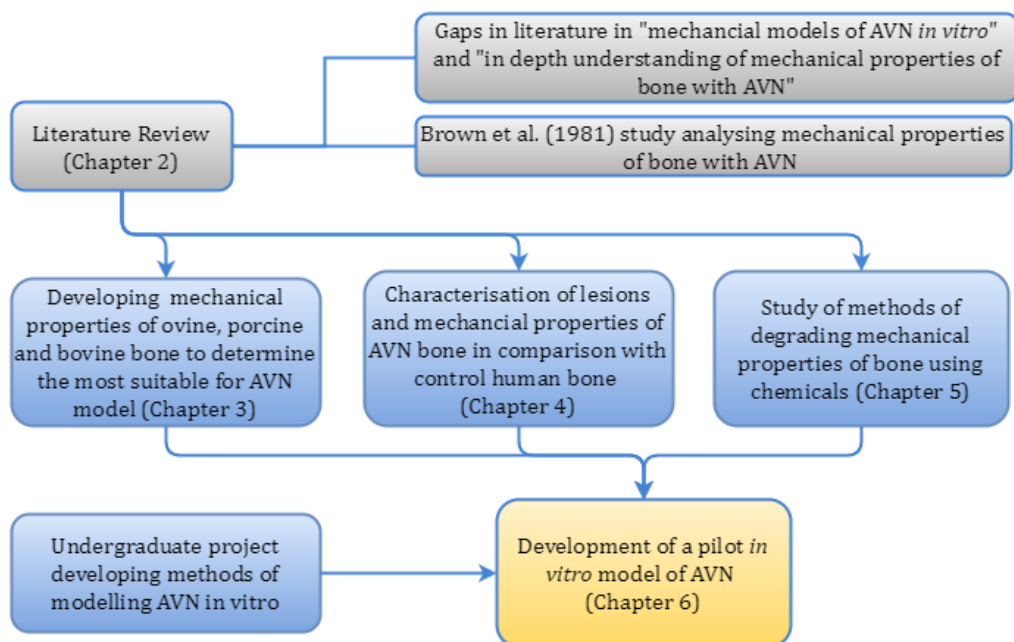


Figure 6-1 – Summary of studies in this thesis. Current chapter is highlighted in yellow and the studies providing direct input into the current chapter are highlighted in blue.

In Chapter 3 of this thesis, the mechanical properties of ovine, porcine and bovine bone were studied in order to determine the most suitable animal tissue

to be used in a mechanical model of AVN. A series of morphological parameters as well as the mechanical properties of the tissues were considered, and it was concluded that porcine femoral heads were most suitable for development of the AVN model.

In order to develop a mechanical model of AVN, the mechanical properties of bone in the model need to be comparable to those seen in AVN femoral heads. It was reported in Chapter 4 of this thesis that AVN femoral head samples tested demonstrated 14.8% decrease in elastic modulus, and 4.2% decrease in yield stress when compared with control human femoral heads. It was also demonstrated that the non-load bearing regions of the AVN femoral heads had higher modulus and yield stress values when compared to the bone plugs from the non-load bearing regions of control femoral heads, and the opposite applied to bone plugs from the load bearing regions of the femoral heads.

In Chapter 5 of this thesis, methods of degrading mechanical properties of bone were discussed. The results demonstrated that HCl was the most effective method of reducing the mechanical strength of bone in a short period of time; however both EDTA and KOH were also effective in mechanically degrading bone. All the chemicals tested in Chapter 5 demonstrated reduction in mechanical properties of bone plugs as shown in figure 5-11, however the effect of this change on the mechanical properties of whole head structures were not analysed. It is difficult to estimate the effect of changing the mechanical properties of one part of the femoral head on the structural properties of the whole head due to the complex shape and morphology of the bone. It is therefore important to understand these effects using experimental analysis.

The work in this chapter is supported by a preliminary project carried out at University of Leeds by fourth year undergraduate students (Appendix G), under the supervision of Dr Sophie Williams<sup>1</sup>, Dr Alison Jones<sup>1</sup>, Dr James Anderson<sup>1,2</sup> and author of this thesis, Mahsa Shahi Avadi<sup>1</sup>. The project was

---

<sup>1</sup> University of Leeds, Leeds, LS2 9JT, United Kingdom

<sup>2</sup> DePuy Synthes Joint Reconstruction, St. Anthony's road, Leeds, LS11 8DT, United Kingdom

carried out in two parts, where one set of students developed experimental models and simulations of AVN, and another set focused on computational modelling and simulation of the disease. Both groups used the findings of Brown et al., (1981) to develop the necrotic regions within porcine femoral heads. The experimental group trialled methods of reducing the mechanical properties of bone, and they succeeded by removing bone plugs from non-load bearing regions of porcine femoral head and using HCl to chemically degrade bone in order to simulate the mechanically weak bone properties seen in AVN tissue. They then placed the degraded bone plug back into the femoral head and secured in place using PMMA bone cement. The group CT scanned these samples and then used a single station hip simulator (SSHS) to apply dynamic loading to weight bearing region of the femoral head and observed contact pressure and fractures. They showed that the AVN “models” fractured with less load cycles when compared to non-treated control porcine femoral heads. They also commented that the fractures occurred at the growth plate region of the femoral head rather than the subchondral region collapse observed in AVN.

This study continued on this work and improved on the mechanical model of AVN developed by the student project, and the findings are reported in this chapter.

## **6.2 Materials and methods**

The pilot model of AVN in this study had two aims: first, to produce a femoral head that demonstrated the reduction in mechanical properties of bone that was seen in AVN femoral heads in Chapter 4, and second, to produce model that contained lesions as seen in the AVN femoral heads.

To produce the lesions, bone plugs were removed from the load-bearing regions of the femoral heads, and following treatment to reduce their mechanical properties, were returned to the femoral head. PMMA bone cement was used to secure the bone plugs in the head.

The method of reducing the mechanical properties of bone using degradation by HCl was adopted, as it degraded bone effectively in a short timeframe as demonstrated in Chapter 5. Treatment time of 6 and 18 hours

were used along with two control sets – one set of femoral heads with bone plug removed and returned without treatment to demonstrate the effects of deforming the tissue, and one set of non-deformed femoral heads as the controls for the study.

**6.2.1 Sample Preparation**

Twelve Porcine femoral head samples from 5-6 month old pigs were received from the abattoir (John Penny & Sons Abattoir, Rawdon, Leeds, UK) and they were dissected following the methods described in section 3.2.4. Bone plugs were removed from load bearing regions of the the femoral heads as demonstrated in section 3.2.5, with the exception that the cartilage was left intact and not removed. Both the bone plugs and the remaining femurs were placed in PBS-soaked tissue paper to maintain moisture until further treatment or testing.

The bone plugs were treated with 1M HCl (prepared as described in section 5.1.1.3) and using the treatment method described in section 5.1.1.7. The remainder of the femoral head was refrigerated at 4°C until required.

The samples were grouped as shown in Table 6-1. A set of control data were also used from the results of mechanical properties of porcine whole head samples from Chapter 3. This was considered acceptable as the method of mechanical testing was consistent with the method used in Chapter 3.

Table 6-1 – Sample groups and treatments applied to each group.

<b>Group (n=4)</b>	<b>Treatment</b>
<b>18 hours</b>	The bone plug was treated in HCl for 18 hours and placed back into the femoral head.
<b>6 hours</b>	The bone plug was treated in HCl for 6 hours and placed back into the femoral head.
<b>0 hours</b>	The bone plug was removed and placed back into the femoral head without any treatment.

Following the treatment allocated to the group, the bone plugs were placed back into the cavity of the parent femoral head. Bone cement (prepared with method described in section 3.2.3.2) was injected in the space between the bone plug and the femoral head in order to fill the gap and seal the bone plug into the head. A small amount of pressure was applied to the bone plug to prevent ejecting until the bone cement had cured.

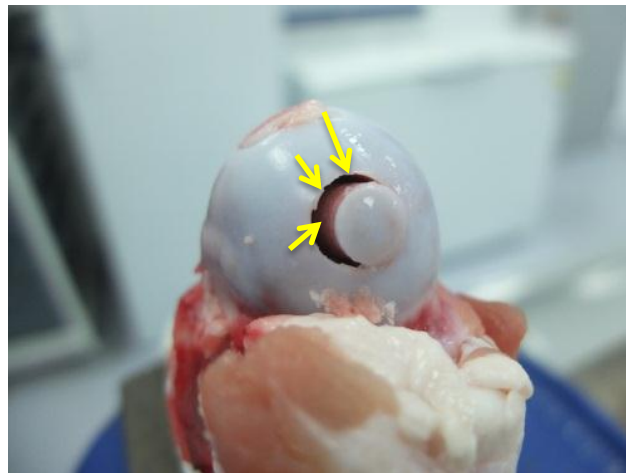


Figure 6-2 - A porcine bone plug that is placed back into the femoral head following treatment in HCl. The cavities (arrows) were filled with bone cement.

After the bone plugs were set into the femoral heads, the heads were prepared as described in section 3.2.6. When the samples were fixed in bone cement, they were stored in refrigerator for maximum of 2 hours before mechanical testing.

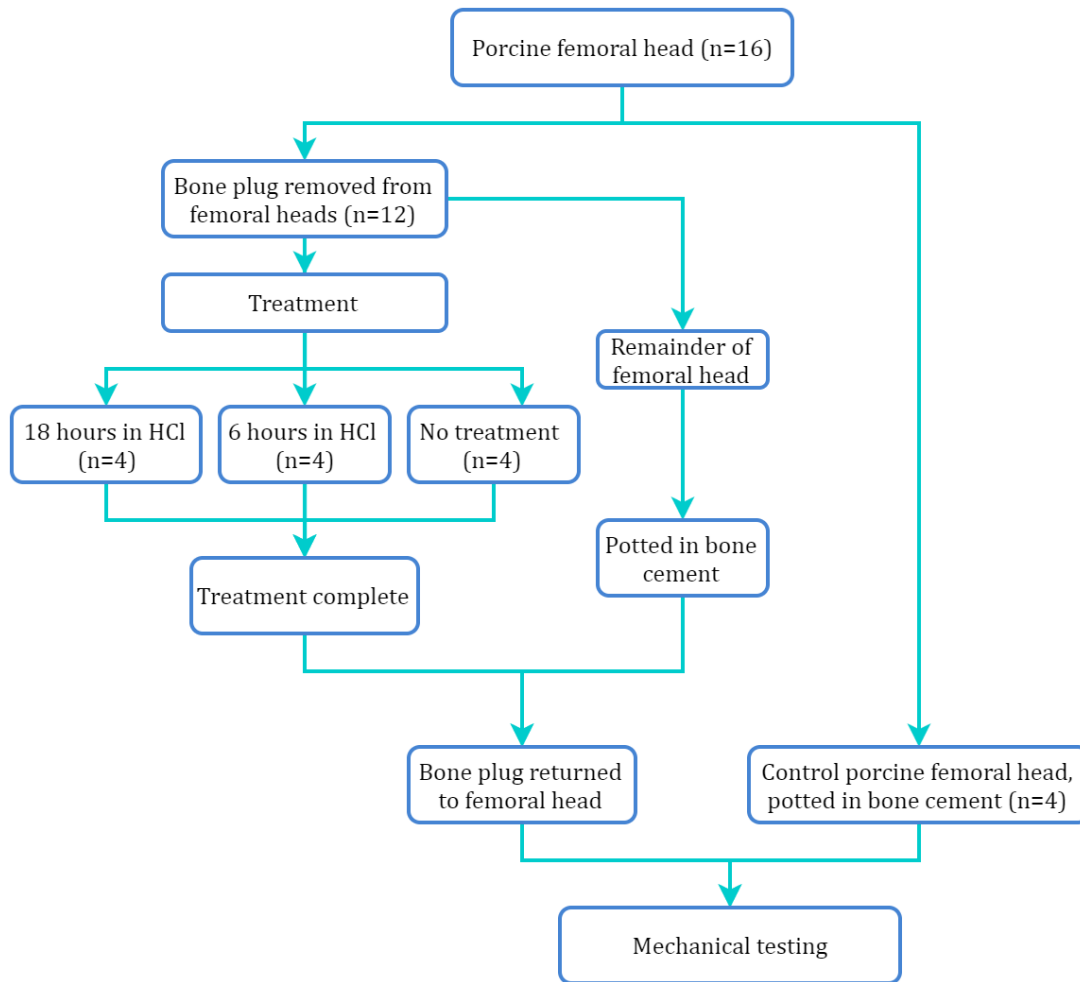


Figure 6-3 – Flow chart demonstrating the sample preparation and treatment paths for the model and control groups.

### 6.2.2 Mechanical Characterisation

Samples were tested in uniaxial compression until failure using the method and apparatus described in section 3.2.9. The loading rate was maintained in order to produce data that were comparable to the findings related to porcine femoral heads tested in Chapter 3. Failure was defined as the point where plastic deformation was initiated, recognised by a significant drop in the compression load.

### 6.3 Results analysis

The results from the mechanical test were saved in .csv format and imported into MATLAB for further analysis. The method used in MATLAB to

analyse the mechanical properties of femoral heads has been explained in section 3.2.10.2.

Analysis of variance (ANOVA) was used to check for significant differences between the means of groups ( $p < 0.05$ ), and Tukey's multiple comparison test was used to establish the groups that were significantly different from each other ( $P < 0.05$ )

## 6.4 Results

The elastic modulus and yield stresses for the various treatments used to replicate mechanical properties of AVN were calculated and are presented in Figure 6-4. The groups with treated bone plugs had significantly lower elastic modulus when compared to both control groups. The group with bone plugs treated for 18 hours had significantly lower yield stress when compared with the other groups.

The red dashed line presents the target reduction in elastic modulus and yield stress from unmodified control groups in order to reproduce changes in the femoral head seen in AVN samples in Chapter 4. The control group with non-treated bone plugs demonstrated the closest values to the target line.

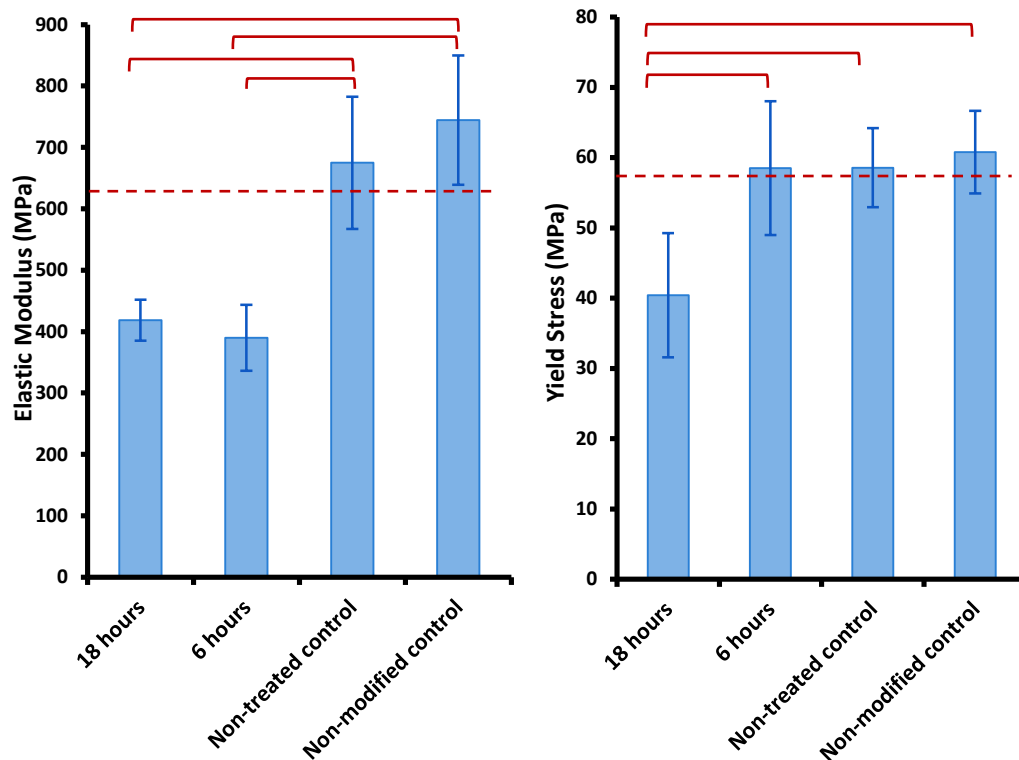


Figure 6-4 –Elastic modulus and yield stresses for femoral heads from treated groups and untreated and unmodified control groups. The error bars demonstrate standard deviation. Red brackets demonstrate significant differences between groups (ANOVA, Tukey’s multiple comparisons test,  $p < 0.05$ ). The red dashed lines demonstrate the desired mechanical properties for an AVN model, based on 14.8% decrease in elastic modulus and 4.2% decrease in yield stresses of unmodified control groups.

## 6.5 Discussion

The aim of this study was to produce an *in vitro* pilot animal mechanical model of AVN by reducing the mechanical properties of porcine bone to represent the reduction in the mechanical properties seen in AVN femoral heads with respect to the control human femoral heads (as demonstrated in Chapter 4).

There have been many attempts at developing animal models of AVN, as discussed in section 2.7. All of the models published to date have been on living animals, and have been to induce AVN in the joint clinically. There have been no published attempts to develop a model of AVN in cadaveric human or animal tissue.

In order to develop a mechanical model of AVN, a series of preliminary studies were undertaken:



1. Firstly, differences in femoral head tissue from different animals needed to be understood. For this study, access was provided to porcine, ovine and bovine tissue and these were studied and compared with human tissue in Chapter 3 of this thesis. Porcine tissue was found to be the most suitable choice, and therefore used in the development of the model of AVN in this chapter.
2. Secondly, femoral head bone with AVN were characterised, and reported in chapter 4. This work determined the target reduction in mechanical properties of bone that is required in a mechanical model of AVN.
3. Thirdly, methods of reducing the mechanical properties of bone were analysed in chapter 5. This work, along with the preliminary work carried out by undergraduate students (Appendix H) determined a suitable method of developing a mechanical model of AVN in animal tissue.

Developing mechanical models of orthopaedic diseases in animal bone has been carried out previously by using decalcification methods to simulate osteoporosis *in vitro* in porcine vertebrae (Ching-yi Lee et al., 2011). Although they reported reduction of biomechanical properties of bone following the decalcification process, they reported that multiple factors determine the success of the disease model in animals, and these include the morphological properties of the model as well as the mechanical properties.

This study developed a pilot model of AVN, and it is believed that in order to develop a successful model, significant effort is required to refine the model. Firstly, a method of developing lesions throughout the femoral head, and not limited to a particular section of the femoral head as seen in AVN femoral heads needs to be established. In this study, bone plugs were removed from the load bearing region of the femoral head, treated in HCl and then placed back into the femoral head using bone cement. This produced a lesion-like area in the load bearing region of the femoral head. In the project carried out by undergraduate students, a method of injecting the bone with HCl was tried, however due to the high density of porcine bone, and the presence of bone marrow, it was unsuccessful in reducing the mechanical properties of bone. In order to allow

for the HCl to enter the trabecular spaces in the bone, either a femoral head with less densely packed trabecular bone such as bovine femoral head can be used, or the bone marrow can be washed out of the femoral head to allow for the demineralisation agent to enter the spacing.

In this study, bone plugs were treated in HCl for 6 and 18 hours, and returned to the femoral heads. These groups were compared with unmodified femoral heads, or modified, but untreated femoral heads (Table 6-1). The untreated control group demonstrated the closest mechanical changes to those required in the model. In order to provide an accurate model of the disease, the treatment time and the treatment agent (type and/or concentration) may need to be refined.

In this study, the assumption was made that the percentage reduction in mechanical properties of bone in AVN when compared with control femoral heads would be replicated in the mechanical model of AVN, rather than the real mechanical properties. This was due to differences that are inherent in the mechanical and morphological properties of porcine and human femoral head tissue, and that the attempt at developing a model with mechanical properties found in AVN would complicate the work in this pilot study. In order to develop a more successful *in vitro* model of AVN, either an animal tissue with more similar mechanical and morphological properties (size, BMD, trabecular density, etc) as human tissue, or cadaveric human tissue will need to be used. The issue, however, with these tissues is that a mechanical model of the disease needs to be reproducible with repeatable parameters, and due to nature of biological tissue this is not possible. It is therefore proposed that the use of artificial materials that reproduce the morphological and mechanical properties of human AVN femoral head tissue needs to be investigated in future work.

## 6.6 Summary of Findings

A pilot model of AVN was developed in study. The model incorporated use of HCl treatment of a section of bone as a method of reducing the mechanical properties of femoral heads. In this study, bone plug sections were removed

from the femoral head and treated in HCl to demineralise the bone and reduce its mechanical properties, and returned to the femoral head to simulate lesions in the femoral head and reduce its structural and mechanical properties. This method successfully simulated diseased bone, however in order to achieve optimum properties of the model, the duration of treatment and concentration of HCl, as well as location of the “lesions” will need to be adjusted.



## Chapter 7. Overall Discussions and Conclusions

Avascular necrosis of the femoral head is a debilitating disease of the hip joint, and to date, there have been no reported effective methods of treating the disease. Many studies have researched the biological characteristics of bone with AVN during different stages of the disease, however very few have considered the importance of the mechanical properties in determining a suitable method of treating the disease.

Interest in studying AVN in femoral heads has increased rapidly in recent years (Figure 7-1). It has historically been a disease affecting the Asian population with a very small number affected in western countries (Chiu et al., 2001; Wong et al., 2005; Lai et al., 2008; Ellams et al., 2011), however with advances in medical research in Asian countries, increasing numbers of published studies have focused on pathologies and the impact of the disease. It has also become the subject of many western studies due to higher interest in introducing medical products and services from the west to Asia.

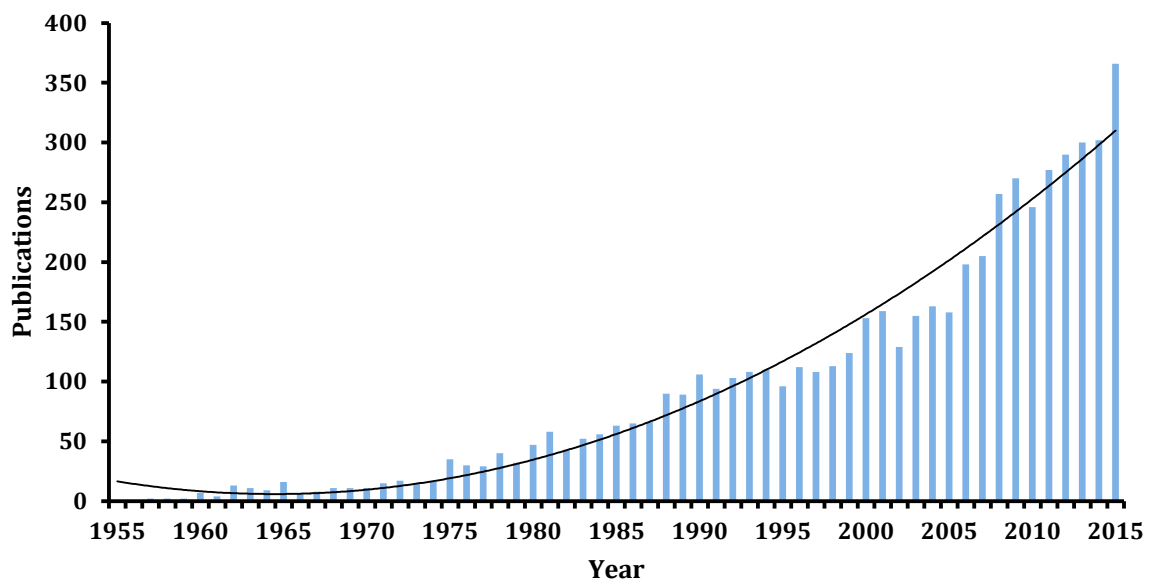


Figure 7-1 – Number of publications per year in PubMed with “Avascular necrosis” or “osteonecrosis” in title or abstract, and related to hip or femoral head. A polynomial trend-line is fitted, demonstrating a positive trend in publications related to avascular necrosis. (PubMed, 2016)

This study was initiated following interest by DePuy Synthes to develop a treatment for AVN that combined a mechanical and biological solution to provide support for the femoral head, while helping bone regenerate. A challenge associated with AVN is that there are currently no valid *in vitro* means of testing the efficacy and safety of a device for the treatment of AVN. This raised the requirement to develop a valid *in vitro* model of AVN.

Currently, there are no mechanical simulation models representing AVN, and any non-medicinal treatment products for mechanical intervention of AVN would need to enter clinical trials directly from development. If a simulation model is successfully developed, it would provide the opportunity to simulate the mechanical failures seen in AVN femoral heads, and provide a mechanism for pre-clinical *in vitro* testing of products aimed at treating AVN.

Several attempts have been made to develop biological models of AVN in animals, and although necrosis of the bone was successfully generated in most of these models, none of the studies carried out on quadrupedal animals reported the mechanical failure observed in AVN in human femoral heads. A study by Conzemius et al. (2002) induced AVN in nineteen emu hips using a combination of ischemic and cryogenic insults, and reported human-like mechanical failure in six of the emus. Although this method was successful in development of AVN-like failure in a third of the hips of the animals, the mechanical properties of the diseased bones were not compared to that seen in human AVN femoral heads. Another issue with animal models of diseases such as AVN, aside from the low-repeatability of the procedures and multifactorial failures of the models, is the cost of acquisition, care, surgery, post-surgical care and slaughter of the animals. In addition, there are many ethical challenges in use of live animals in research. There is significant pressure on researchers to integrate the principles of replacement, refinement and reduction (3Rs) in their research (Russell and Burch, 1959; BBSRC, 2016). These principles require researchers to use:

- Replacement: avoiding or replacing use of animals in research by using methods such as computer modelling, tissue engineering

- Refinement: Improving scientific procedures and husbandry to minimise distress, pain and lasting harm on animal.
- Reduction: minimising animal use by reducing sample numbers or obtaining more information from same number of animals by applying data and resource sharing and improved experimental design.

Development of a mechanical model of AVN *in vitro* using tissue from deceased animals from the food chain would be beneficial as it would replace the use of live animals in research.

### 7.1 Research Objectives

This study aimed to develop a model of AVN that re-produced the mechanical properties of bone observed in femoral heads with AVN. In order to develop a valid model and due to the limited data available on mechanical properties of AVN, a series of studies were carried out to input into the mechanical model of the disease. These are summarised in Figure 7-2.

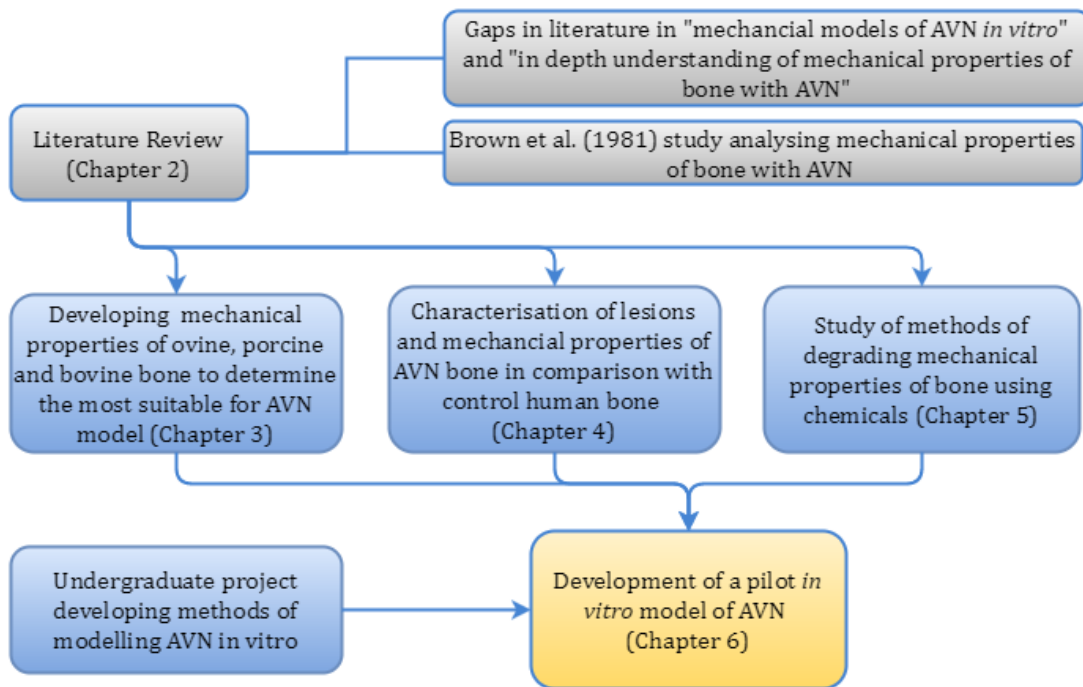


Figure 7-2 – Flowchart showing a summary of studies in this thesis, and the studies feeding into the development of an AVN model.

In order to develop a valid model of bone with AVN, a suitable base material needed to be chosen. For the purpose of this study, bovine, ovine and porcine femoral head tissues were considered, and were characterised (Chapter 3). The findings were then compared with characteristics of control human femoral head tissue, and based on this information, porcine bone was found to be the most suitable choice for use in the mechanical model of AVN.

Following a review of the literature, the study by Brown et al. (1981) was the only published study to the author's knowledge on mechanical properties of bone in AVN. It was argued in Chapter 2 that the reported data was incomplete and did not provide enough information to produce a mechanical model of AVN. A study was thereby designed to characterise the lesions and mechanical properties of bone with AVN, and compare the findings with properties of control human bone (Chapter 4).

A parallel study (Chapter 5) was carried out to determine the effects of chemical degradation of mechanical properties of bone. The use of HCl, EDTA and KOH was assessed. This was in order to reduce the mechanical properties of bone with the objective of reproducing the mechanical characteristics of necrotic bone. This was supplemented by the findings reported by the undergraduate project group and supervised by the author (Appendix H), on methods of reducing the mechanical properties of whole femoral head bone, and recreating fracture modes seen in AVN.

The findings from Chapters 3 to 5 along with the results of the undergraduate project fed into the study to develop a pilot mechanical model of AVN in porcine femoral heads. This was done by reducing the mechanical properties of a bone plug from the load bearing region of the femoral head and returning to the head following degradation (Chapter 6).

## **7.2 Experimental Challenges**

A series of experimental challenges were faced in this project and these are discussed in this section.



### 7.2.1 Access to Human Tissue

AVN is a disease affecting a significantly larger population in Asia Pacific countries when compared to Europe or North America. It is the primary diagnosis of 2% of patients undergoing total hip arthroplasty in England and Wales (Ellams et al., 2011), whereas it is the most common diagnosis for hip arthroplasty procedures in Asia Pacific (Chiu et al., 1997, 2001; Lai et al., 2008).

In order to obtain AVN femoral heads, surgeons in United Kingdom were contacted, however due to the small number of THR surgeries for AVN, access to a sufficient number of samples to produce statistically relevant data was very unlikely. In order to obtain a larger number of tissues, Dr Lee in China was contacted. Following agreement, pathways in which the tissue could be exported to University of Leeds were considered, however this was not possible due to legal challenges in exporting tissue from China. An alternative option was to carry out the experimental work in a local university in China and hence the experimental work was carried out in Xi'an Jiaotong University.

To comply with both UK and Chinese regulations on use of human tissue in research, an extensive research ethics protocol was prepared detailing the work carried out and submitted as part of the application to the ethics committees in the University of Leeds and Xi'an Jiaotong University and Affiliated Hospitals. In order to prepare the research ethics protocol, significant collaboration was undertaken by the Chinese and UK counterparts of the research, and involved detailed experimental planning. This also supported the development of the experimental protocol and allowed for carrying out significant experimental work in a limited timeframe.

During this study, twenty femoral heads were collected from patients undergoing total hip replacement procedure following diagnosis with AVN. These were collected in a period of 13 months, and the experiments were carried out at the half-way point during sample collection and at the end of collection of all of the samples. A substantial variance was seen in samples in this study which may have been due to natural differences in human tissues and the different stages of the disease. Although twenty femoral heads provided this study with a larger data set than has previously been

published for mechanical properties of AVN previously, a larger sample number would have provided this study with the capability to compare the radiological and mechanical properties of bone in different stages of the disease in a more statistically precise form.

Another challenge in this study was that the control tissue used in this study was from a tissue bank in United States. This introduced variance in demographics between the control tissue and AVN tissue, in particular in relation to BMD that was part of the morphology of the bone. It has been demonstrated that bone mineral density is lower in the Asian population when compared with Caucasian or African populations (Woo et al., 2001; Finkelstein et al., 2002a; Barrett-Connor et al., 2005; Walker et al., 2006). There are also differences in the mean hip geometry between races. Yan et al. (2004) reported that the femoral neck diameters in the cohort of Chinese women (n=101) was 10% ( $p < 0.01$ ) smaller than that of Caucasian women (n=246). Similar differences in hip geometries of Chinese subjects versus Caucasians have also been reported by other authors, where Wang et al. (2005) reported shorter femoral neck axis length in Chinese when compared to Caucasians, and Wang et al. (1997) reported shorter hip axis length in Chinese versus Caucasians. These factors along with others such as bone turnover (Finkelstein et al., 2002b) and diet (Wang et al., 1997) may contribute to ethnical differences in mechanical properties of bone.

### 7.2.2 Experimental Limitations

The experiments in this study were conducted in two centres. The characterisation of femoral head samples with AVN was carried out in Xi'an Jiaotong University, whereas the remainder of the experimental work was carried out in University of Leeds. Throughout the project, an attempt was made to ensure a series of factors were kept constant or as close as possible to reduce the variables that may impact the assessed mechanical properties of bone in human or animal tissue and to allow for data obtained at different times to be comparable. The compression rate was maintained constant throughout all of the experiments as that is a factor that can impact the output from a mechanical test (Linde et al., 1991), however due to limitations in the availability of

equipment in Xi'an Jiaotong University, some factors such as resolution of CT images and sample storage times could not be kept constant.

Another difference between the experiments carried out in the two centres was that the CT scanner in Xi'an Jiaotong University did not have the capability to measure BMD of AVN femoral head samples. This would have provided valuable information as the relationship between the mineral content of bone and the different stages of AVN are currently not known. Kubota et al. (2014) measured the regional BMD in 48 hips (36 patients post-collapse and non-collapse) using DEXA, and reported higher BMD in the post-collapse group when compared with non-collapse group ( $p < 0.01$ ), however it is possible that the increase in the observed post-collapse BMD may be due to densification of bone due to collapse or microfracture of the trabecular structure in the measured region rather than increased mineral presence due to accelerated osteoblast activity. In another study, Beckmann et al. (2009) compared the trabecular structure of bone samples from AVN and osteoarthritis femoral heads, and found no significant differences between the bone quality and trabecular microarchitecture between the groups. There have also been reports of possible correlations between AVN and BMD, however they are reports of associated changes in BMD and increased risk of AVN in patients with pre-existing conditions that are also AVN risk factors, such as bone marrow transplants (Tauchmanovà et al., 2003; Kaste et al., 2004) and human immunodeficiency virus (Brown and Crane, 2001). Determining the BMD of bone in different stages of AVN would have proved useful in determining the properties of material required in the mechanical model of AVN by answering the question of whether the BMD related to mechanical properties in AVN, and should be considered in future work.

### **7.3 Future Work**

The work in this thesis has indicated the potential for a refined mechanical model of AVN. However there are many emerging research questions that need to be addressed to allow for development of a suitable animal model for testing treatments proposed for AVN. Some of the considerations are discussed below.

### 7.3.1 Lesions in AVN Femoral Heads

Lesion size (Steinberg et al., 1999) and location (Nishii et al., 2002) are significant factors in determining the prognosis and severity of AVN. Anderson (2015) reviewed 2D slices from MRI and CT scans of AVN patients to develop an *in silico* simulation model of AVN, and demonstrated that lesion properties and morphology significantly affected the stress distributions within the femoral heads. In Chapter 4, it was reported that locations of necrotic lesions are not limited to specific regions in the femoral head, and can exist as one large volume or in many smaller volumes throughout the tissue. The factors influencing the locations and sizes of lesions in the femoral heads need to be understood and secondly, a method of developing lesions in specific regions in the model of AVN needs to be developed.

### 7.3.2 Changes in BMD with AVN

Understanding the mechanical and structural properties of AVN has helped with determining the benchmark properties required from a simulation model of AVN, however changes in BMD of bone with AVN is not understood. Understanding the impact of AVN on the morphological properties of bone such as BMD and trabecular properties will aid in development of a valid model of AVN. If it can be demonstrated that the BMD of bone is altered by AVN, methods of changing BMD of bone can be implemented in development of model of AVN.

### 7.3.3 Finalising Experimental AVN Model

The aim of this project was to develop a mechanical model of AVN. Experimental mechanical models of bone diseases have been developed previously for osteoporosis (Akabay et al., 2007; Ching-yi Lee et al., 2011), however no published experimental models had been developed for AVN prior to this study. The approach used by Akabay et al. (2007) and Ching-yi Lee et al. (2011) for model of osteonecrosis was to demineralise whole spinal vertebrae in EDTA or HCl by placing the whole bone structure in the demineralising solution. The method used in this study adopted this process to demineralise bone and reduce the mechanical properties of bone. This method

successfully reduced the mechanical properties of bone in the model of AVN; however adjustment of the simulation factors of AVN (HCl concentration and time) is necessary in order to develop a model that is representative of the mechanical properties seen in AVN femoral heads.

Other factors that may influence the structural properties of the AVN model include:

- The location of the treated bone section
- Size of the treated bone section, or alternatively use of multiple small bone sections
- Species and age of animal used

#### **7.3.4 Computational Modelling of AVN**

Although computational simulation of AVN was not in the scope of this thesis, the data provided in Chapter 4, where structural and mechanical properties of bone with and without AVN were compared, can provide the data required for computational simulation of the disease. Computational models require validation using an experimental model; development of a final experimental model of AVN can also prove useful in validating the computational model. These models will be useful in reducing the amount of experimental work required on animal tissue, and may be useful in developing models of disease using the parameters of human tissue rather than relying on tissue available via tissue banks or animal tissue.

#### **7.4 Conclusions**

In addition to the work towards development of a mechanical model of AVN, this thesis has contributed through increasing the knowledge and understanding on mechanical and structural properties of bone with AVN. This is new information that facilitates the development of in vitro models of AVN. The work in this thesis has produced a large amount of data that was interpreted to compare the mechanical and structural properties of bone with and without AVN. The findings demonstrated

reduction in yield stress and elastic modulus of bone with AVN when compared with control samples. They also demonstrated that the non-load-bearing regions of bones with AVN had higher yield stress and elastic modulus when compared to samples from the same regions of control samples. This information provided insight into the mechanical properties of AVN beyond what was previously understood, and produced the inputs required for development of an experimental model of AVN.

The morphological properties of the AVN femoral heads were also analysed in this thesis and it was shown that up to 70% of the volume of the femoral heads were covered by necrotic lesions in some cases. The lesions were also spread throughout the femoral heads and were not limited to a particular region. Subchondral fractures were also present around the lesions. Methods of disease classification based on necrotic bone volume estimates have shown a poor ability to predict disease progression. The experiments recorded in this thesis confirmed that there is no relationship between the necrotic bone volume and mechanical properties of the bone, establishing a root cause for the lack of correlation. It was also demonstrated that methods of quantifying lesion sizes, where the lesions are assumed to be limited to a particular region in the femoral head, are not accurate at predicting the stage of the disease. The progress towards developing an *in vitro* mechanical model is a first step in developing a validated method of classifying lesion morphology that can be used as both a prognostic and diagnostic tool.

Developing an *in vitro* model of AVN required understanding of methods to change the mechanical properties of bone in animal tissue. Chemical methods were used to reduce the mechanical properties of bone plugs and these were translated into simulating AVN in femoral heads. The mechanical properties of bone plugs were reduced by immersing them into degrading chemicals for stated time periods and they were placed back into non-treated femoral heads to alter the structural properties of whole bone. The work presented in this thesis produced a pilot model of AVN which successfully demonstrated reduced mechanical properties of bone as seen bone with AVN. This type of *in vitro* model in animal tissue that is available from the food chain, using chemical degradation methods have been used to produce such models to

simulate osteoporosis had not been produced for disease models of AVN. This has provided a significantly more ethical method of simulating AVN in a cheaper and more repeatable manner.





## References

- Aaron, R.K., Ciombor, D.M., 1997. (v) Role of electrical stimulation in the treatment of avascular necrosis of the femoral head. *Current Orthopaedics*. **11**(3), pp. 187–92. doi:10.1016/S0268-0890(97)90033-5
- Aaron, R.K., Lennox, D., Stulberg, B.N., 1997. The natural history of osteonecrosis of the femoral head and risk factors for rapid progression, in: Urbaniak, J.R., Jones, J.J.P. (Eds.), *Osteonecrosis: Etiology, Diagnosis and Treatment*. American Academy of Orthopaedic Surgeons. pp. 261–65.
- Abe, T., Sato, K., Miyakoshi, N., Kudo, T., Tamura, Y., Tsuchida, T., Kasukawa, Y., 1999. Trabecular remodeling processes in the ovariectomized rat: modified node-strut analysis. *Bone*. **24**(6), pp. 591–6.
- Abjornson, C., DePaula, C.A., Kotha, S.P., Johnson, L.A., Guzelsu, N., 1998. Changes in the mechanical and material properties of bone related to increasing molarities of sodium fluoride. *Translations of Orthopaedic Research Society*. **23**, p. 957.
- Adili, A., Trousdale, R.T., 2003. Femoral head resurfacing for the treatment of osteonecrosis in the young patient. *Clinical Orthopaedics and Related Research* **417**, 93–101. doi:10.1097/01.blo.0000096815.78689.3e
- Agarwala, S., Jain, D., Joshi, V.R., Sule, A., 2005. Efficacy of alendronate, a bisphosphonate, in the treatment of AVN of the hip. A prospective open-label study. *Rheumatology (Oxford)*. **44**(3), pp. 352–9. doi:10.1093/rheumatology/keh481
- Agarwala, S., Shah, S., Joshi, V.R., 2009. The use of alendronate in the treatment of avascular necrosis of the femoral head: follow-up to eight years. *Journal of Bone and Joint Surgery, British Volume*. **91**(8), 1013–8. doi:10.1302/0301-620X.91B8.21518
- Akbay, A., Bozkurt, G., Ilgaz, O., Palaoglu, S., Akalan, N., Benzel, E.C., 2007. A demineralized calf vertebra model as an alternative to classic osteoporotic vertebra models for

- pedicle screw pullout studies. *European Spine Journal* **17**(3), pp. 468–73.  
doi:10.1007/s00586-007-0545-1
- AK-Steel, 2007. Stainless Steel 316/316L [Online]. (Accessed 21 April 2016). URL  
[http://www.aksteel.com/pdf/markets\\_products/stainless/austenitic/316\\_316l\\_data\\_sheet.pdf](http://www.aksteel.com/pdf/markets_products/stainless/austenitic/316_316l_data_sheet.pdf)
- Al-Mousawi, F., Malki, A., Al-Aradi, A., Al-Bagali, M., Al-Sadadi, A., Booz, M.M.Y., 2002. Total hip replacement in sickle cell disease. *International Orthopaedics*. **26**(3), pp. 157–61.  
doi:10.1007/s00264-002-0337-5
- Amanatullah, D.F., Strauss, E.J., Di Cesare, P.E., 2011. Current management options for osteonecrosis of the femoral head: part II, operative management. *American Journal of Orthopaedics*. **40**(9), pp. E186–92.
- An, Y.H., 2000. Mechanical Properties of Bone, in: Mechanical Testing of Bone and the Bone-Implant Interface. CRC Press, pp. 41–63.
- An, Y.H., Draughn, R.A., 2000. Mechanical testing of bone and the bone implant interface. CRC Press.
- Anderson, J.A., 2015. In vitro and in silico simulations of femoral heads with avascular necrosis. PhD Thesis, University of Leeds
- Arlet, J., Ficat, R.P., 1960. Is not osteitis condensans ilii merely a variety of sacroiliac arthrosis? Clinical and histopathological study of a case. *Revue du Rhumatisme et des Maladies Ostéo-articulaires* **27**, pp. 358–62.
- Ascenzi, A., Bonucci, E., 1967. The tensile properties of single osteons. *The Anatomical Records*. **158**(4), pp. 375–86. doi:10.1002/ar.1091580403
- Asnis, S.E., Wanek-Sgaglione, L., 1994. Intracapsular fractures of the femoral neck. Results of cannulated screw fixation. *Journal of Bone and Joint Surgery, American Volume*. **76**(12), pp. 1793–803.

- Assouline-Dayana, Y., Chang, C., Greenspan, A., Shoenfeld, Y., Gershwin, M.E.E.E., 2002. Pathogenesis and natural history of osteonecrosis. *Seminars in Arthritis and Rheumatism*. **32**(2), pp. 94–124. doi:10.1053/sarh.2002.33724b
- Astrand, J., Aspenberg, P., 2002. Systemic alendronate prevents resorption of necrotic bone during revascularization. A bone chamber study in rats. *BioMed Central Musculoskeletal Disorders*. **3**(1), p. 19. doi:10.1186/1471-2474-3-19
- Athanasiou, K.A., Zhu, C., Lanctot, D.R., Agrawal, C.M., Wang, X., 2000. Fundamentals of biomechanics in tissue engineering of bone. *Tissue Engineering*. **6**(4), pp. 361–81. doi:10.1089/107632700418083
- Augat, P., Link, T., Lang, T.F., Lin, J.C., Majumdar, S., Genant, H.K., 1998. Anisotropy of the elastic modulus of trabecular bone specimens from different anatomical locations. *Medical Engineering and Physics*. **20**(2), pp. 124–31. doi:10.1016/S1350-4533(98)00001-0
- Bachiller, F.G., Caballer, A.P., Portal, L.F., 2002. Avascular necrosis of the femoral head after femoral neck fracture. *Clinical Orthopaedics and Related Research*. **399**, pp. 87–109.
- Bancroft, J.D., Gamble, M., 2001. *Theory and Practice of Histological Techniques*. Churchill Livingstone.
- Barrett-Connor, E., Siris, E.S., Wehren, L.E., Miller, P.D., Abbott, T.A., Berger, M.L., Santora, A.C., Sherwood, L.M., 2005. Osteoporosis and fracture risk in women of different ethnic groups. *Journal of Bone Mineral Research*. **20**(2), pp. 185–94. doi: 10.1359/JBMR.041007
- Baxter UK, n.d. Baxter UK Product Catalogue - 1000 ml Sterile Water for Irrigation Pour Bottle [WWW Document]. URL <http://www.ecomm.baxter.com/ecatalog/browseCatalog.do?lid=10011&hid=10000&cid=10001&key=9c317911a195cba96145873ea9f62c> (accessed 7.19.13).

- BBSRC, 2016. The replacement, refinement and reduction (3Rs) in research using animals - BBSRC [Online] (Accessed 21 August 2016). URL <http://www.bbsrc.ac.uk/funding/grants/priorities/3rs-research-animals/>
- Beaumont, R., Thornton, J., Wright, M., Young, E., Cowern, M., Musson, S., Devonshire, A., Evans, R., Miller, R., McDowall, K., Smee, C., Smith, B., Holland, M.J., Porteous, M.M., Goldberg, M.A., Rangan, M.A., Rees, M.J., 2013. Public and patient guide to the NJR's 10th annual report, National Joint Registry for England, Wales and Northern Ireland.
- Beckmann, J., Matsuura, M., Grässel, S., Köck, F., Grifka, J., Tingart, M., 2009. A muCT analysis of the femoral bone stock in osteonecrosis of the femoral head compared to osteoarthritis. *Archives of Orthopaedic and Trauma Surgery*. **129**(4), pp. 501–5. doi:10.1007/s00402-008-0666-y
- Bluemke, D.A., Zerhouni, E.A., 1996. MRI of Avascular Necrosis of Bone. *Topics in Magnetic Resonance Imaging*. **8**(4), pp. 231–46.
- Borchers, R.E., Gibson, L.J., Burchardt, H., Hayes, W.C., 1995. Effects of selected thermal variables on the mechanical properties of trabecular bone. *Biomaterials* **16**(7), pp. 545–51. doi:10.1016/0142-9612(95)91128-L
- Boutroy, S., Buxsein, M.L., Munoz, F., Delmas, P.D., 2005. In vivo assessment of trabecular bone microarchitecture by high-resolution peripheral quantitative computed tomography. *The Journal of Clinical Endocrinology and Metabolism* **90**(12), pp. 6508–15. doi:10.1210/jc.2005-1258
- Brinker, M.R., Rosenberg, A.G., Kull, L., Galante, J.O., 1994. Primary total hip arthroplasty using noncemented porous-coated femoral components in patients with osteonecrosis of the femoral head. *Journal of Arthroplasty* **9**(5), pp. 457–68.
- Brockstedt, H., Kassem, M., Eriksen, E.F., Mosekilde, L., Melsen, F., 1993. Age- and sex-related changes in iliac cortical bone mass and remodeling. *Bone* **14**(4), pp. 681–91. 691. doi:10.1016/8756-3282(93)90092-O

- Brown, P., Crane, L., 2001. Avascular Necrosis of Bone in Patients with Human Immunodeficiency Virus Infection: Report of 6 Cases and Review of the Literature. *Clinical Infectious Diseases*. **32**(8), pp. 1221–26.
- Brown, S.J., Pollintine, P., Powell, D.E., Davie, M.W.J., Sharp, C.A., 2002. Regional differences in mechanical and material properties of femoral head cancellous bone in health and osteoarthritis. *Calcified Tissue International*. **71**(3), pp. 227–34.
- Brown, T.D., Baker, K.J., Brand, R.A., 1992. Structural consequences of subchondral bone involvement in segmental osteonecrosis of the femoral head. *Journal of Orthopaedic Research*. **10**(1), pp. 79–87.
- Brown, T.D., Ferguson, A.B., 1980. Mechanical Property Distributions in the Cancellous Bone of the Human Proximal Femur. *Acta Orthopaedica*. **51**(3), pp. 429–37.
- Brown, T.D., Way, M.E., Ferguson, A.B., 1981. Mechanical characteristics of bone in femoral capital aseptic necrosis. *Clinical Orthopaedics and Related Research*. **156**, pp. 240–7.
- Bullough, P.G., DiCarlo, E.F., 1990. Subchondral avascular necrosis: a common cause of arthritis. *Annals of the Rheumatic Diseases*. **49**(6), pp. 412–20. doi:10.1136/ard.49.6.412
- Burr, D.B., Turner, C.H., Naick, P., Forwood, M.R., Ambrosius, W., Sayeed Hasan, M., Pidaparti, R., 1998. Does microdamage accumulation affect the mechanical properties of bone? *Journal of Biomechanics*. **31**(4), pp. 337–45. doi:10.1016/S0021-9290(98)00016-5
- Burstein, A.H., Reilly, D.T., Martens, M., 1976. Aging of bone tissue: mechanical properties. *Journal of Bone and Joint Surgery, American Volume*. **58**(1), pp. 82–6.
- Byrne, D., Mulhall, K., Baker, J., 2010. Anatomy & biomechanics of the hip. *The Open Sports Medicine Journal*. **4**, pp. 51-7.
- Calza, L., Manfredi, R., Chiodo, F., 2003. Osteonecrosis in HIV-infected patients and its correlation with highly active antiretroviral therapy (HAART). *Presse médicale* **32**(13 Pt 1), pp. 595–8.

- Calvé, J., 1910. Sur une forme particuliere de pseudo-coxalgie greffée sur des déformations caracteristiques de l'extremité superieure du femur. *Revista de Chirurgie*. **30**, p. 54.
- Camp, J.F., Colwell, C.W., 1986. Core Decompression of the Femoral Head for Osteonecrosis. *Journal of Bone and Joint Surgery*. **68-A(9)**, pp. 1313–9.
- Carter, D.R., Caler, W.E., 1983. Cycle-dependent and time-dependent bone fracture with repeated loading. *Journal of biomechanical engineering*. **105(2)**, pp. 166–70.
- Carter, D.R., Hayes, W.C., 1976. Bone compressive strength: the influence of density and strain rate. *Science*. **194(4270)**, pp. 1174–6.
- Carter, D.R., Hayes, W.C., 1976a. Fatigue life of compact bone—I effects of stress amplitude, temperature and density. *Journal of Biomechanics*. **9(1)**, pp. 27–34. doi:10.1016/0021-9290(76)90136-6
- Carter, D.R., Hayes, W.C., 1976b. Bone compressive strength: the influence of density and strain rate. *Science*. **194**, pp. 1174–6.
- Carter, D.R., Hayes, W.C., 1977. The compressive behavior of bone as a two-phase porous structure. *Journal of Bone and Joint Surgery, British Volume*. **59(7)**, pp. 954–62.
- Castania, V.A., Silveira, J.W. de S. da, Issy, A.C., Pitol, D.L., Castania, M.L., Neto, A.D., Bel, E.A. Del, Defino, H.L.A., 2015. Advantages of a combined method of decalcification compared to EDTA. *Microscopy Research and Technique*. **78(2)**, pp. 111–8.
- Catto, M., 1977. Ischaemia of bone. *Journal of clinical pathology. Supplement (Royal College of Pathologists)* **11**, pp. 78–93.
- Chao, Y.-C., Wang, S.-J., Chu, H.-C., Chang, W.-K., Hsieh, T.-Y., 2003. Investigation of alcohol metabolizing enzyme genes in Chinese alcoholics with avascular necrosis of hip joint, pancreatitis and cirrhosis of the liver. *Alcohol and alcoholism (Oxford, Oxfordshire)*. **38(5)**, pp. 431–6.
- Chiba, K., Burghardt, A.J., Osaki, M., Majumdar, S., 2013. Heterogeneity of bone microstructure in the femoral head in patients with osteoporosis: an ex vivo HR-pQCT study. *Bone*. **56(1)**, pp. 139–46. doi:10.1016/j.bone.2013.05.019

- Ching-yi Lee, She-Hung Chan, Hung-Yi Lai, Shih-Tseng Lee, 2011. A method to develop an in vitro osteoporosis model of porcine vertebrae: histological and biomechanical study. *Journal of Neurosurgery*. **14**(6), pp. 789-98
- Chiu, K.H., Shen, W.Y., Tsui, H.F., Chan, K.M., 1997. Experience with primary exeter total hip arthroplasty in patients with small femurs. *Journal of Arthroplasty* **12**, pp. 267–72. doi:10.1016/S0883-5403(97)90022-X
- Chiu, K.H., Shen, W.Y., Tsui, H.F., Chan, K.M., 1997. Experience with primary Exeter total hip arthroplasty in patients with small femurs. Review at average follow-up period of 6 years. *Journal of Arthroplasty* **12**(3), pp. 267–72.
- Chiu, K.Y., Ng, T.P., Tang, W.M., Poon, K.C., Ho, W.Y., Yip, D., 2001. Charnley total hip arthroplasty in Chinese patients less than 40 years old. *Journal of Arthroplasty* **16**(1), pp. 92–101. doi:10.1054/arth.2001.19156
- Choi, K., Goldstein, S.A., 1992. A comparison of the fatigue behavior of human trabecular and cortical bone tissue. *Journal of Biomechanics*. **25**(12), pp. 1371–81. doi:10.1016/0021-9290(92)90051-2
- Clarke, B., 2008. Normal bone anatomy and physiology. *Clinical Journal of the American Society of Nephrology*. **3** Supplement 3, pp. S131–9. doi:10.2215/CJN.04151206
- Cong, E., Walker, M.D., 2014. The Chinese skeleton: insights into microstructure that help to explain the epidemiology of fracture. *Bone Research*. **2**, 14009. doi:10.1038/boneres.2014.9
- Conway, J.J., 1993. A scintigraphic classification of Legg-Calvé-Perthes disease. *Seminars in nuclear medicine*. **23**, pp. 274–95.
- Conzemius, M.G., Brown, T.D., Zhang, Y., Robinson, R.A., 2002. A New Animal Model of Femoral Head Osteonecrosis, One that Progresses to Human-Like Bony Mechanical Failure. *Journal of Orthopaedic Research*. **20**(2), pp. 303-9. doi:10.1016/S0736-0266(01)00108-5

- Coogan, P.G., Urbaniak, J.R., 1997. vascularized fibular bone grafting for osteonecrosis of the femoral head. *Current Orthopaedics*. **11**, pp. 179–86.
- Cooper, C., Steinbuch, M., Stevenson, R., Miday, R., Watts, N.B., 2010. The epidemiology of osteonecrosis: findings from the GPRD and THIN databases in the UK. *Osteoporosis International*. **21**(4), pp. 569–77. doi:10.1007/s00198-009-1003-1
- Cory, E., Nazarian, A., Entezari, V., Vartanians, V., Müller, R., Snyder, B.D., 2010. Compressive axial mechanical properties of rat bone as functions of bone volume fraction, apparent density and micro-ct based mineral density. *Journal of Biomechanics*. **43**(5), pp. 953–60. doi:10.1016/j.jbiomech.2009.10.047
- Cristofolini, L., Viceconti, M., Cappello, A., Toni, A., 1996. Mechanical validation of whole bone composite femur models. *Journal of Biomechanics*. **2**(4), pp. 525–35. doi:10.1016/0021-9290(95)00084-4
- Cui, Q., Wang, G.J.J., Su, C.-C., Balain, G., 1997. The Otto Aufranc Award: Lovastatin Prevents Steroid Induced Adipogenesis and Osteonecrosis. *Clinical Orthopaedics and Related Research*. **344**, pp. 8–19.
- Currey, J.D., 1969a. The mechanical consequences of variation in the mineral content of bone. *Journal of Biomechanics*. **2**(1), 1–11. doi:10.1016/0021-9290(69)90036-0
- Currey, J.D., 1969b. The relationship between the stiffness and the mineral content of bone. *Journal of Biomechanics*. **2**(4), pp. 477–80. doi:10.1016/0021-9290(69)90023-2
- Currey, J.D., 1988a. The effects of drying and re-wetting on some mechanical properties of cortical bone. *Journal of Biomechanics*. **21**(5), pp. 439–41. doi:10.1016/0021-9290(88)90150-9
- Currey, J.D., 1988b. The effect of porosity and mineral content on the Young's modulus of elasticity of compact bone. *Journal of Biomechanics*. **21**(2), pp. 131–39.. doi:10.1016/0021-9290(88)90006-1
- Currey, J.D., 2005. Structural heterogeneity in bone: good or bad? *Journal of Musculoskeletal Neuronal Interactions*. **5**(4), p. 317.



- Currey, J.D., 2009. Measurement of the mechanical properties of bone: a recent history. *Clinical Orthopaedics and Related Research*. **467**(8), pp. 1948–54. doi:10.1007/s11999-009-0784-z
- Currey, J.D., Brear, K., Zioupos, P., Reilly, G.C., 1995. Effect of formaldehyde fixation on some mechanical properties of bovine bone. *Biomaterials*. **16**(16), pp. 1267–71. doi:10.1016/0142-9612(95)98135-2
- Currey, J.D., Foreman, J., Laketić, I., Mitchell, J., Pegg, D.E., Reilly, G.C., 1997. Effects of ionizing radiation on the mechanical properties of human bone. *Journal of Orthopaedic Research*. **15**(1), pp. 111–7. doi:10.1002/jor.1100150116
- Currey, J.D. 1970. The mechanical properties of bone. *Clinical Orthopaedics and Related Research*. **73**, pp. 210–31.
- Dalén, N., Hellström, L.G., Jacobson, B., 1976. Bone Mineral Content and Mechanical Strength of the Femoral Neck. *Acta Orthopaedica*. **47**(5), pp. 503–8.
- Day, J.S., Ding, M., van der Linden, J.C., Hvid, I., Sumner, D.R., Weinans, H., 2001. A decreased subchondral trabecular bone tissue elastic modulus is associated with pre-arthritic cartilage damage. *Journal of Orthopaedic Research*. **19**(5), pp. 914–8. doi:10.1016/S0736-0266(01)00012-2
- Dekhtyar, Y., Gamza, A., Tatarinov, a, Jansons, H., 1995. Electron and mechanical properties of bone during heating, evaluated by exoelectron emission and ultrasound. *Biomaterials*. **16**(11), pp. 861–3.
- Doube, M., Kłosowski, M.M., Arganda-Carreras, I., Cordelières, F.P., Dougherty, R.P., Jackson, J.S., Schmid, B., Hutchinson, J.R., Shefelbine, S.J., 2010. BoneJ: Free and extensible bone image analysis in ImageJ. *Bone*, **47**(6), pp. 1076–9. doi:10.1016/j.bone.2010.08.023
- Drescher, W., Weigert, K.P., Bunger, M.H., Ingerslev, J., Bunger, C., Hansen, E.S., 2004. Femoral head blood flow reduction and hypercoagulability under 24 h megadose

- steroid treatment in pigs. *Journal of Orthopaedic Research*. **22**, pp. 501–08.  
doi:10.1016/j.orthres.2003.10.002
- Duchemin, L., Bousson, V., Raossanaly, C., Bergot, C., Laredo, J.D., Skalli, W., Mitton, D., 2008. Prediction of mechanical properties of cortical bone by quantitative computed tomography. *Medical Engineering and Physics*. **30**(3), pp. 321–8.
- Dudkiewicz, I., Covo, A., Salai, M., Israeli, A., Amit, Y., Chechik, A., 2004. Total hip arthroplasty after avascular necrosis of the femoral head: does etiology affect the results? *Archives of Orthopaedic and Trauma Surgery*. **124**(2), pp. 82–5.  
doi:10.1007/s00402-003-0630-9
- Edgerton, B.C., An, K.N., Morrey, B.F., 1990. Torsional strength reduction due to cortical defects in bone. *Journal of Orthopaedic Research*. **8**(6), pp. 851–5.  
doi:10.1002/jor.1100080610
- Ehlinger, M., Moser, T., Adam, P., Bierry, G., Gangi, A., de Mathelin, M., Bonnomet, F., 2011. Early prediction of femoral head avascular necrosis following neck fracture. *Orthopaedics & Traumatology, Surgery & Research*. **97**(1), pp. 79–88.  
doi:10.1016/j.otsr.2010.06.014
- Ellams, D., Forsyth, O., Hindley, P., Mistry, A., Newell, C., Pickford, M., Royall, M., Swanson, M., Blom, A., Clark, E., Dieppe, P., Smith, A., Tobias, J., Vernon, K., Thornton, J., Wright, M., Young, E., Porter, M., Borroff, M., Gregg, P., Howard, M., MacGregor, A., Tucker, K., Esler, C., Jones, A., Porteous, M., Goldberg, A., 2011. National Joint Registry for England and Wales, Available at: [www.njrcentre.org.uk](http://www.njrcentre.org.uk).
- Enright, H., Haake, R., Weisdorf, D., 1990. Avascular necrosis of bone: a common serious complication of allogeneic bone marrow transplantation. *American Journal of Medicine*. **89**(6), pp. 733–8.
- Evans, B.G., Zawadsky, M.W., 2010. The Hip and Femur, in: Wiesel, S.W., Delahay, J.N. (Eds.), *Essentials of Orthopedic Surgery*. Springer, p. 522.

- Evans, F.G., 1973. *Mechanical Properties of Bone*. Charles C Thomas Publisher, Springfield Illinois, USA.
- Evans, F.G., Lebow, M., 1951. Regional differences in some of the physical properties of the human femur. *Journal of Applied Physiology* **3**(9), pp. 563–72.
- Fairbank, A.C., Bhatia, D., Jinnah, R.H., Hungerford, D.S., 1995. Long-term results of core decompression for ischaemic necrosis of the femoral head. *Journal of Bone and Joint Surgery, British Volume*. **77-B**(1), pp. 42–9.
- Fan, Z., Swadener, J.G., Rho, J.Y., Roy, M.E., Pharr, G.M., 2002. Anisotropic properties of human tibial cortical bone as measured by nanoindentation. *Journal of Orthopaedic Research*. **20**(4), pp. 806–10. doi:10.1016/S0736-0266(01)00186-3
- Femur Bone [NURBS] 3D Model Download | 3D CAD Browser [WWW Document], n.d. URL <http://www.3dcadbrowser.com/download.aspx?3dmodel=57576> (accessed 7.1.13a).
- Ficat, R.P., 1985. Idiopathic bone necrosis of the femoral head - early diagnosis and treatment. *Journal of Bone and Joint Surgery, British Volume*. **67-B**(1), pp. 3–9.
- Ficat, R.P., Arlet, J., 1980. Ischemia and necroses of bone, in: Hungerford, D.S. (Ed.), *Ischemia and Necroses of Bone*. Williams and Wilkins, p. 196.
- Fideler, B.M., Vangsness, C.T., Orlando, C., Moore, T., 1995. Gamma Irradiation: Effects on Biomechanical Properties of Human Bone-Patellar Tendon-Bone Allografts. *American Journal of Sports Medicine*. **23**(5), pp. 643–6. doi:10.1177/036354659502300521
- Fink, J.C., Leisenring, W.M., Sullivan, K.M., Sherrard, D.J., Weiss, N.S., 1998. Avascular necrosis following bone marrow transplantation: a case-control study. *Bone*, **22**(1), pp. 67–71.
- Finkelstein, J.S., Lee, M.-L.T., Sowers, M., Ettinger, B., Neer, R.M., Kelsey, J.L., Cauley, J.A., Huang, M.-H., Greendale, G.A., 2002. Ethnic variation in bone density in premenopausal and early perimenopausal women: effects of anthropometric and

- lifestyle factors. *The Journal of Clinical Endocrinology and Metabolism* **87**(7), pp. 3057–67.
- Fisher, D.E., Bickel, W.H., Holley, K.E., Ellefson, R.D., 1972. Corticosteroid-induced aseptic necrosis. II. Experimental study. *Clinical Orthopaedics and Related Research*. **84**, pp. 200–6.
- Friedman, A.W., 2006. Important determinants of bone strength: beyond bone mineral density. *Journal of Clinical Rheumatology*. **12**(2), pp. 70–7. doi:10.1097/01.rhu.0000208612.33819.8c
- Fung, Y., 1993. Biomechanics: mechanical properties of living tissues. Springer.
- Fyda, T.M., Callaghan, J.J., Olejniczak, J., Johnston, R.C., 2002. Minimum ten-year follow-up of cemented total hip replacement in patients with osteonecrosis of the femoral head. *Iowa Orthopaedic Journal*. **22**, pp. 8–19.
- Galante, J., Rostoker, W., Ray, R.D., 1970. Physical properties of trabecular bone. *Calcified Tissue Research*. **5**(1), pp. 236–46. doi:10.1007/BF02017552
- Gardeniers, J.W.M., 1993a. The ARCO perspective for reaching one uniform staging system of osteonecrosis, in: Schoutens, A. (Ed.), *Bone Circulation and Vascularization in Normal and Pathological Conditions*. Plenum Press, p. 375.
- Gardeniers, J.W.M., 1993b. Report of the Committee of Staging and Nomenclature. ARCO News Letter, 5:n°2: 79-82, 1993, in: ARCO Committee on Terminology and Staging: Report on the Committee-Meeting at Santiago de Compostela on Thursday the 14th of October 1993. pp. 79–82.
- Garellick, G., Kärrholm, J., Rogmark, C., Herberts, P., 2010. Swedish Hip Arthroplasty Register Annual Report 2010 [WWW Document]. Swedish Joint Registry. URL <http://www.shpr.se/Libraries/Documents/AnnualReport-2010-2-eng.sflb.ashx> (accessed 7.11.12).

- Gautier, E., Ganz, K., Krügel, N., Gill, T., Ganz, R., 2000. Anatomy of the medial femoral circumflex artery and its surgical implications. *Journal of Bone and Joint Surgery, British Volume*. **82**(5), pp. 679–83.
- Glade, M.J., Krook, L., 1982. Glucocorticoid-induced inhibition of osteolysis and the development of osteopetrosis, osteonecrosis and osteoporosis. *Cornell Veterinarian*. **72**(1), pp. 76–91.
- Glimcher, M.J., Kenzora, J.E., 1979a. The biology of osteonecrosis of the human femoral head and its clinical implications: I. Tissue biology. *Clinical Orthopaedics and Related Research*. **138**, pp. 284-309
- Glimcher, M.J., Kenzora, J.E., 1979b. The Biology of Osteonecrosis of the Human Femoral Head and its Clinical Implications: III. Discussion of the Etiology and Genesis of the Pathological Sequelae; Comments on Treatment. *Clinical Orthopaedics and Related Research*. **140**, pp. 47–50.
- Goldstein, S.A., 1987. The mechanical properties of trabecular bone: dependence on anatomic location and function. *Journal of Biomechanics*. **20**(11-12), pp. 1055–61.
- Goldstein, S.A., Goulet, R., Mccubbrey, D., 1993. Measurement and significance of three-dimensional architecture to the mechanical integrity of trabecular bone. *Calcified Tissue International*. **53**, Supplement 1, pp. 127–33.
- Graves, S., Davidson, D., Lewis, P., Steiger, R. de, Stoney, J., Tomkins, A., Vial, R., Miller, L., Lynch, J., Griffith, L., O'Donohue, G., Lorimer, M., Y L Liu, Stanford, T., Cuthbert, A., Kelly, L., 2014. Annual Report 2014.
- Grynpas, M., 1993. Age and disease-related changes in the mineral of bone. *Calcified Tissue International*. **53**, Supplement 1, pp. S57–64.
- Haba, Y., Lindner, T., Fritsche, A., Schiebenhöfer, A.-K., Souffrant, R., Kluess, D., Skripitz, R., Mittelmeier, W., Bader, R., 2012. Relationship between mechanical properties and bone mineral density of human femoral bone retrieved from patients with

- osteoarthritis. *The Open Orthopaedic Journal*. **6**, pp. 458–63. doi:10.2174/1874325001206010458
- Haba, Y., Skripitz, R., Lindner, T., Köckerling, M., Fritsche, A., Mittelmeier, W., Bader, R., 2012. Bone mineral densities and mechanical properties of retrieved femoral bone samples in relation to bone mineral densities measured in the respective patients. *Scientific World Journal*. 2012, 242403.
- Hamer, A.J., Stockley, I., Elson, R.A., 1999. Changes in allograft bone irradiated at different temperatures. *Journal of Bone and Joint Surgery, British Volume*. **81**(2), pp. 342–4.
- Hengsberger, S., Kulik, A., Zysset, P.K., 2002. Nanoindentation discriminates the elastic properties of individual human bone lamellae under dry and physiological conditions. *Bone*. **30**(1), pp. 178–84. doi:10.1016/S8756-3282(01)00624-X
- Hernigou, P., Voisin, M.C., Marichez, M., Despres, E., Goutallier, D., 1989. Comparison of nuclear magnetic resonance and histology in necrosis of the femoral head. *Revue du rhumatisme et des maladies ostéo-articulaires*. **56**(11), pp. 741–4.
- Heřt, J., Fiala, P., Petrtýl, M., 1994. Osteon orientation of the diaphysis of the long bones in man. *Bone*. **15**(3), pp. 269–77. doi:10.1016/8756-3282(94)90288-7
- Hhawker, H., Neilson, H., Hayes, R.J., Serjeant, G.R., 1982. Haematological factors associated with avascular necrosis of the femoral head in homozygous sickle cell disease. *British Journal of Haematology*. **50**(1), pp. 29–34. doi:10.1111/j.1365-2141.1982.tb01887.x
- Hipp, J.A., Edgerton, B.C., An, K.N., Hayes, W.C., 1990. Structural consequences of transcortical holes in long bones loaded in torsion. *Journal of Biomechanics*. **23**(12), pp. 1261–8.
- Holman, A.J., Gardner, G.C., Richardson, M.L., Simkin, P.A., 1995. Quantitative magnetic resonance imaging predicts clinical outcome of core decompression for osteonecrosis of the femoral head. *Journal of Rheumatology*. **22**(10), pp. 1929–33.

- Holmberg, S., Dalen, N., 1987. Intracapsular pressure and caput circulation in nondisplaced femoral neck fractures. *Clinical Orthopaedics and Related Research*. (219). pp. 124–6.
- Hölzer, A., Pietschmann, M.F., Rösl, C., Hentschel, M., Betz, O., Matsuura, M., Jansson, V., Müller, P.E., 2012. The interrelation of trabecular microstructural parameters of the greater tubercle measured for different species. *Journal of Orthopaedic Research*. **30**(3), pp. 429–34. doi:10.1002/jor.21525
- Hopson, C.N., Siverhus, S.W., 1988. Ischemic Necrosis of the femoral head - Treatment by core decompression. *Journal of Bone and Joint Surgery*. **70-A**(7), pp. 1048–51.
- Hougaard, K., Thomsen, P.B., 1986. Traumatic posterior dislocation of the hip - Prognostic factors influencing the incidence of avascular necrosis of the femoral head. *Archives of Orthopaedic and Traumatic Surgery*. **106**(1), pp. 32–35. doi:10.1007/BF00435649
- Huang, S.-L., He, X.-J., Wang, K.-Z., 2012. Joint replacement in China: progress and challenges. *Rheumatology (Oxford)*. **51**(9), pp. 1525–6. doi:10.1093/rheumatology/kes077
- Huber, M.B., Carballido-Gamio, J., Bauer, J.S., Baum, T., Eckstein, F., Lochmüller, E.M., Majumdar, S., Link, T.M., 2008. Proximal femur specimens: automated 3D trabecular bone mineral density analysis at multidetector CT--correlation with biomechanical strength measurement. *Radiology*. **247**(2), pp. 472–81. doi:10.1148/radiol.2472070982
- Hughes, P.E., Hsu, J.C., Matava, M.J., 2002. Hip Anatomy and Biomechanics in the Athlete. *Sports Medicine and Arthroscopy Review*. **10**(2), pp. 103–14. 114. doi:10.1097/00132585-200210020-00002
- Hungerford, D.S., 2002. Osteonecrosis: Avoiding total hip arthroplasty. *Journal of Arthroplasty*. **17**(4), pp. 121–24. 124. doi:10.1054/arth.2002.33300

- Ichiseki, T., Ueda, Y., Katsuda, S., Kitamura, K., Kaneuji, A., Matsumoto, T., 2006. Oxidative stress by glutathione depletion induces osteonecrosis in rats. *Rheumatology (Oxford)*. **45**(3), pp. 287–90. doi:10.1093/rheumatology/kei149
- Ikeda, S., Morishita, Y., Tsutsumi, H., Ito, M., Shiraishi, A., Arita, S., Akahoshi, S., Narusawa, K., Nakamura, T., 2003. Reductions in bone turnover, mineral, and structure associated with mechanical properties of lumbar vertebra and femur in glucocorticoid-treated growing minipigs. *Bone*. **33**(5), pp. 779–87.
- Imhof, H., Sulzbacher, I., Grampp, S., Czerny, C., Youssefzadeh, S., Kainberger, F., 2000. Subchondral Bone and Cartilage Disease: A Rediscovered Functional Unit. *Investigative Radiology*. **35**(10), pp. 581–8.
- Incavo, S.J., Pappas, C.N., 2004. Diagnosis and classification of avascular necrosis of the hip. *Seminars in Arthroplasty*. **15**(3), pp. 140–4. 144. doi:10.1053/j.sart.2004.10.004
- Instron, 2015. 3300 Dual Column Universal Testing Systems - Instron [WWW Document]. URL <http://www.instron.com/en/products/testing-systems/universal-testing-systems/electromechanical/3300/3360-dual-column> (accessed 12.Jan.2016).
- Iorio, R., Healy, W.L., Abramowitz, A.J., Pfeifer, B.A., 1998. Clinical Outcome and Survivorship Analysis of Core Decompression for Early Osteonecrosis of the Femoral Head. *Journal of Arthroplasty*. **13**(1), pp. 34–41.
- Ito, H., Matsuno, T., Omizu, N., Aoki, Y., Minami, A., 2003. Mid-term prognosis of non-traumatic osteonecrosis of the femoral head. *Journal of Bone and Joint Surgery*. **85-B**(6), pp. 796–801. doi:10.1302/0301-620X.85B6.13794
- Iwata, H., Torii, S., Hasegawa, Y., Itoh, H., Mizuno, M., Genda, E., Kataoka, Y., 1993. Indications and Results of Vascularized Pedicle Iliac Bone Graft in Avascular Necrosis of the Femoral Head. *Clinical Orthopaedics and Related Research*. **295**. pp. 281–8.
- Jergesen, H.E., Khan, A.S., 1997. The Natural History of Untreated Asymptomatic Hips in Patients Who Have Non-Traumatic Osteonecrosis. *Journal of Bone and Joint Surgery*. **7**(3), pp. 359–63.



- Johansson, H.R., Zywiell, M.G., Marker, D.R., Jones, L.C., McGrath, M.S., Mont, M.A., 2011. Osteonecrosis is not a predictor of poor outcomes in primary total hip arthroplasty: a systematic literature review. *International Orthopaedics*. **35**(4), pp. 465–73. doi:10.1007/s00264-010-0979-7
- Jones Jr, J.P., 1993. Fat embolism, intravascular coagulation, and osteonecrosis. *Clinical Orthopaedics and Related Research*. **292**, pp. 294-308.
- Jones, J.P., 1992. Intravascular coagulation and osteonecrosis. *Clinical Orthopaedics and Related Research*. **277**, pp. 41–53.
- Jones, J.P., 2001. Alcoholism, Hypercortisonism, Fat Embolism and Osseous Avascular Necrosis. *Clinical Orthopaedics and Related Research*. **393**, pp. 4–12.
- Jones, J.P., Sakovich, L., 1966. Fat embolism of bone. A roentgenographic and histological investigation, with use of intra-arterial lipiodol, in rabbits. *Journal of Bone and Joint Surgery, American Volume*. **48**(1), pp. 149–64.
- Jones, L.C., Allen, M.R., 2011. Animal Models of Osteonecrosis. *Clinical Reviews in Bone and Mineral Metabolism*. **9**(1), pp. 63–80. doi:10.1007/s12018-011-9090-x
- Jones, L.C., Hungerford, D.S., 2004. Osteonecrosis: etiology, diagnosis, and treatment. *Current Opinions in Rheumatology*. **16**(4), pp. 443–9.
- Joseph, B., 2011. Natural History of Early Onset and Late-Onset Legg-Calve-Perthes Disease. *Journal of Pediatric Orthopaedics*. **31**, pp. S152–5. doi:10.1097/BPO.0b013e318223b423
- Kaneko, T.S., Bell, J.S., Pejicic, M.R., Tehranzadeh, J., Keyak, J.H., 2004. Mechanical properties, density and quantitative CT scan data of trabecular bone with and without metastases. *Journal of Biomechanics*. **37**(4), pp. 523–30. doi:10.1016/j.jbiomech.2003.08.010
- Kang, P., Gao, H., Pei, F., Shen, B., Yang, J., Zhou, Z., 2010. Effects of an anticoagulant and a lipid-lowering agent on the prevention of steroid-induced osteonecrosis in rabbits.

- International Journal of Experimental Pathology*. **91**(3), pp. 235–43.  
doi:10.1111/j.1365-2613.2010.00705.x
- Kaste, S.C., Shidler, T.J., Tong, X., Srivastava, D.K., Rochester, R., Hudson, M.M., Shearer, P.D., Hale, G.A., 2004. Bone mineral density and osteonecrosis in survivors of childhood allogeneic bone marrow transplantation. *Bone Marrow Transplantation*. **33**(4), pp. 435–41.
- Kaye, B., Randall, C., Walsh, D., Hansma, P., 2012. The Effects of Freezing on the Mechanical Properties of Bone. *Open Bone Journal*. **4**(1), pp. 14–9
- Keaveny, T.M., Morgan, E.F., Yeh, O.C., 2009. Bone Mechanics, in: Biomedical Engineering and Design Handbook. pp. 221–44.
- Keaveny, T.M., Pinilla, T.P., Crawford, R.P., Kopperdahl, D.L., Lou, A., 1997. Systematic and random errors in compression testing of trabecular bone. *Journal of Orthopaedic Research*. **15**, pp. 101–10. doi:10.1002/jor.1100150115
- Keaveny, T.M., Wachtel, E.F., Ford, C.M., Hayes, W.C., 1994. Differences between the tensile and compressive strengths of bovine tibial trabecular bone depend on modulus. *Journal of Biomechanics*. **27**(19), pp. 1137–46.
- Keller, T.S., Mao, Z., Spengler, D.M., 1990. Young's modulus, bending strength, and tissue physical properties of human compact bone. *Journal of Orthopaedic Research*. **8**(4), pp. 592–603. doi:10.1002/jor.1100080416
- Kerachian, M.A., Harvey, E.J., Cournoyer, D., Chow, T.Y.K., Séguin, C., 2006. Avascular necrosis of the femoral head: vascular hypotheses. *Endothelium* **13**, 237–44. doi:10.1080/10623320600904211
- Kerboul, M., Thomine, J., Postel, M., Merle D'Aubigne, R., D'Aubigne, R.M., 1974. The conservative surgical treatment of idiopathic aseptic necrosis of the femoral head. *Journal of Bone and Joint Surgery, American Volume*. **56**(2), pp. 291–6.
- Kim, H.K., Su, P.H., Qiu, Y.S., 2001. Histopathologic changes in growth-plate cartilage following ischemic necrosis of the capital femoral epiphysis. An experimental

- investigation in immature pigs. *Journal of Bone and Joint Surgery, American Volume*. **83-A(5)**, pp. 688–97.
- Kinney, J.H., Ladd, A.J., 1998. The Relationship Between Three-Dimensional Connectivity and the Elastic Properties of Trabecular Bone. *Journal of Bone Mineral Research*. **13(5)**, pp. 839–45.
- Knaepler, H., Haas, H., Püschel, H.U., 1991. [Biomechanical properties of heat and irradiation treated spongiosa]. *Unfallchirurgie*. **17(4)**, pp. 194–9.
- Köhler, P., Kreicbergs, A., Strömberg, L., 1986. Physical properties of autoclaved bone. Torsion test of rabbit diaphyseal bone. *Acta orthopaedica Scandinavica*. **57(2)**, pp. 141–5.
- Kondo, N., Tokunaga, K., Ito, T., Arai, K., Amizuka, N., Minqi, L., Kitahara, H., Ito, M., Naito, M., Shu-Ying, J., Oda, K., Murai, T., Takano, R., Ogose, A., Endo, N., 2006. High dose glucocorticoid hampers bone formation and resorption after bone marrow ablation in rat. *Microscopy Research and Technique*. **69(10)**, pp. 839–46. doi:10.1002/jemt.20355
- Koo, K.H., Kim, R., Ko, G.H., Song, H.R., Jeong, S.T., 1995. Preventing collapse in early necrosis of the femoral head. *Journal of Bone and Joint Surgery, British Volume*. **77-B(6)**, pp. 870–4.
- Koo, K.-H.H., Ahn, I.O., Kim, R., Song, H.R., Jeong, S.T., Na, J.B., Kim, Y.S., Cho, S.H., 1999. Bone marrow edema and associated pain in early stage osteonecrosis of the femoral head: prospective study with serial MR images. *Radiology*. **213(3)**, pp. 715–22.
- Kopecky, K.K., Braunstein, E.M., Brandt, K.D., Filo, R.S., Leapman, S.B., Capello, W.N., Klatte, E.C., 1991. Apparent avascular necrosis of the hip: appearance and spontaneous resolution of MR findings in renal allograft recipients. *Radiology* **179(2)**, pp. 523–7.
- Kotha, S.P., Walsh, W.R., Pan, Y., Guzelsu, N., 1998. Varying the mechanical properties of bone tissue by changing the amount of its structurally effective bone mineral content. *Bio-medical Materials and Engineering*. **8(5-6)**, pp. 321–34.

- Kristensen, K.D., Pedersen, N.W., Kiaer, T., Starklint, H., 1991. Core decompression in femoral head osteonecrosis: 18 Stage I hips followed up for 1-5 years. *Acta orthopaedica Scandinavica*. **62**(2), pp. 113–4.
- Kubota, S., Inaba, Y., Kobayashi, N., Ike, H., Takagawa, S., Ikenishi, T., Naka, T., Saito, T., 2014. Property Of Bone Mineral Density In Osteonecrosis Of The Femoral Head - Comparison Between Collapse And Non-collapse Group-, in: ORS Annual Meeting Proceedings. p. Poster 1769.
- Kwok-Sui, L., 2008. A Practical Manual for Musculoskeletal Research. World Scientific Publishing Company.
- Lafage, M.H., Balena, R., Battle, M.A., Shea, M., Seedor, J.G., Klein, H., Hayes, W.C., Rodan, G.A., 1995. Comparison of alendronate and sodium fluoride effects on cancellous and cortical bone in minipigs. A one-year study. *Journal of Clinical Investigation*. **95**(5), pp. 2127–33. doi:10.1172/JCI117901
- Lafforgue, P., 2006. Pathophysiology and natural history of avascular necrosis of bone. *Joint, Bone, Spine: Revue du Rhumatisme*. **73**(5), pp. 500–7. doi:10.1016/j.jbspin.2006.01.025
- Lai, K.-A.A., Shen, W.-J.J., Yang, C.-Y.Y., Shao, C.-J.J., Hsu, J.-T.T., Lin, R.-M.M., 2005. The use of alendronate to prevent early collapse of the femoral head in patients with nontraumatic osteonecrosis. A randomized clinical study. *Journal of Bone and Joint Surgery, American Volume*. **87**(10), pp. 2155–9. doi:10.2106/JBJS.D.02959
- Lai, Y.-S.S., Wei, H.-W.W., Cheng, C.-K.K., 2008. Incidence of hip replacement among national health insurance enrollees in Taiwan. *Journal of Orthopaedic Surgery and Research*. **3**, p. 42.
- Laitinen, K., Välimäki, M., 1991. Alcohol and bone. *Calcified Tissue International*. **49**(S1), pp. S70–3. doi:10.1007/BF02555094
- Lavernia, C.J., Sierra, R.J., Grieco, F.R., 1999. Osteonecrosis of the femoral head. *Journal of American Academy of Orthopaedic Surgeons*. **7**(4), pp. 250–61.

- Lazenby, R., 1986. Porosity-geometry interaction in the conservation of bone strength. *Journal of Biomechanics*. **19**(3), pp. 257–8.
- Lee, C.K., Hansen, H.T., Weiss, A.B., 1980. The “Silent Hip” of idiopathic ischemic necrosis of the femoral head in adults. *Journal of Bone and Joint Surgery*. **62-A**(5), pp. 795–800.
- Legg, A., 1910. An obscure affliction of the hip joint. *Boston Medical Surgery Journal*. **62**, p. 202.
- Li, B., Aspden, R.M., 1997. Composition and mechanical properties of cancellous bone from the femoral head of patients with osteoporosis or osteoarthritis. *Journal of Bone Mineral Research*. **12**(4), pp. 641–51. doi:10.1359/jbmr.1997.12.4.641
- Li, B., Aspden, R.M., 1997. Mechanical and material properties of the subchondral bone plate from the femoral head of patients with osteoarthritis or osteoporosis. *Annals of the Rheumatic Diseases*. **56**(4), pp. 247–54.
- Li, D., Bi, L., Meng, G., Wang, J., Lv, R., Liu, M., Liu, J., Hu, Y., 2011. Mineral status and mechanical properties of cancellous bone exposed to hydrogen peroxide for various time periods. *Cell and Tissue Banking*. **12**(1), pp. 51–8. doi:10.1007/s10561-009-9161-0
- Lieberman, J.R., Conduah, A., Urist, M.R., 2004. Treatment of Osteonecrosis of the Femoral Head with Core Decompression and Human Bone Morphogenetic Protein. *Clinical Orthopaedics and Related Research*. **429**, pp. 139–45.
- Lieberman, J.R.J.R.R.R., 2004. Core decompression for osteonecrosis of the hip. *Clinical Orthopaedics and Related Research*. **418**, pp. 29–33.
- Lim, B.-H., Lim, S.-J., Moon, Y.-W., Park, Y.-S., 2012. Cementless total hip arthroplasty in renal transplant patients. *Hip International : the Journal of Clinical and Experimental Research on Hip Pathology and Therapy*. **22**(5), pp. 516–20. doi:10.5301/HIP.2012.9471
- Lindahl, O., Lindgren, A.G., 1967. Cortical bone in man. II. Variation in tensile strength with age and sex. *Acta orthopaedica Scandinavica*. **38**(2), pp. 141–7.

- Linde, F., Nørgaard, P., Hvid, I., Odgaard, A., Søballe, K., 1991. Mechanical properties of trabecular bone. Dependency on strain rate. *Journal of Biomechanics*. **24**(9), pp. 803–9.
- Linde, F., Sørensen, H.C.F., 1993. The effect of different storage methods on the mechanical properties of trabecular bone. *Journal of Biomechanics*. **26**(10), pp. 1249–52. doi:10.1016/0021-9290(93)90072-M
- Liu, X.S., Walker, M.D., McMahon, D.J., Udesky, J., Liu, G., Bilezikian, J.P., Guo, X.E., 2011. Better skeletal microstructure confers greater mechanical advantages in Chinese-American women versus white women. *Journal of Bone Mineral Research*. **26**(8), pp. 1783–92. doi:10.1002/jbmr.378
- Loder, R.T., Skopelja, E.N., 2011. The Epidemiology and Demographics of Legg-Calvé-Perthes' Disease. *ISRN Orthopedics*. **2011**, pp. 1–14. doi:10.5402/2011/504393
- Loizou, C.L., Parker, M.J., 2009. Avascular necrosis after internal fixation of intracapsular hip fractures; a study of the outcome for 1023 patients. *Injury*. **40**(11), pp. 1143–6. doi:10.1016/j.injury.2008.11.003
- Ludwig, J., Lauber, S., Lauber, H.J., Dreisilker, U., Raedel, R., Hotzinger, H., 2001. High-energy shock wave treatment of femoral head necrosis in adults. *Clinical Orthopaedics and Related Research*. **387**, pp. 119–26.
- Lu-Yao, G.L., Keller, R.B., Littenberg, B., Wennberg, J.E., 1994. Outcomes after displaced fractures of the femoral neck. A meta-analysis of one hundred and six published reports. *Journal of Bone and Joint Surgery, American Volume*. **76**(1), pp. 15–25.
- Lykissas, M.G., Gelalis, I.D., Kostas-Agnantis, I.P., Vozonelos, G., Korompilias, A. V, 2012. The role of hypercoagulability in the development of osteonecrosis of the femoral head. *Orthopaedic Reviews*. **4**(2), p. e17. doi:10.4081/or.2012.e17
- Ma, H., Zeng, B., Li, X., Chai, Y., 2008. [Experimental study on avascular necrosis of femoral head induced by methylprednisolone combined with lipopolysaccharide in rabbits]. *Zhongguo Xiu Fu Chong Jian Wai Ke Za Zhi*. **22**(3), pp. 265–70.

- Maeda, S., Kita, A, Fujii, G., Funayama, K., Yamada, N., Kokubun, S., 2003. Avascular necrosis associated with fractures of the femoral neck in children: histological evaluation of core biopsies of the femoral head. *Injury*. **34**(4), pp. 283–6.
- Magnussen, R.A., Guilak, F., Vail, T.P., 2005a. Cartilage degeneration in post-collapse cases of osteonecrosis of the human femoral head: altered mechanical properties in tension, compression, and shear. *Journal of Orthopaedic Research*. **23**(3), 576–83. doi:10.1016/j.orthres.2004.12.006
- Magnussen, R.A., Guilak, F., Vail, T.P., 2005b. Articular cartilage degeneration in post-collapse osteonecrosis of the femoral head. Radiographic staging, macroscopic grading, and histologic changes. *Journal of Bone and Joint Surgery, American Volume*. **87**(6), pp. 1272–7. doi:10.2106/JBJS.D.01936
- Malizos, K.N., Karantanas, A.H., Varitimidis, S.E., Dailiana, Z.H., Bargiotas, K., Maris, T., 2007. Osteonecrosis of the femoral head: etiology, imaging and treatment. *European Journal of Radiology*. **63**(1), pp. 16–28. doi:10.1016/j.ejrad.2007.03.019
- Manggold, J., Sergi, C., Becker, K., Lukoschek, M., Simank, H.-G., 2002. A new animal model of femoral head necrosis induced by intraosseous injection of ethanol. *Laboratory Animals*. **36**(2), pp. 173–80.
- Marciniak, D., Furey, C., Shaffer, J.W.W., 2005. Osteonecrosis of the Femoral Head A Study of 101 Hips Treated with Vascularized Fibular Grafting. *Journal of Bone and Joint Surgery*. **87-A**(4), pp. 742–7. doi:10.2106/JBJS.D.02774
- Marotti, G., 1993. A New Theory of Bone Lamellation. *Calcified tissue international* 53, S47–S56.
- Martens, M., van Audekercke, R., de Meester, P., Mulier, J.C., 1986. Mechanical behaviour of femoral bones in bending loading. *Journal of Biomechanics* 19, 443–454. doi:10.1016/0021-9290(86)90021-7

- Martens, M., Van Audekercke, R., Delpont, P., De Meester, P., Mulier, J.C., 1983. The mechanical characteristics of cancellous bone at the upper femoral region. *Journal of Biomechanics*. **16**(12), pp. 971–83.
- Martin, R.B., Boardman, D.L., 1993. The effects of collagen fiber orientation, porosity, density, and mineralization on bovine cortical bone bending properties. *Journal of Biomechanics*. **26**(9), pp. 1047–54. doi:10.1016/S0021-9290(05)80004-1
- Martin, R.B., Burr, D.B., Sharkey, N.A., 1998. *Skeletal Tissue Mechanics*. Springer.
- Martin, R.B., Ishida, J., 1989. The relative effects of collagen fiber orientation, porosity, density, and mineralization on bone strength. *Journal of Biomechanics*. **22**(5), pp. 419–26. doi:10.1016/0021-9290(89)90202-9
- Massari, L., Fini, M., Cadossi, R., Setti, S., Traina, G.C., 2006. Biophysical stimulation with pulsed electromagnetic fields in osteonecrosis of the femoral head. *Journal of Bone and Joint Surgery, American Volume*. **88**(Supplement 1), pp. 56–60. doi:10.2106/JBJS.F.00536
- Matos, M.A., de Alencar, R.W., da Rocha Matos, S.S., 2007. Avascular necrosis of the femoral head in HIV infected patients. *The Brazilian Journal of Infectious Diseases*. **11**(1), pp. 31–4.
- Matsui, M., Saito, S., Ohzono, K., Sugano, N., Saito, M., Takaoka, K., Ono, K., 1992. Experimental steroid-induced osteonecrosis in adult rabbits with hypersensitivity vasculitis. *Clinical Orthopaedics and Related Research*. **277**, pp. 61–72.
- Matsusaki, H., Noguchi, M., Kawakami, T., Tani, T., 2005. Use of vascularized pedicle iliac bone graft combined with transtrochanteric rotational osteotomy in the treatment of avascular necrosis of the femoral head. *Archives of Orthopaedic and Trauma Surgery*. **125**(2), pp. 95–101. doi:10.1007/s00402-004-0777-z
- Mazières, B., Marin, F., Chiron, P., Moulinier, L., Laroche, M., Cantagrel, A., Amigues, J.M., 1997. Influence of the volume of osteonecrosis on the outcome of core



- decompression of the femoral head. *Annals of the Rheumatic Diseases*. **56**, pp. 747–50.
- McCalden, R.W., McGeough, J.A., Barker, M.B., Court-Brown, C.M., 1993. Age-Related Changes in the Tensile Properties of Cortical Bone - The relative importance of change in porosity, mineralization and microstructure. *Journal of Bone and Joint Surgery*. **75**(8), pp. 1193–205.
- McCormack, J., Stover, S.M., Gibeling, J.C., Fyhrie, D.P., 2012. Effects of mineral content on the fracture properties of equine cortical bone in double-notched beams. *Bone*. **50**(6), pp. 1275-80.
- McElhaney, J., Alem, N., Roberts, V.L., 1970. A porous block model for cancellous bones. ASME, New York N.Y.
- McElhaney, J., Fogle, J., Byars, E., Weaver, G., 1964. Effect of enamling on the mechanical properties of beef bone. *Journal of Applied Physiology*. **19**(6), 1234–6.
- McKenzie, W.M.C., 2013. Examples in Structural Analysis, Second Edition - CRC Press Book, Second. ed. CRC Press.
- McLaughlin, F., Mackintosh, J., Hayes, B.P., McLaren, A., Uings, I.J., Salmon, P., Humphreys, J., Meldrum, E., Farrow, S.N., 2002. Glucocorticoid-induced osteopenia in the mouse as assessed by histomorphometry, microcomputed tomography, and biochemical markers. *Bone*. **30**(6), pp. 924–30.
- McLure, S., 2012. Improving models for translational research in osteoarthritis. University of Leeds.
- Mehta, P., Nelson, M., Brand, A., Boag, F., 2013. Avascular necrosis in HIV. *Rheumatology International*. **33**(1), pp. 235–8. doi:10.1007/s00296-011-2114-5
- Menezes, N.M., Connolly, S.A., Shapiro, F., Olear, E.A., Jimenez, R.M., Zurakowski, D., Jaramillo, D., 2007. Early ischemia in growing piglet skeleton: MR diffusion and perfusion imaging. *Radiology*. **242**(1), pp. 129–36. doi:10.1148/radiol.2421050680

- Merle D'Aubigné, R., Postel, M., Mazabraud, A., Massias, P., Gueguen, J., France, P., 1965. Idiopathic necrosis of the femoral head in adults. *Journal of Bone and Joint Surgery, British Volume*. **47**(4), pp. 612–33.
- Meyers, M.H., 1988. Osteonecrosis of the femoral head: pathogenesis and long-term results of treatment. *Clinical Orthopaedics and Related Research*. **231**, pp. 51–61.
- Mitchell, M.D., Kundel, H.L., Steinberg, M.E., Kressel, H.Y., Alavi, A., Axel, L., 1986. Avascular necrosis of the hip: comparison of MR, CT, and scintigraphy. *American Journal of Roentgenology*. **147**(1), pp. 67–71.
- Mont, M.A., Carbone, J.J., Fairbank, A.C., 1996a. Core decompression versus nonoperative management for osteonecrosis of the hip. *Clinical Orthopaedics and Related Research*. **324**, pp. 169–78.
- Mont, M.A., Fairbank, A.C., Krackow, K.A., Hungerford, D.S., 1996b. Corrective osteotomy for osteonecrosis of the femoral head. *Journal of Bone and Joint Surgery, American Volume*. **78**(7), pp. 1032–8.
- Mont, M.A., Hungerford, D.S., 1995. Non-traumatic avascular necrosis of the femoral head. *Journal of Bone and Joint Surgery, American Volume*. **77**(3), pp. 459–74.
- Mont, M.A., Marulanda, G.A., Jones, L.C., Saleh, K.J., Gordon, N., Hungerford, D.S., Steinberg, M.E., 2006. Systematic analysis of classification systems for osteonecrosis of the femoral head. *Journal of Bone and Joint Surgery, American Volume*. **88**(Suppl 3), pp. 16–26.
- Morgan, E.F., Keaveny, T.M., 2001. Dependence of yield strain of human trabecular bone on anatomic site. *Journal of Biomechanics*. **34**(5), pp. 569–77. doi:10.1016/S0021-9290(01)00011-2
- Motomura, G., Yamamoto, T., Miyanishi, K., Jingushi, S., Iwamoto, Y., 2004. Combined effects of an anticoagulant and a lipid-lowering agent on the prevention of steroid-induced osteonecrosis in rabbits. *Arthritis and rheumatism* **50**, 3387–91.

- Motomura, G., Yamamoto, T., Yamaguchi, R., Ikemura, S., Nakashima, Y., Mawatari, T., Iwamoto, Y., 2011. Morphological analysis of collapsed regions in osteonecrosis of the femoral head. *Journal of Bone and Joint Surgery, British Volume*. **93-B(2)**, pp. 184–7. doi:10.1302/0301-620X.93B2
- MP Biomedicals, 2015. Phosphate Buffered Saline Tablets, Dulbecco's Formula, 1X [WWW Document]. Catalogue. URL [http://www4.mpbio.com/ecom/docs/proddata.nsf/\(webtds2\)/28103](http://www4.mpbio.com/ecom/docs/proddata.nsf/(webtds2)/28103) (accessed 2.23.15).
- Munemoto, M., Kido, A., Sakamoto, Y., Inoue, K., Yokoi, K., Shinohara, Y., Tanaka, Y., 2016. Analysis of trabecular bone microstructure in osteoporotic femoral heads in human patients: in vivo study using multidetector row computed tomography. *BMC Musculoskeletal Disorders*. **17**, p. 13.
- Nakata, K., Masuhara, K., Nakamura, N., Shibuya, T., Sugano, N., Matsui, M., Ochi, T., Ohzono, K., 1996. Inducible osteonecrosis in a rabbit serum sickness model: deposition of immune complexes in bone marrow. *Bone*. **18(6)**, pp. 609–15.
- Neumayr, L.D., Aguilar, C., Earles, A.N., Jergesen, H.E., Haberkern, C.M., Kammen, B.F., Nancarrow, P.A., Padua, E., Milet, M., Stulberg, B.N., Williams, R.A., Orringer, E.P., Graber, N., Robertson, S.M., Vichinsky, E.P., 2006. Physical therapy alone compared with core decompression and physical therapy for femoral head osteonecrosis in sickle cell disease. Results of a multicenter study at a mean of three years after treatment. *Journal of Bone and Joint Surgery, American Volume*. **88(12)**, pp. 2573–82. doi:10.2106/JBJS.E.01454
- Nishii, T., Sugano, N., Miki, H., Hashimoto, J., Yoshikawa, H., 2006. Does Alendronate Prevent Collapse in Osteonecrosis of the Femoral Head? *Clinical Orthopaedics and Related Research*. **443**, pp. 273–9. doi:10.1097/01.blo.0000194078.32776.31
- Nishii, T., Sugano, N., Ohzono, K., Sakai, T., Haraguchi, K., Yoshikawa, H., 2002a. Progression and cessation of collapse in osteonecrosis of the femoral head. *Clinical Orthopaedics and Related Research*. **400**, pp. 149–57.

- Nishii, T., Sugano, N., Ohzono, K., Sakai, T.T., Sato, Y., Yoshikawa, H., 2002. Significance of lesion size and location in the prediction of collapse of osteonecrosis of the femoral head: a new three-dimensional quantification using magnetic resonance imaging. *Journal of Orthopaedic Research*. **20**(1), pp. 130–6. doi:10.1016/S0736-0266(01)00063-8
- NJR, 2015. NJR Reports - Patient Characteristics [WWW Document]. URL [http://www.njrreports.org.uk/hips-primary-procedures-patient-characteristics/H04v9NJR?reportid=191E3463-99EA-4E3C-A5B3-8F3FE7546023&defaults=Filter\\_\\_Calendar\\_Year=%22MAX%22,H\\_\\_Filter\\_\\_Joint=%22Hip%22](http://www.njrreports.org.uk/hips-primary-procedures-patient-characteristics/H04v9NJR?reportid=191E3463-99EA-4E3C-A5B3-8F3FE7546023&defaults=Filter__Calendar_Year=%22MAX%22,H__Filter__Joint=%22Hip%22) (accessed 19.Apr.2016).
- Nyman, J.S., Leng, H., Dong, X.N., Wang, X., 2009. Differences in the mechanical behavior of cortical bone between compression and tension when subjected to progressive loading. *Journal of the Mechanical Behaviour of Biomedical Materials*. **2**(6), pp. 613–9.
- Ohman, C., Dall’Ara, E., Baleani, M., Van Sint Jan, S., Viceconti, M., 2008. The effects of embalming using a 4% formalin solution on the compressive mechanical properties of human cortical bone. *Clinical Biomechanics*. **23**(10), pp. 1294–8.
- Ohzono, K., Takaoka, K., Saito, S., Saito, M., Matsui, M., Ono, K., 1992. Intraosseous arterial architecture in nontraumatic avascular necrosis of the femoral head. Microangiographic and histologic study. *Clinical Orthopaedics and Related Research*. **277**, pp. 79–88.
- Okazaki, S., Nishitani, Y., Nagoya, S., Kaya, M., Yamashita, T., Matsumoto, H., 2009. Femoral head osteonecrosis can be caused by disruption of the systemic immune response via the toll-like receptor 4 signalling pathway. *Rheumatology (Oxford)*. **48**(3), pp. 227–32. doi:10.1093/rheumatology/ken462
- Orban, H.B., Cristescu, V., 2009. Avascular necrosis of the femoral head. *Medica*. **4**(7), pp. 26–34.

- Panjabi, M.M., Krag, M., Summers, D., Videman, T., 1985. Biomechanical time-tolerance of fresh cadaveric human spine specimens. *Journal of Orthopaedic Research*. **3**(3), pp. 292–300. doi:10.1002/jor.1100030305
- Papapetrou, P.D., 2009. Bisphosphonate-associated adverse events. *Hormones*. **8**(2), pp. 96–110.
- Pappas, J.N., 2000. The musculoskeletal crescent sign. *Radiology*. **217**(1), pp. 213–4. doi:10.1148/radiology.217.1.r00oc22213
- Parfitt, A.M., Drezner, M.K., Glorieux, F.H., Kanis, J.A., Malluche, H., Meunier, P.J., Ott, S.M., Recker, R.R., 1987. Bone histomorphometry: standardization of nomenclature, symbols, and units. Report of the ASBMR Histomorphometry Nomenclature Committee. *Journal of Bone Mineral Research*. **2**(6), pp. 595–610. doi:10.1002/jbmr.5650020617
- Peled, E., Bejar, J., Zinman, C., Boss, J.H., Reis, D.N., Norman, D., 2009. Prevention of distortion of vascular deprivation-induced osteonecrosis of the rat femoral head by treatment with alendronate. *Archives of Orthopaedic and Trauma Surgery*. **129**(2), pp. 275–9. doi:10.1007/s00402-008-0656-0
- Pelker, R.R., Friedlaender, G.E., Markham, T.C., Panjabi, M.M., Moen, C.J., 1984. Effects of freezing and freeze-drying on the biomechanical properties of rat bone. *Journal of Orthopaedic Research*. **1**(4), pp. 405–11. doi:10.1002/jor.1100010409
- Pena-Rodriguez, M.E., 2013. Statistical Process Control for the FDA-Regulated Industry. ASQ Quality Press.
- Peng, G.-S., Yin, J.-H., Wang, M.-F., Lee, J.-T., Hsu, Y.-D., Yin, S.-J., 2002. Alcohol sensitivity in Taiwanese men with different alcohol and aldehyde dehydrogenase genotypes. *Journal of the Formosan Medical Association*. **101**(11), pp. 769–74.
- Peng, G.-S., Yin, S.-J., 2009. Effect of the allelic variants of aldehyde dehydrogenase ALDH2\*2 and alcohol dehydrogenase ADH1B\*2 on blood acetaldehyde concentrations. *Human Genomics*. **3**(2), pp. 121–7.

- Perilli, E., Briggs, A.M., Kantor, S., Codrington, J., Wark, J.D., Parkinson, I.H., Fazzalari, N.L., 2012. Failure strength of human vertebrae: prediction using bone mineral density measured by DXA and bone volume by micro-CT. *Bone*. **50**(6), pp. 1416–25. doi:10.1016/j.bone.2012.03.002
- Perthes, G., 1913. Uber osteochondritis deformans juvenilis. *Archiv fur Klinische*. **101**, p. 779.
- PlatinumTraining, 2015. Platinum Training | BioSkills Labs, Consulting, Anatomical Management [WWW Document]. URL <http://platinumtraining.org/> (accessed 9.Jan.2016).
- Polesello, G., Sakai, D.S., Ono, N.K., Honda, E.K., Guimaraes, R.P., Júnior, W.R., 2009. The importance of the diagnosis of subchondral fracture of the femoral head, how to differentiate it from avascular necrosis and how to treat it. *Revista Brasileira de Ortopedia*. **44**(2), pp. 102–5.
- Prasad, P., Donoghue, M., 2013. A comparative study of various decalcification techniques. *Indian Journal of Dental Research*. **24**(3), pp. 302–8.
- PubMed, 2016. PubMed - NCBI [WWW Document]. URL <http://www.ncbi.nlm.nih.gov/pubmed/>
- Pufe, T., Scholz-Ahrens, K.E., Franke, A.T.M., Petersen, W., Mentlein, R., Varoga, D., Tillmann, B., Schrezenmeir, J., Glüer, C.C., 2003. The role of vascular endothelial growth factor in glucocorticoid-induced bone loss: evaluation in a minipig model. *Bone*. **33**(6), pp. 869–76.
- Ramachandran, M., Ward, K., Brown, R.R., Munns, C.F., Cowell, C.T., Little, D.G., 2007. Intravenous bisphosphonate therapy for traumatic osteonecrosis of the femoral head in adolescents. *Journal of Bone and Joint Surgery, American Volume*. **89**(8), pp. 1727–34.

- Ramchandani, V.A., 2013. Genetics of Alcohol Metabolism, in: Watson, R.R., Preedy, V.R., Zibadi, S. (Eds.), Alcohol, Nutrition, and Health Consequences. Humana Press, Totowa, NJ, pp. 15–25.
- Rasband, W.S., 1997. ImageJ, U. S. National Institutes of Health, Bethesda, Maryland, USA [WWW Document]. URL <http://imagej.nih.gov/ij/> (accessed 2.23.15).
- Rasouljan, R., Raeisi Najafi, A., Chittenden, M., Jasiuk, I., 2013. Reference point indentation study of age-related changes in porcine femoral cortical bone. *Journal of Biomechanics*. **46**(10), pp. 1689–96.
- Reis, N.D., Schwartz, O., Militianu, D., Ramon, Y., Levin, D., Norman, D., Melamed, Y., Shupak, A., Goldsher, D., Zinman, C., 2003. Hyperbaric oxygen therapy as a treatment for stage-I avascular necrosis of the femoral head. *Journal of Bone and Joint Surgery, British Volume*. **85**(3), pp. 371–5.
- Rho, J.Y., Currey, J.D., Zioupos, P., Pharr, G.M., 2001. The anisotropic Young's modulus of equine secondary osteons and interstitial bone determined by nanoindentation. *Journal of Experimental Biology*. **204**(10), pp. 1775–81.
- Rho, J.Y., Hobatho, M.C., Ashman, R.B., 1995. Relations of mechanical properties to density and CT numbers in human bone. *Medical Engineering and Physics*. **17**(5), pp. 347–355. doi:10.1016/1350-4533(95)97314-F
- Rho, J.Y., Kuhn-Spearing, L., Zioupos, P., 1998. Mechanical properties and the hierarchical structure of bone. *Medical Engineering and Physics*. **20**(2), pp. 92–102.
- Rho, J.Y., Roy, M., Pharr, G.M., 2000. Comments on “Elastic modulus and hardness of cortical and trabecular bone lamellae measured by nanoindentation in the human femur.” *Journal of Biomechanics*. **33**(10), p. 1335. doi:10.1016/S0021-9290(99)00228-6
- Rho, J.Y., Roy, M.E., Tsui, T.Y., Pharr, G.M., 1999a. Elastic properties of microstructural components of human bone tissue as measured by nanoindentation. *J. Biomed. Mater. Res*. **45**(1), pp. 48–54.

- Rho, J.Y., Zioupos, P., Currey, J.D., Pharr, G.M., 1999b. Variations in the individual thick lamellar properties within osteons by nanoindentation. *Bone*. **25**(3), pp. 295–300. doi:10.1016/S8756-3282(99)00163-5
- Russell, N.A., Rives, A., Pelletier, M.H., Bruce, W.J., Walsh, W.R., 2013. The effect of sterilization on the mechanical properties of intact rabbit humeri in three-point bending, four-point bending and torsion. *Cell and Tissue Banking*. **14**(2), pp. 231-42.
- Russell, W.M.S., Burch, R.L., 1959. *The Principles of Humane Experimental Technique*. Methuen.
- Saito, S., Takaoka, K., Ono, K., Minobe, Y., Inoue, A., 1985. Residual deformities related to arthrotic change after Perthes' disease. *Archives of Orthopaedic and Traumatic Surgery* **104**, pp. 7–14. doi:10.1007/BF00449949
- Sakamoto, M., Shimizu, K., Iida, S., Akita, T., Moriya, H., Nawata, Y., 1997. Osteonecrosis Of The Femoral Head: A Prospective Study With MRI. *Journal of Bone and Joint Surgery, British Volume*. **79**(2), pp. 213–9.
- Sakamoto, Y., Yamamoto, T., Motomura, G., Sakamoto, A., Yamaguchi, R., Iwasaki, K., Zhao, G., Karasuyama, K., Iwamoto, Y., 2013. Osteonecrosis of the femoral head extending into the femoral neck. *Skeletal Radiology*. **42**(3), pp. 433–6. doi:10.1007/s00256-012-1525-z
- Salehpour, A., Butler, D.L., Proch, F.S., Schwartz, H.E., Feder, S.M., Doxey, C.M., Ratcliffe, A., 1995. Dose-dependent response of gamma irradiation on mechanical properties and related biochemical composition of goat bone-patellar tendon-bone allografts. *Journal of Orthopaedic Research*. **13**(6), pp. 898–906. doi:10.1002/jor.1100130614
- Scanco Medical, n.d. XtremeCT : Clinical microCT : Systems & Solutions : SCANCO Medical AG [WWW Document]. URL <http://www.scanco.ch/en/systems-solutions/clinical-microct/xtremect.html> (accessed 22.Jul.2014).
- Schaffler, M.B., Burr, D.B., 1988. Stiffness of compact bone: Effects of porosity and density. *Journal of Biomechanics*. **21**(1), pp. 13–6.



*Nature Methods*. **9**, 671–675. doi:10.1038/nmeth.2089

Seal, B.L., Otero, T.C., 2001. Polymeric biomaterials for tissue and organ regeneration. *Materials Science and Engineering*. **34**(4-5), pp. 147–230.

Sedlin, E.D., Hirsch, C., 1966. Factors affecting the determination of the physical properties of femoral cortical bone. *Acta orthopaedica Scandinavica*. **37**(1), pp. 29–48.

Seeman, E., 2008. Bone quality: the material and structural basis of bone strength. *Journal of Bone and Mineral Metabolism*. **26**(1), pp. 1–8. doi:10.1007/s00774-007-0793-5

Séguin, C., Kassis, J., Busque, L., Bestawros, A., Theodoropoulos, J., Alonso, M.-L., Harvey, E.J., 2008. Non-traumatic necrosis of bone (osteonecrosis) is associated with endothelial cell activation but not thrombophilia. *Rheumatology (Oxford)*. **47**(8), pp. 1151–5. doi:10.1093/rheumatology/ken206

Seiler, J.G., Kregor, P.J., Conrad, E.U., Swiontkowski, M.F., 1996. Posttraumatic osteonecrosis in a swine model. *Acta Orthopaedica Scandinavia*. **67**(3), pp. 249–254.

*Journal of biomechanics* **42**, 510–6. doi:10.1016/j.jbiomech.2008.11.026

Shapiro, F., Connolly, S., Zurakowski, D., Menezes, N., Olear, E., Jimenez, M., Flynn, E., Jaramillo, D., 2009. Femoral head deformation and repair following induction of ischemic necrosis: a histologic and magnetic resonance imaging study in the piglet. *Journal of Bone and Joint Surgery, American Volume*. **91**(12), pp. 2903–14.

Shen, Y.-C., Fan, J.-H., Edenberg, H.J., Li, T.-K., Cui, Y.-H., Wang, Y.-F., Tian, C.-H., Zhou, C.-F., Zhou, R.-L., Wang, J., Zhao, Z.-L., Xia, G.-Y., 1997. Polymorphism of ADH and ALDH Genes among Four Ethnic Groups in China and Effects upon the Risk for Alcoholism. *Alcoholism: Clinical and Experimental Research*. **21**(7), pp. 1272–7.

Silva, M.J., Ulrich, S.R., 2000. In vitro sodium fluoride exposure decreases torsional and bending strength and increases ductility of mouse femora. *Journal of Biomechanics*. **33**(2), pp. 231–4.

- Smith, C.W., Kearney, J.N., 1996. The effects of irradiation and hydration upon the mechanical properties of tendon. *Journal of Materials Science: Materials in Medicine*. **7**(11), pp. 645–650. doi:10.1007/BF00123402
- Smith, F.B., 1959. Effects of Rotatory and Valgus Malpositions on Blood Supply to the Femoral Head Observations at Arthroplasty. *Journal of Bone and Joint Surgery. – American Volume*. **41**(5), pp. 800–15.
- Søgaard, C.H., Mosekilde, L., Schwartz, W., Leidig, G., Minne, H.W., Ziegler, R., 1995. Effects of fluoride on rat vertebral body biomechanical competence and bone mass. *Bone*. **16**(1), pp. 163–9.
- Steffen, R.T., Athanasou, N.A., Gill, H.S., Murray, D.W., 2010. Avascular necrosis associated with fracture of the femoral neck after hip resurfacing: Histological assesment of femoral bone from retrieval specimens. *Journal of Bone and Joint Surgery, British Volume*. **92-B**(6), pp. 787–93.
- Steinberg, D.R., Steinberg, M.E., Garino, J.P., Dalinka, M., Udupa, J.K., 2006. Determining lesion Size in Osteonecrosis of the Femoral Head. *Journal of Bone and Joint Surgery*. **88-A**(3), pp. 27–34.
- Steinberg, M.E., Bands, R.E., Parry, S., Hoffman, E., Chan, T., Hartman, K.M., 1999. Does lesion size affect the outcome in avascular necrosis? *Clinical Orthopaedics and Related Research*. **367**, pp. 262–71.
- Steinberg, M.E., Hayken, G.D., Steinberg, D.R., 1995. A quantitative system for staging avascular necrosis. *Journal of Bone and Joint Surgery, British Volume*. **77-B**(1), pp. 34–41.
- Stevens, K., Tao, C., Lee, S.-U., Salem, N., Vandevenne, J., Cheng, C., Neumann, G., Valentin-Opran, A., Lang, P., 2003. Subchondral fractures in osteonecrosis of the femoral head: comparison of radiography, CT, and MR imaging. *AJR. American Journal of Roentgenology*. **180**(2), pp. 363–8. doi:10.2214/ajr.180.2.1800363

- Strømsøe, K., Høiseth, A., Alho, A., Kok, W.L., 1995. Bending strength of the femur in relation to non-invasive bone mineral assessment. *Journal of Biomechanics*. **28**(7), pp. 857–61. doi:10.1016/0021-9290(95)95274-9
- Stulberg, B.N., Bauer, T.W., Belhobek, G.H., 1990. Making core decompression work. *Clinical Orthopaedics and Related Research*. **261**, 186-95.
- Sugioka, Y., 1984. Transtrochanteric rotational osteotomy in the treatment of idiopathic and steroid-induced femoral head necrosis, Perthes' disease, slipped capital femoral epiphysis, and osteoarthritis of the hip. Indications and results. *Clinical Orthopaedics and Related Research*. **169**, pp. 12–23.
- Sugioka, Y., Yamamoto, T., 2008. Transtrochanteric posterior rotational osteotomy for osteonecrosis. *Clinical Orthopaedics and Related Research*. **466**, pp. 1104–9. doi:10.1007/s11999-008-0192-9
- Swanson, S.A. V., Freeman, M.A.R., Day, W.H., 1971. The fatigue properties of human cortical bone. *Medical & Biological Engineering* 9, 23–32. doi:10.1007/BF02474401
- Swiontkowski, M.F., Tepic, S., Rahn, B. a, Cordey, J., Perren, S.M., M Perren, S., 1993. The effect of fracture on femoral head blood flow: Osteonecrosis and revascularization studied in miniature swine. *Acta orthopaedica Scandinavica*. **64**(2), pp. 196–202.
- Takano-Murakami, R., Tokunaga, K., Kondo, N., Ito, T., Kitahara, H., Ito, M., Endo, N., 2009. Glucocorticoid inhibits bone regeneration after osteonecrosis of the femoral head in aged female rats. *The Tohoku Journal of Experimental Medicine*. **217**(1), pp. 51–8.
- Takao, M., Sugano, N., Nishii, T., Sakai, T., Nakamura, N., Yoshikawa, H., 2009. Different magnetic resonance imaging features in two types of nontraumatic rabbit osteonecrosis models. *Magnetic Resonance Imaging*. **27**(2), pp. 233–9.
- Tan, E., Lim, E.C.P., Teo, Y., Lim, Y., Law, H., Sia, A.T., 2009. Ethnicity and OPRM variant independently predict pain perception and patient-controlled analgesia usage for post-operative pain. *Molecular Pain*. **5**, p. 32. doi:10.1186/1744-8069-5-32

- Tank, P.W., Gest, T.R., 2008. Lippincott Williams and Wilkins Atlas of Anatomy (Point (Lippincott Williams & Wilkins)). Lippincott Williams & Wilkins,US.
- Tauchmanovà, L., De Rosa, G., Serio, B., Fazioli, F., Mainolfi, C., Lombardi, G., Colao, A., Salvatore, M., Rotoli, B., Selleri, C., 2003. Avascular necrosis in long-term survivors after allogeneic or autologous stem cell transplantation: a single center experience and a review. *Cancer*. **97**(10), pp. 2453–61.
- Taylor, S.D., Tsiridis, E., Ingham, E., Jin, Z., Fisher, J., Williams, S., 2011. Comparison of human and animal femoral head chondral properties and geometries. *Proceedings of the Institution of Mechanical Engineers, Part H: Journal of Engineering in Medicine*. **226**(1), pp. 55–62.
- Thickman, D., Axel, L., Kressel, H.Y., Steinberg, M., Chen, H., Velchick, M., Fallon, M., Dalinka, M., 1986. Magnetic resonance imaging of avascular necrosis of the femoral head. *Skeletal Radiology*. **15**(2), pp. 133–40.
- Thomasson, H.R., Edenberg, H.J., Crabb, D.W., Mai, X.L., Jerome, R.E., Li, T.K., Wang, S.P., Lin, Y.T., Lu, R.B., Yin, S.J., 1991. Alcohol and aldehyde dehydrogenase genotypes and alcoholism in Chinese men. *American Journal of Human Genetics*. **48**(4), pp. 677–81.
- Tofferi, J.K., Diamond, H.S., 2012. Avascular necrosis treatment & management [WWW Document]. Medscape Reference: Drugs, Diseases & Procedures. URL <http://emedicine.medscape.com/article/333364-treatment#a1128> (accessed 7.10.12).
- Trading Economics, 2015. China Average Yearly Wages [WWW Document]. URL <http://www.tradingeconomics.com/china/wages> (accessed 9.Apr.2016).
- Turner, C.H., Burr, D.B., 1993. Basic biomechanical measurements of bone: A tutorial. *Bone*, **14**(4), pp. 595–608.
- Turner, C.H., Garetto, L.P., Dunipace, A.J., Zhang, W., Wilson, M.E., Grynpas, M.D., Chachra, D., McClintock, R., Peacock, M., Stookey, G.K., 1997. Fluoride treatment increased

- serum IGF-1, bone turnover, and bone mass, but not bone strength, in rabbits. *Calcified Tissue International*. **61**(1), pp. 77–83.
- van Haaren, E.H., van der Zwaard, B.C., van der Veen, A.J., Heyligers, I.C., Wuisman, P.I.J.M., Smit, T.H., 2008. Effect of long-term preservation on the mechanical properties of cortical bone in goats. *Acta Orthopaedica*. **79**(5), pp. 708–16.
- Vanleene, M., Rey, C., Ho Ba Tho, M.C., 2008. Relationships between density and Young's modulus with microporosity and physico-chemical properties of Wistar rat cortical bone from growth to senescence. *Medical Engineering and Physics*. **30**(8), pp. 1049–56.
- Viceconti, M., Toni, A., Brizio, L., Rubbini, L., Borrelli, A., 1996. The effect of autoclaving on the mechanical properties of bank bovine bone. *La Chirurgia Degli Organi Di Movimento*. **81**(1), pp. 63–8.
- Viguet-Carrin, S., Garnero, P., Delmas, P.D., 2006. The role of collagen in bone strength. *Osteoporosis International*. **17**(3), pp. 319–36.
- Villemure, I., Stokes, I.A.F., 2009. Growth plate mechanics and mechanobiology. A survey of present understanding. *Journal of Biomechanics*. **42**(12), pp. 1793–803. doi:10.1016/j.jbiomech.2009.05.021
- Wachter, N., Krischak, G., Mentzel, M., Sarkar, M., Ebinger, T., Kinzl, L., Claes, L., Augat, P., 2002. Correlation of bone mineral density with strength and microstructural parameters of cortical bone in vitro. *Bone*. **31**(1), pp. 90–5.
- Wagner, D.W., Lindsey, D.P., Beaupre, G.S., 2011. Deriving tissue density and elastic modulus from microCT bone scans. *Bone*. **49**(5), pp. 931–8. doi:10.1016/j.bone.2011.07.021
- Walker, M.D., Babbar, R., Opotowsky, A.R., Rohira, A., Nabizadeh, F., Badia, M. Della, Chung, W., Chiang, J., Mediratta, A., McMahon, D., Liu, G., Bilezikian, J.P., 2006. A referent bone mineral density database for Chinese American women. *Osteoporosis International*. **17**(6), pp. 878–87.

- Wallace, R.J., Pankaj, P., Simpson, A.H.R.W., 2013. The effect of strain rate on the failure stress and toughness of bone of different mineral densities. *Journal of Biomechanics*. **46**(13), pp. 2283–7. doi:10.1016/j.jbiomech.2013.06.010
- Wang, C.-J., Wang, F.-S., Yang, K.D., Huang, C.-C., Lee, M.S.-S., Chan, Y.-S., Wang, J.-W., Ko, J.-Y., 2008. Treatment of osteonecrosis of the hip: comparison of extracorporeal shockwave with shockwave and alendronate. *Archives of Orthopaedic and Trauma Surgery*. **128**(9), pp. 901–8. doi:10.1007/s00402-007-0530-5
- Wang, C.-J.J., Wang, F.-S., Huang, C.-C., Yang, K.D., Weng, L.-H., Huang, H.-Y., 2005. Treatment for osteonecrosis of the femoral head: comparison of extracorporeal shock waves with core decompression and bone-grafting. *Journal of Bone and Joint Surgery, American Volume*. **87**(11), pp. 2380–7.
- Wang, K., Wang, C., Wu, Y., Chen, H., 2006. [Changes of vessel in steroid-induced osteonecrosis of femoral head: experimental study of rabbits]. *Zhonghua Yi Xue Za Zhi*. **86**(29), pp. 2024–7.
- Wang, M.C., Aguirre, M., Bhudhikanok, G.S., Kendall, C.G., Kirsch, S., Marcus, R., Bachrach, L.K., 1997. Bone mass and hip axis length in healthy Asian, black, Hispanic, and white American youths. *Journal of Bone Mineral Research*. **12**(11), pp. 1922–35.
- Wang, X., Bank, R.A., Shen, X., Te Koppele, J.M., Athanasiou, K.A., Agrawal, C.M., 1999. Heat induced collagen denaturation and its effects on bone mechanical integrity, in: *Proceedings of the First Joint BMES/EMBS Conference. 1999 IEEE Engineering in Medicine and Biology 21st Annual Conference and the 1999 Annual Fall Meeting of the Biomedical Engineering Society (Cat. No.99CH37015)*. IEEE, p. 493. doi:10.1109/IEMBS.1999.802571
- Wang, X., Bank, R.A., TeKoppele, J.M., Agrawal, C.M., 2001. The role of collagen in determining bone mechanical properties. *Journal of Orthopaedic Research*. **19**(6), pp. 1021–6.

- Wang, X., Nyman, J.S., 2007. A novel approach to assess post-yield energy dissipation of bone in tension. *Journal of Biomechanics*. **40**(3), pp. 674–677. doi:10.1016/j.jbiomech.2006.02.002
- Wang, X., Nyman, J.S., Dong, X.N., Leng, H., Reyes, M., 2010. Fundamental Biomechanics in Bone Tissue Engineering. *Synthesis Lectures on Tissue Engineering*. **2**(1), pp. 1–225. doi:10.2200/S00246ED1V01Y200912TIS004
- Wang, X.-F., Duan, Y., Beck, T.J., Seeman, E., 2005. Varying contributions of growth and ageing to racial and sex differences in femoral neck structure and strength in old age. *Bone*. **36**(9), pp. 978–86.
- Wang, Y., Ohtsuka-Isoya, M., Shao, P., Sakamoto, S., Shinoda, H., 2002. Effects of methylprednisolone on bone formation and resorption in rats. *Japanese Journal of Pharmacology*. **90**(3), pp. 236–46.
- Wei, B.F., Ge, X.H., 2011. Treatment of osteonecrosis of the femoral head with core decompression and bone grafting. *Hip International*. **22**, pp. 206 – 10.
- Weiner, S., Wagner, H.D., 1998. THE MATERIAL BONE: Structure-Mechanical Function Relations. *Annual Reviews of Materials Science*. **28**(1), pp. 271–98.
- Weinstein, R.S., 2012. Glucocorticoid-induced osteonecrosis. *Endocrine*. **41**(2), pp. 183–90. doi:10.1007/s12020-011-9580-0
- Wen, Q., Ma, L., Chen, Y.-P., Yang, L., Luo, W., Wang, X.-N., 2008. A rabbit model of hormone-induced early avascular necrosis of the femoral head. *Biomedical and Environmental Sciences*. **21**(5), pp. 398–403. doi:10.1016/S0895-3988(08)60060-4
- Winwood, K., Zioupos, P., Currey, J.D., Cotton, J.R., Taylor, M., 2006. Strain patterns during tensile, compressive, and shear fatigue of human cortical bone and implications for bone biomechanics. *Journal of Biomedical Materials Research Part A*. **79**(2), pp. 289–97. doi:10.1002/jbm.a.30796

- Wong, G.K.C., Poon, W.S., Chiu, K.H., 2005. Steroid-induced avascular necrosis of the hip in neurosurgical patients: epidemiological study. *ANZ Journal of Surgery*. **75**(6), pp. 409–10. doi:10.1111/j.1445-2197.2005.03389.x
- Woo, J., Li, M., Lau, E., 2001. Population bone mineral density measurements for Chinese women and men in Hong Kong. *Osteoporosis International*. **12**(4), pp. 289–95.
- Wu, S., Jia, H., Hans, D., Lan, J., Wang, L., Li, J., Cai, Y., 2009. Assessment of volumetric bone mineral density of the femoral neck in postmenopausal women with and without vertebral fractures using quantitative multi-slice CT. *Journal of Zhejiang University Science Part B*. **10**(7), pp. 499–504. doi:10.1631/jzus.B0820409
- Wynnyckyj, C., Omelon, S., Savage, K., Damani, M., Chachra, D., Gryn timer, M.D., 2009. A new tool to assess the mechanical properties of bone due to collagen degradation. *Bone*. **44**(5), pp. 840–8. doi:10.1016/j.bone.2008.12.014
- Wynnyckyj, C., Omelon, S., Willett, T.L., Kyle, K., Goldberg, H., Gryn timer, M.D., 2011. Mechanism of bone collagen degradation due to KOH treatment. *Biochimica et Biophysica Acta*. **1810**(2), pp. 192–201.
- XtremeCT scanner [WWW Document], n.d. URL <http://www.scanco.ch/en/systems-solutions/clinical-microct.html> (accessed 7.22.14b).
- Yamamoto, T., 2012. Subchondral insufficiency fractures of the femoral head. *Clinical Orthopaedic Surgery*. **4**(3), pp. 173–80.
- Yamamoto, T., Hirano, K., Tsutsui, H., Sugioka, Y., Sueishi, K., 1995. Corticosteroid enhances the experimental induction of osteonecrosis in rabbits with Shwartzman reaction. *Clinical Orthopaedics and Related Research*. **316**, pp. 235–43.
- Yan, L., Crabtree, N., Reeve, J., Zhou, B., Dequeker, J., Nijs, J., Falch, J., Prentice, A., 2004. Does hip strength analysis explain the lower incidence of hip fracture in the People's Republic of China? *Bone*. **34**(3), pp. 584–8.



- Yang, L., Boyd, K., Kaste, S.C., Kamdem Kamdem, L., Rahija, R.J., Relling, M. V, 2009. A mouse model for glucocorticoid-induced osteonecrosis: effect of a steroid holiday. *Journal of Orthopaedic Research*. **27**(2), pp. 169–75. doi:10.1002/jor.20733
- Yao, H., Dao, M., Carnelli, D., Tai, K., Ortiz, C., 2011. Size-dependent heterogeneity benefits the mechanical performance of bone. *Journal of the Mechanics and Physics of Solids*. **59**(1), pp. 64–74. doi:10.1016/j.jmps.2010.09.012
- Yen, C., Tu, Y., Ma, C., Yu, S., Kao, F., Lee, M.S., 2006. Osteonecrosis of the Femoral Head : Comparison of Clinical Results for Vascularized Iliac and Fibula Bone Grafting. *Journal of Bone and Joint Surgery, British Volume*. **22**(1), pp. 21–24.
- YXLON, n.d. YXLON [WWW Document]. URL <http://www.yxlon.com/Products/X-ray-systems/Y-Cheetah> (accessed 19.Jun.2015).
- Zhang, F., Chang, J., Lu, J., Lin, K., Ning, C., 2007. Bioinspired structure of bioceramics for bone regeneration in load-bearing sites. *Acta Biomaterialia*. **3**(6), pp. 896–904. doi:10.1016/j.actbio.2007.05.008
- Zhao, D., Xu, D., Wang, W., Cui, X., 2006. Iliac Graft Vascularization for Femoral Head Osteonecrosis. *Clinical Orthopaedics and Related Research*. **442**, pp. 171–9. 179. doi:10.1097/01.blo.0000181490.31424.96
- Zioupos, P., Wang, X., Currey, J., 1996. The accumulation of fatigue microdamage in human cortical bone of two different ages in vitro. *Clinical Biomechanics*. **11**(7), pp. 365–75. 375. doi:10.1016/0268-0033(96)00010-1
- Zysset, P.K., Guo, X.E., Hoffler, C.E., Moore, K.E., Goldstein, S.A., 1999. Elastic modulus and hardness of cortical and trabecular bone lamellae measured by nanoindentation in the human femur. *Journal of Biomechanics*. **32**(10), pp. 1005–1012. doi:10.1016/S0021-9290(99)00111-6



## Appendix A

**Matlab programme used for assessing the mechanical properties of bone**



Matlab Programme	Commands
<pre> clc; clear all; close all outputpath = 'input path'; PathStr = 'output path'; Files = dir(fullfile(PathStr, '*.xlsx')); N = length(Files);  dimen = dlmread('SampleProperties.csv', ',',1,3); Data = cell(N,1); H = (1:N)';  for k=1:N  Data{k}=xlsread(fullfile(PathStr,Files(k).name), 'A:B');      contarea{k} = dimen(k,2);     origlength{k} = dimen(k,1);      machineload{k} = Data{k}(:,1)     machineext{k} = Data{k}(:,2);     compload{k} = [[(machineload{k})*2.5]+69]     compext{k} = [(machineext{k})/3]      engstress{k} = compload{k}/contarea{k};     engstrain{k} = compext{k}/origlength{k};      x{k} = engstrain{k};           %strain until yield index value     y{k} = engstress{k};           %stress until yield index value     ymax{k} = max(engstress{k})     xmax{k} = max(engstrain{k})      %plots graph     f{k} = figure(k);     L1{k} = plot(x{k}, y{k}, 'k');      hold on; [x2{k}, y2{k}] = ginput(2) yrange{k} = range(y{k}) outputname{k} = dimen(k,1)     %give cell with output info x_lim{k}=xlim; y_lim{k}=ylim;  [x3{k}, y3{k}] = ginput(1) YieldStress{k} = y3{k} %To place crosshairs on the line hold on </pre>	<p>Open file and determine input and output paths and number of files</p> <p>Read file with sample dimensions</p> <p>Start loop programme for each file</p> <p>Read load and displacement values</p> <p>Import contact area and original length in mm</p> <p>Convert the output load and displacement to real load (as a result of magnification by fixtures in Chapter 4)</p> <p>Calculate stress and strain</p> <p>Calculate stress and strain until yield</p> <p>Plot stress/strain graphs</p>

```

        scatter(x2{k},y2{k}, 'filled',
'MarkerFaceColor', [0.8 0 0.8]);
        scatter(x3{k},y3{k}, 'filled',
'MarkerFaceColor', [0.2 0 0.8]);

        hold on;

        lineObj{k}=fit(x2{k},y2{k} , 'poly1');
%essentially you are fitting a line to point set
(x,y)

        new_lim_x{k}=0:0.05:[max(engstrain{k})];
%decrease 0.1 to achieve finer resolution

new_lim_y{k}=feval(lineObj{k},new_lim_x{k});hold
on;

        L2{k} = plot((new_lim_x{k}),[new_lim_y{k}]);
axis([0 xmax{k} 0 ymax{k}])
        hold on
        grid off;

        xlabel('Engineering Strain');
%X axis label
        ylabel('Engineering Stress,MPa');
%Y axis label
        hold off;
        Names = (k);
        title(Names);

        saveas(f{k}, strcat(outputpath,
'graph',int2str(k)), 'jpg');

        xgrad{k} = x2{1,k}(2,1)-x2{1,k}(1,1)
        ygrad{k} = y2{1,k}(2,1)-y2{1,k}(1,1)
        modulus{k} = ygrad{k}/xgrad{k}
        Var{k}= [k;modulus{k};YieldStress{k}];

end

%headers
header = {'MatlabID', 'E', 'YieldStress'};
%output data transformed
dt=[cell2mat(Var)'];

%output with headers in a dataset
ds = dataset({dt,header{:}})

%dataset exported into a text file in outputpath
export(ds,'file',strcat(outputpath,
'output.txt'))

```

Save graphs

Calculate elastic modulus

End loop

Save data

## **Appendix B**

**Ethics protocol for use of control human tissue**







Sophie Williams  
Institute of Medical and Biological Engineering  
School of Mechanical Engineering  
University of Leeds  
Leeds, LS2 9JT

**MaPS and Engineering joint Faculty Research Ethics Committee (MEEC FREC)  
University of Leeds**

12 September 2016

Dear Sophie

**Title of study**            **Development of research techniques to assist surgical interventions of the hip**  
**Ethics reference**        **MEEC 13-002**  
**Grant reference**        **EP/G012172/1**

I am pleased to inform you that the application listed above has been reviewed by the MaPS and Engineering joint Faculty Research Ethics Committee (MEEC FREC) and I can confirm a favourable ethical opinion as of the date of this letter. The following documentation was considered:

<i>Document</i>	<i>Version</i>	<i>Date</i>
MEEC 13-002 130912 WILLIAMS Submitted ethics form for human hip tissue.pdf	1	12/09/13
MEEC 13-002 130912 WILLIAMS Submitted protocol for human hip tissue.pdf	1	12/09/13
MEEC 13-002 Generic risk assessment (SPW) for ethics 205113.PDF	1	12/09/13

Please notify the committee if you intend to make any amendments to the original research as submitted at date of this approval, including changes to recruitment methodology. All changes must receive ethical approval prior to implementation. The amendment form is available at <http://ris.leeds.ac.uk/EthicsAmendment>.

Please note: You are expected to keep a record of all your approved documentation, as well as documents such as sample consent forms, and other documents relating to the study. This should be kept in your study file, which should be readily available for audit purposes. You will be given a two week notice period if your project is to be audited. There is a checklist listing examples of documents to be kept which is available at <http://ris.leeds.ac.uk/EthicsAudits>.

We welcome feedback on your experience of the ethical review process and suggestions for improvement. Please email any comments to [ResearchEthics@leeds.ac.uk](mailto:ResearchEthics@leeds.ac.uk).

Yours sincerely

Jennifer Blaikie  
Senior Research Ethics Administrator, Research & Innovation Service  
On behalf of Professor Gary Williamson, Chair, [MEEC FREC](#)  
CC: Faculty Research & Innovation Office





Please read each question carefully, taking note of instructions and completing all parts. If a question is not applicable please indicate so. The superscripted numbers (eg<sup>8</sup>) refer to sections of the guidance notes, available at [www.leeds.ac.uk/ethics](http://www.leeds.ac.uk/ethics). Where a question asks for information which you have previously provided in answer to another question, please just refer to your earlier answer rather than repeating information.

Research ethics training courses: <http://www.sddu.leeds.ac.uk/sddu-research-ethics-courses.html>

To help us process your application enter the following reference numbers, if known and if applicable:

Ethics reference number:	EP/G012172/1
Student number and/ or grant reference:	EPSRC Programme grant in Biotribology of Catilage EP/G012172/1 PhD students, Avadi 200662543 and Pallan 200274266

## PART A: Summary

### A.1 Which [Faculty Research Ethics Committee](#) would you like to consider this application?<sup>2</sup>

- Arts and PVAC (PVAR)  
 Biological Sciences (BIOSCI)  
 ESSL/ Environment/ LUBS (AREA)  
 MaPS and Engineering (MEEC)  
 Medicine and Health (Please specify a subcommittee):
  - Leeds Dental Institute (DREC)
  - Health Sciences/ LIGHT/ LImm
  - School of Healthcare (SHREC)
  - Medical and Dental Educational Research (EdREC)
  - Institute of Psychological Sciences (IPSREC)

### A.2 Title of the research<sup>3</sup>

Development of research techniques to assess surgical interventions of the hip

### A.3 Principal investigator's contact details<sup>4</sup>

Name ( <i>Title, first name, surname</i> )	Dr Sophie Williams
Position	Associate Professor
Department/ School/ Institute	Institute of Medical and Biological Engineering, School of Mechanical Engineering
Faculty	Engineering
Work address ( <i>including postcode</i> )	School of Mechanical Engineering, University of Leeds, Leeds LS2 9JT
Telephone number	0113 343 2214
<b>University of Leeds</b> email address	s.d.williams@leeds.ac.uk

**A.4 Purpose of the research:**<sup>5</sup> (Tick as appropriate)

- Research
- Educational qualification: **Please specify:** PhD research (for Pallan and Avadi)
- Educational Research & Evaluation<sup>6</sup>
- Medical Audit or Health Service Evaluation<sup>7</sup>
- Other

**A.5 Select from the list below to describe your research:** (You may select more than one)

- Research on or with human participants
- Research with has potential significant environmental impact.<sup>8</sup> If yes, please give details:  
\_\_\_\_\_
- Research working with data of human participants
  - New data collected by questionnaires/interviews
  - New data collected by qualitative methods
  - New data collected from observing individuals or populations
  - Research working with aggregated or population data
  - Research using already published data or data in the public domain
- Research working with human tissue samples<sup>9</sup>

**A.6 Will the research involve any of the following:**<sup>10</sup> (You may select more than one)

***If your research involves any of the following an application must be made to the National Research Ethics Service (NRES) via IRAS [www.myresearchproject.org.uk](http://www.myresearchproject.org.uk) as NHS ethical approval will be required. There is no need to complete any more of this form. Contact [governance-ethics@leeds.ac.uk](mailto:governance-ethics@leeds.ac.uk) for advice.***

- Patients and users of the NHS (including NHS patients treated in the private sector)<sup>11</sup>
- Individuals identified as potential participants because of their status as relatives or carers of patients and users of the NHS
- Research involving adults in Scotland, Wales or England who lack the capacity to consent for themselves<sup>12</sup>
- A prison or a young offender institution in England and Wales (and is health related)<sup>14</sup>
- Clinical trial of a medicinal product or medical device<sup>15</sup>
- Access to data, organs or other bodily material of past and present NHS patients<sup>9</sup>
- Use of human tissue (including non-NHS sources) where the collection is not covered by a Human Tissue Authority licence<sup>9</sup>
- Foetal material and IVF involving NHS patients
- The recently deceased under NHS care
- None of the above

**You must inform the Research Ethics Administrator of your NRES number and approval date once approval has been obtained.**

If the University of Leeds is not the Lead Institution, or approval has been granted elsewhere (e.g. NHS) then you should contact the local Research Ethics Committee for guidance. The UoL Ethics Committee need to be assured that any relevant local ethical issues have been addressed.

**A.7 Will the research involve NHS staff recruited as potential research participants (by virtue of their professional role) or NHS premises/ facilities?**

Yes  No

If yes, ethical approval must be sought from the University of Leeds. Please note that NHS R&D approval is needed in addition: [www.myresearchproject.org.uk](http://www.myresearchproject.org.uk). Contact [governance-ethics@leeds.ac.uk](mailto:governance-ethics@leeds.ac.uk) for advice.

**A.8 Will the participants be from any of the following groups? (Tick as appropriate)**

- Children under 16<sup>16</sup>
- Adults with learning disabilities<sup>12</sup>
- Adults with other forms of mental incapacity or mental illness
- Adults in emergency situations
- Prisoners or young offenders<sup>14</sup>
- Those who could be considered to have a particularly dependent relationship with the investigator, eg members of staff, students<sup>17</sup>
- Other vulnerable groups
- No participants from any of the above groups

**Please justify the inclusion of the above groups, explaining why the research cannot be conducted on non vulnerable groups.**

**It is the researcher's responsibility to check whether a DBS check is required and to obtain one if it is needed.**

See also <http://www.homeoffice.gov.uk/agencies-public-bodies/dbs> and [http://store.leeds.ac.uk/browse/extra\\_info.asp?modid=1&prodid=2162&deptid=34&compid=1&prodvarid=0&catid=243](http://store.leeds.ac.uk/browse/extra_info.asp?modid=1&prodid=2162&deptid=34&compid=1&prodvarid=0&catid=243).

**A.9 Give a short summary of the research<sup>18</sup>**

*This section must be completed in **language comprehensible to the lay person**. Do not simply reproduce or refer to the protocol, although the protocol can also be submitted to provide any technical information that you think the ethics committee may require. This section should cover the main parts of the proposal.*

This protocol outlines a series of research studies using human hip joints obtained from deceased donors via a commercial tissue bank in the USA using ethically approved processes. The studies aim to develop research techniques to assess surgical interventions in the hip, this includes:

- Assessment of contact mechanics, experimentally and computationally, this will provide information about the stress and strain that tissues in the joint are subjected too, and the likelihood of damage.
- Assessment of mechanical properties of the bone and soft tissues (such as the labrum and cartilage), to help us better understand the effects of different loading.
- Assessment of the biological characteristics of the bone and soft tissues (such as the labrum and cartilage), much is known about cartilage properties, but little is known about the labrum. We are interested in how it's characteristics differ to those of cartilage.

Information gained will be used to develop computational models and experimental simulations of the natural hip joint in a healthy and diseased state. Diseases to be considered include avascular necrosis and those affecting joint geometry such as femoroacetabular impingement and dysplasia.

**A.10 What are the main ethical issues with the research and how will these be addressed?**<sup>19</sup>

Indicate any issues on which you would welcome advice from the ethics committee.

The main ethical issues to be considered include:

- Consent of tissue donors, the commercial tissue bank states that it has reviewed the processes by which consent for research from the donor or authorising party was obtained (to the best their knowledge), in accordance with all applicable state and federal laws (USA) and regulations (specifically the Human Anatomical Gift Act) prior to recovery and distribution.
- Disposal of donor tissue, this will done respectfully following local guidelines in accordance with the HTA
- Data protection, all donor samples will be coded prior to receipt at the University. All data will be stored and used in accordance with University guidelines; that also meet the requirements of the HTA.

**PART B: About the research team****B.1 To be completed by students only**<sup>20</sup>

Qualification working towards (eg Masters, PhD)	PhD
Supervisor's name (Title, first name, surname)	Dr Sophie Williams
Department/ School/ Institute	Institute of Medical and Biological Engineering, School of Mechanical Engineering
Faculty	Engineering
Work address (including postcode)	School of Mechanical Engineering, University of Leeds, Leeds LS2 9JT
Supervisor's telephone number	0113 343 2214
Supervisor's email address	s.d.williams@leeds.ac.uk
Module name and number (if applicable)	

**B.2 Other members of the research team (eg co-investigators, co-supervisors)**<sup>21</sup>

Name (Title, first name, surname)	Dr Alison Jones (Co-Investigator)
Position	Lecturer
Department/ School/ Institute	Institute of Medical and Biological Engineering, School of Mechanical Engineering
Faculty	Engineering
Work address (including postcode)	School of Mechanical Engineering, University of Leeds, Leeds LS2 9JT
Telephone number	0113 343 2099
Email address	a.c.jones@leeds.ac.uk

Name (Title, first name, surname)	Dr Qianqian Wang (Researcher on study)
Position	Research Fellow
Department/ School/ Institute	Institute of Medical and Biological Engineering, School of Mechanical Engineering
Faculty	Engineering
Work address (including postcode)	School of Mechanical Engineering, University of Leeds, Leeds LS2 9JT
Telephone number	0113 343 5011
Email address	q.wang@leeds.ac.uk

Name (Title, first name, surname)	Dr Junyan Li (Researcher on study)
Position	Research Fellow
Department/ School/ Institute	Institute of Medical and Biological Engineering, School of Mechanical Engineering
Faculty	Engineering
Work address (including postcode)	School of Mechanical Engineering, University of Leeds, Leeds LS2 9JT
Telephone number	0113 343 5011
Email address	menjlic@leeds.ac.uk

Name (Title, first name, surname)	Masha Avadi (Researcher on study)
Position	PhD research student
Department/ School/ Institute	Institute of Medical and Biological Engineering, School of Mechanical Engineering
Faculty	Engineering
Work address (including postcode)	School of Mechanical Engineering, University of Leeds, Leeds LS2 9JT
Telephone number	0113 343 2164
Email address	mnmsa@leeds.ac.uk

Name (Title, first name, surname)	Rachel Pallan (Researcher on study)
Position	PhD research student
Department/ School/ Institute	Institute of Medical and Biological Engineering, School of Mechanical Engineering
Faculty	Engineering
Work address (including postcode)	School of Mechanical Engineering, University of Leeds, Leeds LS2 9JT
Telephone number	0113 343 2164
Email address	mn06rp@leeds.ac.uk

## Part C: The research

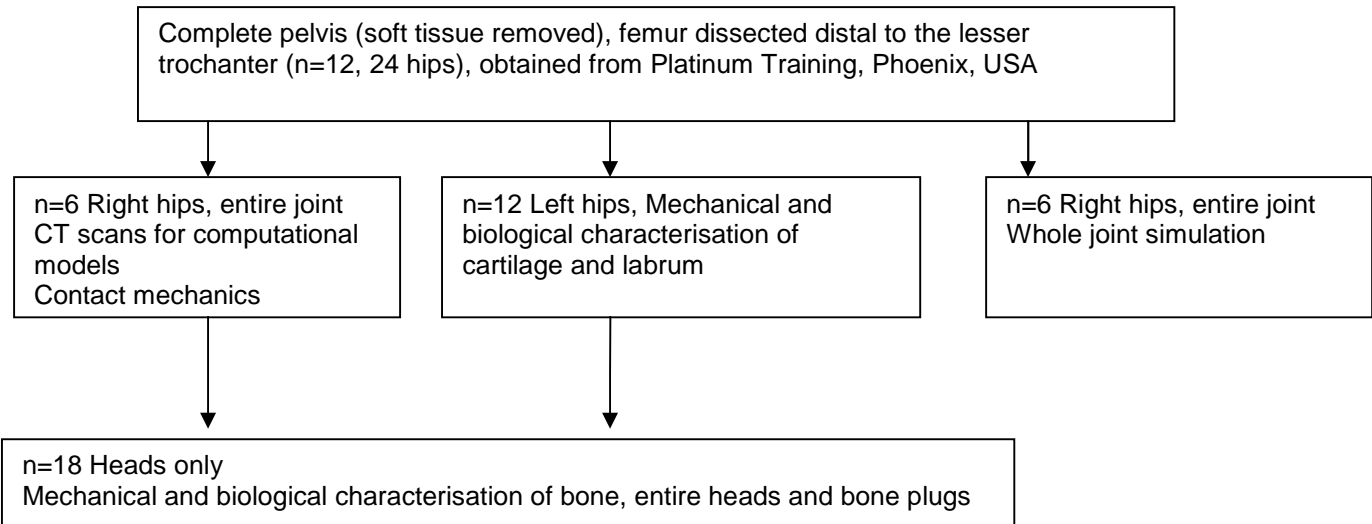
### C.1 What are the aims of the study?<sup>22</sup> (Must be in language comprehensible to a lay person.)

- Provide medical images for use in donor sample (hip joint specific) computational models to predict contact mechanics (ie areas of the joint that contact under load)
- Compare the contact mechanics in porcine and human joints (and also comparison to predictions generated by computational models)
- Characterise the biological and mechanical properties of human hip joint tissue (bone, cartilage and labrum) and compare to porcine and diseased human tissue (e.g. femoral heads with AVN, subject of another study protocol and ethics approval)
- Assess the tribological behaviour (wear and friction) of natural human hip joints in a joint simulator, and compare to porcine hip joints
- Modify the whole joint simulation to include altered pathologies

**C.2 Describe the design of the research. Qualitative methods as well as quantitative methods should be included.** (Must be in language comprehensible to a lay person.)

*It is important that the study can provide information about the aims that it intends to address. If a study cannot answer the questions/ add to the knowledge base that it intends to, due to the way that it is designed, then wasting participants' time could be an ethical issue.*

Twelve pelvis sections (24 hips) will be purchased from Platinum Training. Samples will be used in testing as described in the flow chart below, it should be noted that there may be slight deviations from the proposed numbers of samples used in each study if technical issues arise or results dictate further testing is required in a particular area.



The research described in the flow diagram above is further detailed below:

- CT scans for computational models, medical images of the donor tissue will be taken using Computed Tomography scanners. Information on shape and structure of the bone will be used in computational models. The computational models will be used to assess the contact areas in hips under load and motion.
- Contact mechanics will be assessed experimentally. Hip joints (the acetabulum and femoral head) will be loaded and the areas of contact assessed, orientation and loads will be varied to assess the effect of different scenarios
- Mechanical and biological characterisation of cartilage and labrum, these tissues will be mechanically characterised (assessing for properties such as strength, stiffness etc). Data will be compared to that generated in other studies (e.g. where we use porcine tissue as a substitute for human tissue, or compared to diseased human tissue). Biological characterisation will include histology (microscopic examination of tissue by sectioning and staining) and immunohistochemistry to identify tissue constituents.
- Mechanical characterisation of bone, entire heads and bone plugs. Bone will be mechanically characterised (assessing for properties such as strength, stiffness etc). Data will be compared to that generated in other studies (e.g. where we use porcine tissue as a substitute for human tissue, or compared to diseased human tissue). Biological characterisation will include histology (microscopic examination of tissue by sectioning and staining) and immunohistochemistry to identify tissue constituents.

**C.3 What will participants be asked to do in the study?**<sup>23</sup> (e.g. number of visits, time, travel required, interviews)

Via a commercial tissue bank (Platinum Training), donors or their next of kin will have completed an informed consent form to donate their tissue for research purposes on their death. University Researchers will not interface with donors / families directly at any time.

**C.4 Does the research involve an international collaborator or research conducted overseas?**<sup>24</sup>

(Tick as appropriate)

Yes  No

**If yes, describe any ethical review procedures that you will need to comply with in that country:**

**Describe the measures you have taken to comply with these:**

Include copies of any ethical approval letters/ certificates with your application.



### C.5 Proposed study dates and duration

Research start date (DD/MM/YY): 01/10/13 Research end date (DD/MM/YY): 30/09/2015

Fieldwork start date (DD/MM/YY): \_\_\_\_\_ Fieldwork end date (DD/MM/YY): \_\_\_\_\_

### C.6. Where will the research be undertaken? (i.e. in the street, on UoL premises, in schools)<sup>25</sup>

The donors samples will be sent to the Faculty of Biological Sciences and gross dissection conducted there. Samples will be stored in the Faculty of Biological Sciences. Experimental work will be undertaken in the Faculties of Biological Sciences and Engineering. Room details are provided in the protocol.

## RECRUITMENT & CONSENT PROCESSES

*How participants are recruited is important to ensure that they are not induced or coerced into participation. The way participants are identified may have a bearing on whether the results can be generalised. Explain each point and give details for subgroups separately if appropriate.*

### C.7 How will potential participants in the study be:

(i) identified?

(ii) approached?

(iii) recruited?<sup>26</sup>

We are not recruiting donors to the study; this will be done by Platinum Training in accordance with the Uniform Anatomical Gift Act (USA).

### C.8 Will you be excluding any groups of people, and if so what is the rationale for that?<sup>27</sup>

*Excluding certain groups of people, intentionally or unintentionally may be unethical in some circumstances. It may be wholly appropriate to exclude groups of people in other cases*

The exclusion criteria for this study is:

1. Donors that have osteoarthritis in the hip, or suffered a broken hip, or had hip surgery (as described on the donor medical and social history questionnaire
2. Donors with serological results indicating a transmissible disease

This is (1) for scientific reasons relating to the research being carried out and (2) safety of researchers

### C.9 How many participants will be recruited and how was the number decided upon?<sup>28</sup>

*It is important to ensure that enough participants are recruited to be able to answer the aims of the research.*

No formal power calculation has been conducted; however, previous work has suggests that the numbers of repeats we are proposing are adequate for this work.

If you have a formal power calculation please replicate it here.

*Remember to include all advertising material (posters, emails etc) as part of your application*

### C10 Will the research involve any element of deception?<sup>29</sup>

If yes, please describe why this is necessary and whether participants will be informed at the end of the study.

No

### C.11 Will **informed consent** be obtained from the research participants?<sup>30</sup>

Yes  No

**If yes, give details of how it will be done. Give details of any particular steps to provide information (in addition to a written information sheet) e.g. videos, interactive material. If you are not going to be obtaining informed consent you will need to justify this.**

Donor samples will be ordered and purchased from Platinum Training, Phoenix, USA. Platinum Training abides by the Uniform Anatomical Gift Act, a copy of their consent form is included in the protocol.

If **participants are to be recruited from any of potentially vulnerable groups, give details of extra steps taken to assure their protection. Describe any arrangements to be made for obtaining consent from a legal representative.**

**Copies of any written consent form, written information and all other explanatory material should accompany this application.** The information sheet should make explicit that participants can withdraw from the research at any time, if the research design permits.

Sample information sheets and consent forms are available from the University ethical review webpage at <http://ris.leeds.ac.uk/InvolvingResearchParticipants>.

**C.12 Describe whether participants will be able to withdraw from the study, and up to what point (eg if data is to be anonymised). If withdrawal is not possible, explain why not.**

If we were to receive a request from Platinum Training regarding the withdrawal of a donor, we would remove those samples from the study and dispose of them in the manner requested by Platinum Training. We would remove and destroy any data collected on that donor from the study.

**C.13 How long will the participant have to decide whether to take part in the research?<sup>31</sup>**

*It may be appropriate to recruit participants on the spot for low risk research; however consideration is usually necessary for riskier projects.*

The consent and decision making process of the donor / their next of kin will be in line with the requirements of the Uniform Anatomical Gift Act.

**C.14 What arrangements have been made for participants who might not adequately understand verbal explanations or written information, or who have special communication needs?<sup>32</sup> (e.g. translation, use of interpreters etc. It is important that groups of people are not excluded due to language barriers or disabilities, where assistance can be given.)**

The consent and decision making process of the donor / their next of kin will be in line with the requirements of the Uniform Anatomical Gift Act.

**C.15 Will individual or group interviews/ questionnaires discuss any topics or issues that might be sensitive, embarrassing or upsetting, or is it possible that criminal or other disclosures requiring action could take place during the study (e.g. during interviews or group discussions)?<sup>33</sup> The [information sheet](#) should explain under what circumstances action may be taken.**

Yes  No *If yes, give details of procedures in place to deal with these issues.*

**C.16 Will individual research participants receive any payments, fees, reimbursement of expenses or any other incentives or benefits for taking part in this research?<sup>34</sup>**

Yes  No

**If Yes, please describe the amount, number and size of incentives and on what basis this was decided.**

## RISKS OF THE STUDY

### C.17 What are the potential benefits and/ or risks for research participants?<sup>35</sup>

The research participants are deceased donors, who have (via an informed consent process) allowed their body to be used for research. All information the University receives about the donors will be anonymous, and they will not be identifiable.

### C.18 Does the research involve any risks to the researchers themselves, or people not directly involved in the research? *Eg lone working*<sup>36</sup>

Yes  No

*If yes, please describe:* \_\_\_\_\_

Is a [risk assessment](#) necessary for this research?

**NB: Risk assessments are a University requirement for all fieldwork taking place off campus. For guidance contact your Faculty Health and Safety Manager or visit <http://www.leeds.ac.uk/safety/fieldwork/index.htm>.**

Yes  No If yes, please include a copy of your risk assessment form with your application.

All research will be conducted on the University campus. A generic risk assessment for the use of human tissue for research is attached; risk assessments will be completed for specific activities relating to this work in a similar manner using established quality assurance systems in the Institute of Medical and Biological Engineering.

## DATA ISSUES

### C.19 Will the research involve any of the following activities at any stage (including identification of potential research participants)? (Tick as appropriate)

- Examination of personal records by those who would not normally have access
  - Access to research data on individuals by people from outside the research team
  - Electronic transfer of data
  - Sharing data with other organisations
  - Exporting data outside the European Union
  - Use of personal addresses, postcodes, faxes, e-mails or telephone numbers
  - Publication of direct quotations from respondents
  - Publication of data that might allow identification of individuals to be identified
  - Use of audio/visual recording devices
  - FLASH memory or other portable storage devices
- Storage of personal data on or including any of the following:
- Manual files
  - Home or other personal computers
  - Private company computers
  - Laptop computers

**C.20. How will the research team ensure confidentiality and security of personal data? E.g. anonymisation procedures, secure storage and coding of data.**<sup>37</sup> Refer to <http://ris.leeds.ac.uk/ResearchDataManagement> for advice

The identity of the patients will not be known to investigators at the University of Leeds, all donor samples will only be identified by Platinum Training's unique donor code, and this will be used throughout the study. Details of the donor sample (e.g. serological report, Medical and social history questionnaire) will be stored on the Achiever system. This system and associated safeguards have been approved by the Human Tissue Authority.

Most data will be processed using university computers, though personal computers may also be used (however, these will be encrypted in accordance with University of Leeds IT policies). All study data will be stored on university networked drives which are regularly backed up, additionally backups of this data will be stored at the site. Access to all study data will be restricted to those directly involved with the research.

The three-dimensional images, characterisation data and corresponding computer models will be stored on a secure, HTA compliant data server. This data and computer simulation capability will be used going forward to investigate the effectiveness of treatments for the hip in a virtual environment. In addition the images and derived models will be used to enrich teaching and public engagement activities.

Data from this study will be used to produce manuscripts for publication in research journals. The data will also be used for internal and external research seminars and for teaching or public engagement purposes where deemed appropriate, all of which is in line with current guideline issued by the Human Tissue Authority. Data associated with the project will be stored for at least 10 years (in accordance with RCUK guidelines) following completion.

**C.21 For how long will data from the study be stored? Please explain why this length of time has been chosen.**<sup>38</sup>

*RCUK guidance states that data should normally be preserved and accessible for ten years, but for some projects it may be 20 years or longer.*

**Students:** *It would be reasonable to retain data for at least 2 years after publication or three years after the end of data collection, whichever is longer.*

10 years, in accordance with RCUK guidance, there are no compelling reasons to store the data for longer

## CONFLICTS OF INTEREST

**C.22 Will any of the researchers or their institutions receive any other benefits or incentives for taking part in this research over and above normal salary or the costs of undertaking the research?**<sup>39</sup>

Yes  No

If yes, indicate how much and on what basis this has been decided

**C.23 Is there scope for any other conflict of interest?**<sup>40</sup> *For example will the research funder have control of publication of research findings?*

Yes  No **If yes, please explain**

As part of the DePuy Technology Partnership (which supports one part of the proposed study), DePuy has the right to review (but not refuse) research publication

**C.24 Does the research involve external funding? (Tick as appropriate)**

Yes  No **If yes, what is the source of this funding?**

EPSRC grant (Biotribology of cartilage), EPSRC studentship (Case award with DePuy Synthes), Industry (DePuy Technology Partnership)

## PART D: Declarations

### Declaration by Chief Investigators

1. The information in this form is accurate to the best of my knowledge and belief and I take full responsibility for it.
2. I undertake to abide by the University's ethical and health & safety guidelines, and the ethical principles underlying good practice guidelines appropriate to my discipline.
3. If the research is approved I undertake to adhere to the study protocol, the terms of this application and any conditions set out by the Research Ethics Committee.
4. I undertake to seek an ethical opinion from the REC before implementing substantial amendments to the protocol.
5. I undertake to submit progress reports if required.
6. I am aware of my responsibility to be up to date and comply with the requirements of the law and relevant guidelines relating to security and confidentiality of patient or other personal data, including the need to register when necessary with the appropriate Data Protection Officer.
7. I understand that research records/ data may be subject to inspection for audit purposes if required in future.
8. I understand that personal data about me as a researcher in this application will be held by the relevant RECs and that this will be managed according to the principles established in the Data Protection Act.
9. I understand that the Ethics Committee may choose to audit this project at any point after approval.

### Sharing information for training purposes: Optional – please tick as appropriate:

- I would be content for members of other Research Ethics Committees to have access to the information in the application in confidence for training purposes. All personal identifiers and references to researchers, funders and research units would be removed.

### Principal Investigator

Signature of Principal Investigator:

(This needs to be an actual signature rather than just typed. Electronic signatures are acceptable)

Print name: Dr Sophie Williams                      Date:        10 September 2013

### Supervisor of student research: I have read, edited and agree with the form above.

Supervisor's signature: .

(This needs to be an actual signature rather than just typed. Electronic signatures are acceptable)

Print name: Dr Sophie Williams                      Date:        10 September 2013

Please submit your form **by email** to [researchethics@leeds.ac.uk](mailto:researchethics@leeds.ac.uk) or if you are in the Faculty of Medicine and Health [FMHUniEthics@leeds.ac.uk](mailto:FMHUniEthics@leeds.ac.uk). **Remember to include any supporting material** such as your participant information sheet, consent form, interview questions and recruitment material with your application.

### To help speed up the review of your application:

- Answer the questions in plain English, avoid using overly technical terms and acronyms not in common use.
- Answer all the questions on the form, including those with several parts (refer to the [guidance](#) if you're not sure how to answer a question or how much detail is required).
- Include any relevant supplementary materials such as
  - Recruitment material (posters, emails etc)
  - [Sample participant information sheet](#)
  - [Sample consent form](#). Include different versions for different groups of participants eg for children and adults, clearly indicating which is which.
  - Signed [risk assessment](#) (required for all activities taking place off-campus).
- If you are not going to be using participant information sheets or consent forms explain why not and how informed consent will be otherwise obtained.
- If you are a student it is essential that you discuss your application with your supervisor.
- Submit a [signed copy](#) of the application, preferably electronically. Students' applications need to be signed by their supervisors as well.

# Study Protocol

## Development of research techniques to assess surgical interventions of the hip

---

**Academic supervisor (Chief investigator):** Dr Sophie Williams

**Investigation protocol prepared by:** Dr Sophie Williams

**Protocol version:** Version 1 10 September 2013

## 1. Executive summary

This protocol outlines a series of research studies using human hip joints obtained from deceased donors via a commercial tissue bank in the USA using ethically approved processes. The studies aim to develop research techniques to assess surgical interventions in the hip, this includes:

- Assessment of contact mechanics, experimentally and computationally
- Assessment of mechanical properties of the bone and soft tissues (such as the labrum and cartilage)
- Assessment of the biological characteristics of the bone and soft tissues (such as the labrum and cartilage)

Information gained will be used to develop computational models and experimental simulations of the natural hip joint in a healthy and diseased state. Diseases to be considered include avascular necrosis and those affecting joint geometry such as femoroacetabular impingement and dysplasia.

The main ethical issues to be considered include:

- Consent of tissue donors, the commercial tissue bank states that it has reviewed the processes by which consent for research from the donor or authorising party was obtained (to the best their knowledge), in accordance with all applicable state and federal laws (USA) and regulations (specifically the Human Anatomical Gift Act) prior to recovery and distribution.
- Disposal of donor tissue, this will done respectfully following local guidelines in accordance with the HTA
- Data protection, all donor samples will be coded prior to receipt at the University. All data will be stored and used in accordance with University guidelines; that also meet the requirements of the HTA.



## 2. Introduction

In England and Wales in 2011, over 80,000 total hip replacement surgeries were performed. These were predominantly for patients with osteoarthritis, a debilitating condition that causes degeneration of the joint, limiting mobility and causing pain. A small percentage of patients required hip replacements due to avascular necrosis (AVN). AVN is a condition where the blood supply to the bone of the femoral head is interrupted, cells die and the bone properties change. This often leads to the femoral head collapsing, necessitating total hip replacement.

Currently, interventions in the hip are limited, often to non-invasive methods such as physiotherapy and pain relief, and when these are no longer effective joint replacement. Some patients have benefitted from surgery that has modified the shape of their joint. In these instances they may have a condition such as dysplasia that reduces the amount of the head that is covered by acetabulum or femoroacetabular impingement where a bony prominence on the head impinges against the acetabulum or the acetabulum “over covers” the head, again causing impingement. In the case of AVN, there is scope for replacing just the diseased region of bone to provide structural support and prevent the collapse of the femoral head.

The development of these clinical techniques would be enhanced by improved scientific understanding of the hip joint. The development and success of total hip replacements has been supported by laboratory testing using in vitro simulators that mimic motions and loads of normal walking in the hip, subjecting the prosthesis to similar conditions to those in vivo. Adverse loading conditions can also be assessed. An in vitro simulation system of the natural hip (i.e. a mechanical simulator in which a natural hip joint is mounted and subjected to loads and motions similar to those experienced in vivo) would aid assessment of less invasive surgical approaches in the hip.

## 3. Aims

This study will support a programme of work to develop computational and experimental research techniques to better assess surgical interventions of the hip joint; including:

- Minimally invasive techniques for avascular necrosis of the femoral head (AVN)
- Surgery for non-normal hip pathologies, for example labral tears, femoroacetabular impingement (FAI), and hip dysplasia

The research techniques to be developed include:

- Computational models based on CT scans of human hip joint, to assess contact mechanics
- Assessment of the contact mechanics of the natural hip joint experimentally
- A single station hip joint simulator, where the entire hip joint is placed in a simulator that will mimic loads and motions experienced by the natural hip. This will be used to assess the wear and friction of the natural joint, and effect of surgical interventions
- A simulator model (as described in the previous point) that includes AVN of the femoral head

Studies developing these models have been primarily completed using porcine tissue, however, validation of the models developed against human tissue is required, and this is the focus of the project described. Specifically the human tissue will be used to meet the following objectives:

- Provide medical images for use in donor sample (hip joint specific) computational models to predict contact mechanics
- Compare the contact mechanics in porcine and human joints (and also comparison to predictions generated by computational models)
- Characterise the biological and mechanical properties of human hip joint tissue (bone, cartilage and labrum) and compare to porcine and diseased human tissue (e.g. femoral heads with AVN, subject of another study protocol and ethics approval)
- Assess the tribological behaviour (wear and friction) of natural human hip joints in a joint simulator, and compare to porcine hip joints
- Modify the whole joint simulation to include altered pathologies (for example, AVN, FAI, etc)

## 4. Investigation personnel and responsibilities

### 4.1. Training

All staff and students working with human tissue will be appropriately trained in the collection, storage and use of human tissue samples under the Leeds Teaching Hospitals Trust and University of Leeds Human Tissue Authority Research Licence (12352). All users of human tissue (including PI's and administrative staff directly involved) will complete an induction program (CDOC024, Faculty of Biological Sciences), which is an overview of the whole process required for an individual to use human tissue, including training, health and safety aspects (COSHH and risk assessment) and occupation health screening. All researchers will be registered to work with human tissue in the University (CDOC004, Faculty of Biological Sciences) and undertake training as set out in CDOC003 (Faculty of Biological Sciences). On going training will also be provided, documented and reviewed at least annually as part of the formal document audit which is carried out by the Persons Designate or their nominated representative.

### 4.2. Chief investigator

The chief investigator will be responsible for:

- Maintaining the study documentation
- Communications with Platinum Training regarding the acquisition of tissue
- Allocating the tissue when it has been received from Platinum Training
- Supervision of those working with data and tissue described in this protocol
- Ensuring University policies are met in relation to working with human tissue

### 4.3. Researchers

Only researchers (PhD students and post-doctoral research fellows / assistants) involved in the projects described in this protocol and associated projects will study the donor tissue supplied. All researchers will undergo training as described in 4.1. Researchers will be responsible for the adherence to human tissue protocols in relation to the work undertaken.

### 4.4. Platinum Training

Platinum training will provide tissue as requested on the (draft) Tissue Request Form (Appendix 1) on a commercial basis. Researchers at the University of Leeds will ensure the donor tissue's use is in

accordance with the Master agreement for Transfer of Bio Materials (Appendix 2). The chief investigator will be responsible for communicating with Platinum Training.

## 5. Study procedures

### 5.1. Obtaining donor samples

Samples will be ordered and purchased from Platinum Training, Phoenix, USA. Platinum Training aims to “provide non-transplantable, human cadaveric tissue for medical research, education and development, and other uses demonstrating scientific merit”. Platinum Training states that it has reviewed the processes by which consent or authorisation for research from the donor or authorising party was obtained (to the best their knowledge), in accordance with all applicable state and federal laws and regulations prior to recovery and distribution. A copy of the consent form used is attached (Appendix 3), and Platinum Training abides by the Uniform Anatomical Gift Act. For further details, of the agreement with Platinum Training, see “Agreement for the transfer of non-transplantable human cadaveric tissue” (Appendix 2).

Platinum Training will provide serological test reports (sample attached, Appendix 4) and patient information as shown on the “sample medical and social history questionnaire” (Appendix 5). Only donor tissue that meets the inclusion / exclusion criteria stated in this protocol will be sent.

The donor samples and all associated information will only be labelled with a unique donor identification number (given by Platinum Training), no one at the University of Leeds will receive the donors name.

Prior to receipt of tissues the Persons Designate or their nominated representative will be informed of the shipment and authorise this. The authority to import human samples form (CDOC014) and the associated core document pertaining to Acquisition and Transfer (CDOC013) outline the procedures to be followed to import human samples and the SOP described will be followed at all times.

#### 5.1.1. Inclusion criteria

- Donors who meet Platinum Training’s requirements regarding tissue donation and have signed a consent form (Appendix 3)
- Male or female donors aged 18-65 years
- Donors with no history of osteoarthritis in the hip, or suffered a broken hip, or had hip surgery (as described on the donor medical and social history questionnaire (Appendix 5).

#### 5.1.2. Exclusion criteria

- Donors that have osteoarthritis in the hip, or suffered a broken hip, or had hip surgery (as described on the donor medical and social history questionnaire (Appendix 5).
- Donors with serological results indicating a transmissible disease (Appendix 4)

### 5.2. Transport, storage, handling and disposal of donor samples

Platinum Training will arrange shipping of donor samples from the USA to the University of Leeds (Garstang South 6.61, Faculty of Biological Sciences) this will be in accordance with the code of practice issued by the Human Tissue Authority (Code of Practice 8 – Import and Export of Human

Bodies, Body Parts and Tissue) this is described locally by a core document (CDOC013). Samples will be sent fresh-frozen and shipped at -20°C. A record will be made of the state of the samples upon arrival to ensure they have not been temperature abused and that the samples are fit to be used.

Once received donor samples will be entered onto the University of Leeds / Leeds Teaching Hospital Trust Achiever system that tracks all donor samples until disposal. In the University donor tissue will be treated with universal precautions following locally agreed standard operating procedures (CDOC 018). At all times tissue will be treated with respect and in compliance with the Human Tissue Act, 2004.

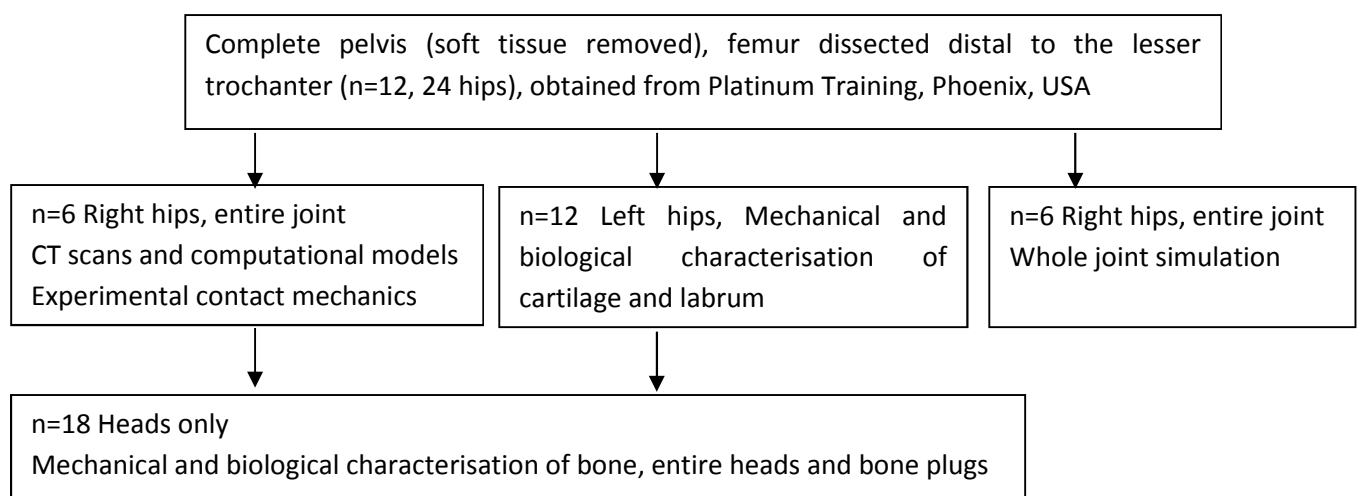
Samples will be stored in locked -40 °C freezers in Garstang South 6.61, Faculty of Biological Sciences where access is limited to only authorised personnel. The storage of human tissue will be carried out in accordance with the guidelines set out by the Human Tissue Authority. Samples will only be removed from storage (for a maximum of seven days) to carry out the experimental testing described in the experimental methodologies.

Experimental studies detailed are expected to be conducted from October 2013 to Spetember 2015. Tested donor samples will be disposed of at the end of the study. Untested samples will be stored in the Faculty of Biological Sciences under the Leeds Teaching Hospital Trust and University of Leeds Human Tissue Authority Research Licence (12352) for future associated studies, which will receive local ethical approval prior to any research being carried out.

If a request from Platinum Training was received regarding the withdrawal of a donor, those samples would be removed from the study and disposed of in the manner requested by Platinum Training. Any data collected on that donor would be removed from the study and destroyed.

### 5.3. Experimental plan for utilisation of donor samples

Twelve pelvis sections (24 hips) will be purchased from Platinum Training. Samples will be used in testing as described in Figure 1, it should be noted that there may be slight deviations from the proposed numbers of samples used in each study if technical issues arise or results dictate further testing is required in a particular area.



**Figure 1 Schematic showing the use of the twelve pelvis sections received.**

## 5.4. Experimental methodologies

### 5.4.1. Gross donor sample preparation

Gross dissection of the defrosted donor pelvis samples will take place in room 6.61 (Faculty of Biological Sciences). Soft tissue will be removed (but the hip capsule will be kept intact). The donor pelvis will be sectioned in two, to provide a right and left hemi-pelvis sample. At each stage of preparation, details will be logged on the Achiever system. Further sample preparation is described in the following sections, and will be distinct for the different experimental studies.

### 5.4.2. CT scan

Experimental work described in this section will be carried out in the Metrology laboratory (B44), School of Mechanical Engineering. The samples will be imaged at a high resolution (where bone micro-structure is visible) in a micro-Computed Tomography scanner (e.g.  $\mu$ CT 80 or XtremeCT, SCANCO Medical AG, Brüttisellen, Switzerland ).

### 5.4.3. MRI Scan

Three 3cm wide sections of acetabulum will be harvested across the cartilage and labrum interface from six acetabular joints. The samples will be scanned using a 9T magnetic resonance image scanner (Department of Physics, University of Leeds, Leeds), with a 3D FLASH scan for approximately 48 hours. Other scan sequences may be investigated. A 3T clinical scanner (Leeds Musculoskeletal Bioengineering Research Unit, Chapel Allerton Hospital, Leeds) may also be used.

### 5.4.4. Contact mechanics

Experimental work described in this section will be carried out in Frank Parkinson, Tissue Engineering laboratory (G32), School of Mechanical Engineering. The hemi-pelvis samples will be further dissected, in the following way: the hip capsule will be carefully dissected and the ligament teres cut, so the acetabulum and femur are separated. The femur will be cut with a bone saw at the lesser trochanter, and excess bone will be removed from the posterior of the acetabulum.

The methodology that will be adopted for assessment of the contact mechanics is detailed in the local SOP (07.14, Institute of Medical and Biological Engineering). In summary, the head and acetabulum will be mounted in appropriate fixtures and installed in an Instron testing machine. A dye (one component of the Microset compound) will be applied to one surface and the head and acetabulum will be subjected to a load. The contact areas will show a transfer of dye that can be imaged and analysed. This process will be repeated for a range of loads and positions of the head and acetabulum.

### 5.4.5. Mechanical characterisation

Experimental work described in this section will be carried out in the Frank Parkinson, Tissue Engineering laboratory (G32) and the metrology laboratory (B44), School of Mechanical Engineering. Cartilage, labral and bone tissue will be characterised using established methods for confined, unconfined and indentation testing to establish mechanical properties.

#### 5.4.5.1. Cartilage and labrum

Prior to mechanical characterisation geometric measurements will be taken of the acetabulum, femoral head and labral tissue (n=6) using digital callipers at various locations, and other appropriate mapping techniques.

Cartilage and labral pins (including bone) will be harvested from the femoral head and acetabulum. Stiffness, compression and permeability testing will be undertaken by placing the pins (n=6) in a chamber and applying a load to represent *in vivo* conditions. The displacement of the interface between the load application point and the tissue will be measured using an ultrasound transducer. A non-linear curve of fit of the experimental compressive consolidation curve (displacement vs. time) to the theoretical consolidation of a poroelastic solid under axial loading will be used to determine the stiffness and compressive modulus, and permeability of the tissues.

Rectangular cartilage and labral sections will be harvested from the femoral head and acetabulum and shaped into a dog bone outline. Tensile testing will be carried out on an Instron uniaxial testing frame where the samples (n=6) will be spring loaded until failure. The load and specimen extension will be recorded in order to determine the tensile strength of the tissues.

In order to determine the friction coefficient and damage threshold of cartilage and labral tissue, acetabular cartilage and labral pins (including bone) and femoral head cartilage sections will be harvested. The acetabular cartilage and labral tissue will be articulated against femoral head cartilage (n=6) using an in-house pin on plate machine with an applied load to represent *in vivo* conditions. A piezoelectric transducer will be used to measure force, which will then be converted into volts using a charge meter and data acquisition unit, this will then be inputted into a computer to determine the coefficient of friction as a function of time. A talysurf will also be used to analyse the wear scar of the tissues to determine the surface roughness and wear volume.

#### **5.4.5.2. Bone**

Bone plugs will be taken from the femoral heads. The plugs will then be potted into bone cement at the distal end of the plug. This will be done by flattening the proximal end of the samples, leaving bone for fixation. During all the processes, saline solution will be used to maintain hydration of the samples. Compression testing will be performed on the samples, where axial load will be applied under displacement control onto the samples until failure. Failure will be defined at the point where plastic deformation is initiated. A pressure sensitive film will be used to estimate the contact area during loading. The load-displacement data will be recorded. The data will be used to calculate the elastic modulus, compressive strength as well as yield strength. Other information such as work to failure and brittleness will also be calculated.

Intact head samples will also be assessed and compression testing will be performed. An axial load will be applied under displacement control onto the centre of the spherical femoral head until failure. Failure will be defined at the point where plastic deformation is initiated. A pressure sensitive film will be used to estimate the contact area during loading. The load-displacement data will be recorded at a rate of 10Hz. The data will be used to calculate the elastic modulus, compressive strength as well as yield strength. Work to failure and brittleness will also be calculated.

#### **5.4.6. Biological characterisation**

Experimental work described in this section will be carried out in laboratory 6.66 (Garstang South, Faculty of Biological Sciences). Tissue (cartilage, labrum and bone) samples will be prepared using established techniques and quantitative, histological and immunohistochemical characterisation carried out.

Cartilage pins (with bone attached) and labral sections will be harvested from acetabulum and femoral heads.

In order to determine the water, glycosaminoglycan and collagen content of labral and cartilage tissue, the tissues will be macerated and freeze dried, then digested using papain or acid hydrolysis and added to DMB dye or chloramine T and Ehrlich's reagent. Their absorbance's will be read on a spectrophotometer at varying wavelengths.

In order to qualitatively analyse cartilage labral and bone tissues using histology, cartilage pins will initially be decalcified. The cartilage labral and bone tissues (n=6) will then be fixed and undergo tissue processing in a series of ethanol, xylene and paraffin wax solutions. Tissues will be embedded using paraffin wax and sectioned using a microtome. Sections will then be transferred onto glass slides to be stained and mounted. Examples of the stains to be used include Haematoxylin and Eosin, Alcian blue, Sirius red, and Miller's elastin.

In order to qualitatively analyse cartilage and labral tissues using immunohistochemistry, tissues (n=6) will either be rapidly fresh frozen in liquid nitrogen and sectioned using a cryostat or formalin fixed paraffin embedded and sectioned on a microtome. Sections will then be transferred onto glass slides to be labelled. If formalin fixed paraffin embedded samples are used antigen retrieval may be required. A number of antibodies will be raised against various constituents for example; collagen I, II, III, VI, IX, X and XI, myeline, laminin, epithelial cells, smooth muscle, and elastin.

#### 5.4.7. Whole joint simulation

Head and acetabulum samples will be dissected to enable them to be mounted in the simulator. The following simulators may be used:

- Pendulum friction simulator, capable of axial loading, flexion-extension motion and measurement of friction at the reciprocating interface (ie between the head and acetabulum)
- Single station hip simulator, capable of axial loading and application of flexion-extension, abduction adduction, and internal-external rotation motions. The load and motion patterns can be controlled to provide a simulated gait cycle

The environment will be controlled (temperature, lubrication etc) as appropriate to mimic the conditions in vivo. The samples will be subjected to repeated cycles and cartilage degeneration will be assessed using established methods of grading and biological assays. Load, motion and alignment will be altered to assess the friction and degradation under different conditions assessed.

### 5.5.Data analysis and use of data

#### 5.5.1. CT images

The high resolution micro-Computed Tomography images of each sample will be used to: analyse tissue structure; take characteristic measurements; construct sample-specific computer models; and calculate mechanical behaviour through computer modelling techniques (such as finite element analysis).

#### 5.5.2. Experimental data

Experimental data will be analysed using established methods and subjected to statistical comparison as appropriate.

## 5.6. Reporting

Data will be reported in PhD theses by research students, and at the Institute's internal meetings. We will seek to publish the data as appropriate at national and international conferences, as well as in peer reviewed journals. Additionally, information will also be disseminated to researchers in associated fields within the Institute of Medical and Biological Engineering.

Platinum Training will be acknowledged as the tissue source in all publications (as described in Appendix 2).

## 6. Ethical considerations

### 6.1. Research Ethics committee approval

The protocol has received favourable review by the Faculty Research Ethics Committee for the Schools of Mathematics; Physical Sciences and Engineering at the University of Leeds (reference EP/G012172/1).

### 6.2. Consent of tissue donors

Platinum Training states that it has reviewed the processes by which consent or authorisation for research from the donor or authorising party was obtained (to the best their knowledge), in accordance with all applicable state and federal laws (USA) and regulations (specifically the Human Anatomical Gift Act<sup>1</sup>) prior to recovery and distribution.

### 6.3. Data protection

The identity of the patients will not be known to investigators at the University of Leeds, all donor samples will only be identified by Platinum Training's unique donor code, and this will be used throughout the study. Details of the donor sample (e.g. serological report, Medical and social history questionnaire) will be stored on the Achiever system. This system and associated safeguards have been approved by the Human Tissue Authority.

Most data will be processed using university computers, though personal computers may also be used (however, these will be encrypted in accordance with University of Leeds IT policies). All study data will be stored on university networked drives which are regularly backed up, additionally backups of this data will be stored at the site. Access to all study data will be restricted to those directly involved with the research.

The three-dimensional images, characterisation data and corresponding computer models will be stored on a secure, HTA compliant data server. This data and computer simulation capability will be used going forward to investigate the effectiveness of treatments for the hip in a virtual environment. In addition the images and derived models will be used to enrich teaching and public engagement activities.

Data from this study will be used to produce manuscripts for publication in research journals. The data will also be used for internal and external research seminars and for teaching or public engagement purposes where deemed appropriate, all of which is in line with current guideline

---

<sup>1</sup> <http://www.uniformlaws.org/Act.aspx?title=Anatomical%20Gift%20Act%20%282006%29>



issued by the Human Tissue Authority. Data associated with the project will be stored for at least 10 years (in accordance with RCUK guidelines) following completion.

#### **6.4. Disposal of donor tissue**

Tissue samples will be disposed of respectfully in line with the Human Tissue Authorities code of practise on disposal of human tissue (Code of Practice 5) this is described locally in a core document (CDOC 012) and SOP (SOP126). Histological slides and small tissue samples may be retained following the study, these will be stored in the Faculty of Biological Sciences under the Leeds Teaching Hospital Trust and University of Leeds Human Tissue Authority Research Licence (12352). Further research or teaching using these slides / samples would be the subject of a further ethics application.

### **7. Appendices**

**Appendix 1 Tissue request form**

**Appendix 2 Agreement for the transfer of non-transplantable human cadaveric tissue**

**Appendix 3 Sample consent form used by Platinum Training**

**Appendix 4 Example serological report form**

**Appendix 5 Sample Medical and Social History Questionnaire (information collected by Platinum Training)**



## Appendix C

**Matlab programme used for analysis of CT images**



Matlab Programme	Commands
<pre> clc; clear all; close all path = 'inputpath'; outputpath = 'outputpath'; p = which('filename.dcm'); filelist = dir([fileparts(p) filesep 'firstfile.dcm']); fileNames = {filelist.name}'; N = length(filelist) writerObj = VideoWriter('outputvideo.avi'); writerObj.FrameRate = 5; open(writerObj);  info = dicominfo('firstfile.dcm'); PixelSize = info.PixelSpacing; Pixel = PixelSize(1,1)  for m = 1:N I{m} = dicomread(fullfile(path,filelist(m).name)); colormap(gray)  se = strel('disk',6); clims = [0 50000] A{m} = imagesc(I{m}, clims)  colormap(gray) level{m} = graythresh(I{m}) Mask1{m} = im2bw(A{m},0.55);  Mask2{m} = im2bw(A{m},0.22)  closeImage{m} = imclose(Mask1{m},se); OpenSoft{m} = imopen(Mask2{m},se); subtract{m} = imsubtract(Mask2{m},Mask1{m}); imagesc  f{m} = [subplot(2,3,1), imshow(A{m} ), title('Original Image'), subplot(2,3,2), imshow(Mask1{m}), title('Bone Mask'), subplot(2,3,3), imshow(Mask2{m}), title('Soft Tissue Mask')... subplot(2,3,4), imshow(OpenSoft{m}), title('Soft Tissue Opened'), subplot(2,3,5), imshow(closeImage{m}), title('Bone Mask Closed'), subplot(2,3,6), imshow(subtract{m}), title({'Soft Tissue Mask subtracted'; 'from Closed Image'})]; saveas(gcf, [strcat(outputpath,'Slice',int2str(m)),'.jpg']); SliceVolume{m} = [(bwarea(subtract{m}))*((Pixel)^3)] frame = getframe(gcf) writeVideo(writerObj, frame); </pre>	<p>Import file and determine output file locations</p> <p>Read pixel size from DICOM file</p> <p>Start loop programme Read image and produce masks on image to produce output image.</p>

```
end
format long
TotalVolume = sum( cell2mat(SliceVolume), 2)
```

End loop programme  
Calculate total volume

## **Appendix D**

### **Ethics Protocol for use of femoral head tissue with AVN**







Mahsa Shahi Avadi  
Institute of Medical and Biological Engineering  
School of Mechanical Engineering  
University of Leeds  
Leeds, LS2 9JT

**MaPS and Engineering joint Faculty Research Ethics Committee (MEEC FREC)  
University of Leeds**

12 September 2016

Dear Mahsa

**Title of study**            **Assessment of femoral heads with avascular necrosis**  
**Ethics reference**        **MEEC 13-001**

I am pleased to inform you that the application listed above has been reviewed by the MaPS and Engineering joint Faculty Research Ethics Committee (MEEC FREC) and following receipt of your response to the Committee's initial comments, I can confirm a favourable ethical opinion as of the date of this letter. The following documentation was considered:

<i>Document</i>	<i>Version</i>	<i>Date</i>
MEEC 13-001 130909 MSA_signed_ Investigation protocol (2).pdf	1	09/09/13
MEEC 13-001 130909 MSA_signed_fieldwork-assessment-form-medium-risk.pdf	1	09/09/13
MEEC 13-001 130909_signed_ MSA Unviersity ethics.pdf	1	09/09/13

Committee members made the following comments about your application:

- Some committee members expressed a concern that something in the element of choice (free to withdraw without giving a reason, no penalty for not taking part, etc.) is lost in the translation to Mandarin. Members suggested having the translation of the consent form re-translated back into English by a third party to ensure that the translation is correct in essence as well as technically correct.
- Please refer to the ISS encryption policy for information about taking encrypted equipment/ data abroad.  
[http://iss.leeds.ac.uk/info/357/information\\_security/977/encryption](http://iss.leeds.ac.uk/info/357/information_security/977/encryption)

Please notify the committee if you intend to make any amendments to the original research as submitted at date of this approval, including changes to recruitment methodology. All changes must receive ethical approval prior to implementation. The amendment form is available at <http://ris.leeds.ac.uk/EthicsAmendment>.

Please note: You are expected to keep a record of all your approved documentation, as well as documents such as sample consent forms, and other documents relating to the study. This should be kept in your study file, which should be readily available for audit purposes. You will be given a two week notice period if your project is to be audited. There is a checklist listing examples of documents to be kept which is available at <http://ris.leeds.ac.uk/EthicsAudits>.

We welcome feedback on your experience of the ethical review process and suggestions for improvement. Please email any comments to [ResearchEthics@leeds.ac.uk](mailto:ResearchEthics@leeds.ac.uk).

Yours sincerely

Jennifer Blaikie  
Senior Research Ethics Administrator, Research & Innovation Service  
On behalf of Professor Gary Williamson, Chair, [MEEC FREC](#)

CC: Student's supervisor(s)

**UNIVERSITY OF LEEDS RESEARCH ETHICS COMMITTEE APPLICATION FORM <sup>1</sup>**



**UNIVERSITY OF LEEDS**

Please read each question carefully, taking note of instructions and completing all parts. If a question is not applicable please indicate so. The superscripted numbers (eg<sup>8</sup>) refer to sections of the guidance notes, available at [www.leeds.ac.uk/ethics](http://www.leeds.ac.uk/ethics). Where a question asks for information which you have previously provided in answer to another question, please just refer to your earlier answer rather than repeating information.

Research ethics training courses: <http://ris.leeds.ac.uk/EthicsTraining>

To help us process your application enter the following reference numbers, if known and if applicable:

Ethics reference number:	
Student number	<b>200662543 (Mahsa Shahi Avadi)</b>

**PART A: Summary**

**A.1 Which Faculty Research Ethics Committee would you like to consider this application?<sup>2</sup>**

- Arts and PVAC (PVAR)
- Biological Sciences (BIOSCI)
- ESSL/ Environment/ LUBS (AREA)
- MaPS and Engineering (MEEC)
- Medicine and Health (Please specify a subcommittee):
  - Leeds Dental Institute (DREC)
  - School of Healthcare (SHREC)
  - School of Medicine (SoMREC)
  - Institute of Psychological Sciences (IPSREC)

**A.2 Title of the research<sup>3</sup>**

Assessment of femoral heads with avascular necrosis

**A.3 Principal investigator's contact details<sup>4</sup>**

Name ( <i>Title, first name, surname</i> )	Dr Sophie Williams
Position	Associate Professor
Department/ School/ Institute	Institute of Medical and Biological Engineering, School of Mechanical Engineering.
Faculty	Engineering
Work address ( <i>including postcode</i> )	Room 435, School of Mechanical Engineering, University of Leeds Woodhouse Lane, Leeds, LS2 9JT
Telephone number	+44 (0)113 3432214
<b>University of Leeds</b> email address	s.d.williams@leeds.ac.uk

**A.4 Purpose of the research:**<sup>5</sup> (Tick as appropriate)

- Research
- Educational qualification: ***Please specify: PhD project***
- Educational Research & Evaluation<sup>6</sup>
- Medical Audit or Health Service Evaluation<sup>7</sup>
- Other

**A.5 Select from the list below to describe your research:** (You may select more than one)

- Research on or with human participants
- Research with has potential significant environmental impact.<sup>8</sup> If yes, please give details:  
\_\_\_\_\_
- Research working with data of human participants
  - New data collected by questionnaires/interviews
  - New data collected by qualitative methods
  - New data collected from observing individuals or populations
  - Research working with aggregated or population data
  - Research using already published data or data in the public domain
- Research working with human tissue samples<sup>9</sup>

**A.6 Will the research involve any of the following:**<sup>10</sup> (You may select more than one)

***If your research involves any of the following an application must be made to the National Research Ethics Service (NRES) via IRAS [www.myresearchproject.org.uk](http://www.myresearchproject.org.uk) as NHS ethical approval will be required. There is no need to complete any more of this form. Contact [governance-ethics@leeds.ac.uk](mailto:governance-ethics@leeds.ac.uk) for advice.***

- Patients and users of the NHS (including NHS patients treated in the private sector)<sup>11</sup>
- Individuals identified as potential participants because of their status as relatives or carers of patients and users of the NHS
- Research involving adults in Scotland, Wales or England who lack the capacity to consent for themselves<sup>12</sup>
- A prison or a young offender institution in England and Wales (and is health related)<sup>14</sup>
- Clinical trial of a medicinal product or medical device<sup>15</sup>
- Access to data, organs or other bodily material of past and present NHS patients<sup>9</sup>
- Use of human tissue (including non-NHS sources) where the collection is not covered by a Human Tissue Authority licence<sup>9</sup>
- Foetal material and IVF involving NHS patients
- The recently deceased under NHS care
- None of the above

**You must inform the Research Ethics Administrator of your NRES number and approval date once approval has been obtained.**

*If the University of Leeds is not the Lead Institution, or approval has been granted elsewhere (e.g. NHS) then you should contact the local Research Ethics Committee for guidance. The UoL Ethics Committee need to be assured that any relevant local ethical issues have been addressed.*

**A.7 Will the research involve NHS staff recruited as potential research participants (by virtue of their professional role) or NHS premises/ facilities?**

Yes     No

*If yes, ethical approval must be sought from the University of Leeds. Please note that NHS R&D approval is needed in addition: [www.myresearchproject.org.uk](http://www.myresearchproject.org.uk). Contact [governance-ethics@leeds.ac.uk](mailto:governance-ethics@leeds.ac.uk) for advice.*

**A.8 Will the participants be from any of the following groups? (Tick as appropriate)**

- Children under 16<sup>16</sup>
- Adults with learning disabilities<sup>12</sup>
- Adults with other forms of mental incapacity or mental illness
- Adults in emergency situations
- Prisoners or young offenders<sup>14</sup>
- Those who could be considered to have a particularly dependent relationship with the investigator, eg members of staff, students<sup>17</sup>
- Other vulnerable groups
- No participants from any of the above groups

**Please justify the inclusion of the above groups, explaining why the research cannot be conducted on non vulnerable groups.**

The clinical investigators may have a dependant relationship with the potential participants, i.e. patients. The clinical investigators will not attempt to influence the decision of the patients to be recruited in this study.

**It is the researcher's responsibility to check whether a DBS check is required and to obtain one if it is needed.** See also <http://www.homeoffice.gov.uk/agencies-public-bodies/dbs> and [http://store.leeds.ac.uk/browse/extra\\_info.asp?modid=1&prodid=2162&deptid=34&compid=1&prodvarid=0&catid=243](http://store.leeds.ac.uk/browse/extra_info.asp?modid=1&prodid=2162&deptid=34&compid=1&prodvarid=0&catid=243).

**A.9 Give a short summary of the research<sup>18</sup>**

*This section must be completed in language comprehensible to the lay person. Do not simply reproduce or refer to the protocol, although the protocol can also be submitted to provide any technical information that you think the ethics committee may require. This section should cover the main parts of the proposal.*

Avascular necrosis of the femoral head is one of the main reasons for a total hip replacement in Asia. It affects the femoral head (ball in the ball/socket joint of the hip) and it occurs following disruption of the blood flow into the femoral head after either trauma or high alcohol or steroid intake. The loss of blood in the bone results in the death of the bone, which eventually leads to the collapse of the femoral head under the loads in the hip.

The overall aim of this project is to create a validated laboratory simulation of the avascular necrosis of the femoral head, which may be used to test treatments aimed at avascular necrosis of the femoral head. In order to do this, femoral heads with avascular necrosis need to be characterised so their mechanical and biological properties are better understood. This proposal relates to the collection of femoral heads with AVN during hip replacement surgery at a hospital in China. The heads are normally discarded, and we are seeking to collect and characterise these.

**A.10 What are the main ethical issues with the research and how will these be addressed?**<sup>19</sup>  
*Indicate any issues on which you would welcome advice from the ethics committee.*

This research requires use of human tissue, specifically femoral head tissue with avascular necrosis, removed from patients during total hip replacement procedures. The removal of the femoral head is a routine practice in this type of surgery, therefore does not require further removal of tissue or extra surgery time. The tissue is normally discarded; however with the consent of the patients the femoral heads will be used for this study.

This research is “non-invasive” in that it will have no effect on the way that the patient is treated, and no extra examination or treatment directly associated with it. Hence the key ethical challenges are obtaining informed consent and maintenance of patient confidentiality

This research will be conducted according to the moral code set out by latest version of the Declaration of Helsinki.

**PART B: About the research team**

**B.1 To be completed by students only**<sup>20</sup>

Qualification working towards (eg Masters, PhD)	PhD
Supervisor's name (Title, first name, surname)	Dr Sophie Williams
Department/ School/ Institute	Institute of Medical and Biological Engineering, School of Mechanical Engineering
Faculty	Engineering
Work address (including postcode)	Room 435, School of Mechanical Engineering, University of Leeds Woodhouse Lane, Leeds, LS2 9JT
Supervisor's telephone number	+44 (0)113 3432214
Supervisor's email address	s.d.williams@leeds.ac.uk
Module name and number (if applicable)	

**B.2 Other members of the research team (eg co-investigators, co-supervisors)**<sup>21</sup>

Name ( <i>Title, first name, surname</i> )	Miss Mahsa Shahi Avadi
Position	PhD student (co-investigator)
Department/ School/ Institute	Institute of Medical and Biological Engineering, School of Mechanical Engineering
Faculty	University of Leeds
Work address ( <i>including postcode</i> )	School of Mechanical Engineering, University of Leeds Woodhouse Lane, Leeds, LS2 9JT
Telephone number	00447932430588
Email address	<a href="mailto:mnmsa@leeds.ac.uk">mnmsa@leeds.ac.uk</a>

Name ( <i>Title, first name, surname</i> )	Prof Zhongmin Jin
Position	Co-investigator

Department/ School/ Institute	Institute of Advanced Manufacturing Technology School of Mechanical Engineering,
Faculty	Xi'an Jiaotong University
Work address (including postcode)	No 99 Yanxiang Rd., Yanta District, Xi'an City, Shaanxi Province, 710054, P.R. of China
Telephone number	0086-029-83395013
Email address	<a href="mailto:z.jin@leeds.ac.uk">z.jin@leeds.ac.uk</a>

Name (Title, first name, surname)	Mr James Anderson
Position	PhD student and co-supervisor
Department/ School/ Institute	Institute of Medical and Biological Engineering, School of Mechanical Engineering
Faculty	Faculty of Engineering
Work address (including postcode)	School of Mechanical Engineering, University of Leeds Woodhouse Lane, Leeds, LS2 9JT
Telephone number	
Email address	<a href="mailto:mniaa@leeds.ac.uk">mniaa@leeds.ac.uk</a>

Name (Title, first name, surname)	Mr Junyan Li
Position	Postgraduate research student and research assistant (co- investigator)
Department/ School/ Institute	Institute of Medical and Biological Engineering, School of Mechanical Engineering
Faculty	Faculty of Engineering
Work address (including postcode)	School of Mechanical Engineering, University of Leeds Woodhouse Lane, Leeds, LS2 9JT
Telephone number	
Email address	<a href="mailto:mnlj@leeds.ac.uk">mnlj@leeds.ac.uk</a>

Name (Title, first name, surname)	Prof Yusheng Qiu
Position	Professor, Director of Department of Orthopaedics (Clinical Investigator)
Department/ School/ Institute	First Affiliated Hospital School of Medicine, Xi'an Jiaotong University
Faculty	
Work address (including postcode)	No. 277, Yanta West Road Xi'an, Shaanxi Province 710061, P.R.China
Telephone number	+86 29 85323934
Email address	



Name (Title, first name, surname)	Dr Meng Li
Position	Attending Surgeon, Department of Orthopaedics (Clinical investigator)
Department/ School/ Institute	First Affiliated Hospital School of Medicine, Xi'an Jiaotong University
Faculty	
Work address (including postcode)	No. 277, Yanta West Road Xi'an, Shaanxi Province 710061, P.R.China
Telephone number	+86 29 85323935
Email address	drleemon@163.com

### Part C: The research

#### C.1 What are the aims of the study?<sup>22</sup> (Must be in language comprehensible to a lay person.)

The aim of this project is to characterise the mechanical and biological properties of bone from femoral head (the ball in the ball-socket hip joint) with avascular necrosis. The results of the study will be used to create a model of the disease in laboratory, which can then be used for testing of treatments and interventions aimed at avascular necrosis of the femoral head.

#### C.2 Describe the design of the research. Qualitative methods as well as quantitative methods should be included. (Must be in language comprehensible to a lay person.)

*It is important that the study can provide information about the aims that it intends to address. If a study cannot answer the questions/ add to the knowledge base that it intends to, due to the way that it is designed, then wasting participants' time could be an ethical issue.*

The research objectives are divided into 6 stages, and a chart showing these steps is also shown in Appendix D.

The study described in part 4 of the above objectives relates to this application.

- 1) Study the characteristics of animal bone as a pilot study in order to generate the techniques required to study the desired characteristics of the bone. These tests will include CT scanning, mechanical compression testing, and possibly 3-point bending on various dimensions of the bone.
- 2) Establish possible methods of changing the material properties of bone that can be used in a later stage to create the model. These may include heating, freezing, degradation using chemicals, etc. The effects of these methods on the mechanical properties of the bone will be recorded.
- 3) Mechanical properties of healthy human bones obtained from a tissue bank (subject to a different study protocol and ethical approval) will be studied in order to validate them against the mechanical properties of the animal bones, and calculate any differences in the mechanical properties.
- 4) Mechanical properties of femoral heads with avascular necrosis will be studied using the techniques established and used prior to this test on the animal femoral heads. These properties will be measured in two parts. First, a series of complete femoral heads will be tested, where they will be scanned using computed tomography to obtain the morphology of the bone, and then

compressed under a load to calculate their mechanical properties such as strength of the bone as well as the amount of work taken to break the bone. The second group of femoral heads will be sectioned into smaller pieces. The areas of necrotic tissue will be identified by computed tomography scanning, and comparative compression tests will be performed on these areas and the areas identified as healthy to calculate a ratio in strength between dead and healthy tissue. The mechanical properties will be recorded and the results will be used to develop a model of the disease.

- 5) The techniques established in (2) will be used to change the material properties of animal femoral heads and obtain the mechanical properties studied in (4).
- 6) The model will be validated *in vitro*.

**C.3 What will participants be asked to do in the study?**<sup>23</sup> (e.g. number of visits, time, travel required, interviews)

This study will require no additional clinic visits by the patient. During a routine appointment, they will be asked to provide informed consent. Their surgery will progress normally, and when the femoral head is removed it will be collected for this research (rather than disposed of). Clinical staff will complete the case report form (CRF) using information in patient notes.

**C.4 Does the research involve an international collaborator or research conducted overseas?**<sup>24</sup>  
(Tick as appropriate)

Yes     No

**If yes, describe any ethical review procedures that you will need to comply with in that country:**

The clinical investigator resides in Xi'an City, China (see section B2). Following ethical approval from university of Leeds, ethical approval will be sought from the local hospital ethics committee in Xi'an, China.

**Describe the measures you have taken to comply with these:**

This process will be initiated by submission of a protocol to the hospital ethics committee, who will provide written approval prior to initiation of the project.

Include copies of any ethical approval letters/ certificates with your application.

**C.5 Proposed study dates and duration**

Research start date (DD/MM/YY): 01/Oct/2011    Research end date (DD/MM/YY):30/Aug/2016

Fieldwork start date (DD/MM/YY): Once ethical approval has been granted and appropriate number of samples has been collected.

Fieldwork end date (DD/MM/YY): Upon completion of experimental work.

**C.6. Where will the research be undertaken?** (i.e. in the street, on UoL premises, in schools)<sup>25</sup>

The data as well as tissues will be obtained from the affiliated hospitals of Xi'an Jiaotong University, China. The mechanical tests will be undertaken in Institute of Advance Manufacturing Technology, School of Mechanical Engineering, Xi'an Jiaotong University, Xi'an City, China.

The data will be analysed during the researcher's (Mahsa Avadi) stay in China, and also upon return to UK. Data as well as patient information will be stored on a campus server file room store with access limited to named members of the research team.

**RECRUITMENT & CONSENT PROCESSES**

*How participants are recruited is important to ensure that they are not induced or coerced into participation. The way participants are identified may have a bearing on whether the results can be generalised. Explain each point and give details for subgroups separately if appropriate.*

**C.7 How will potential participants in the study be:**

**(i) identified?**

Potential patients will be identified by the collaborating surgeon (clinical investigator) based on their routine CT and MR images. The surgeon will identify whether the patient requires a total hip replacement procedure due to avascular necrosis.

**(ii) approached?**

Once identified as potential candidates, they will be approached for recruitment at a hospital visit.

**(iii) recruited?**<sup>26</sup>

The study will be verbally explained by their clinician and they will be given a Patient Information Leaflet, an example of which is held in Appendix B, to keep. If they wish, they can sign a Patient Consent form at the time, or take one away with them for further consideration. If they complete the consent form they will be included in the study. An example of the patient consent form is located in appendix C.

**C.8 Will you be excluding any groups of people, and if so what is the rationale for that?**<sup>27</sup>

*Excluding certain groups of people, intentionally or unintentionally may be unethical in some circumstances. It may be wholly appropriate to exclude groups of people in other cases*

- Subjects who, in the opinion of the Clinical Investigator, have an existing condition that would compromise their participation
- Subjects who have previously undergone any type of surgery for avascular necrosis in the affected hip
- Subjects who have marked atrophy or deformity in the upper femur
- Subjects who are unable to give informed consent
- Subjects with transmissible diseases
- Subjects with active local or systemic infection

**C.9 How many participants will be recruited and how was the number decided upon?**<sup>28</sup>

*It is important to ensure that enough participants are recruited to be able to answer the aims of the research.*

Initially, a minimum of 30 patients will be recruited. Following testing these femoral heads, variance between data will be calculated, and a power calculation will be performed to check how many further patients are required. The number of patients recruited may also be limited by the availability of suitable patients within the affiliated hospitals.

If you have a formal power calculation please replicate it here.

Remember to include all advertising material (posters, emails etc) as part of your application

**C10 Will the research involve any element of deception?**<sup>29</sup>

If yes, please describe why this is necessary and whether participants will be informed at the end of the study.

N/A

**C.11 Will informed consent be obtained from the research participants?**<sup>30</sup>

Yes  No

**If yes, give details of how it will be done. Give details of any particular steps to provide information (in addition to a written information sheet) e.g. videos, interactive material. If you are not going to be obtaining informed consent you will need to justify this.**

Once identified as potential candidates, they will be approached for recruitment. The study will be verbally explained by the clinician in Mandarin (local language), and they will be given a Patient Information Leaflet (appendix B) and Patient Consent Form (Appendix C). If they complete the consent form they will be included in the study. The consent form will be kept in a sealed envelope (labelled with the patient code) with the data. It will not be opened unless required to prove that consent was given.

The patient information leaflet and patient consent form will both be translated into mandarin Chinese using a professional translation company following the approval of this ethics application.

**If participants are to be recruited from any of potentially vulnerable groups, give details of extra steps taken to assure their protection. Describe any arrangements to be made for obtaining consent from a legal representative.**

N/A

**Copies of any written consent form, written information and all other explanatory material should accompany this application. The information sheet should make explicit that participants can withdraw from the research at any time, if the research design permits.**

Sample information sheets and consent forms are available from the University ethical review webpage at <http://ris.leeds.ac.uk/InvolvingResearchParticipants>.

**C.12 Describe whether participants will be able to withdraw from the study, and up to what point (eg if data is to be anonymised). If withdrawal is not possible, explain why not.**

Yes. As described in the patient information leaflet, if the patient decides to withdraw from the study, they should inform their clinician in writing. The clinician will identify the appropriate patient number and transfer the request to the academic supervisor, who will remove the sample from the database.

**C.13 How long will the participant have to decide whether to take part in the research?**<sup>31</sup>

*It may be appropriate to recruit participants on the spot for low risk research; however consideration is usually necessary for riskier projects.*

The patients will have time between being recommended for surgery and the date before their surgery to decide if they want to take part in the research. It is believed that most patients will be able to decide immediately. As there is low risk to the patient, this is seen as appropriate.

**C.14 What arrangements have been made for participants who might not adequately understand verbal explanations or written information, or who have special communication needs?**<sup>32</sup> *(e.g. translation, use of interpreters etc. It is important that groups of people are not excluded due to language barriers or disabilities, where assistance can be given.)*

The patient information and consent forms will be translated into Mandarin Chinese by a professional translation company once the English text has been approved. The final translations will be submitted to the local ethics committee in China.

**C.15 Will individual or group interviews/ questionnaires discuss any topics or issues that might be sensitive, embarrassing or upsetting, or is it possible that criminal or other disclosures requiring action could take place during the study (e.g. during interviews or group discussions)?**<sup>33</sup> *The [information sheet](#) should explain under what circumstances action may be taken.*

Yes  No *If yes, give details of procedures in place to deal with these issues.*

**C.16 Will individual research participants receive any payments, fees, reimbursement of expenses or any other incentives or benefits for taking part in this research?**<sup>34</sup>

Yes  No

*If Yes, please describe the amount, number and size of incentives and on what basis this was decided.*

**RISKS OF THE STUDY**

**C.17 What are the potential benefits and/ or risks for research participants?**<sup>35</sup>

It is unlikely that the patients who participate in the study will benefit directly from the research due to the predicted time-line for the research project. Because the interaction with the participants is limited to use of tissue gathered during their routine clinical care (and normally discarded), the only risk to the participants associated with the study is disclosure of personal data.

**C.18 Does the research involve any risks to the researchers themselves, or people not directly involved in the research? Eg lone working<sup>36</sup>**

Yes  No

**If yes, please describe:** \_\_\_\_\_

**Is a risk assessment necessary for this research?**

Yes  No If yes, please include a copy of your risk assessment form with your application.

*NB: Risk assessments are a University requirement for all fieldwork taking place off campus. For guidance contact your Faculty Health and Safety Manager or visit <http://www.leeds.ac.uk/safety/fieldwork/index.htm>.*

#### **DATA ISSUES**

**C.19 Will the research involve any of the following activities at any stage (including identification of potential research participants)? (Tick as appropriate)**

- Examination of personal records by those who would not normally have access
  - Access to research data on individuals by people from outside the research team
  - Electronic transfer of data
  - Sharing data with other organisations
  - Exporting data outside the European Union
  - Use of personal addresses, postcodes, faxes, e-mails or telephone numbers
  - Publication of direct quotations from respondents
  - Publication of data that might allow identification of individuals to be identified
  - Use of audio/visual recording devices
  - FLASH memory or other portable storage devices
- Storage of personal data on or including any of the following:
- Manual files
  - Home or other personal computers
  - Private company computers
  - Laptop computers

**C.20. How will the research team ensure confidentiality and security of personal data? E.g. anonymisation procedures, secure storage and coding of data.<sup>37</sup> Refer to <http://ris.leeds.ac.uk/ResearchDataManagement> for advice**

All patient specific data will be anonymised prior to transfer from the hospital: Patients' names and addresses will be removed and the data codified using a number. The numbers will be sequential: e.g. 001 – 002, etc.

Demographic information with the patient numbers will be transferred using a case report form (Appendix A). The content of each case report form will be loaded into a database, using the patient number to maintain traceability.

Once at University of Leeds, the data will be transferred to the University of Leeds server room file store, and access to the data will be limited to named members of the research team based on need.

Part of the data processing will be carried out off-campus while tests are being performed in China. An encrypted external hard drive with Sophos security software will be used to transfer data off-site. The data will be processed directly from the encrypted hard-disk and will not be exposed any shared networks.

The original consent forms will be stored with the clinical investigator in Xi'an, China, and will not be opened unless necessary to prove consent. A copy of the consent form will be added to the patient's clinical notes at the hospital. Once consent has been obtained, the clinical investigator will report this in the case report form, with the patient number and the date of consent as well as the details of whom the consent is obtained by.

**C.21 For how long will data from the study be stored? Please explain why this length of time has been chosen.**<sup>38</sup>

*RCUK guidance states that data should normally be preserved and accessible for ten years, but for some projects it may be 20 years or longer.*

**Students:** *It would be reasonable to retain data for at least 2 years after publication or three years after the end of data collection, whichever is longer.*

10 years following collection of the data, which is approximately 7-8 years after the completion of the PhD.

\_\_\_\_\_ years, \_\_\_\_\_ months

#### CONFLICTS OF INTEREST

**C.22 Will any of the researchers or their institutions receive any other benefits or incentives for taking part in this research over and above normal salary or the costs of undertaking the research?**<sup>39</sup>

Yes  No

If yes, indicate how much and on what basis this has been decided

**C.23 Is there scope for any other conflict of interest?**<sup>40</sup> *For example will the research funder have control of publication of research findings?*

Yes  No ***If yes, please explain***

Mahsa Shahi Avadi is a PhD student with funding from EPSRC and CASE funding from DePuy Synthes. As part of the funding agreement, DePuy Synthes will be able to review publications prior to submission. This is covered by a contract, relating to the CASE funding with DePuy Synthes.

**C.24 Does the research involve external funding? (Tick as appropriate)**

Yes  No ***If yes, what is the source of this funding?***

Mahsa Shahi Avadi is funded by Centre of Excellence in Medical and Biological Engineering (EPSRC). CASE top-up Funding is provided DePuy Synthes.

**PART D: Declarations**

**Declaration by Chief Investigators**

1. The information in this form is accurate to the best of my knowledge and belief and I take full responsibility for it.
2. I undertake to abide by the University's ethical and health & safety guidelines, and the ethical principles underlying good practice guidelines appropriate to my discipline.
3. If the research is approved I undertake to adhere to the study protocol, the terms of this application and any conditions set out by the Research Ethics Committee.
4. I undertake to seek an ethical opinion from the REC before implementing substantial amendments to the protocol.
5. I undertake to submit progress reports if required.
6. I am aware of my responsibility to be up to date and comply with the requirements of the law and relevant guidelines relating to security and confidentiality of patient or other personal data, including the need to register when necessary with the appropriate Data Protection Officer.
7. I understand that research records/ data may be subject to inspection for audit purposes if required in future.
8. I understand that personal data about me as a researcher in this application will be held by the relevant RECs and that this will be managed according to the principles established in the Data Protection Act.
9. I understand that the Ethics Committee may choose to audit this project at any point after approval.

**Sharing information for training purposes:** Optional – please tick as appropriate:

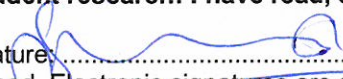
- I would be content for members of other Research Ethics Committees to have access to the information in the application in confidence for training purposes. All personal identifiers and references to researchers, funders and research units would be removed.

**Principal Investigator**

Signature of Principal Investigator:  (This needs to be an actual signature rather than just typed. Electronic signatures are acceptable)

Print name: DR SOPHIE WILLIAMS Date: (dd/mm/yyyy): 09/09/13.

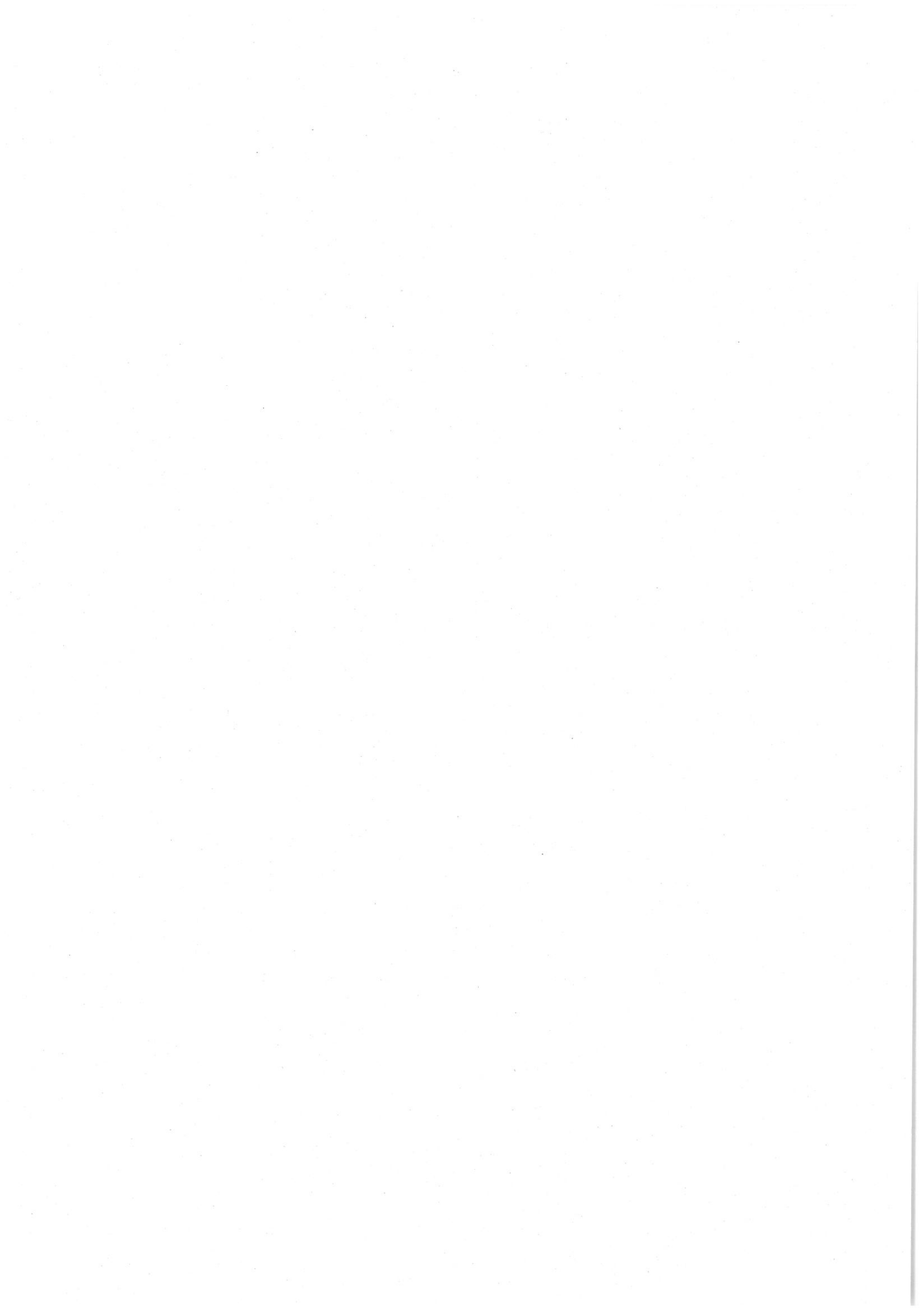
**Supervisor of student research: I have read, edited and agree with the form above.**

Supervisor's signature:  (This needs to be an actual signature rather than just typed. Electronic signatures are acceptable)

Print name: DR SOPHIE WILLIAMS Date: (dd/mm/yyyy): 09/09/13.

Please submit your form **by email** to [researchethics@leeds.ac.uk](mailto:researchethics@leeds.ac.uk) or if you are in the Faculty of Medicine and Health [FMHUniEthics@leeds.ac.uk](mailto:FMHUniEthics@leeds.ac.uk). **Remember to include any supporting material** such as your participant information sheet, consent form, interview questions and recruitment material with your application.





## Appendix A: Example of the case report form contents

### Assessment of femoral heads with AVN

Case report form revision and date: [DRAFT] 01 August 2013

A case report form must be provided with each subject included in the study.

Patient number	
Clinician's name	
Date of interview	
Does the patient meet the following inclusion and exclusion criteria?	Yes / No
Has consent been obtained from the patient? If yes, please state the name of the person who obtained the consent and the date of consent.	Yes / No

Subjects who fulfil the following inclusion and exclusion criteria will be considered eligible for inclusion into this investigation:

#### ***Inclusion criteria***

- Male or female subjects aged 18 years or above and skeletally mature at the point of screening for participation
- Subjects with avascular necrosis of the femoral head
- Subjects undergoing total hip replacement procedure as part of their treatment routine
- Subjects who are able to give voluntary, written informed consent to participate in this clinical investigation and from whom consent has been obtained

#### ***Exclusion criteria***

- Subjects who, in the opinion of the Clinical Investigator, have an existing condition that would compromise their participation and follow-up in this study.
- Subjects who have previously undergone any type of surgery for avascular necrosis in the affected hip
- Subjects who have marked atrophy or deformity in the upper femur
- Subjects who are unable to give informed consent
- Subjects with transmissible diseases
- Subjects with active local or systemic infection

When did the patient first present to an orthopaedic clinician (Month / Year)?	
When did first onset of pain occur?	
How old is the patient?	
What sex is the patient?	
What weight is the patient in kg?	
What height is the patient in cm?	

## **Appendix B: Example of Patient Information Leaflet contents**

### **Assessment of femoral heads with AVN – in vitiation to donate femoral head for research**

You are being invited to donate the bone that will be removed at surgery to research. Please read the following information carefully and discuss it with others if you wish. Take time to decide whether or not you wish to take part.

#### **What is the Purpose of the Study?**

You have a condition in your hip called avascular necrosis. This means that some of the bone in the ball part of your hip joint has died, and it has reached a stage where you need to undergo total hip replacement. The aim of this study is to investigate how this condition affects the hip, and to try to develop better treatment techniques. To do this, the bone tissue that is removed from your hip during your surgery will be used to analyse the condition in your hip and help us understand it better.

#### **Do I have to take part?**

Participation in this study is entirely voluntary; it is up to you to decide whether or not to take part. If you do decide to take part you will be given this information sheet to keep and be asked to sign a consent form; and you are still free to withdraw at any time and without giving a reason. This will not affect the care you receive.

#### **What will happen to me if I take part?**

There will be no change in your current treatment if you choose to allow us to use your tissue and data in our study. We only intend to use the bone that is removed from the hip in any regular total hip replacement procedure (which would normally be destroyed following surgery); so you will not have to attend hospital any more than normal, and will not be subject to treatments or pain that are not part of the standard of care at your hospital.

#### **What do I have to do?**

If you agree to let us use your tissue and data, it is important that you fill in the consent form. Apart from that, there will be no difference in the treatment that you receive. If at any time you no longer wish us to use your tissue and data, you must tell your surgeon.

#### **What are the possible disadvantages and risks of taking part?**

Normally, the tissue that is removed from the patient during total hip replacement is disposed of by the hospital. However if you decide to take part in this study, it will be provided to us by your surgeon and staff hospital for research.

If you consent to take part in this study, your data will be made anonymous (your name and address will be replaced by a number) and shared with a research group at the University of Leeds (UK). The data and information we get from you will still be treated as confidential information and will not be distributed in public.

#### **What are the possible benefits of taking part?**

There may be no direct benefit to you in taking part. However, the research that is being conducted may help people with the same condition as you in the future by helping develop better treatments for the disease.

#### **Will my taking part in this study be kept confidential?**

Yes. The data that is provided to the University of Leeds by your hospital will be anonymous, and will be treated as confidential information. It is likely that other people will see the data that is being used, but it will not be possible to identify you personally.

Information may be recorded on paper and/or on a computer database at the hospital. The University of Leeds will also have copies of the paper forms and the database. Prior to transfer to the University of Leeds, your data will be encoded (your name and address will be removed and you will only be identified by a study number and initials). The encoded data will be processed under the supervision and responsibility of the University of Leeds. The University of Leeds will take steps to ensure that the encoded data is protected and confidentiality maintained at all times. The reports published from such

data may be used for regulatory, scientific or commercial purposes and may be published, but it will not be possible to identify you.

**What will happen to the results of the research study?**

The information may be published at scientific meetings and in medical journals.

**Who is organising and funding the research?**

The research is being conducted by the Institute of Medical and Biological Engineering at The University of Leeds in the United Kingdom. The research is funded by Engineering and Physical Sciences Research Council (EPSRC) and DePuy Synthes.

**Who has reviewed the study?**

*[Note to reviewers: where I have written XXXXXX, I intend to provide the correct contact details once they have been provided.]*

The University of Leeds Ethics Committee, and the [XXXXXX] have given ethical approval for this study. If you should wish to make a complaint about the conduct of this study please contact

**Contact for Further Information**

If at any time you have any questions concerning the study then please contact:

**[XXXXXX Investigator's name and contact details]**

Academic investigator's details

**Thank you for considering taking part in this study.**

# Appendix C: Example of Patient Consent Form contents

## Assessment of femoral heads with AVN

Patient Study Number: \_\_\_\_\_

### Patient consent

Please initial box

I confirm that I have read and understand the patient information sheet (version ..... ) for the above research study. I have had the opportunity to ask questions and have had these answered satisfactorily.

I understand that my participation is voluntary and that I am free to withdraw at any time without giving any reason, without my medical care or legal rights being affected.

I understand that researchers at the University of Leeds and other academic institutions will have access to and test the tissue that is removed from my hip during my total hip replacement surgery.

I understand that researchers at the University of Leeds will have access to personal information that is relevant to the research. I give permission for these individuals to obtain, store and process such information.

I agree to take part in the above study.

\_\_\_\_\_  
Name of Patient

\_\_\_\_\_  
Date

\_\_\_\_\_  
Signature

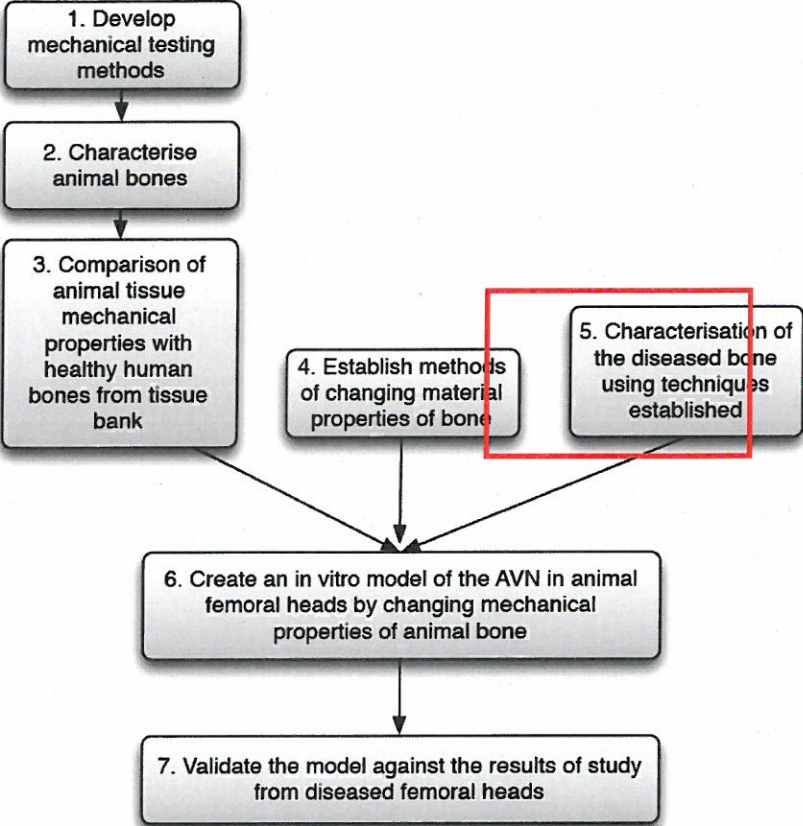
\_\_\_\_\_  
Name of Clinical Investigator

\_\_\_\_\_  
Date

\_\_\_\_\_  
Signature

# Appendix D: Diagram showing project objectives

Please note, the objectives of the study detailed in this protocol is highlighted with a red box



### To help speed up the review of your application:

- Answer the questions in plain English, avoid using overly technical terms and acronyms not in common use.
- Answer all the questions on the form, including those with several parts (refer to the [guidance](#) if you're not sure how to answer a question or how much detail is required).
- Include any relevant supplementary materials such as
  - Recruitment material (posters, emails etc)
  - [Sample participant information sheet](#)
  - [Sample consent form](#). Include different versions for different groups of participants eg for children and adults, clearly indicating which is which.
  - Signed [risk assessment](#) (required for all activities taking place off-campus).
- If you are not going to be using participant information sheets or consent forms explain why not and how informed consent will be otherwise obtained.
- If you are a student it is essential that you discuss your application with your supervisor.
- Submit a [signed copy](#) of the application, preferably electronically. Students' applications need to be signed by their supervisors as well.





---

# Investigation protocol

---

Protocol to assess human femoral heads with avascular necrosis in collaboration with Xi'an Jiaotong University, P R China

**Academic investigator:** Mahsa Shahi Avadi

**Academic supervisor:** Dr. Sophie Williams

**Investigation protocol prepared by:** Mahsa Shahi Avadi

**Protocol version:** 1 (01 August 2013)

**Approval signature**

This protocol consists of 27 pages plus appendices and is agreed by:

Dr. Sophie Williams

Academic supervisor

---

Mahsa Shahi Avadi

Academic investigator

---

I, the undersigned, have read and understood the Investigation Protocol specified above, and agree on the contents. The Investigation Protocol will serve as a basis for co-operation in the study.

Academic collaborator Name            1. Prof Z Jin  
Collaborator Address                    Room: A429  
    Institute of Advanced Manufacturing Technology  
    School of Mechanical Engineering,  
    Xi'an Jiaotong University  
    No 99 Yan Xiang Road, Yanta District  
    Xi'an City, Shaanxi Province, 710054  
    P.R. of China  
Investigator telephone number        0086-029-83395013  
Investigator e-mail address            Zhongmin@mail.xjtu.edu.cn

Investigator signature                    .....

Date of signature                            .....

Academic collaborator Name            2. Dr Manyi Wang  
Collaborator Address                    Office B-421  
    Institute of Advanced Manufacturing Technology  
    School of Mechanical Engineering  
    Xi'an Jiaotong University  
    No 99 Yan Xiang Road  
    Xi'an City, Shaanxi Province, 710054  
    P.R. China  
Investigator telephone number        0086-029-83395382  
Investigator e-mail address            manyiwang@mail.xjtu.edu.cn  
Investigator signature                    .....

Date of signature                            .....

Clinical Investigator Name           1. Yusheng Qiu  
Professor, Director of Department of Orthopaedics  
First Affiliated Hospital  
School of Medicine, Xi'an Jiaotong University  
No. 277, Yanta West Road  
Xi'an, Shaanxi Province 710061,  
P.R.China  
t: +86 29 85323934 (Office).

Investigator signature           .....

Date of signature                 .....

2. Meng Li  
Attending Surgeon, Department of Orthopaedics  
First Affiliated Hospital  
School of Medicine, Xi'an Jiaotong University  
No. 277, Yanta West Road  
Xi'an, Shaanxi Province 710061,  
P.R.China  
t: +86 29 85323935 (Office).

Investigator e-mail address       drleemon@163.com

Investigator signature           .....

Date of signature                 .....

3. Prof. Shuangli Zhou  
  
Clinical investigator  
  
Associate Professor, Vice Director of Department of  
Orthopaedics  
  
First Affiliated Hospital  
  
School of Medicine, Xi'an Jiaotong University

No.277 Yanta West Road

Xi'an City, Shaanxi Province 710061

P.R.China

Investigator telephone number

0086-029-85323938

Investigator signature

.....

Date of signature

.....

## Contents

---

1	Executive Summary.....	8
2	Introduction .....	9
3	Roles and Responsibilities.....	10
3.1	Clinical Investigator (or person appointed by the clinical investigator) .....	10
3.2	Academic supervisor and academic collaborator roles .....	10
3.3	Academic investigators .....	10
4	Overall study objectives.....	11
5	Selection of Subjects .....	13
5.1	Inclusion criteria.....	13
5.2	Exclusion criteria .....	13
6	Investigation procedures .....	13
6.1	Patient recruitment.....	14
6.1.1	Informed Consent .....	14
6.1.2	Subject eligibility .....	15
6.1.3	Clinical and imaging assessments .....	15
7	Tissue Storage, Disposal and Transport.....	16
7.1	Transport.....	16
7.2	Storage .....	16
7.3	Disposal.....	16
8	Study Design.....	16
8.1.1	Sample size.....	16
8.1.2	$\mu$ CT scan protocol .....	17
8.1.3	Mechanical testing protocol .....	17
8.1.4	Histology on bone samples .....	18
9	Results.....	18
9.1	$\mu$ CT images.....	18

9.2	Demographics.....	19
9.3	Mechanical testing .....	19
9.4	Histology.....	19
10	Risk/benefit analysis.....	19
11	Ethical Considerations .....	19
11.1	Research Ethics committee approval.....	20
11.2	Informed consent .....	20
11.3	Data protection .....	20
11.3.1	Anonymisation.....	20
11.3.2	Data storage, handling and transfer.....	21
11.3.3	Consent forms .....	21
11.3.4	End of study.....	21
11.4	Declaration of Helsinki .....	21
11.5	Case report form completion .....	21
12	References.....	23
13	Appendix A: Example of the case report form contents .....	25
13.1	Inclusion criteria .....	25
13.2	Exclusion criteria .....	25
14	Appendix B: Example of Patient Information Leaflet contents	<b>Error! Bookmark not defined.</b>
15	Appendix C: Example of Patient Consent Form contents ..	<b>Error! Bookmark not defined.</b>

## 1 Executive Summary

TITLE	Properties of femoral heads with avascular necrosis
FUNDING	UK based PhD studentship (sponsored by an EPSRC CASE award with top-up funding by DePuy Synthes)
OBJECTIVES	The aim of this project is to establish the mechanical and biological characteristics of human femoral heads (removed and normally discarded at hip replacement surgery) with avascular necrosis and use the information gathered to identify analogous materials that can be used in a mechanical model of avascular necrosis.
INDICATION	Skeletally mature subjects with avascular necrosis of the femoral head who are due to undergo total hip replacement procedure to treat the affected hip
INVESTIGATION DESIGN	Patients with avascular necrosis of the femoral head undergoing hip replacement surgery will be consented, their affected femoral head will be removed in surgery (normally this would be discarded) and replaced with a hip replacement. The mechanical and biological characteristics of the removed femoral head. The properties studied will then be replicated in a laboratory simulation model of the disease.
NUMBER OF SUBJECTS	A minimum of 30 avascular necrotic femoral heads are required, with no upper limit
TARGET POPULATION	<p><b>Inclusion criteria</b></p> <ul style="list-style-type: none"> <li>• Male or female subjects aged 18 years or above and skeletally mature at the point of screening for participation</li> <li>• Subjects with avascular necrosis of the femoral head</li> <li>• Subjects undergoing total hip replacement procedure as part of their treatment routine</li> <li>• Subjects who are able to give voluntary, written informed consent to participate in this clinical investigation and from whom consent has been obtained</li> </ul> <p><b>Exclusion criteria</b></p> <ul style="list-style-type: none"> <li>• Subjects who, in the opinion of the Clinical Investigator, have an existing condition that would compromise their participation</li> <li>• Subjects who have previously undergone any type of surgery for avascular necrosis in the affected hip</li> <li>• Subjects who have marked atrophy or deformity in the upper femur</li> <li>• Subjects who are unable to give informed consent</li> <li>• Subjects with transmissible diseases</li> <li>• Subjects with active local or systemic infection</li> </ul>
SAFETY	This investigation does not impact upon the patients' normal care and uses tissue that would normally be discarded.



## 2 Introduction

Avascular necrosis (AVN) is the term given to an orthopaedic disease whereby osteocytes (bone cells) die as a result of interruption of blood supply to the bone [1]. It may be referred to with other terms, such as osteonecrosis, ischaemic necrosis and osseous ischemia [2]. It commonly occurs in the femoral head, but can occur in other skeletal sites such as the knee, shoulder, and ankle [3]. In the femoral head, it commonly results in the collapse of the femoral head following a series of pathological events. Following this point, the articular surface becomes arthritic and the patients commonly undergo total hip replacement surgery [4].

The majority of the sufferers of AVN are younger people, with average age in the Chinese population who underwent total hip replacement due to avascular necrosis reported as 50 years old [5]. AVN is also the most common diagnosis for patients undergoing total hip replacement in Asia [6,7,8]. In Europe and US, it is less prevalent [1,9,10,11].

Two factors affect the rate of the collapse of the femoral head: size and position of the lesion as well as the material properties of the dead and remodelling bone. If these factors are studied, a laboratory mechanical model of the disease may be developed. The developed model will be advantageous both in clinical and industrial aspects. The clinical advantages are that it will help choose the most effective treatment for patients suffering with AVN, following diagnosis. From an industrial point of view, it will allow optimisation and development of suitable orthopaedic implants aimed at treating AVN efficiently.

The aim of this project is to identify the mechanical and biological properties of the diseased femoral heads collected from patients suffering from avascular necrosis. By identifying these mechanical properties, development of an in vitro animal model with matching properties to the diseased femur will be possible. This model can then go on to be validated in vitro against the data from the diseased femoral heads, and then used to test new treatments and interventions in vitro.

This protocol defines the process of subject selection, collection of femoral heads, and characterisation. It also defines the means of ensuring patient confidentiality and obtaining informed consent.

## 3 Roles and Responsibilities

### 3.1 Clinical Investigator (or person appointed by the clinical investigator)

- The Clinical Investigators role is to co-ordinate the clinical aspects of this study: patient recruitment and assessment
- They are responsible for recruiting patients that satisfy the requirements of the inclusion and exclusion criteria.
- They are responsible for informing the patient about the study and obtaining consent in accordance with the Investigational Procedures defined in this protocol
- They are responsible for co-ordinating collection of the required information (case report form, CRF) and its anonymisation
- They are responsible for ensuring that the patient consent form is sent in a sealed envelope and is transferred to the Academic Investigator with the required data.

### 3.2 Academic supervisor and academic collaborator roles

- The academic investigators role is to maintain the study documentation and perform data analysis.
- They are responsible for maintaining an investigation file that contains a record of all approved documentation, consent forms and other documents relating to the study.
- They are responsible for ensuring that the data protection requirements of this protocol are met.
- They are responsible for supervising the data analysis described in this protocol.

### 3.3 Academic investigators

They will follow the protocol described in terms of the experimental studies

## 4 Overall study objectives

The aim of this project is to characterise diseased femoral heads collected from patients suffering from avascular necrosis. By identifying these mechanical and biological properties, development of an *in vitro* animal model with matching properties to the diseased femoral heads will be possible. This model can then go on to be validated *in vitro* against the data from the diseased femoral heads, and then used to test new treatments and interventions *in vitro*.

The objectives of the overall study are as follows, and the aim of this protocol is described in part 5:

- 1) Develop techniques to characterise the mechanical properties of bone. These techniques will include CT scanning and mechanical compression testing on various dimensions of bone samples from femoral head.
- 2) Compare mechanical properties of bone from porcine, ovine and bovine femoral head tissue and choose the most suitable species for further testing and the final model of the disease.
- 3) Compare mechanical properties of animal tissue with mechanical properties of healthy human bones received from a tissue bank.
- 4) Establish possible methods of changing the material properties of bone that can be used in a later stage to create the model. These may include heating, freezing, degradation using chemicals, etc. The effects of these methods on the mechanical properties of the bone will be recorded.
- 5) Mechanical properties of femoral heads with avascular necrosis will be studied using the techniques established and used on the animal femoral heads. The mechanical properties will be recorded and the results will be used to develop a model of the disease. The heads will also be assessed using standard histology techniques.
- 6) The findings from characterisation of diseased bones and animal tissue will be combined with the methods established to change the material properties of bone to create an *in vitro* model of avascular necrosis in animal femoral heads.
- 7) The model will be validated *in vitro* against the results of study from diseased femoral heads.

A diagram showing the project objectives can be viewed in Fig. 4-1.

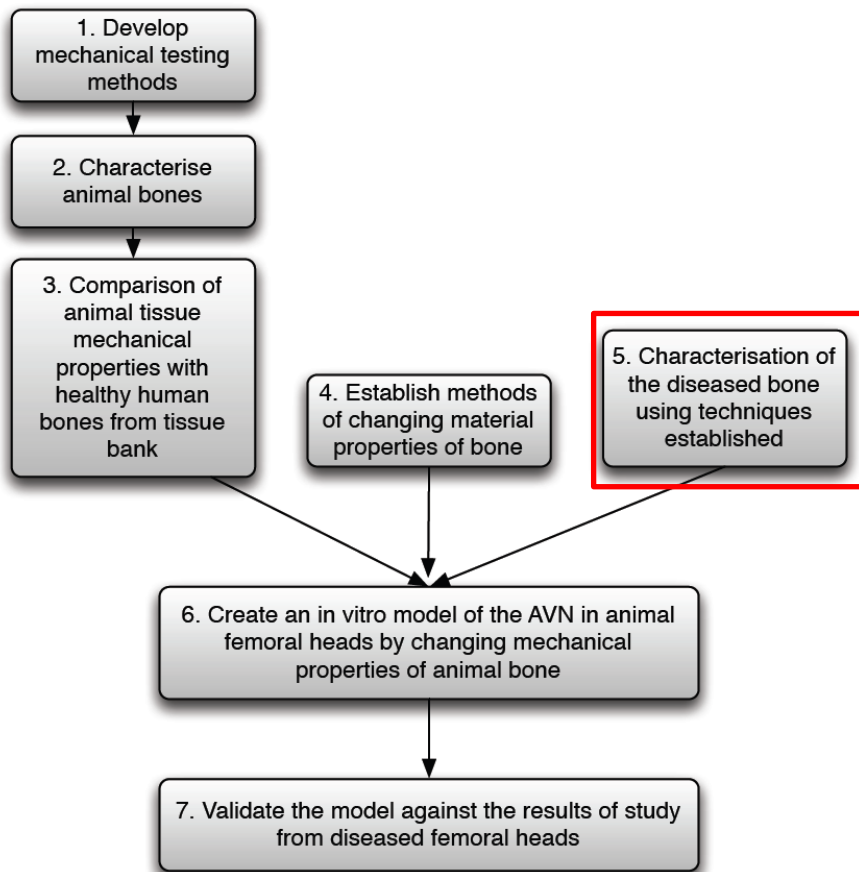


Fig. 4-1 - Diagram showing project objectives, the objectives of the study detailed in this protocol is highlighted with a red box

## 5 Selection of Subjects

The subjects for this study will be patients from Xian Jiaotong University First Affiliated Hospital. Subjects who fulfil the following inclusion and exclusion criteria will be considered eligible for inclusion into this investigation:

### 5.1 Inclusion criteria

- Male or female subjects aged 18 years or above and skeletally mature at the point of screening for participation
- Subjects with avascular necrosis of the femoral head
- Subjects undergoing total hip replacement procedure as part of their treatment routine
- Subjects who are able to give voluntary, written informed consent to participate in this clinical investigation and from whom consent has been obtained

### 5.2 Exclusion criteria

- Subjects who, in the opinion of the Clinical Investigator, have an existing condition that would compromise their participation and follow-up in this study.
- Subjects who have previously undergone any type of surgery for avascular necrosis in the affected hip
- Subjects who have marked atrophy or deformity in the upper femur
- Subjects who are unable to give informed consent
- Subjects with transmissible diseases
- Subjects with active local or systemic infection

## 6 Investigation procedures

The flow diagram in Fig. 6-1 shows the investigation procedure, and further details are described in the following sections.

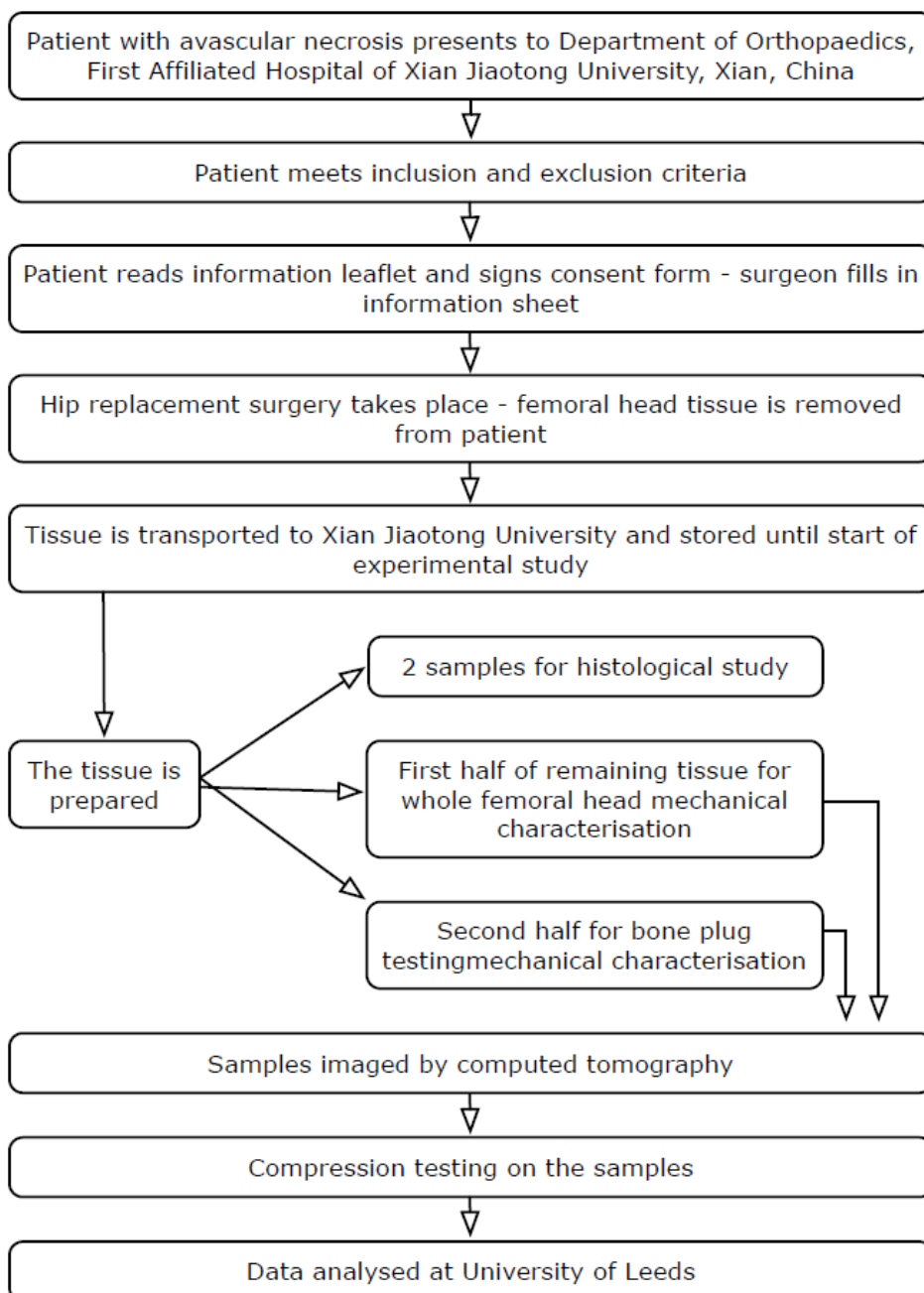


Fig. 6-1 – Flow diagram showing the investigational procedure for this study

## 6.1 Patient recruitment

This study does not affect the standard of care provided for the patient. It uses femoral head tissue which is routinely removed and discarded during total hip replacement surgery, at this time the patient's natural hip is replaced with a total hip replacement.

### 6.1.1 INFORMED CONSENT

Subjects who are deemed to meet the inclusion and exclusion criteria for this investigation by the Clinical Investigator will be given a verbal explanation of the nature of their condition, the purpose of this investigation, and the requirements of their involvement. They will be provided with a patient information sheet (Appendix B, when this study is approved this will be

translated into Mandarin, by a commercial translating company) and given sufficient time prior to their surgery to decide whether they wish to participate in this investigation.

Any queries that the subjects may have regarding this clinical investigation will be addressed by the Clinical Investigator or another member of the investigative team.

Subjects will be informed that they are free to obtain further information at any time, that they are free to withdraw their consent and to discontinue their participation in the investigation at any time without affecting their quality of care.

Subjects will be made aware that their personal data (as shown on the case report form, appendix A) will be collected and processed by the investigative team in accordance with the Declaration of Helsinki; that the results of this investigation may be published, but that their confidentiality will be maintained at all times and that it will not be possible to identify them from any data presented.

If the subject is willing to participate in this investigation, written informed consent will be obtained using the patient consent form (Appendix C when this study is approved this will be translated into Mandarin, by a commercial translating company)). The patient consent form must be signed before any data or tissue is transferred from the hospital site to research investigators. The consent form will be sealed in an envelope and transferred with the case report form and tissue. The envelope will remain sealed unless verification of patient consent is required.

### 6.1.2 SUBJECT ELIGIBILITY

Once written informed consent has been obtained the subject is considered to have been enrolled in the study. Each enrolled subject will be added to the study database and allocated the next available subject number as defined in section 11.3.1.

The Case Report Form (CRF, Appendix A) will be completed as a record of adherence to the inclusion and exclusion criteria noted in section 5.

### 6.1.3 CLINICAL AND IMAGING ASSESSMENTS

Each subject considered to be eligible for entry into this investigation will have the following information recorded in the CRF after providing written informed consent:

- Demographic details: Age, Sex, Weight, Height,
- Approximate date of first onset of pain
- Approximate date of first presentation to an orthopaedic clinician

The content of each CRF will be loaded into a central database, using the allocated subject number to maintain traceability. The original copies will be archived by the academic supervisor on University of Leeds property.

## 7 Tissue Storage, Disposal and Transport

### 7.1 Transport

The tissue will be transported from the First Affiliated hospital to Xi'an Jiatong university using locally approved procedures, in a sealed cool box clearly labelled with the contents of the box. The tissue will be transferred by a person assigned by the clinical investigator. The same transport method will be used to transfer the used tissue back to the hospital for disposal.

### 7.2 Storage

The samples will be stored in Xi'an Jiaotong University in an assigned freezer for human tissue at approximately -20°C when tests are not being performed on them. In between tests, the samples will be stored in an assigned refrigerator at approximately 4°C.

### 7.3 Disposal

Following the end of the experimental procedures, the tissues will be disposed of respectfully in the incinerator of the hospital from which tissues were originally obtained. Any requests of the patient regarding disposal will be respected and carried out if possible, following locally approved procedures.

## 8 Study Design

This study will include different experimental procedures. MicroCT scans of the femoral heads following removal will be taken, mechanical testing will be performed on the femoral heads to obtain mechanical properties of the entire head and smaller bone plugs and histology will be carried out in order to biologically characterise the tissue.

### 8.1.1 SAMPLE SIZE

No formal sample size formulae have been used to calculate the number of samples required for the study. The number will depend on the possible number of patients that can be recruited within the short timeframe of the PhD. Since the data gathered from the femoral heads are to be used in creating the in vitro simulation later in the project (point 6 in section 4), samples will need to be collected and tested before December 2014.

A minimum of 20 femurs will be specified for the entire study. No upper limit will be specified for this study.



Out of the samples obtained, two will be used for histological analysis, and the remaining femoral heads will be divided into two groups, in one group the whole femoral head will be mechanically assessed and in the second group, bone plugs will be taken and mechanically assessed.

### 8.1.2 $\mu$ CT SCAN PROTOCOL

A part of the experimental protocol includes scanning the samples using a micro computed tomography ( $\mu$ CT) scanner. This is a procedure where the equipment scans thin slices of the sample using an X-ray and combines them to generate a three-dimensional structure of the sample. It provides very detailed information about the morphology of the sample.

All samples will be scanned using a  $\mu$ CT scanner (Y. Cheetah, manufactured by YXLON, Germany) based in Institute of Advanced Manufacturing Technology, School of Mechanical Engineering, Xian Jiaotong University in the presence of a calibration phantom to allow estimates of density prior to mechanical and biological testing. The images will be taken at a resolution (voxel size) of 82 $\mu$ m.

### 8.1.3 MECHANICAL TESTING PROTOCOL

In order to calculate the mechanical properties of the avascular necrotic bone, mechanical testing will be performed on the bone specimens. These tests will be performed using a mechanical testing machine (model PLD-5kN, manufactured by Xi'an Li Chuang Materials Testing Ltd) based in Institute of Advanced Manufacturing Technology, School of Mechanical Engineering, Xian Jiaotong University on bone plugs as well as whole bone samples.

#### 8.1.3.1 Compression testing on entire femoral heads

One group of the femoral heads collected for mechanical testing will be prepared for whole sample tests by dissecting the soft tissue from the samples to end with a clean bone sample for CT scanning. The base of the sample will be potted in cement and prepared for CT scan and compression testing. During this process, the articular surface will be maintained, and kept hydrated using a tissue paper soaked in saline solution.

Compression testing will be performed on the samples, where axial load will be applied under displacement control onto the centre of the spherical femoral head until failure. Failure will be defined at the point where plastic deformation is initiated. A pressure sensitive film will be used to estimate the contact area during loading. The load-displacement data will be recorded at a rate of 10Hz. The data will be used to calculate the elastic modulus, compressive strength as well as yield strength. Work to failure and brittleness will also be calculated.

### 8.1.3.2 Compression testing on bone plugs

The remainder of the femoral heads will be prepared for tests on bone plugs of the femoral head. From each femoral head, osteochondral plugs of 9mm diameter and approximately  $20 \pm 5$ mm diameter length will be removed using a stainless steel corer. The plugs will then be potted into cement at the distal end of the plug. This will be done by flattening the proximal end of the samples, leaving approximately 5-8mm of bone for fixation. During all the processes, saline solution will be used to maintain hydration of the samples [3].

Compression testing will be performed on the samples, where axial load will be applied under displacement control onto the samples until failure [2]. Failure will be defined at the point where plastic deformation is initiated. A pressure sensitive film will be used to estimate the contact area during loading. The load-displacement data will be recorded. The data will be used to calculate the elastic modulus, compressive strength as well as yield strength. Other information such as work to failure and brittleness will be calculated.

### 8.1.4 HISTOLOGY ON BONE SAMPLES

The histology tests will be carried out in Department of Biology, Xi'an Jiaotong university, Xian, China. The test will be carried out by an experienced technician appointed by the collaborative supervisor, and the photographs of the results will be analysed by Mahsa Shahi Avadi.

The bone samples will be fixed in 10% neutral buffered formalin for 12-24 hours. The bone will then be sectioned using a band saw into thinner (3-5mm) sections. The sections will be made in the coronal plane and then fixed in formalin for a further 24-48 hours. The bone sections will then be decalcified using ethylene-diaminetetracetic acid (EDTA). The sections will then be sliced before staining with haematoxylin and eosin (H&E). Following staining, the slices will be examined using a microscope at various magnifications to obtain a good degree of comparison between the two extents of disease in the bone.

## 9 Results

### 9.1 $\mu$ CT images

The results from the CT Scans will be used to create a map of bone mineral density and porosity of the diseased femoral head with respect to the location on the bone in the femoral heads. The findings will be compared with the scans of healthy femoral heads from another study. This will then be used to understand the changes in the properties of femoral head bone following avascular necrosis and to replicate a similar situation in the simulation model of the disease.

## 9.2 Demographics

Subject demographic details will be summarised and used in conjunction with the CT images and the mechanical testing data to report the extent of the disease in each case.

## 9.3 Mechanical testing

The results from the mechanical testing will be obtained as load versus displacement data. The results will then be used to calculate the elastic modulus, compressive strength, yield strength, work to failure and brittleness for each specimen. They will then be used in conjunction with the CT images to understand the mechanical properties of different regions of femoral heads with avascular necrosis. The results will be used to create a simulation model of the disease in animal femoral heads in vitro.

## 9.4 Histology

Histological analysis will be used to determine the biological properties at different stages of the disease. The findings from images of the femoral head with severe and medium avascular necrosis pathogenesis will also be compared with a histological analysis of a normal femoral head from a further study. It is aimed that these findings will provide comparison basis for evaluation of biological state of the femoral heads with avascular necrosis, when compared with CT images and mechanical properties.

## 10 Risk/benefit analysis

This is an evaluation that characterises bone tissue from patients that is removed and normally discarded as part of the patients' normal treatment during total hip replacement surgery. Thus the study should not impact on the patients' level of care, or increase the risk of physical harm to them. The principal risk to patients is loss of confidentiality of their personal medical information. This risk has been mitigated by the development of a data anonymisation, transfer, storage and processing protocol that reduces the risk of disclosure to a practicable minimum.

Given the time-line for this investigation (approximately 3 years, the duration of the PhD study), the results of the study are unlikely to benefit the participants directly. However, the study has the potential to improve the treatments patients receive to treat AVN for future patients.

## 11 Ethical Considerations

## 11.1 Research Ethics committee approval

The protocol has been reviewed by the Faculty Research Ethics Committee for the Schools of Mathematics; Physical Sciences and Engineering at the University of Leeds.

Prior to commencing the trial, approval will be obtained from the local hospital ethics committee for First Affiliated Hospital of Xian Jiaotong University.

## 11.2 Informed consent

Once identified as potential candidates, patients will be approached for recruitment during their next routine hospital visit. The study will be verbally explained by the clinician, and patients will be given a patient information leaflet and consent form with a return envelope to take away if they wish. If patients complete the consent form they will be included in the study. The consent form will be sent to the IMBE research team by the clinical investigator in a sealed envelope. The envelope will be marked with the patient identification number as defined in section 11.3.1. It will not be opened unless required to prove that consent was given.

If the patient decides to withdraw from the study, they should inform their clinician. The clinician will identify the appropriate patient number and transfer the request to the academic supervisor, who will remove the sample from the database. Patients are informed that withdrawal from the study does not impact their care in any way.

It is acknowledged that some patients may not adequately understand written or verbal information in English. To accommodate these patients, the documentation will be provided in their Chinese Mandarin

Examples of the patient information sheet and consent form are available in appendix B and C.

## 11.3 Data protection

### 11.3.1 ANONYMISATION

All patient specific data will be anonymised prior to transfer from the hospital: Patients' names and addresses will be removed and the data codified using a number that identifies the patient. This identification number will consist of the next available incrementing number. For example, the first patient enrolled will be given the number 001; the second will be allocated 002.

In addition to tissue, personal information will be transferred using a case report form (Appendix A). The content of each case report form will be loaded into a database, using the patient number to maintain trace-ability.

### 11.3.2 DATA STORAGE, HANDLING AND TRANSFER

Part of the data processing will be carried out off-campus while tests are being performed in China. An encrypted external hard drive with Sophos security software will be used to transfer data off-site. The data will be processed directly from the encrypted hard-disk and will not be exposed any shared networks.

The results from the micro-CT scans and mechanical and histological testing will be processed on the researcher's personal computer as well as a university computer. The patient name or details will not be used to process these data, and only the patient number will be used for all data analysis. When using a personal computer, the data will be processed directly from and stored on an encrypted external hard drive with Sophos security software. The raw data will also be backed up on the University of Leeds server.

Demographical information about the patient as obtained in the case report form will be stored and used anonymously and linked to the patient number.

### 11.3.3 CONSENT FORMS

The original consent forms will be stored with the clinical investigator in Xi'an, China, and will not be opened unless necessary to prove consent. A copy of the consent form will be added to the patient's clinical notes at the hospital. Once consent has been obtained, the clinical investigator will report this in the case report form, with the patient number and the date of consent as well as the details of whom the consent is obtained by.

### 11.3.4 END OF STUDY

The data will be stored on the University of Leeds server for 10 years following publication of data.

## 11.4 Declaration of Helsinki

This investigation will be conducted in accordance with the relevant articles of the latest version of the Declaration of Helsinki.

## 11.5 Case report form completion

A case report form must be provided for each subject included in the study.

The case report form (Appendix A) is required to identify the diagnosis and clinical progression of the disease at the time of surgery.

During the first interview, the following data will be captured:

- Demographic details: Age, Sex, Weight, Height,

- Approximate date of first onset of pain
- Approximate date of first presentation to an orthopaedic clinician

In addition to collecting these demographics, the clinician will review the inclusion and exclusion criteria to assess whether the patient's eligibility status has changed.

The case report form will be transported with the tissue. The details will be logged on the study database. An example of the case report form is shown in Appendix A.

## 12 References

- 1 Cooper, C, Steinbuch, M, Stevenson, R, Miday, R and Watts, N B (2010) "The epidemiology of osteonecrosis findings from the GPRD and THIN databases in the UK." *Osteoporosis international: a journal established as result of cooperation between the European Foundation for Osteoporosis and the National Osteoporosis Foundation of the USA*, 21(4), pp. 569–77.
- 2 Jones, John Paul (1971) "Alcoholism, Hypercortisonism, Fat Embolism and Osseous Avascular Necrosis," in *Idiopathic Ischemic Necrosis of the Femoral Head in Adults*, pp. 112–132.
- 3 Assouline-Dayana, Y., Chang, Christopher, Greenspan, Adam, Shoenfeld, Yehuda and Gershwin, M.E. E (2002) "Pathogenesis and natural history of osteonecrosis." *Seminars in Arthritis and Rheumatism*, 32(2), pp. 94–124.
- 4 Tofferi, J K and Diamond, H S (2012) "Avascular necrosis treatment & management." *Medscape Reference: Drugs, Diseases & Procedures*. [online] Available from: <http://emedicine.medscape.com/article/333364-treatment#a1128> (Accessed 10 July 2012)
- 5 Lai, Yu-Shu S, Wei, Hung-Wen W and Cheng, Cheng-Kung K (2008) "Incidence of hip replacement among national health insurance enrollees in Taiwan." *Journal of Orthopaedic Surgery and Research*, 3, p. 42.
- 6 Wong, G K C, Poon, W S and Chiu, K H (2005) "Steroid-induced avascular necrosis of the hip in neurosurgical patients: epidemiological study." *ANZ journal of surgery*, 75(6), pp. 409–10.
- 7 Chiu, K H, Shen, W Y, Tsui, H F and Chan, K M (1997) "Experience with primary exeter total hip arthroplasty in patients with small femurs. Review at average follow-up period of 6 years." *The Journal of arthroplasty*, 12(3), pp. 267–72.
- 8 Chiu, K Y, Ng, T P, Tang, W M, Poon, K C, et al. (2001) "Charnley total hip arthroplasty in Chinese patients less than 40 years old." *The Journal of arthroplasty*, 16(1), pp. 92–101.
- 9 Garellick, G, Kärrholm, J, Rogmark, C and Herberts, P (2010) "Swedish Hip Arthroplasty Register Annual Report 2010." *Swedish Joint Registry*. [online] Available from: <http://www.shpr.se/Libraries/Documents/AnnualReport-2010-2-eng.sflb.ashx> (Accessed 11 July 2012)
- 10 Ellams, D, Forsyth, O, Hindley, P, Mistry, A, et al. (2011) *National Joint Registry for England and Wales*,
- 11 Mont, MA and Hungerford, DS (1995) "Non-traumatic avascular necrosis of the femoral head." *The Journal of Bone & Joint Surgery, American Volume*, 77(3), pp. 459–474.
- 12 Malizos, K N, Karantanas, A H, Varitimidis, S E, Dailiana, Z H, et al. (2007) "Osteonecrosis of the femoral head: etiology, imaging and treatment." *European journal of radiology*, 63(1), pp. 16–28.
- 13 Lavernia, C J, Sierra, R J and Grieco, F R (1999) "Osteonecrosis of the femoral head." *The Journal of the American Academy of Orthopaedic Surgeons*, 7(4), pp. 250–61.

- 14 Gautier, E, Ganz, K, Krügel, N, Gill, T and Ganz, R (2000) "Anatomy of the medial femoral circumflex artery and its surgical implications." *The Journal of bone and joint surgery. British volume*, 82(5), pp. 679–83.
- 15 Radcliffe, I a J, Prescott, P, Man, H S and Taylor, M (2007) "Determination of suitable sample sizes for multi-patient based finite element studies." *Medical engineering & physics*, 29(10), pp. 1065–72.
- 16 Bryan, R, Nair, P B and Taylor, M (2009) "Use of a statistical model of the whole femur in a large scale, multi-model study of femoral neck fracture risk." *Journal of Biomechanics*, 42(13), pp. 2171–6.



## 13 Appendix A: Example of the case report form contents

### Assessment of femoral heads with AVN

Case report form revision and date: **[DRAFT] 01 August 2013**

A case report form must be provided with each subject included in the study.

Patient number	
Clinician's name	
Date of interview	
Does the patient meet the following inclusion and exclusion criteria?	Yes / No
Has consent been obtained from the patient?	Yes / No
If yes, please state the name of the person who obtained the consent and the date of consent.	

Subjects who fulfil the following inclusion and exclusion criteria will be considered eligible for inclusion into this investigation:

#### 13.1 Inclusion criteria

- Male or female subjects aged 18 years or above and skeletally mature at the point of screening for participation
- Subjects with avascular necrosis of the femoral head
- Subjects undergoing total hip replacement procedure as part of their treatment routine
- Subjects who are able to give voluntary, written informed consent to participate in this clinical investigation and from whom consent has been obtained

#### 13.2 Exclusion criteria

- Subjects who, in the opinion of the Clinical Investigator, have an existing condition that would compromise their participation and follow-up in this study.
- Subjects who have previously undergone any type of surgery for avascular necrosis in the affected hip
- Subjects who have marked atrophy or deformity in the upper femur
- Subjects who are unable to give informed consent
- Subjects with transmissible diseases
- Subjects with active local or systemic infection


When did the patient first present to an orthopaedic clinician (Month / Year)?	
When did first onset of pain occur?	
How old is the patient?	
What sex is the patient?	
What weight is the patient in kg?	
What height is the patient in cm?	



## Appendix E

**Risk assessment for experimental work in Xi'an Jiaotong University**

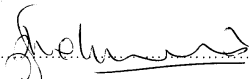


FACULTY OF ENGINEERING – RISK ASSESSMENT		 <b>UNIVERSITY OF LEEDS</b>
<i>Experimental work in Xi'an Jiaotong University – Placement risk assessment</i>	Assessment N <sup>o</sup>	
<i>Xi'an Jiaotong University, China</i>	Lab 02	

Preliminary notes
<ul style="list-style-type: none"> <li>• Risk assessment must be conducted by Academic supervisor/Principal Investigator/Manager.</li> <li>• Other team members and/or people involved or affected by the activities must be consulted in the construction of the risk assessment.</li> <li>• Academic supervisor/Pis/Managers and other team members must ensure that the control arrangements and safe systems of work are followed.</li> <li>• Academic supervisor/Pis/Managers must review this risk assessment at least annually, or in the event of incident, accident or changes to operating/maintenance procedures/personnel.</li> <li>• Review of risk assessment must be conducted by the Academic supervisor/PI/Manager and initialled and dated in the space provided.</li> </ul>

Reference information
<ul style="list-style-type: none"> <li>• Health and Safety at Work etc Act 1974</li> <li>• Management of Health and Safety at Work Regulations 1999</li> </ul>

Copies
<ul style="list-style-type: none"> <li>• Original signed risk assessment must be retained by the Academic supervisor/PI/Manager in their office.</li> <li>• A copy (and any appendices) must be retained in the health and safety file in the workplace.</li> <li>• A digital copy must be forwarded by email to the Faculty Safety Team before work begins.</li> </ul>

Academic supervisor/PI/Manager's approval				
ACADEMIC SUP/PI/MANAGER	PRINT NAME	SIGNATURE	EMAIL/TELEPHONE	DATE
<b>Dr Sophie Williams</b>	Sophie Williams		<b>mensw@leeds.ac.uk</b>	<b>02/09/2014</b>

RA review [to be dated initialled by Academic supervisor/PI/MANAGER]							
Date of next review due:							
Date review completed:							
Initials:							

- The aim of this risk assessment is to provide information on the types of risks and hazards that employees, students and others may be exposed to, arising from the activities described. •

Countersignatures (other members of risk assessment team) [Only if applicable – see Faculty RA Procedures]				
ROLE	PRINT NAME	SIGNATURE	EMAIL/TELEPHONE	DATE
Student	Mahsa Avadi		<a href="mailto:mnmsa@leeds.ac.uk">mnmsa@leeds.ac.uk</a>	02/09/14

## IDENTIFICATION OF RISKS, CONTROLS & ACTIONS

**Consequence/Severity of Harm (C) x Likelihood of harm being realised (L) = Risk Rating [see table following]**

HAZARD TYPE	WHO MAY BE HARMED?	RISK RATING WITHOUT CONTROLS C x L = E,H,M,L,T	CURRENT CONTROL MEASURES (IF ANY)	NEW RISK RATING C x L = E,H,M,L,T	ADDITIONAL CONTROL MEASURES IDENTIFIED	FINAL RISK RATING C x L = E,H,M,L,T	ACTION BY (& DEADLINE)
Hazard from radiation	Student and lab users	High	CT scanner is surrounded by protective casing.  Training has been carried out on the CT Scanner safety and will be reviewed prior to use.	Trivial	A safe distance from the scanner will be maintained during activity of the radiation tube. This will be decided following advice from the technician responsible for radiation monitoring.  Prior to use, all casing and cables will be checked to be intact.	Trivial	
Hazard from use of biological tissue – Human	Student and lab users	High	Personal protective clothing will be used during use of biological tissue. This includes gloves, lab coats and safety specs.	High	The student has been trained on use of human tissue in iMBE laboratories, and will be carrying out the experimental work following iMBE procedures. Further local induction will be carried out.  The tissue will be prepared in an area dedicated for human tissue dissection and will not be mixed with other animal tissue used in the	Trivial	

- The aim of this risk assessment is to provide information on the types of risks and hazards that employees, students and others may be exposed to, arising from the activities described. •

					<p>lab.</p> <p>Student has been vaccinated for infectious diseases that can be transmitted from biological tissue, including Hepatitis A and B.</p> <p>Following use of human tissue, all the containers used as well as the surfaces will be cleaned using Virkon cleaning solution.</p> <p>Any tissue will be stored in a dedicated freezer space for human tissue. The samples will be placed in double packaging. Any liquids will be placed in pots and double bagged before placing in freezer. All tissues will be disposed of together.</p> <p>During the dissection of the samples, drill or saw may be used to prepare the tissue. At this point, the student will prepare use a face shield in order to protect from small debris and aerosols.</p> <p>During CT scanning of human tissue, the samples will be placed in a sealed pot prior to being placed in the scanner. The sample will remain in sealed box until return to the preparation room.</p> <p>During mechanical testing of the samples, the samples will be delivered to the lab where the testing equipment is located in a sealed pot. The user will wear personal protective clothing. A plastic film will be used to cover the</p>		
--	--	--	--	--	---	--	--

• The aim of this risk assessment is to provide information on the types of risks and hazards that employees, students and others may be exposed to, arising from the activities described. •

					mechanical testing machine and nearby benches. Any spillages will be cleaned using Virkon. A plastic film will be taped to the machine to be used as a protective screen in case of escape of fluids towards the lab user.		
Use of mechanical testing equipment	Student and lab users	High	Limits are applied on the software in order to prevent excessive loads	Medium	<p>The student will be trained on the testing equipment before use.</p> <p>The student will operate the testing machine using the software which has limits applied.</p> <p>In order to prevent injury due to high loads, during operation of machine, the student will keep a safe distance from the machine.</p>	Trivial	
Experimental work in a foreign lab	Student	Medium	Training has been carried out on the testing equipment and induction has been given to the laboratory procedures	Medium	<p>The student will be trained on all the equipment and policies of the laboratory with the help of a translator (if needed).</p> <p>Where the student feels the policies do not cover the health and safety aspects that are required, the student will review the risk assessment, and where possible, follow the policies of iMBE, such as good laboratory practice and safety during use of mechanical testing equipment.</p> <p>Where the student finds the health and safety policies insufficient, or finds that the controls in place do not protect the student or other users in the lab, she will stop the work, and contact the supervisors in iMBE for a review of the risk assessment.</p>	Trivial	

• The aim of this risk assessment is to provide information on the types of risks and hazards that employees, students and others may be exposed to, arising from the activities described. •



					The student will follow the points in this risk assessment in order to prevent injuries to her and other lab users.		

COMMUNICATION OF RISK ASSESSMENT FINDINGS TO THOSE INVOLVED				
	METHOD	YES	DATE	COMMENTS
<b>METHODS OF COMMUNICATION USED</b>	Local induction			
	Details of risk assessment discussed and agreed			
	Copy of risk assessment available			
	Controls covered by local protocols & procedures			
	Safety Handbook location notified			
	Toolbox talk			
	Team meeting			
	Email circulation			
	Other – Invitation by letter to retired members			

Consequence/Severity	Likelihood of harm being realised (L)
----------------------	---------------------------------------

• The aim of this risk assessment is to provide information on the types of risks and hazards that employees, students and others may be exposed to, arising from the activities described. •

of Harm (C)	Remote Possibility	Possible	Likely	Highly probable	Virtual Certainty
Minor injury or illness	Trivial	Trivial	Low	Low	Low
Injury/illness requiring medical attention	Trivial	Low	Medium	Medium	High
Injury/illness involving more than 3 days off work	Low	Medium	Medium	High	High
Major injury or long term illness	Low	Medium	High	Extreme	Extreme
Fatal injury/illness	Low	High	High	Extreme	Extreme

- The aim of this risk assessment is to provide information on the types of risks and hazards that employees, students and others may be exposed to, arising from the activities described. •

RISK RATING = (C x L/S)		ACTION & TIMESCALES
Extreme	E	Work must not be started or continued until the risk level has been reduced. While the control measures should be cost-effective, the legal duty to reduce the risk is absolute. This means that if it is not possible to reduce the risk, even with unlimited resources, then the work must not be started or must remain prohibited.
High	H	Work must not be started until the risk has been reduced. Considerable resources may have to be allocated to reduce the risk. Where the risk involves work in progress, the problem should be remedied as quickly as possible. (Action within 1 Week)
Medium	M	Efforts should be made to reduce the risk, but the costs of prevention should be carefully measured and limited. Depending on the number of people exposed to the hazard risk reduction measures should normally be implemented (Action within 1 Month)
Low	L	Consideration should be given to cost-effective solutions, or improvements that impose minimal operating standards which will maintain Low level of risk. Monitoring is required to ensure that the controls are maintained. (Review Assessment Annually)
Trivial	T	No action is required to deal with trivial risks, and no documentary records need be kept (insignificant risk)(Review Assessment Annually)

- The aim of this risk assessment is to provide information on the types of risks and hazards that employees, students and others may be exposed to, arising from the activities described. •





## Placement Risk Management Action Plan Form

This form is optional, but will help to ensure you fulfil all the requirements of the Protocol on Risk Management of Student Placements.

For guidance on who completes and how to complete this form, please refer to the Overall Guidance - Placements and Guide to Risk Profiling Placements which can be found at [www.leeds.ac.uk/safety](http://www.leeds.ac.uk/safety). These guidance documents also point to areas where help in completion of this form can be gained.

<b>Contact Information</b>	
<b>Placement Provider</b> Company Name, Name of contact, Address and contact details	Institute of Advanced Manufacturing Technology School of Mechanical Engineering, Xi'an Jiaotong University No 99 Yan Xiang Road, Yanta District, Xi'an City, Shaanxi Province, 710054 P.R. of China
<b>Student (s)</b> Name, Student ID number, Contact details while on placement	Mahsa Shahi Avadi 200662543 Mobile: 00447932430588 e-mail: <a href="mailto:mnmsa@leeds.ac.uk">mnmsa@leeds.ac.uk</a>
<b>Faculty / School, Academic Tutor Name</b>	Institute of Medical and Biological Engineering School of Mechanical engineering University of Leeds PhD supervisor: Dr Sophie Williams
<b>Placement Coordinator</b> <i>(if different from the Academic Tutor)</i> Name and Contact details	
<b>Dates of Placement</b> (from / to)	24 September 2014 – 09 October 2014

<b>Other details of Placement</b> Job Title	Experimental work on analysis of femoral heads with avascular necrosis
--	--

<b>General Information</b>					
			<b>Follow up Action</b>	<b>Action By</b>	<b>Action Completed</b>
<b>A</b>	Has the Placement Provider returned a completed Tripartite Agreement?	Yes			
	Has the Student returned a completed Tripartite Agreement?	Yes	.		
<b>B</b>	Has the Placement Provider agreed to and / or signed any specific University information?	Yes	A contract was signed by the placement provider agreeing to meet the requirements of the placement.	Sophie Williams	
<b>C</b>	Has the Placement Provider been used in the past?	Yes	By Mahsa Avadi during May 2013		
	If so was health and safety reviewed after previous placement(s)?	Yes			
	If yes are there any unresolved concerns - what are they?	No	All concerns have been resolved through a risk assessment.		
<b>D</b>	If the Placement Provider has been used in the past have there been significant accidents / incidents or other concerns?	No			
	If yes have these concerns been resolved satisfactorily?	Yes / No			

Title:	Placements- Risk Management Action Plan: PDF	Number:	PRSG5.11	Issue date:	01/11	Page Number	Page 2 of 6
--------	--	---------	----------	-------------	-------	-------------	-------------

E	If the placement involves a medium/high risk activity, does the Placement Provider have access to in house professional health and safety advice?	No	There is medium/high risk during the placement due to the nature of the lab work, however all these issues are resolved through a risk assessment, and through application of iMBE safety protocols in the placement.		
---	---	----	---	--	--

Placement Risk Profile (from guide to risk profiling and actions to reduce risk)				
Factor	Risk Level	Follow up Action	Action By	Action Completed
<b>F</b> Work Factors	Low	The student will be undertaking experimental work on human tissue, where dissection, CT imaging and mechanical testing will be involved. In order to reduce the risk from the work, a risk assessment of the experimental work has been carried out and is attached. The student will follow iMBE safety protocols where possible. The student is vaccinated for Hepatitis A and B, and Tetanus, and has undergone an assessment by her GP for the nature of work in China. Personal protection equipment is provided to the student for use during experiments. The student will be fully trained on test equipment and inducted on the local safety regulations of the laboratory. The risk assessment will be reviewed on the student's arrival in Xi'an and before work commences to ensure it covers all risks.		
<b>G</b> Travel and Transportation Factors	Low	The student will use air travel to Xi'an. On arrival at Xi'an, a mixture of taxi and bus may be used to travel around city and to the university/hospital.		



<b>H</b>	Location and / or regional Factors	Low	The student will respect all cultural and regional rules in Xi'an. Any travel advice by <a href="http://www.gov.uk">www.gov.uk</a> will be followed. Any situations which may lead to political tension will be avoided.		
<b>I</b>	General / Environmental Health Factors	Low	Xi'an is a highly polluted city, and the air may cause respiratory issues. Nose filters have been provided to the student to reduce the particles inhaled. The student will close windows and remain indoors where possible on days when pollution is highest. The tap water in China is not safe to drink, and only bottled water will be consumed.		
<b>J</b>	Individual Student Factors	Low	-		
<b>K</b>	Insurance Limitations	Low			

### Final Conclusion

		Follow up Action	Action By	Action Completed
Has the student had a briefing prior to the placement beginning?	Yes			
Is a pre-placement site visit required prior to approval?	No			
Are residual risks tolerable?	Yes			

**Action plan prepared by:**

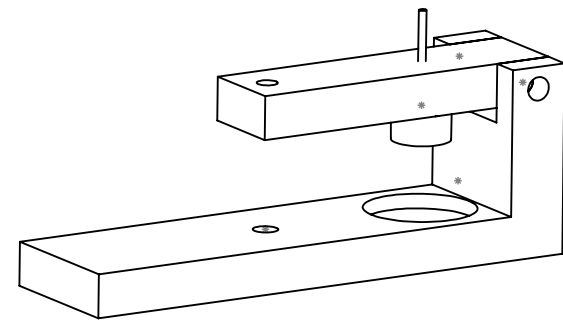
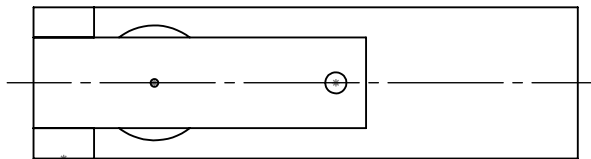
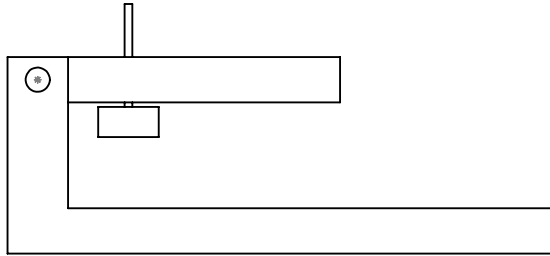
Mahsa Avadi

<b>Role:</b>	Student
<b>Date:</b>	17/09/14
<b>Placement Approved by: (Head of School or</b>	
<b>Role:</b>	
<b>Date:</b>	

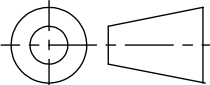
## Appendix F

**Drawings of fixtures designed for experimental work in Xi'an Jiaotong University**





DO NOT  
SCALE IF IN  
DOUBT ASK



THE UNIVERSITY OF LEEDS  
SCHOOL OF MECHANICAL ENGINEERING

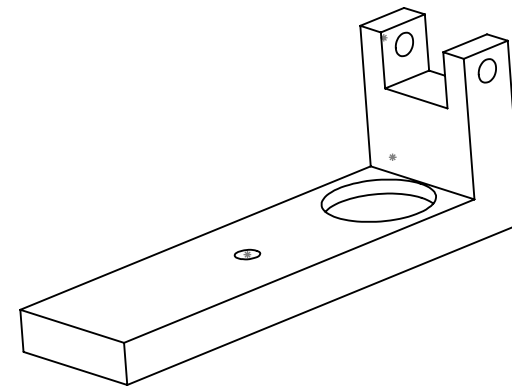
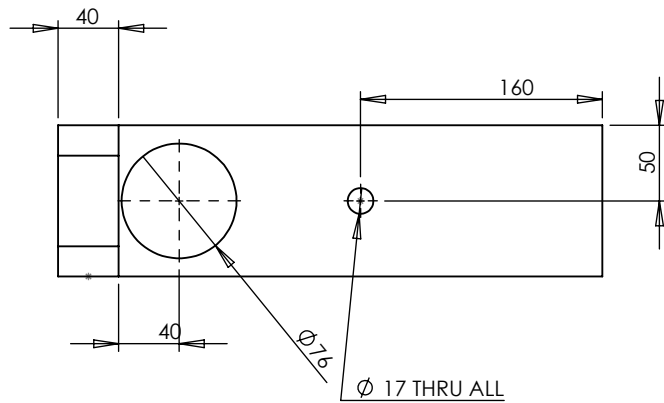
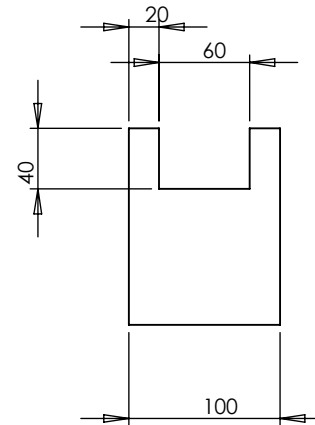
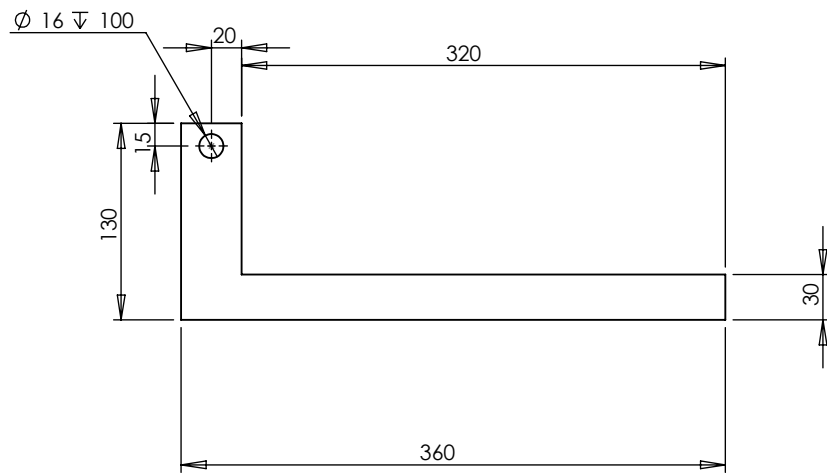
DATE :13.3.14

SCALE 1:5

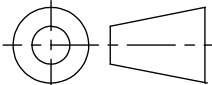
TITLE: Fixture for use with human tissues in CT scanner in Xi'an China

DRAWN BY: M S  
AVADI

DWG NO:



DO NOT  
SCALE IF IN  
DOUBT ASK



THE UNIVERSITY OF LEEDS  
SCHOOL OF MECHANICAL ENGINEERING

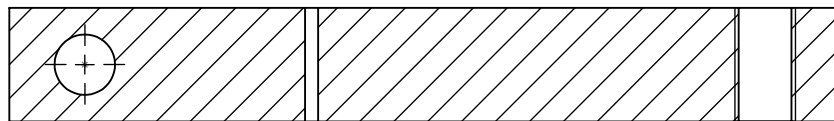
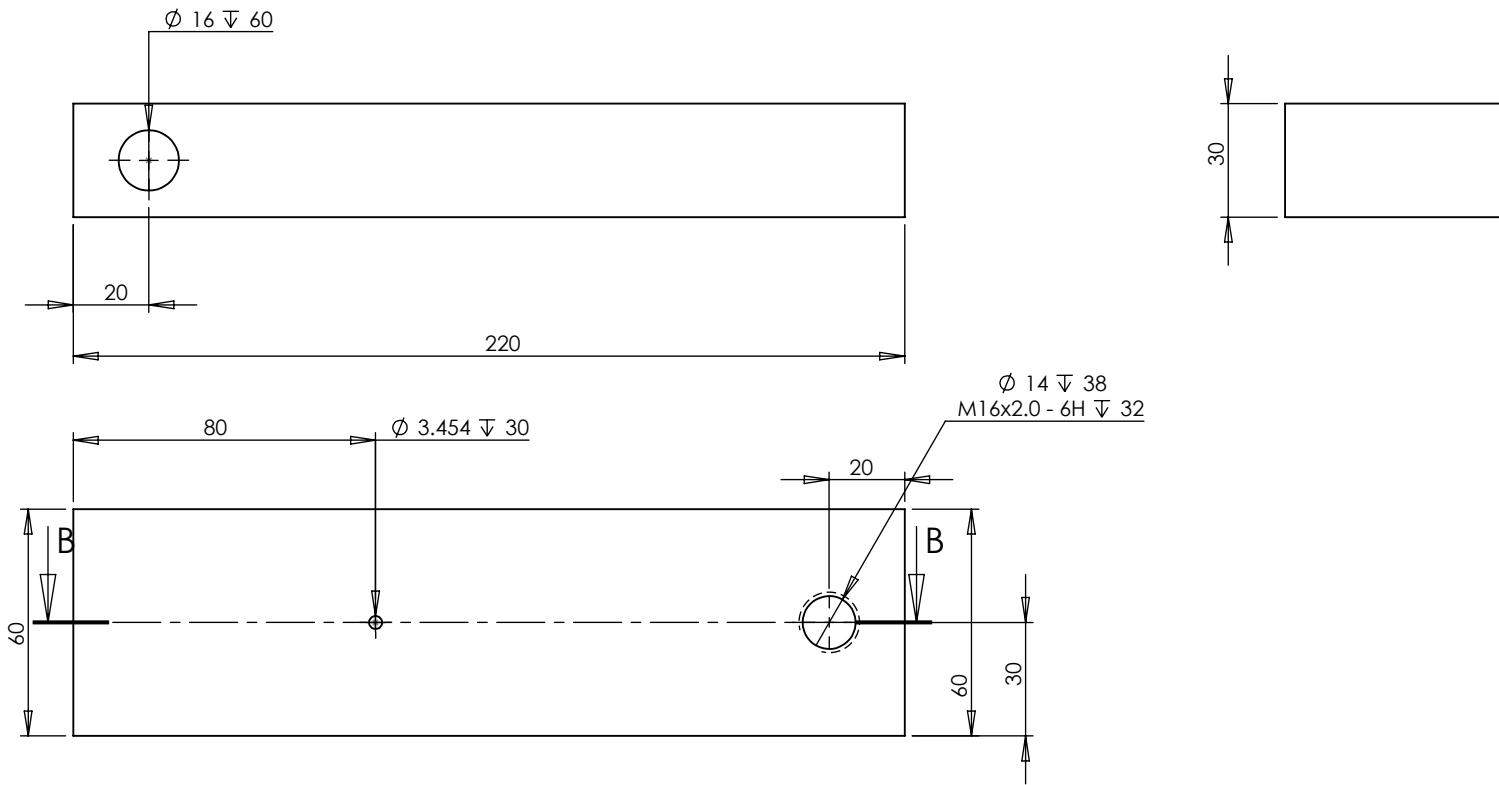
DATE :13.3.14

SCALE 1:5

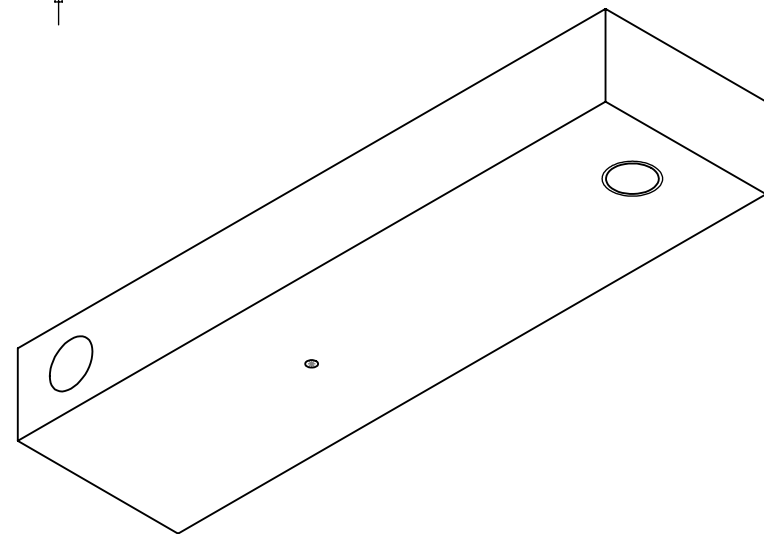
TITLE: Fixture for use with human tissues in CT scanner in Xi'an China

DRAWN BY: M S  
AVADI

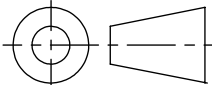
DWG NO:



SECTION B-B



DO NOT  
SCALE IF IN  
DOUBT ASK



THE UNIVERSITY OF LEEDS  
SCHOOL OF MECHANICAL ENGINEERING

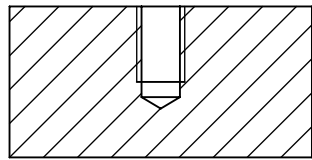
DATE :13.3.14

SCALE 1:2

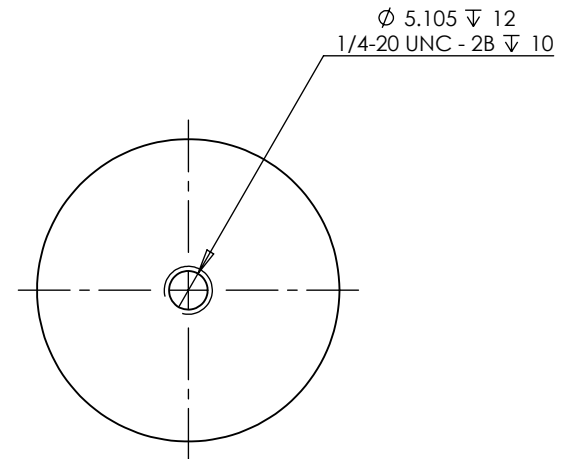
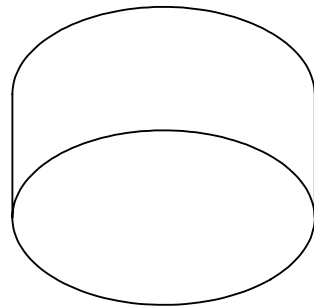
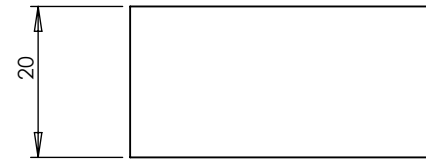
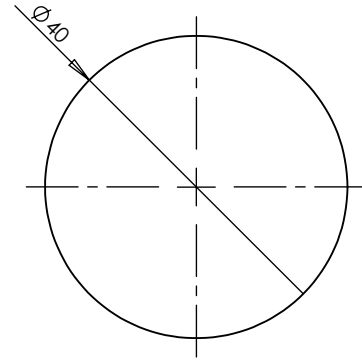
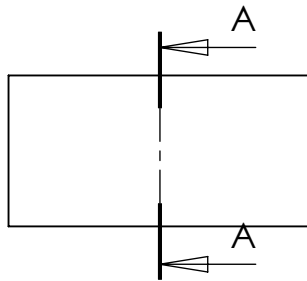
TITLE: Fixture for use with human tissues in CT scanner in Xi'an China

DRAWN BY: M S  
AVADI

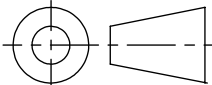
DWG NO:



SECTION A-A  
SCALE 1 : 1



DO NOT  
SCALE IF IN  
DOUBT ASK



THE UNIVERSITY OF LEEDS  
SCHOOL OF MECHANICAL ENGINEERING

DATE :13.3.14

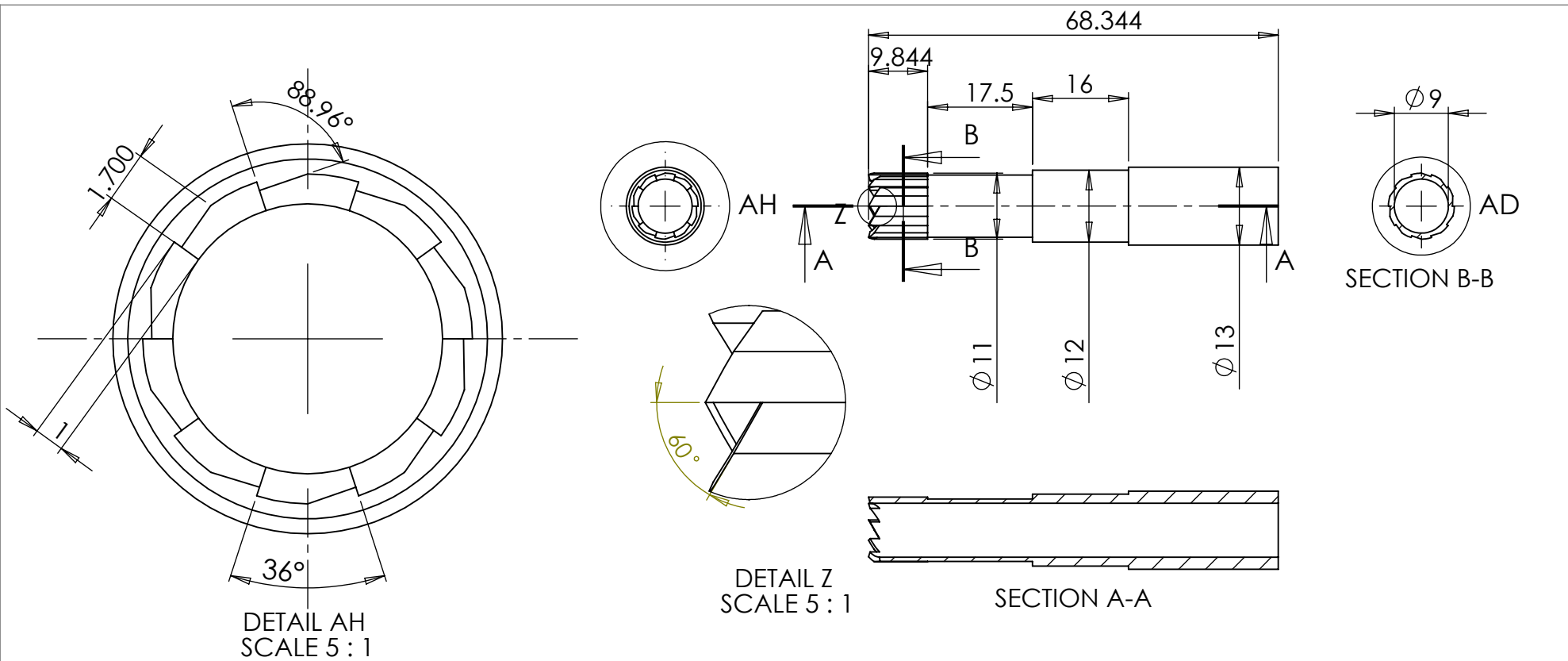
SCALE 1:1

TITLE: Fixture for use with human tissues in CT scanner in Xi'an China

DRAWN BY: M S  
AVADI

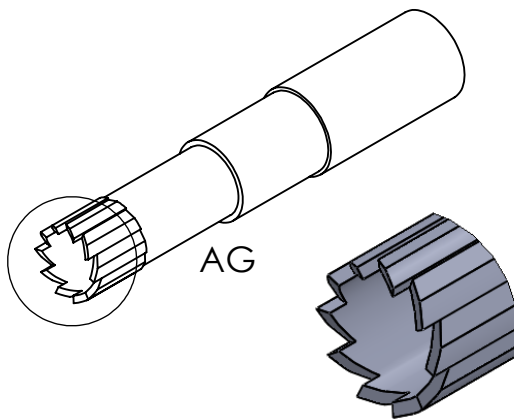
DWG NO:





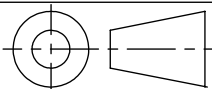
Material: Stainless steel to BS970  
Grade 303S21

Remove all sharp edges except  
for cutter teeth.



DETAIL AG  
SCALE 2 : 1

DO NOT  
SCALE IF IN  
DOUBT ASK



THE UNIVERSITY OF LEEDS  
SCHOOL OF MECHANICAL ENGINEERING

DATE :13.3.14

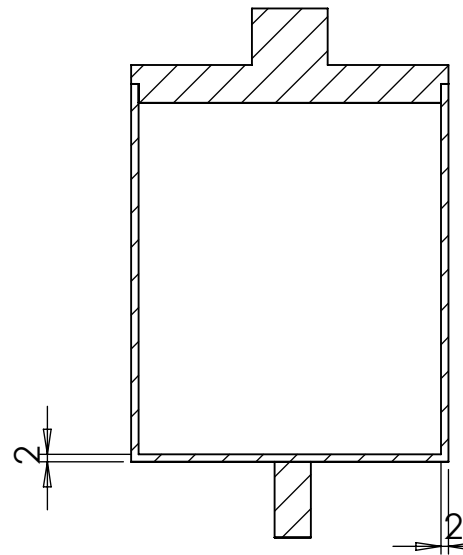
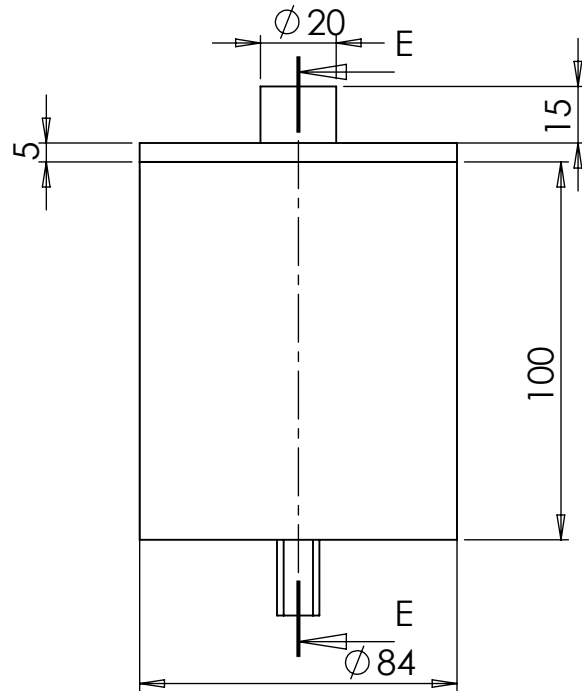
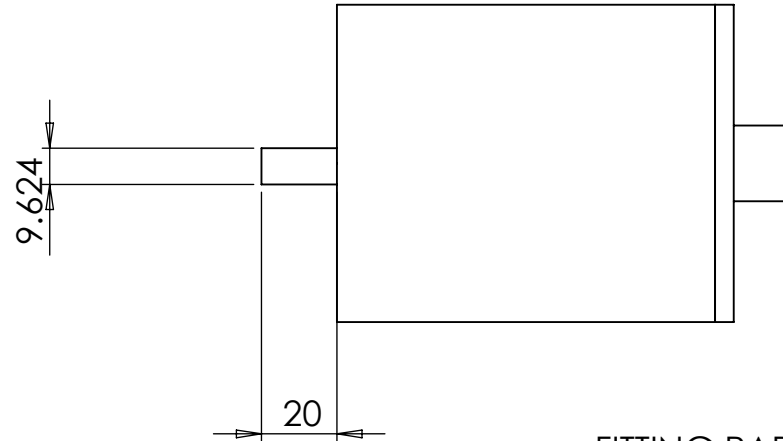
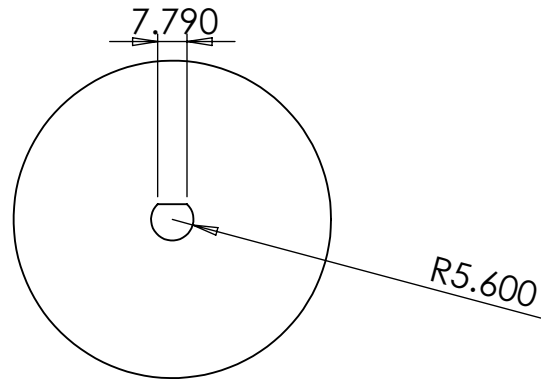
SCALE 1:1

TITLE: 9mm Dia Bone plug cutter

DRAWN BY: M S  
AVADI

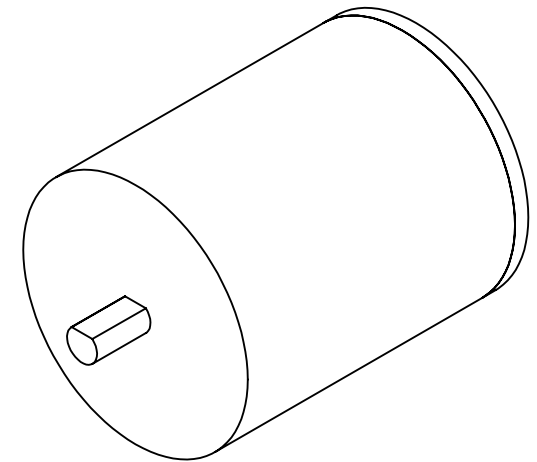
DWG NO:





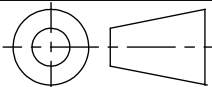
SECTION E-E

FITTING PART NEEDS TO BE PERMANENTLY FIXED TO THE SAMPLE POT. THE LID WILL BE SEPERATE, BUT NEEDS A TIGHT FIT WITH SAMPLE POT.



ALL MATERIALS: PEEK

DO NOT SCALE IF IN DOUBT ASK



THE UNIVERSITY OF LEEDS  
SCHOOL OF MECHANICAL ENGINEERING

DATE :13.3.14

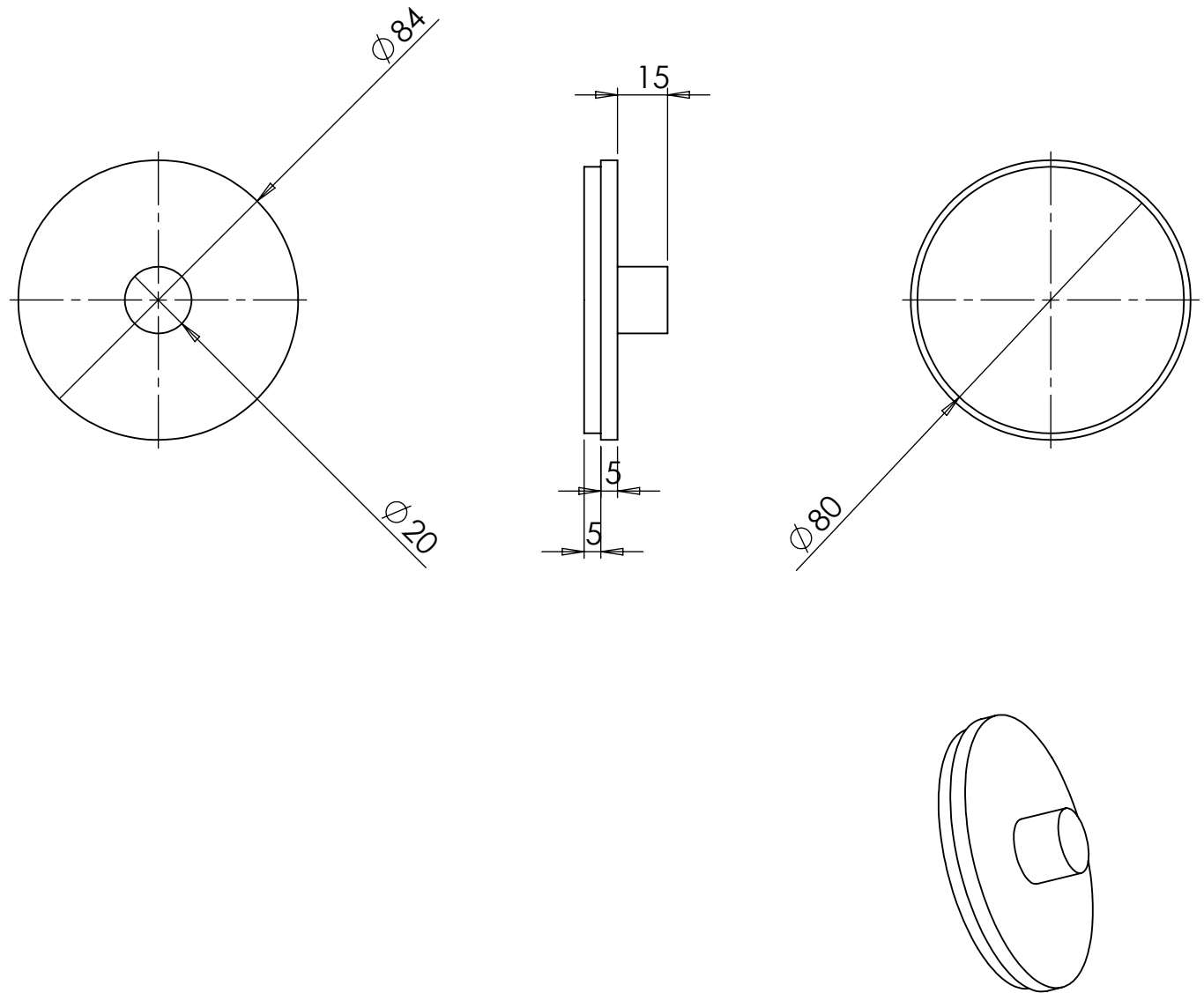
SCALE 1:2

TITLE: Fixture for use with human tissues in CT scanner in Xi'an China  
ASSEMBLY DRAWING  
ALL DIMENSIONS IN MM

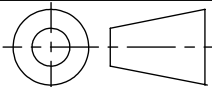
DRAWN BY: M S AVADI

DWG NO:

POT LID PART DRAWING



DO NOT  
SCALE IF IN  
DOUBT ASK



THE UNIVERSITY OF LEEDS  
SCHOOL OF MECHANICAL ENGINEERING

DATE :13.3.14

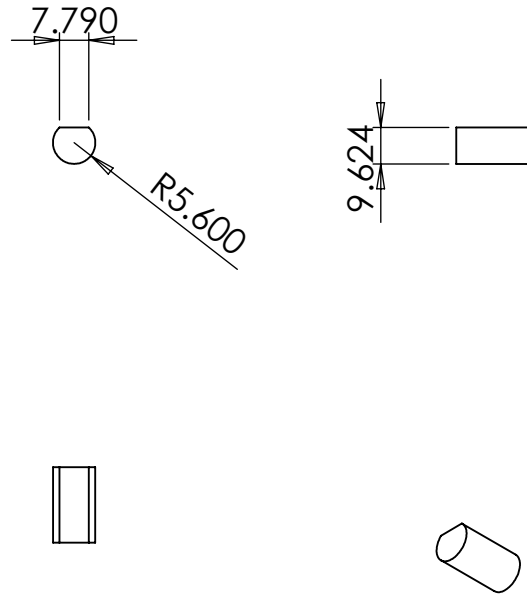
SCALE 1:2

TITLE: Fixture for use with human tissues in CT scanner in Xi'an China

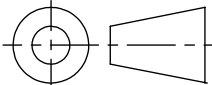
DRAWN BY: M S  
AVADI

DWG NO:

# FITTING PART DRAWING



DO NOT  
SCALE IF IN  
DOUBT ASK



THE UNIVERSITY OF LEEDS  
SCHOOL OF MECHANICAL ENGINEERING

DATE :13.3.14

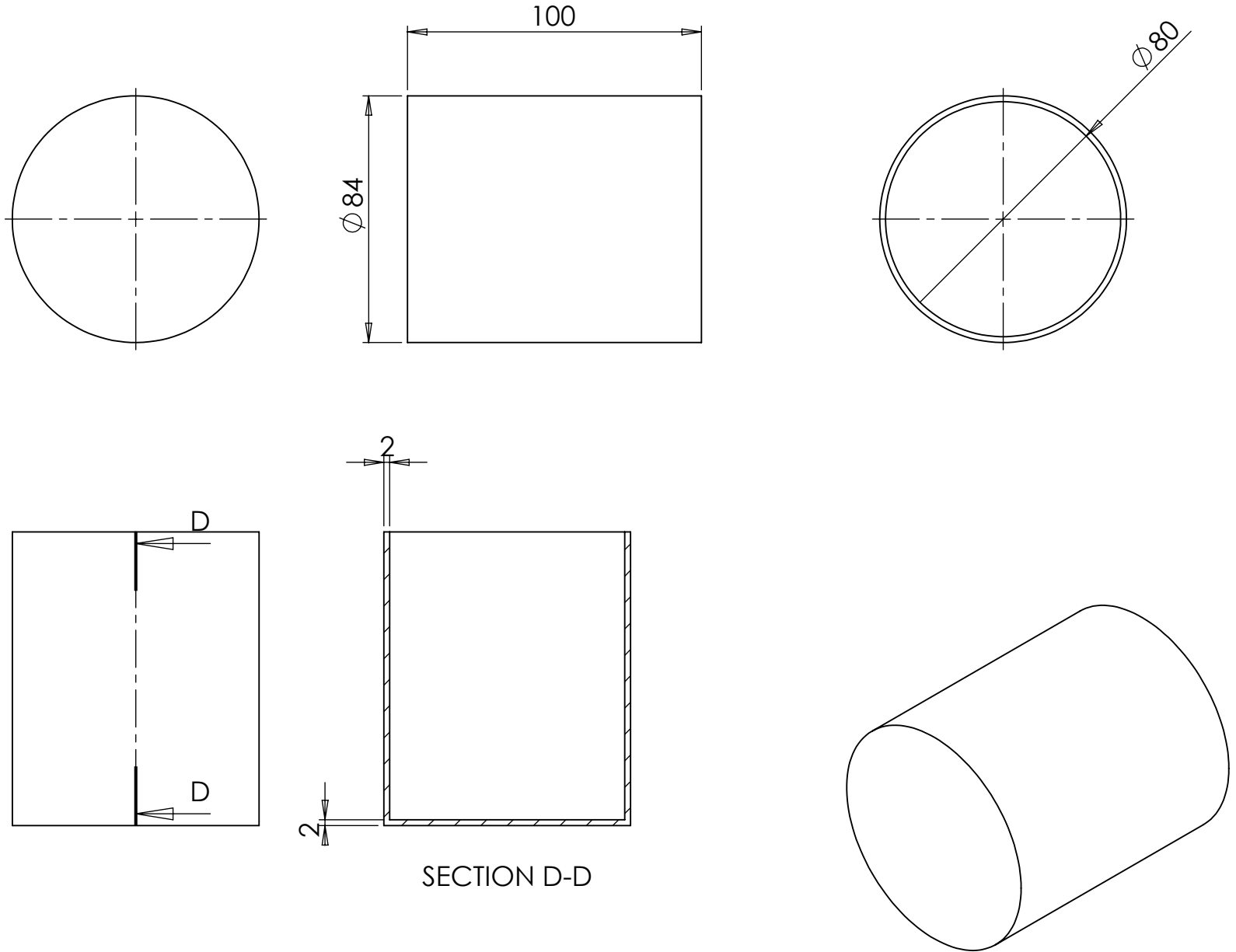
SCALE 1:2

TITLE: Fixture for use with human tissues in CT scanner in Xi'an China

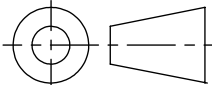
DRAWN BY: M S  
AVADI

DWG NO:

SAMPLE POT PART DRAWING



DO NOT  
SCALE IF IN  
DOUBT ASK



THE UNIVERSITY OF LEEDS  
SCHOOL OF MECHANICAL ENGINEERING

DATE :13.3.14

SCALE 1:2

TITLE: Fixture for use with human tissues in CT scanner in Xi'an China

DRAWN BY: M S  
AVADI

DWG NO:

## **Appendix G**

### **Patient Characteristics**





Specimen number	Test specimen number	Date of Surgery	Date of onset of pain	Date presented to Doctor	Age (y)	Gender	Mass (kg)	Height (cm)	Side of hip	BMI
MSA-ML-20140210-01R	A1	08/02/2014	01/01/2001	01/03/2003	51	F	56	157	R	22.7
MSA-ML-20140402-02L	A2	29/03/2014	01/02/2006	01/07/2006	65	F	45	163	L	16.9
MSA-ML-20140429-03R	A3	27/04/2014	01/03/2004	01/03/2004	60	F	55	162	R	21.0
MSA-ML-20140528-04L	A4	26/05/2014	01/01/2011	01/02/2011	77	F	62	163	L	23.3
MSA-ML-20140618-05L	A5	18/06/2014	15/05/2013	10/02/2014	63	F	67	158	L	26.8
MSA-ML-20140812-06R	A6	10/08/2014	10/05/2010	08/06/2012	60	F	50	161	R	19.3
MSA-ML-20140820-07L	A7	19/08/2014	01/09/2013	05/10/2013	62	M	58	165	L	21.3
MSA-ML-20140804-08L	A8	29/08/2014	20/05/2014	26/05/2014	65	F	63	160	L	24.6
MSA-ML-20140929-09L	A9	27/09/2014	28/06/2005	01/08/2012	56	F	56	158	L	22.4
MSA-ML-20141016-10L	A10	15/10/2014	05/06/2012	10/08/2012	63	M	56	173	L	18.7
MSA-ML-20141027-11L	A11	25/10/2014	20/05/2002	30/04/2002	47	M	117	180	L	36.1
MSA-ML-20141103-12R	A12	01/11/2014	10/08/2012	20/06/2012	59	M	55	174	R	18.2
MSA-ML-20141112-13R	A13	25/10/2014	20/05/2002	30/04/2002	47	M	117	180	R	36.1
MSA-ML-20141112-14R	A14	10/11/2014	05/10/2010	02/09/2010	52	M	67	176	R	21.6
MSA-ML-20141208-15R	A15	05/12/2014	07/10/2013	20/09/2013	62	M	64	168	R	22.7
MSA-ML-20141209-16R	A16	06/12/2014	30/05/2013	10/04/2013	65	M	57	162	R	21.7
MSA-ML-20150114-17L	A17	10/01/2015	20/10/2005	10/08/2005	51	M	63	174	L	20.8
MSA-ML-20150128-18L	A18	29/01/2015	03/12/2013	10/11/2013	62	M	53	169	L	18.6
MSA-ML-20150309-19R	A19	06/03/2015	20/03/2002	10/03/2002	56	F	49	163	R	18.4
MSA-ML-20150309-20L	A20	06/03/2015	20/03/2002	10/03/2002	56	F	49	163	L	18.4

## Appendices

Appendices

## **Appendix H**

**Report for preliminary undergraduate study**



# MECHANICAL INVESTIGATION OF THE COLLAPSE OF THE HUMAN HIP JOINT DUE TO AVASCULAR NECROSIS

*Ben Cowley, Anthony Fear, Katherine Macdougall, Mavra Mahmood*

## ABSTRACT

A method of developing a model of Avascular necrosis (AVN) in porcine femoral heads has been carried out by decalcifying bone using hydrochloric acid (HCl). 30 hours of HCl saturation resulted in an 83% reduction in elastic modulus and 57% reduction in yield strength. A fundamental in-vitro model was developed to determine the amount of time and load required to induce collapse. In all collapsed femurs, fracture was located at the neck and initiated from the growth plate. Two and three-dimensional finite element (FE) models were generated to investigate the mechanical influence of lesion size on the femoral head. Homogenous and inhomogeneous 3D models were also developed using Computed Tomography (CT) images of a treated femur. Models were loaded via a regime that applied a distributed force over the femoral head, replicating both experimental and physiological conditions. Models were analysed to determine locations of possible collapse, and results were compared to experimental models with both showing high stresses induced in the neck. However, due to a growth plate within the porcine tissue, experimental results were compromised.

**Keywords** — Avascular necrosis, finite element, bone decalcification.

## 1. INTRODUCTION

Avascular necrosis (AVN) is the death of bone cells due to a disruption of the blood supply (1), inducing infarcted areas of bone (lesions). AVN is a progressive disease than most commonly occurs in the femoral head (2). If left untreated this disorder can eventually result in collapse of the femoral head, requiring a total hip replacement (THR). Collapse of the femoral head is a complex biomechanical event and the risk of collapse is governed by the extent and location of the lesion. Steinberg et al. (1) reported that lesions occupying over 30% of the femoral head are defined as 'severe' and have a higher incidence of collapse. Early

diagnosis and treatment of AVN can prevent the requirement of a THR; and preserve the mechanical function of the femoral head.

Lesions leading to collapse are most commonly located in the weight bearing area of the femoral head (3). The loss of blood supply to bone decreases the bones resistance to stresses (4) leading to fractures within the necrotic areas. Subsequently, this causes the collapse of the articular surface due to the accumulation of fractures in the trabeculae. This induces the characteristic crescent shaped collapse recorded clinically (5). Brown et al (6) documented a reduction of mechanical properties in post-collapse necrotic bone; 72% reduction in elastic modulus and a 52% reduction in yield strength.

Various investigations have used finite element (FE) models to establish theoretical models for the collapse of necrotic femoral heads (7, 8). These studies determine the effect of lesion size and location on likelihood of failure (8). Bone is an inhomogeneous anisotropic material, but most FE investigations model bone as a homogeneous and isotropic material to reduce computational time. However, this reduces the accuracy of the models produced due to misrepresentation of the material properties.

Locations of collapse have been determined subchondral bone and deep necrotic regions (7). Clinically, findings of Motomura et al. (3) determined that in advanced lesions, collapse occurred within the subchondral bone. All 30 of the retrieved femoral heads displayed failure at the interface between the necrotic bone and the sclerotic layer that demarcates the lesion at the lateral boundary.

Necrotic femoral heads collapse due to high impact trauma or accumulative fatigue failure as a result of the high contact forces generated daily. Peak loads at the hip joint were determined during a number of activities (9). Findings revealed subjects loaded their hips at 238% body weight (BW) during normal walking. Furthermore, strenuous activities such as

jogging and stumbling result in high contact forces of 550% and 870% BW, respectively (10).

The current investigation was carried out to derive useful information to support DePuy's pre-collapse treatment research. To the authors' knowledge, there are no known published papers which document an in-vitro experimental replication of AVN. The aims of this investigation were to:

- Degrade bone properties to mimic the properties of necrotic bone
- Develop an experimental method of replicating AVN in porcine femoral heads
- Develop fixtures and protocol for mechanical testing
- Induce collapse in the experimental AVN model due to severe loading conditions
- Investigate, using FE models, the effect of lesion size on the mechanisms of collapse
- Investigate the effects of applying homogenous and inhomogeneous material properties to AVN FE models
- Predict possible locations of failure in FE models and compare against experimental results

## 2. METHODOLOGY

This investigation was comprised of several studies: experimentally degrading bone; applying this to the femoral head; replicate the physiological loading experimentally and computationally; and determine likely locations of collapse using accurate FE models.

### 2.1. Experimental investigation

#### 2.1.1. Assessment of mechanical properties

Bone plugs were extracted from porcine femoral heads and tested under loading using an Instron machine (system 5900). Data for force and displacement were used to calculate the elastic modulus and yield strength of each sample. Mineral content was quantified by Computed Tomography (CT) imaging the bone plugs to obtain values for bone mass density (BMD) ( $\text{mgHA}/\text{m}^3$ ).

Samples were saturated in 0.5M Ethylenediaminetetraacetic (EDTA) for 2, 3 and 4 days or 0.5M hydrochloric acid (HCl) for 18, 24, and 30 hours. These samples underwent the same material testing and imaging as the control group. The affected region was measured from individual CT slices to determine the extent of decalcification.

#### 2.1.2. AVN model

To decalcify the bone within the femoral head, acid was initially injected. However, this approach was ineffective. Hence, a new method was devised involving drilling a 6mm diameter cavity of 30mm depth from the underside of the femoral head to the weight bearing region. This cavity was filled with HCl for 30 hours. Two bone plugs were extracted from a donor femur of which one was treated with HCl for 30 hours. The partially decalcified bone plug was replaced in the cavity, followed by a healthy plug. The femur was CT scanned to observe evidence of decalcification.

#### 2.1.3. Fixture designs

A design was optimized in a 3D CAD package (SolidWorks, Dassault, USA) to form a jig, meant for positioning and alignment of porcine femoral heads. After validation of designs, the femoral heads were fixated and a testing protocol was devised for loading. CT scanning, SSHS software evaluation, and contact pressure analysis were undertaken.

An artificial acetabular cup was designed and manufactured; a 42mm diameter chamfer was incorporated into the design. Additionally, the cup depth was reduced by 8mm, and a groove was cut into the edge of the surface to avoid impingement of the femoral neck. The centre of rotation (COR) of the components was set using the jig in Figure 1.

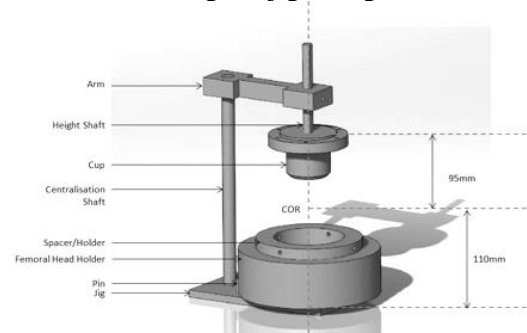


Fig. 1: CAD model for the experimental fixation set-up.

#### 2.1.4. Head fixation

Six porcine femurs were cemented into the inferior component (femoral head holder). To aid fixation bone marrow in the shaft was removed and holes were drilled into the femur. The femur was aligned so the weight-bearing region was consistent with the COR and clamped into place. The cement was poured into the inferior component in a liquid state and left to set for 30-40 minutes.

### 2.1.5. Loading

Three healthy and three treated hips were loaded through the single station hip simulator (SSHS). A dynamic load of 300-4000N was applied to the weight-bearing portion of the femoral head.

Tests were run in increments of 2 hours at a frequency of 1 Hz (1 cycle/second). Each femoral head was CT scanned after 3 and 6 hours of loading; unless premature fracture occurred. Adduction-abduction (AA) torque and axial force motor position (AFMP) were measured using SSHS software. Additionally, theoretical contact pressure analysis was undertaken to appreciate the effect of contact area on contact pressure.

## 2.2. Computational investigation

All models produced were developed and analysed using finite element software (ABAQUS/CAE 6.12-2, Simula Inc, USA).

### 2.2.1. 2D modelling

Six 2D FE models (Table 1) were developed to determine the effect of the addition of cortical and/or sclerotic bone within the femoral head. The effect of altering lesion size was also investigated for mild, moderate, and severe AVN, by modelling lesions occupying 15%, 30% and 45% of the femoral head volume respectively. in accordance with the classification system of Steinberg et al. (1).

**Table 1: Components of 2D models.**

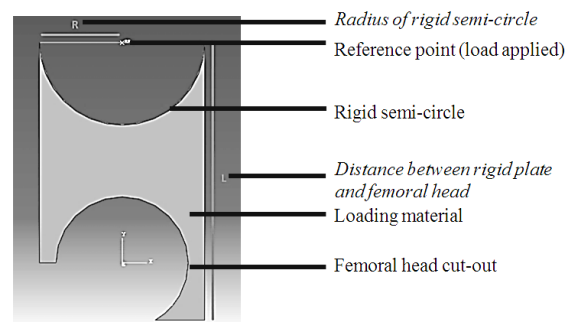
Model	Components
0	Cancellous bone only (benchmark)
1	Lesion and cancellous bone
2	Lesion, cancellous and cortical bone covering the lesion.
3	Lesion, cancellous and cortical bone that covers the cancellous bone only.
4	Lesion, cancellous bone and sclerotic layer surrounding lesion.
5	Lesion, cancellous bone, sclerotic layer surrounding the lesion and cortical bone covering the cancellous bone only.

The femoral head geometry was simplified to a 48mm diameter circle with a horizontal cut-off 12mm below the centerline. To represent physiological conditions, the head was angled at 30° from the horizontal (11) and a boundary condition of zero displacement and rotation was applied to the underside of the femoral head. Necrotic regions were represented as wedge-shaped zones with reduced mechanical properties (7) in accordance to experimental findings (6), the apex of which was located in the center of the femoral head.

Lesions were located in the posterosuperior portion of the femoral heads, which is supplied by the lateral epiphyseal arteries; obstruction of these vessels could result in necrosis (12). When cortical and sclerotic bone were included in models, a thickness of 1mm was assigned (13, 14). Each model was constructed with lesions of 15% and 30% subtended at the apex. *Model 1* was also generated with a 135° lesion.

In accordance with literary values, elastic moduli of 18 GPa and 0.6 GPa were assigned to cortical and cancellous bone respectively. A Poisson's ratio of 0.3 was assigned to all components. A modulus reduction of 72% was applied to necrotic bone and a 44% increase was applied to sclerotic bone (6). Material properties were assumed to be homogenous and isotropic with linear elastic properties.

A 2D loading regime was developed to apply a stress profile comparable to that as experienced in vivo. The loading regime consisted of two parts; a low modulus loading material representing the articular cartilage and a rigid hemisphere to which a point load was applied (Figure 2.). Sensitivity tests were carried out to best represent the physiological loading conditions experienced by the femoral head. The following parameters were varied to achieve this; distance between the femoral head and rigid hemisphere, elastic modulus of the loading material, radius of the rigid hemisphere and the magnitude of the load.



**Fig. 2: Diagram showing the 2D FE loading regime.**

To verify the models and to determine an optimum seed size for each component, mesh convergence testing was conducted. Due to its geometrical complexity, *Model 5* was selected (Table 1). The seed size determined via this process was applied to all other models, ensuring accuracy throughout results.

Due to the nature of the models produced, it was not possible to validate the models through comparative calculations. To test the validity of the loading regime, the stress distribution produced was compared with literary values (9, 10, 15). To test the validity of the models, results were compared with the findings of Brown et al., (16).

2.2.2. 3D modelling

Inhomogeneous and homogeneous 3D models were generated from CT scans of the treated and viable porcine femur. The CT scans were analysed and manipulated using proprietary software (ScanIP, Simpleware, UK) to develop FE models. A series of image processing steps were undertaken to obtain an accurate geometry for the models.

The loading regime from the 2D models was adapted to 3D models to replicate the loading applied in the experimental investigation, by applying a distributed load of 4kN over the femoral head. To represent physiological conditions and link with the experimental method, the distal end of the modelled femur was restricted from displacement/rotation in all axes. The elastic moduli for the loading cylinder and hemisphere were applied in terms of the experimentally derived modulus value (Table 2). The modulus value applied was 100 times smaller and 1000 times larger than the modulus of the cylinder and the hemisphere respectively. A Poisson’s ratios of 0.5 was applied to the hemisphere.

The final models were meshed at the lowest seed size possible given the computational power available. For validation, results from the final models were compared with previous literary investigations.

Homogeneous model

Homogenous material properties, determined via experimental testing (30 hours HCl treatment, Table 4) were applied to appropriate sections of the models. 3D lesions representing 15% and 30% volumes of the femoral head were constructed using SolidWorks (Dassault Systems, USA) and positioned in the weight-bearing region. Lesions

generated were cone shaped and maintained a radius of curvature matching the femoral head.

Inhomogeneous model

Inhomogeneous material properties were applied throughout the models using greyscale (GS) values from the CT scans. Two conversion factors were determined from viable and treated bone plugs. The conversion factors were calibrated by matching the experimental elastic modulus values with the assigned modulus values from the FE models. The conversion factors were then applied to appropriate areas of the FE models. To test the validity of the conversion process, assigned modulus values from the final model were compared with experimentally derived elastic modulus values.

2.3. Key outputs and comparisons

There were a number of links between separate investigations within the project, with all linking to the final computation and experimental models produced, as shown in Figure 3.

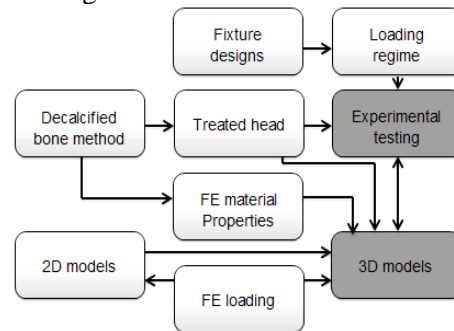


Fig. 3: Schematic showing the links between separate investigations within the project.

3. RESULTS

3.1. Experimental study

3.1.1. Assessment of mechanical properties

Average values taken from 10 healthy control plugs were found to have the properties listed in Table 2.

Table 2: Average material properties for control bone plugs.

E (MPa)	Yield (MPa)	BMD mgHA/cm <sup>3</sup>	Area (mm <sup>3</sup> )
189	9.79	314	68.3

Average values for elastic modulus, yield, BMD and area of decalcification for EDTA treated bone plugs are given in Table 3. The percentage difference was



calculated using the corresponding values in Table 2. These results demonstrate the trend expected; a reduction in mechanical properties was recorded as the duration of EDTA treatment increased. The area of decalcification also increased.

**Table 3: Average material properties and corresponding reductions of EDTA treated bone plugs.**

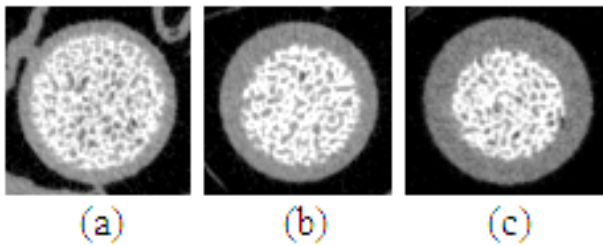
Duration (days)	E (MPa) (% diff.)	Yield (MPa) (% diff.)	BMD (mgHA/cm <sup>3</sup> ) (% diff.)	Decalcified Area (%)
2	107 (-43.4%)	8.44 (-13.8%)	248 (-21.0%)	27.5%
3	77.5 (-59.0%)	5.96 (-39.1%)	227 (-27.2%)	39.7%
4	56.8 (-69.9%)	5.35 (-45.4%)	193 (-45.4%)	46.8%

The properties of samples treated with HCl are presented in Table 4. The results display a similar trend to EDTA treatment. However, a greater reduction in properties was achieved in a shorter duration with HCl (elastic modulus decreased by 74.8% after 18 hours, compared to a 69.9% reduction after 4 days of EDTA treatment). The most extensive decalcification was recorded after 30 hour treatment which demonstrated an 83.3% reduction in elastic modulus and a 57.4% reduction in yield stress.

**Table 4: Average material properties and corresponding reductions of HCl treated bone plugs.**

Duration (hours)	E (MPa) (% diff.)	Yield (MPa) (% diff.)	BMD (mgHA/cm <sup>3</sup> ) (% diff.)	Decalcified Area (% area)
18	47.6 (-74.8%)	4.77 (-51.2%)	240 (-23.6%)	27.1%
24	47.2 (-75.0%)	5.12 (-47.7%)	172 (-45.3%)	46.4%
30	31.6 (-83.3%)	4.18 (-57.4%)	156 (-50.2%)	55.1%

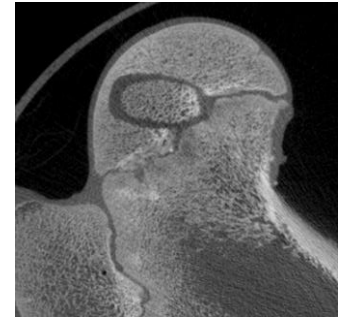
Dark grey regions of the circular cross section in the CT images, shown in Figure 4, indicate decalcified bone. As with EDTA, the area of decalcification increased with time of HCl treatment.



**Fig. 4: CT images showing the cross section of HCl treated bone plugs after (a) 18 hours, (b) 24 hours and (c) 30 hours.**

**3.1.2. AVN model**

The CT images revealed the treated area to be in the desired location under the surface of the weight-bearing region. The darker grey areas within the femoral head show a sufficient level of decalcification in the replaced plug (Figure 5). Additionally, there was evidence of decalcification beyond the cavity wall, as the cavity was also treated with HCl. Across this region of the femoral head the bone had considerably reduced properties, in accordance with the reductions shown in Table 4.



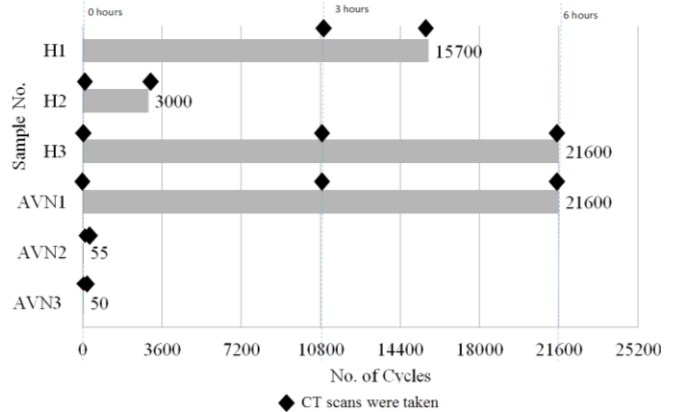
**Fig. 5: CT image of the final treated model, showing areas of decalcification.**

**3.1.3. Fixture validation**

The optimal jig design ensured no impingement. Cup deformation was not recorded under high loading, validating the design. Centralisation of the femoral head was achieved by the designed set-up. The weight bearing portion of the femoral head was well aligned with the COR.

**3.1.4. Fracture**

Results showed treated femoral heads fractured at faster rates than healthy femoral heads (min. cycles for treated fracture=50, min. cycles for healthy fracture=3000) (Figure 6).



**Fig. 6: The number of cycles to fracture and time at which CT scans were taken.**

**3.1.5. Contact pressure and head deformation**

Plastic deformation of the femoral head increased the contact area between the cup and head, and hence a

reduction in contact pressure. The theoretical contact pressure ranged from 2.5 to 3.6 MPa.

A reduction in AA torque (Figure 7) and an increase in AFMP (Figure 8) verified femoral head deformation. A maximum increase of 59% and 98% in AFMP and AA torque were observed for specimen H1 respectively.

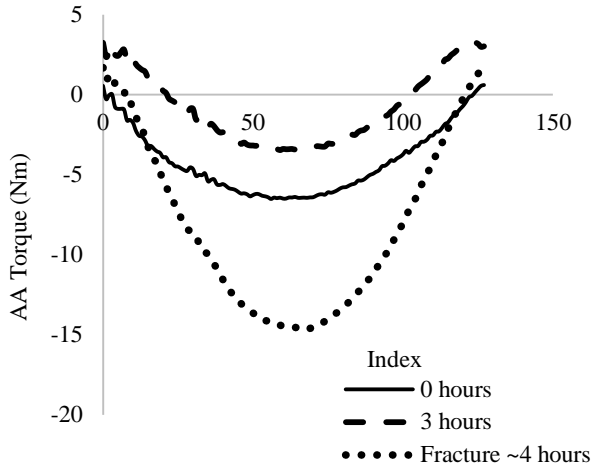


Fig. 7: Variation in AA torque for H1.

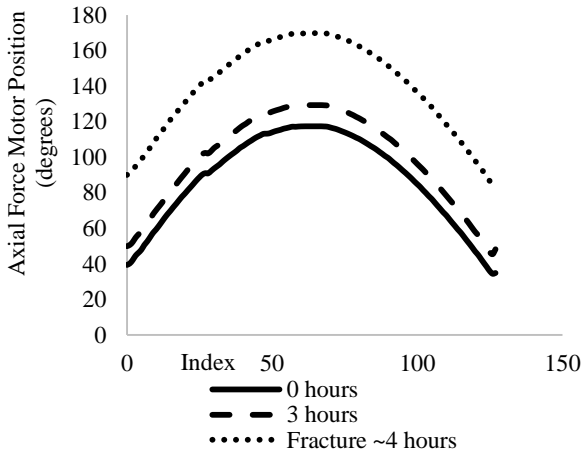


Fig. 8: Variation in AFMP for H1

3.1.6. CT analysis

Post - loading

In all failed femurs (67%), fracture occurred at the neck. Microfractures were observed around interfaces displaying a modulus mismatch: i.e. the growth plate and ossified bone tissue (Figure 9); or the growth plate and treated bone. These microfractures increased as loading time increased. Between 3 hours and collapse, the fracture size increased by 5.6mm (H2).

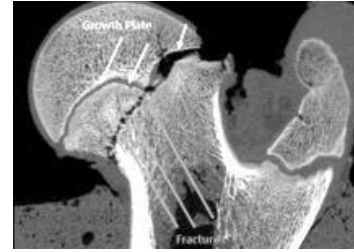


Fig. 9: A CT image of sample H2 post fracture. Arrows indicate the location of fracture initiation at the growth plate.

3.2. Computational study

3.2.1. 2D results

Loading regime

Computational testing determined the parameters shown in Table 5 produced an optimized stress profile.

Table 5: Optimal ratios for 2D loading.

Parameter	Value
Rigid semi-circle radius	$\cong 1.25 * r_{femoral\ head}$
Loading material elastic modulus	$\cong 0.01 * E_{femoral\ head}$
Distance between rigid semi-circle and femoral head	$\cong 2.7 * r_{rigid\ plate}$
Load	0.5kN

These values produced the stress profile presented in Figure 10.

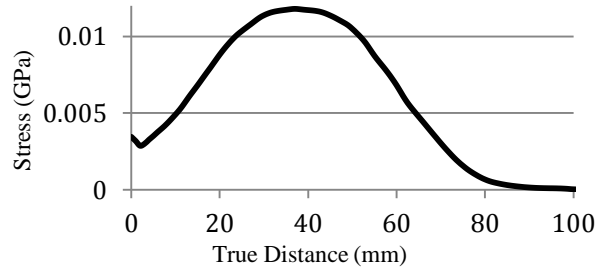


Fig. 10: Stress distribution over the femoral head.

2D Model analysis

An increase in displacement was recorded in models with greater lesion size, shown in Figure 11.

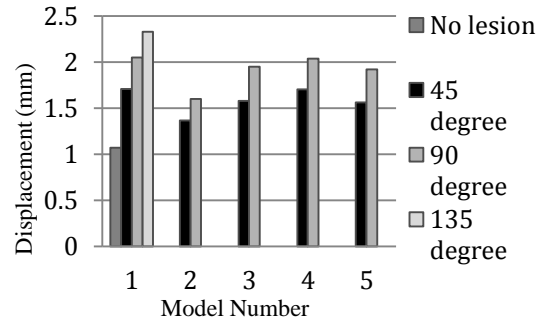
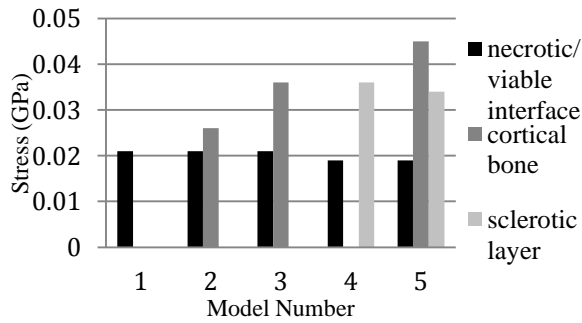


Fig. 11: The effect of lesion angle on displacement of the femoral head.

**Table 6: Range of Hounsfield values and assigned elastic modulus (E) values for 3D models.**

Model	Range of Hounsfield Units	Conversion Factor	Range of Assigned E (GPa)	Experimentally Derived E (GPa)	Average E from Literature (GPa)
Viable	Minimum - 0	$7.116 \times 10^{-5}$	Minimum - 0.01687	Viable cancellous - 0.188966	Viable cancellous - 0.584 Viable cortical - 18.08
	Maximum - 4693		Maximum - 0.2879		
	Peak - 1616		Average - 0.1519		
Treated	Viable Minimum - 0	$3.2 \times 10^{-5}$ for viable bone	Viable Minimum - 0.01559	Viable cancellous - 0.188966	Viable cancellous - 0.584 Viable cortical - 18.08
	Viable Maximum - 4574		Viable Maximum - 0.29627		
	Viable Peak - 1629		Viable Average - 0.1715		
	Treated Minimum - 0	$3.2 \times 10^{-5}$ for treated bone	Treated Minimum - 0.00554	Treated cancellous - 0.03164	Necrotic cancellous - 0.16352 Necrotic cortical - 5.0624
	Treated Maximum - 3394		Treated Maximum - 0.0942		
	Treated Peak - 1617		Treated Average - 0.0498		

Peak stress in Model 1 was generated at the lateral interface of the viable/necrotic bone. The addition of the cortical and/or sclerotic bone had minor effects of the general stress distributions throughout the femoral heads. However, higher stress levels were generated within the added cortical/sclerotic bone, as shown in Figure 12. Higher stresses were generated within the cortical and sclerotic bone for smaller lesion models. Stresses along the lateral boundary of the viable/necrotic tissue were independent of lesion size.



**Figure 12: Effects of the addition of cortical bone and sclerotic layer on the stresses generated in 2D models.**

### 3.2.2. 3D results

#### Homogenous model

The maximum displacement within the models increased with lesion size. The displacement profiles consistently presented the crescent shape induced during subchondral collapse.

The maximum von Mises stresses found in all models was located in the inferior femoral neck. Stress values doubled with the addition of the lesion, independent of lesion size. In both lesion models, stresses of 7MPa were recorded through the lateral viable/necrotic interface. In larger lesions, stresses of 8.7MPa were generated at the top of the lesion, whereas in smaller lesions, large stresses occurred near the lateral boundary.

Strain throughout the femur increased with the inclusion of lesions. In both models the peak strain occurred at the femoral neck, reaching 0.056 and 0.044 for the 15% and 30% lesion models respectively. A large area of strain was also induced in the top of the smaller lesion, with values reaching 0.055 at the lateral boundary of the lesion. A lesser peak stain of 0.04 was recorded at the top of the larger lesion.

#### Inhomogeneous model

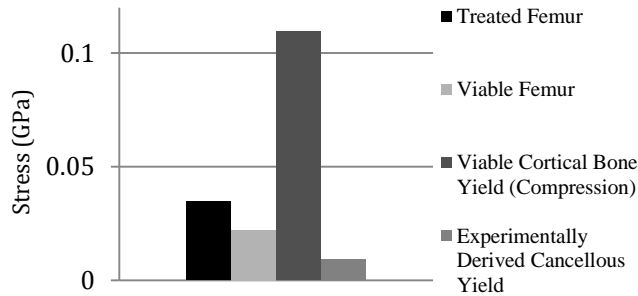
##### Greyscale conversion

The reduction in Hounsfield units between the viable and treated bone shows effective decalcification, presented in Table 6. Comparison between the experimentally derived elastic modulus values and the assigned modulus values in the FE models, demonstrates accurate conversion of GS values. Experimental values lay within the range of assigned values. However, assigned values were significantly lower than human literary elastic modulus values.

##### Model analysis

Comparison of the viable and treated models showed an increase in displacement of 12.9% in the treated model.

Similarly to the homogenous models, peak compressive stresses were located in the inferior femoral neck. Compressive stresses increased by 55% with the inclusion of the lesion. Peak tensile stresses were generated in the superior femoral neck and increased by 211% with the inclusion of a lesion. No stresses generated were great enough to cause yield if compared to literary values of human bone, shown in Figure 13. However, if compared to the yield stress value derived experimentally, 9.79MPa, extensive areas of yielding were induced.



**Fig. 13: Peak compressive von Mises stresses generated through inhomogeneous models, compared to literary and experimentally derived yield values.**

A significant increase in von Mises stress of 548% was recorded in the subchondral bone above the lesion in the treated model.

Strain levels also increased by 52% from the viable model to the treated model, with peak strain being generated in the upper femoral neck.

## 5. DISCUSSION

### 5.1. Experimental

#### 5.1.1. Bone treatment

The assessment of bone material properties revealed HCl to be the most efficient method of degrading bone with a reduction of 83.3% in elastic modulus after 30 hours. This is comparable to the reduction in necrotic bone recorded by Brown et al. (6). This method was therefore used to treat the femoral head to develop an area of degraded bone.

The bone plug replacement method produced a lesion-like area of degraded bone properties in the desired location of the femoral head. It can be assumed that this region of the femoral head has properties similar to that reported for 30 hours of HCl treatment (Table 4). This was a repeatable method to replicate the mechanical properties seen in AVN, in which the size and location of the degraded bone can be controlled.

#### 5.1.2. Loading protocol

To the authors' knowledge there is no published report which documents porcine gait. Additionally, the weight-bearing region of pigs is unknown and therefore could differ to humans. Therefore the rapid collapse observed could be due to the high loads applied to an incorrect location.

A dynamic load was applied to the porcine femoral head, and hence the stress distribution on the hip was not a realistic representation.

It was observed that reducing the inclination angle (rotating anti-clockwise) changed the weight-

bearing region, whereas increasing the angle (rotating clockwise) caused impingement of the neck. The angle differed from the anatomical angle in the human hip joint; which could cause irregular stress distributions and consequently, early fracture.

High contact pressures arose due to the small diameters of femoral heads, relative to the cup diameter (average porcine head diameter=37.5mm, cup diameter=42mm). The treatment method created a modulus mismatch between the treated and viable bone. High stress concentrations generated in this area caused microfractures. The presence of the growth plate caused a secondary modulus mismatch, from which cracks generally initiated.

### 5.2. Computational

#### 5.2.1. Loading

The 2D loading regime was validated via comparison with stress magnitudes recorded by Duan et al. (15) and stress profiles recorded by Brown et al. (6). It was concluded that the regime applied accurate loading conditions resembling those experienced in vivo.

#### 5.2.2. 2D models

Displacement increased with lesion size. Peak displacements were induced within the lesions due to the reduced mechanical properties. The distributed load generated a crescent shaped deformation profile. Reduced displacement of around 20% was recorded in *Model 2*, due to the cortical shell providing structural support to the femoral head.

The presence of the lesion significantly increased stress distributions and peak values. Maximum stresses were generated in *Model 1* at the lateral interface between the lesion and the viable bone, due to a modulus mismatch. Higher stresses were induced within the cortical/sclerotic bone due to higher elastic modulus values. However, the inclusion of these components had little effect on the stresses generated throughout the femoral head.

Validation of the 2D results is not feasible as there are no comparable investigations.

#### 5.2.3. Homogenous 3D model

For all lesion sizes, crescent shaped displacement profiles were generated, in accordance with findings of Steinberg et al. (1) and results recorded clinically (3). For both lesions, maximum displacements around 5mm were induced, which are greater than the 4mm depression assumed to be severe (1). Consequently, it can be assumed that repeated deformations of this

magnitude are likely to cause microfractures within the necrotic tissue, which would eventually lead to collapse.

Peak stresses were located in the inferior femoral neck. This result is validated by the increased thickness of cortical bone in the femoral neck, observed in the CT scans, in accordance to Wolff's law. Stress levels at this location doubled with the inclusion of lesions. As the necrotic region was unable to withstand load, increased stresses were distributed through the proximal femur.

Lesion size had negligible effect on the magnitude of stresses generated at the lateral necrotic/viable interface. However, larger lesions displayed peak stresses around the apex, located within the viable cancellous bone. In accordance with findings of Motomura (3), an increase in lesion size induced larger stress concentrations in the weight bearing region, at the top of the lesion. The synergistic effect of this, combined with fatigue loading, could lead to subchondral collapse, as recorded clinically.

Strain values throughout the head increased with the inclusion of the lesion due to a combination of increased displacements and complex stress redistributions.

#### *5.2.4. Inhomogeneous 3D model*

After conversion from GS values, elastic modulus values reduced by 61% within areas of treated bone. This is comparable to the 72% reduction recorded by Brown et al (6), validating the conversion process. However, elastic modulus values are significantly less than literary values for human bone (Table 6). This affected the results recorded, and induced unrealistic results, such as displacement values of up to 14.85mm. The introduction of the treated area increased displacements, promoting trabecular collapse.

Peak compressive stresses were generated within the higher modulus cortical bone in the inferior femoral neck. Stress values increased throughout the treated model relative to the viable model. The location of peak stresses relates with experimental results, as failure occurred in the femoral neck in all collapsed models.

When comparing induced stress values to literary yield values of human bone, no areas of yield were recorded. However, when compared to experimentally derived values of yield for porcine tissue, extensive areas of yield occurred. However, experimentally derived yield values from immature

porcine tissue will differ to that of mature human literary values.

### **5.3. Comparisons of experimental and computational models**

Fracture occurred at the neck in all collapsed experimental models. This is consistent with high stresses in the superior femoral neck for all computational models. It must be emphasized that fractures initiated at the growth plate for all experimentally collapsed models. The influence of the growth plate was overlooked in all computational models.

The 3D FE loading regime was designed to replicate the experimental protocol. However, simulating dynamic cyclic loading in computational models was beyond the scope of this project. This limited the comparisons available between computational and experimental models. High conformity, achieved in computational loading eliminated concentrated contact pressures. However, this was not possible in experimental loading, consequently producing high contact stresses which may have contributed towards premature collapse.

It must be emphasised that no effects of accumulative damage were considered in computational models. This is physiologically unrealistic and limits the validation between experimental and computational models. Due to the poor fatigue resistance of bone (17), the breakdown of necrotic trabeculae is likely to occur progressively due to repeated loading. This phenomenon was overlooked in the FE models, and therefore it was unlikely that failure would be induced with the application of a single load.

### **5.4. Limitations**

A relatively small sample size was used throughout the bone plug study with results showing relatively large levels of variation. This reduced the reliability and accuracy of average values. Subsequently this affected the material properties assigned to FE models.

The extent of the affected area was limited by the method of treatment. It was not possible to involve the weight bearing subchondral bone within the treated area, were collapse is often recorded clinically (3).

Treated heads were left out of refrigeration and exposed to air for over 30 hours prior to loading, significantly longer than untreated models. This may have caused degradation of the bone, contributing to premature collapse.

The mechanical integrity of the final experimental models was reduced by drilling during treatment. Speculatively, this damage would affect the specimens beyond that observed in necrotic femoral heads.

Numerous simplifications were applied to FE models in order to reduce computational time. The linear elastic homogenous material properties applied, inherently misrepresent component bone tissues. Hence the accuracy of stress distributions is reduced. Yield strength deficits within the bone are overlooked, a critical factor in the initiation of collapse.

The geometry of the modelled lesions were simplified, inducing inaccurate stress distributions. Peak stresses and strains were generated at the apex and corners of the lesions which may be model specific. The representative lesions implanted in the weight bearing regions of homogenous models altered the geometry, by engulfing the fovea capitis.

Interpretation of the CT images was qualitative and subjective, as the orientation of femurs varied between scans.

## 6. CONCLUSION

A successful method was developed to replicate AVN within the porcine femoral head via an acid decalcification process. A repeatable test protocol, including fixation and loading, was developed to replicate physiological conditions. Generally, collapse was induced in treated femoral heads in a lesser time than in viable femoral heads. However, fractures were initiated at the growth plates, suggesting misrepresentative failure locations.

FE models concluded that an increase in lesion size, increased displacement of the femoral head, promoting collapse. Homogeneous and inhomogeneous material properties were successfully applied to 3D models, highlighting probable locations of failure. Agreement was observed between the obtained results and literary findings.

Peak stresses generated in the neck of FE models, linked well with experimental results. However, locations of experimental failure were influenced by the growth plate.

### 6.1. Advancements

Further investigations could alter the size and location of the treated area, by adapting the size of the replaced plug and varying the location of the cavity.

Mature tissue should be used to prevent crack initiation at the growth plate. Ideally, human tissue

should be used, as geometrical differences between porcine and human femurs may alter the stress distributions generated.

Further FE models could include cyclic loading and accumulative fatigue, inducing realistic gradual breakdown of the femoral head.

Furthermore, variations of the gait cycle should be applied both computationally and experimentally, to thoroughly investigate the hip joint.

## ACKNOWLEDGEMENTS

All the support and guidance from mentors Dr. Alison Jones and Dr. Sophie Williams is gratefully acknowledged. Thanks also go to Mahsa Shahi Avidi, Dr. Qianqian Wang, James Anderson and Nazir-Ahmed Karbanee for their support through the project.

## REFERENCES

1. Steinberg, M. et al. A quantitative system for staging avascular necrosis. *Journal of Bone & Joint Surgery, British Volume*. 1995, **77-B**(1), pp.34-41.
2. Pappas, J.N. The Musculoskeletal Crescent Sign 1. *Radiology*. 2000, **217**(1), pp.213-214.
3. Motomura, G. et al. Morphological analysis of collapsed regions in osteonecrosis of the femoral head. *Journal of Bone & Joint Surgery, British Volume*. 2011, **93**(2), pp.184-187.
4. Rothschild, B.M. *Rheumatology: a primary care approach*. Yorke Medical Books, 1982.
5. Mont, M.A. and Hungerford, D.S. Non-traumatic avascular necrosis of the femoral head. *The Journal of bone and joint surgery. American volume*. 1995, **77**(3), p.459.
6. BROWN, T.D. et al. Mechanical characteristics of bone in femoral capital aseptic necrosis. *Clinical Orthopaedics and Related Research*. 1981, **156**, pp.240-247.
7. Brown, T.D. et al. A non-linear finite element analysis of some early collapse processes in femoral head osteonecrosis. *J Biomech*. 1982, **15**(9), pp.705-715.
8. Sugano, N. et al. Prognostication of osteonecrosis of the femoral head in patients with systemic lupus erythematosus by magnetic resonance imaging. *Clinical Orthopaedics and Related Research*. 1994, (305), pp.190-199.
9. Bergmann, G. et al. Hip contact forces and gait patterns from routine activities. *J Biomech*. 2001, **34**(7), pp.859-871.
10. Bergmann, G. et al. Hip joint loading during walking and running, measured in two patients. *J Biomech*. 1993, **26**(8), pp.969-990.
11. Steele, D.G. *The anatomy and biology of the human skeleton*. Texas A&M University Press, 1988.
12. Sevvit, S. and Thompson, R. The distribution and anastomoses of arteries supplying the head and neck of the femur. *Journal of Bone & Joint Surgery, British Volume*. 1965, **47**(3), pp.560-573.
13. Rodríguez-Soto, A.E. et al. Texture analysis, bone mineral density, and cortical thickness of the proximal femur: fracture risk prediction. *Journal of computer assisted tomography*. 2010, **34**(6), pp.949-957.
14. Treece, G.M. et al. High resolution cortical bone thickness measurement from clinical CT data. *Medical image analysis*. 2010, **14**(3), pp.276-290.
15. DUAN, Y. et al. THE HIP STRESS LEVEL ANALYSIS FOR HUMAN ROUTINE ACTIVITIES. *Biomedical Engineering: Applications, Basis and Communications*. 2005, **17**(03), pp.153-158.
16. Brown, T.D. et al. Stress transmission anomalies in femoral heads altered by aseptic necrosis. *J Biomech*. 1980, **13**(8), pp.687-699.
17. Carter, D.R. et al. Fatigue behavior of adult cortical bone: the influence of mean strain and strain range. *Acta Orthopaedica*. 1981, **52**(5), pp.481-490.